Changes of address (with advance notice of fifteen days) and communications regarding subscriptions and payments should be mailed to the Secretary of the Institute, at 450 Ahnaip St., Menasha, Wisconsin, or 1 East 79 Street, New York 21, N. Y.

* Numerals in parentheses following Directors' names designate Region number.

PROCEEDINGS OF THE I.R.E.

Published Monthly by

The Institute of Radio Engineers, Inc.

VOLUME 39 — *September, 1951* — NUMBER 9

PROCEEDINGS OF THE I.R.E.

INSTITUTE NEWS AND RADIO NOTES

Responsibility for the contents of papers published in the PROCEEDINGS OF THE I.R.E. rests upon the authors. Statements made in papers are not binding on the Institute or its members.

I.R.E. Professional Group Founders

R. A. Heising
Originator, Professional Group System

W. L. Everitt
First Chairman, Professional Groups Committee

W. R. G. Baker
Present Chairman Professional Groups Committee

Dorman D. Israel
Broadcast and Television Receivers

Lewis Winner
Broadcast Transmission Systems

J. G. Brainerd
Circuit Theory

Ernst Weber
Instrumentation

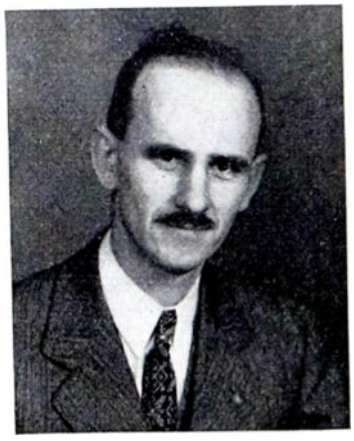

M. M. Hubbard
Nuclear Science

R. F. Rollman
Quality Control

and Professional Group Chairmen

JOHN E. KETO
Airborne Electronics

GEORGE SINCLAIR
Antennas and Propagation

B. B. BAUER
Audio

RALPH I. COLE
Engineering Management

EUGENE MITTELMANN
Industrial Electronics

NATHAN MARCHAND
Information Theory

W. J. MAYO-WELLS
Radio Telemetry and Remote Control

AUSTIN BAILEY
Vehicular Communications

What Is Nuclear Engineering?*

ALVIN M. WEINBERG†

This paper is published with the approval of the IRE Professional Group on Nuclear Science, and has been secured through the co-operation of that Group.—*The Editor.*

IF I WERE to answer the question, "what is radio engineering," or "what is electrical engineering," or "what is chemical engineering," I could with good point say, "radio engineering is what radio engineers do," or "electrical engineering is what electrical engineers do," or "chemical engineering is what chemical engineers do." Should I try to answer the question, "what is nuclear engineering," by saying "nuclear engineering is what nuclear engineers do," I should hardly be giving an intelligible answer—not only because what nuclear engineers do is supposed to be secret, but, perhaps more important, because what nuclear engineers are supposed to do is, in a sense, not very well defined. This is partly a symptom of transition of nuclear technology from an applied science to an engineering art, a transition during which the job of the engineer and the scientist overlap—but it is also a reflection of the inherent difficulties which exist in establishing valid objectives for nuclear energy development.

I shall therefore try, in answering the question, "what is nuclear engineering," to give first what I think are valid and worthwhile objectives for the nuclear energy effort in the United States.

The wretched international situation at first sight makes it superfluous to seek objectives for nuclear-energy development beyond the needs dictated by military necessity. These needs include weapon development, production of fissionable materials for weapons, either in reactors or in diffusion plants, and development of high temperature, mobile nuclear reactors for propulsion of military vehicles such as ships or aircraft. And indeed, it is probable that nuclear-energy development will in the foreseeable future strongly resemble aircraft development in that both are curiously mixed military and nonmilitary technologies which reflect, in microcosm, our larger mixed military-nonmilitary civilization.

Yet there are at least two reasons why nuclear-energy development must seek objectives beyond the strictly military. The first is that, from a very long-range viewpoint, it is probable that nuclear prime movers will have to tide our civilization over from its current dependence on stored photosynthetic energy (i.e., coal and oil) to an ultimate dependence on currently produced photosynthetic energy (burning of green plants, and the like). Our civilization *can* survive without supersonic aircraft; it *cannot* survive without an alternate large-scale energy source, such as uranium fission, to take over when coal and oil give out. Thus, in an ultimate sense, nuclear energy ought to enter into the fabric of our civilization in a manner somehow more important—and more intimate—than that of aircraft propulsion. From this viewpoint, nuclear energy is too important to our civilization for its future to be tied to military needs alone.

The second reason for nuclear-energy development seeking some of its objectives beyond the military is that the course of development of nuclear-powered prime movers for military needs lies only partly along the same road as the development of nuclear prime movers for civilian needs.

There are two main objectives of military reactor development: production of fissionable material and propulsion of military vehicles. The basic requirement for propulsive machinery is that it be small and light; the basic requirement for a fissionable material producer is that it produce cheaply. On the other hand, the basic requirement for a civilian reactor is, on the whole, that it produce useful energy cheaply, regardless of its size or weight. Thus the objectives of civilian nuclear energy—cheap power—are not quite the same as the objectives of military nuclear energy—compact power and fissionable material—and, in general, the paths which are appropriate to further military nuclear energy are only partly the paths which would further civilian nuclear energy. It is only in a reactor which produces both fissionable material and cheap electrical power that there is an objective of the clearest validity since it would combine the long-term civilian objective (power) with a continuing military objective (fissionable material).

In spite of my belief that nuclear energy does ultimately represent an extraordinarily important part of our civilization's energy resources—and therefore its ultimate objectives must be found rather independently of the military—I concede that as a practical matter the present military impetus has given great point to the reactor-development program. For the next generation it is probable that this military-nonmilitary duality will characterize nuclear-energy development.

A neutron chain reactor is unique among sources of thermal energy in that the rate of energy release in a reactor is independent of the temperature at which the energy is generated. This, of course, results from the fact that the Arrhenius factor strongly enters into the rate of reaction in the chemical binding energy range where the reaction energy is of the order of KT; but it enters not at all in a nuclear reaction where the energies are many orders of magnitude greater than KT. This basic independence of nuclear-energy release from temperature has allowed the development of reactors to proceed along two parallel threads which are characterized by temperature and purpose. There is a low-temperature thread which is exemplified by the large-scale plutonium producers at Hanford, and there is a high-temperature thread exemplified by the projected naval or aircraft reactors. For a given total energy release, the required heat-transfer surface is smaller the higher the temperature drops. This in substance means that a compact reactor which produces useful power must be a high-temperature one, and, quite apart from questions of thermal efficiency, this is the reason why the military mobile reactors belong to the high-temperature genus.

On the other hand, where reactor size is unimportant there is incentive to run at low temperature—both because, at low temperature, materials are generally more adequate and because the very best moderator, heavy water, is inherently a low-temperature material. In a conventional steam power station where the prime motivation is fuel economy, advantages in material performance which accrue from low pressure and temperature are more than balanced by the thermodynamic or fuel-efficiency advantage of high temperature. In a nuclear power plant where fuel efficiency is secondary to plant efficiency, the incentive to run at high temperature is much smaller. In fact, it is my own belief that the dominant kind of nuclear power plant will be a rather low-temperature, low-thermal efficiency system which will combine the long-term objectives of fissionable material and power production, and in which all compromises will be made in the interest of over-all low cost. The fissionable material produced from such low-temperature power reactors will presumably be available for weapon or for high-temperature, high-efficiency mobile systems; but since the uses for the highly compact high-temperature systems will be specialized, it is my guess that in the foreseeable future it will be these rather low-temperature fissionable material power producers which will represent the main stream of nuclear-energy development.

Such combination Pu or U^{233} and power producers would supply increasingly large amounts of the country's power. It is my belief that the development of networks of such dual-purpose plants is the main job of nuclear engineering since it is by successful operation of such networks—more than by the successful propulsion of military vehicles—that the long-term importance of nuclear energy can be demonstrated.

* Decimal classification: 539. Original manuscript received by the Institute, April 30, 1951.
An address presented, 1951 IRE National Convention, New York, N. Y., March 22, 1951.
† Oak Ridge National Laboratory, Oak Ridge, Tenn.

There is the rather practical question in deciding on a power producer of whether it should be a breeder or a converter, i.e., should it convert newly dug U^{235} into Pu^{239} or U^{233}, or should it increase the total supply of U^{233} or Pu^{239}? That breeding is the ultimate choice is clear since eventually we will run out of U^{235}. But the cost of breeding, per atom of newly bred material, should be higher than the cost of conversion, and, therefore, a balance must be struck between the cost of digging less enriched ores against the cost of producing expensive bred material. The question of whether it pays to invest one's money in a breeder or an additional ore processing plant is by no means easy to answer. At some price for a pound of uranium ore it makes more sense to breed, rather than to convert. What that price is, I do not know.

Granted that some kind of nuclear reactors which will produce power and fissionable material are of long-term significance, what about the other large-scale engineering systems—the isotope separators; will they occupy any long-term important position in nuclear-energy development? While it is too early to say, I think there is a fair chance that isotope separators will be important even in the long run for the following reason: a chain reactor using natural uranium stops when a rather small amount of its U^{235} is burned up. The problem then is whether it pays to dig new uranium out of the ground or whether it pays to ship the depleted uranium back to the diffusion plant to re-enrich it. Just as in the choice of breeders versus converters, so here the answer to the question does it pay to re-enrich depends on the ore cost. Since, as high-grade ores are worked out, raw U will almost certainly increase in price, it is possible that re-enriching will prove of long-term importance, i.e., isotope separation will possibly retain its significance. Thus, a nuclear power-plant system might include an ore plant which supplies normally enriched U to a large central power plant which, after burning part of the U^{235}, returns its waste product to a diffusion plant for re-enriching. The economic engineering of such a complex will clearly depend on an integrated analysis of the whole reactor-diffusion plant complex which takes account, say, of the fact that part of the power from the reactor must be fed back into the diffusion plant.

But at this stage, when not one single kilowatt of electrical energy has yet been extracted from nuclear fission, it is a little far-fetched to try to make blueprints for huge reactor-isotope separation plants. It is enough to examine the overriding reactor problems.

Although a nuclear chain reactor is a nuclear system, the fission process, after all, involves neutrons and splitting uranium nuclei; the practical development of nuclear energy is primarily a nonnuclear, a chemical, question. In this respect it is no different from other thermodynamic technologies which depend for their success on the integrity of materials at elevated temperatures.

The investigation of materials, and of their properties at elevated temperatures and high levels of radiation, thus becomes perhaps the overriding problem in the development of high-performance nuclear reactors. Because of nuclear considerations, the spectrum of atomic species which is allowable in a chain reactor is rather different from that ordinarily encountered in engineering practice; such materials as Zr, Be, and even Hf, which were almost chemical rarities in prenuclear energy days, are commonplace now.

That the center of effort in nuclear energy should pass from the study of nuclear phenomena to the study of chemical phenomena is inherent in the nature of the fission process. No less than 35 different chemical elements are produced by uranium fission. But, as I have already mentioned, the technology has become heavily chemical (and metallurgical) particularly because it must rely, for its engineering realization, on a spectrum of atomic species different than that required for any other technology, and therefore little explored, and it must rely on them under conditions of heat and radiation unlike those encountered elsewhere. For example, the curious changes in metals which result from heavy particle bombardment turn out more and more to color the design choices available to reactor designers.

I think the understanding that nuclear technology is primarily a chemical technology has been a very happy and important turn of events which has been held back no little by the historically dominant role of physicists in nuclear energy. It is particularly important because, if nuclear energy's long-term objective of cheap fissionable material and power is to be attained, it will be necessary to treat the reactor and its associated chemical plants as a unit and to make design choices and design compromises not on the basis of what is needed to optimize the reactor alone or the chemical plant alone but what is required to optimize the whole system. The chemical properties of the reactor materials will certainly be involved in any such balance.

While chemical (and metallurgical) problems seem to be overriding now, largely because nuclear energy must seek its ends at temperatures which allow useful power (but even at their lowest make chemical reactions go fast), there are countless second-order problems in practically all the fields of science. For example, the embarrassing fact that the biological organism has no effective sensory apparatus for nuclear radiation makes it necessary to devise artificial sensory instruments, such as ionization chambers, either for radiation protection or for reactor control. Again, to choose at random a field of interest to electronic engineers, the development of servo systems for control of nuclear reactors, while unimportant as long as the reactors were incapable of rapid response—as in the case with large unenriched machines—becomes important as the power-density demand on the reactor increases. In general, the scientific synthesis which seems to be required for the effective prosecution of nuclear energy is perhaps broader in scope and in scale than that required for any other large-scale technology. The scope comes about mainly because intense penetrating radiation, being a phenomenon essentially unknown on our planet, must be investigated almost from scratch. The scale comes from military pressure, which makes it important to push these investigations with greatest speed. This combination gives rise to the large atomic-energy laboratories with their staffs of mathematicians, biologists, theoretical, nuclear, and solid physicists, metallurgists, and engineers.

The job of the nuclear engineer in all this will be to help in the precise formulation of objectives, to understand the essentials of the scientific synthesis which is basic to nuclear reactor development, and to reduce this synthesis to engineering practice. That the scientific synthesis, covering as it does mathematics, nuclear and solid-state physics, chemistry, metallurgy, and biology, is enormously broad, is only part of the difficulty which besets the nuclear engineer. After all, aeronautical engineering or radio engineering also require a considerable scientific synthesis. But I think the real difficulty in nuclear engineering is that reactors are so expensive, and, until our objectives are made thoroughly valid, the incentive to build them is relatively so weak that not enough reactors are built and running to establish a true nuclear-engineering tradition. The engineer is a builder: his art is the sum of separate experience gained in trying to make things work. An engineering science has great difficulty progressing vigorously if it almost never builds anything.

The dilemma in which nuclear engineering finds itself is, I believe, unique to it. I know of no other technology of comparable scale in which the number of different units produced is so small, and therefore the rate at which practical engineering data are accumulated is, relative to the effort spent, so low.[1]

As I have said, the paucity of reactors stems first from their expense, and second from the weakness of their motivation. Our motivation, because of the military situation, has recently become much better established than I would judge was the case at the time the Atomic Energy Act was first framed. There is still the question of expense. To overcome this block, to make reactor development a true *experimental* science, it has become customary to do what are called reactor experiments, i.e., small rather cheap, but complete, reactors which demonstrate the feasibility of certain kinds of reactor configuration. Of these, the Experimental Breeder and the Homogeneous Reactor Experiment are examples.

The United States is a rich country, and it has been possible for us to make engineering progress by building and by profiting from our mistakes. But in nuclear-energy development, even with the extensive use of reactor experiments, it is hardly likely that we shall ever have the experimental flexibility which is possible in an engineering art whose units are smaller and less expensive.

It will therefore be necessary for the nuclear engineer to subject his notions to extensive analysis before he commits them to hardware; and this analysis will, in many cases, be surprisingly like theoretical physics.

Nuclear engineering in its broadest sense is thus not very different from nuclear science; this overlap stems primarily from the

[1] Eugene Wigner has pointed out that the Mercury boiler development shares in this respect the same difficulties as reactor development.

newness of the field, from the fact that only five years separated the first-observed fission from the first high-powered chain reactor. As the technology progresses, the nuclear engineer must more and more encroach on the scientist's prerogatives; this encroachment I think the scientist must encourage. In this, the nuclear scientists—perhaps particularly the nuclear physicists—have often shirked their duty. It was they who devised the first chain reactors and who worked out the theory of the chain reactor. It is up to them either to codify their work in a straightforward and consistent manner so that the nuclear engineer can take over or to become nuclear engineers themselves. That to too great an extent they have done neither is a serious criticism which can hardly be excused by the fact that day-to-day pressure has been unrelenting since the war.

I have talked so far about nuclear engineering in its broadest terms as the conception, design, and synthesis of complete workable reactor systems, which by their success add to the motivation for atomic energy development. This, while being the central aspect of nuclear engineering, is of course the activity in which fewest nuclear engineers will participate. Most nuclear engineers will be component developers: they will develop heat exchangers, they will design liquid-metal pumps, they will compute critical masses, and they will build ion chambers. I suppose in this respect nuclear engineers will be much like other engineers. Yet even for the component developers there will be a necessity for acquiring knowledge on a broad scale precisely because, as yet, the knowledge which is required for specific tasks is nowhere systematized, and precisely because the engineering and the science are coming of age simultaneously.

That nuclear engineering, whether on component scale or systems scale, makes demands on the engineer possibly more stringent than any other technology seems clear. In a sense, nuclear-energy development puts our whole system of engineering education to test, and it is by no means certain that our engineering education system will meet this test adequately. For we nuclear engineers, like the original Manhattan Project scientists, have our necks way out. While we have demonstrated the validity of our occupation as far as production of nuclear explosives is concerned, we have not yet demonstrated its validity as far as long-term atomic power is concerned. We are gambling several hundred million dollars, not to speak of very large human effort, on the notion that nuclear energy will pay off—that it will really enter as a significant part of our life—that the promise in nuclear energy envisaged by the framers of the Atomic Energy Act can be fulfilled. It is certainly too early to insure success in this gamble; yet the stakes are enormous, and we nuclear engineers take as a primary article of faith that it is only lack of human ingenuity, not nature, which could possibly prevent us from achieving final success.

The JETEC Approach to the Tube-Reliability Problem*

JEROME R. STEEN†, FELLOW, IRE

Summary—**The need for reliability in electron-tube operation has increased several fold during the past few years and has far outdistanced corresponding quality-evaluation methods. Not only has this been evidenced by requirements in civilian applications, but also, and even more important, in military fields where several thousand tubes may be needed in a single piece of equipment. In an attempt to overcome the deficiency in present evaluation methods an entirely new approach is offered—that of analyzing and specifying tube-population mortality rates and tube-population characteristic depreciation rates. This concept shifts the emphasis from the individual to the group, and is more susceptible to scientific treatment and evaluation.**

FOR THE PAST several years the subject of reliable tubes, and that of reliable components of other kinds as well (such as, resistors, condensers, and the like) have received considerable attention. There have been numerous meetings, conferences, seminars, and even conventions devoted entirely to the problem of tube and component reliability in various classes of equipment, such as industrial and military as opposed to those intended for use in the home-entertainment field.

Although a great deal of progress has been made, much remains to be done; consequently, JETEC undertook a review of the situation. It is true that several manufacturers have been working for some time on various lines of "reliable" or "premium" tubes for military and commercial applications. What appears essential, however, is a more unified method of approach which, it is hoped, can be realized through more complete industry participation.

It might be noted here that while the subject of this paper is "The JETEC Approach to the Tube-Reliability Problem" the following discussion is the author's own interpretation of what has transpired in JETEC committee meetings and in discussions with JETEC committee personnel. Although JETEC discussions are still in the early stages, the way in which the tube-reliability problem may be examined has been pointed out.

It might be well to describe the organization and functioning of JETEC. The letters "JETEC" refer to the Joint Electron-Tube Engineering Council. JETEC is sponsored both by the National Electrical Manufacturers Association and the Radio-Television Manufacturers Association, and gets its policy guidance from two directors, one of whom is appointed by each organization. In addition, there are six council members, three of whom are appointed by NEMA and three by RTMA. These six elect a chairman from their group and operate as an autonomous body.

As JETEC standards material is formulated, the proposals are submitted to the parent organizations for approval, that is, they become subject to the routine standardization procedures either of NEMA or RTMA, or of both. Upon approval by either or both of the parent organizations this JETEC standards material becomes the official standards of such approving organizations. Formulation of these standards takes place either in line committees, of which there are seven, or in staff committees, of which there are four.

The Committee on Sampling Procedure is a staff committee since it operates across all activities, while, for example, the Committee on Receiving Tubes is a line committee since it is concerned directly with the standardization activities of a particular classification of tubes. Chairmen of the line and staff committees are staff members of JETEC. These eleven staff members, together with six council members, meet periodically to carry on the standardization activities of the tube-manufacturing industry.

In returning to the subject at hand I should like to say that the JETEC approach to this problem is a positive one in that the preparation of some specific recommendations is intended. A great deal of effort has been expended in some instances, and tubes with improved reliability have appeared on the market. Usually, however, the production is low and the cost high, and in many cases the user cannot afford to pay the price. Therefore, it is important that the JETEC approach be both positive and constructive.

According to Webster the word "reliable" is amplified as follows: "That may be relied upon; worthy of confidence; trustworthy." An example given was, "We can speak of a railroad train as reliable when it can be depended upon to arrive on time."

From the above, therefore, it appears that the concept of reliability may take one of several different forms. For example, a tube may be considered reliable if it operates for a long time in a simple noncritical circuit without giving trouble; if it operates for a long period of time with little or no change in essential characteristics; if large quantities operate for a certain lesser period with practically no early failures; or if it operates un-

* Decimal classification: R331.5. Original manuscript received by the Institute, February 21, 1951; revised manuscript received, April 24, 1951. Presented at the AIEE-IRE Conference on Electron Tubes for Computers (in collaboration with the panel on electron tubes of the Research and Development Board) at Atlantic City, N. J., on December 11, 1950.

† Director of Quality Control, Sylvania Electric Products Inc., 1740 Broadway, New York, N. Y.

der conditions of extreme vibration and/or shock without failure.

From the above, therefore, it can be seen that the word "reliable" covers so many different facets of tube operation that before any conclusion can be drawn as to whether a tube is reliable it must be determined on just what basis reliability is to be evaluated. Reliability for use in flip-flop circuits, for example, would be based on an entirely different premise than reliability resulting from a low vital-defect failure rate in a transoceanic cable installation or from a very high stability of some electrical characteristic essential for use in a piece of accurate measuring equipment or in maintaining an industrial control process.

Therefore, the JETEC approach to the tube-reliability problem is first to develop objective and realistic tube ratings based upon the application for which the tube is intended. These ratings will relate to one of the categories mentioned previously or to some new category not yet fully recognized. In most instances there will be a well-defined starting point based upon previous experience with the same or with a similar type of application. Occasionally, however, a brand-new application will appear, and in this case it may be necessary to go back to fundamentals.

After a tube type has been conceived objectively and rated realistically for the application in mind, the next step is the development of adequate specifications, both product and acceptance, by which the quality of the product may be determined and maintained. These adequate specifications must be based on actual tests and on life tests performed under conditions approximating as closely as possible the range of application requirements.

After adequate specifications have been developed for defining and evaluating, they should be supplemented and extended forward into production and assembly processes as well as into the realm of incoming parts and materials; they may extend even into vendors' plants. These systematic manufacturing processes should be established and maintained in such a manner that a maximum of information becomes available as supporting evidence of tube quality. In that event, acceptance specifications may be written with a mimum of complexity and in such a manner that when considered together with systematic product controls and realistic tube ratings they will give a very complete picture of tube quality.

Up to this time our comments have dealt almost entirely with generalities. To be useful, however, in connection with computers and other specialized applications it is important not only to discuss the background, the reasons, and the advantages of such a course of action but also to present, in a somewhat orderly manner, recommendations for carrying out such a program.

First, let us take the case of an application where something is known concerning the operating requirements. In this instance an existing tube type may be selected; if nothing quite suitable is available, appropriate design modifications can be made. It will be necessary in the very beginning to start keeping data systematically on all important characteristics as well as on those which may assume importance later. The important thing, however, is to make certain that any data which are kept are capable of being integrated into the over-all picture with a maximum of efficiency and a minimum of confusion. Let us consider now some of the general classes of characteristics for which information (adequate information) is required.

Perhaps the largest and most important group of items to be considered includes the electrical characteristics, such as plate current, transconductance, and the like, whose distributions are essentially normal. In these applications, where reliability is dependent upon uniformity and dispersion of electrical characteristics, reliability becomes a matter of maintaining and controlling these characteristics within a reasonable limit. This can be done most effectively by considering the tube type as a whole and by maintaining adequate controls during production, both upon the dispersion of the characteristics and upon their process averages.

As soon as data, indicating the process capabilities as defined in terms of product standard deviation (dispersion) and product process average shift, are available, it then becomes possible to correlate the relationship between equipment requirement on one hand and process capability on the other. As the development proceeds, changes may be made in one or the other, depending upon the many economic considerations involved.

The process standard deviation mentioned before is that which indicates the within-group variability of a characteristic. One of the best methods for determining this is by means of the simple control chart. The analysis of a considerable amount of data on commercial tube types indicates that limits of plus- and minus-one standard deviation (sigma) of the characteristic in question can be used as a starting point for limits of process average shift.

Let us assume, for example, that standard deviations of 300 micromhos and 0.5 milliamperes are representative of normal within-group manufacturing variations for type WXYZ, having bogey ratings of 5,000 micromhos and 7.5 milliamperes, respectively. If these were the two important electrical characteristics to be considered, the tube rating sheet might include the following:

Rated product average (bogey)	5,000 mhos	7.5ma
Maximum product standard deviation	300 mhos	0.5ma
Maximum product average shift	300 mhos	0.5ma.

Now let us turn to the matter of vital defects, always an important item whenever reliability of operation is paramount. Here, also, it is preferable to evaluate and to rate the tube type in terms of the product and process rather than in terms of the individual. In other words, the equipment designer should be more interested in over-all product mortality than in failure of an individual since definite design consideration can be given to the former. With this in mind, it seems logical to specify life in terms of maximum allowable failure rate, which might appear graphically, as shown in Fig. 1, or on the specification sheet as follows:

Maximum failure rate to 100 hours—1.0 per cent/100 hrs
Maximum failure rate 100 to 1000 hours —0.5 per cent/100 hrs
Maximum failure rate 1000 to 10,000 hours—0.25 per cent/100 hrs.

Once the life function has been evaluated on an engineering basis so that its expectancy may be specified with a reasonable degree of assurance, it should be possible to remove tube making from the status of an art to that of the realm of a science. Only when this has been accomplished will the equipment people be able to realize the full benefits from any particular design. For example, a recent military design specification states that in government equipment maximum operating conditions should not exceed 80 per cent of commercial ratings for normal government use and 50 per cent of commercial ratings for critical government use.

In addition to controlling inoperatives during life, it is often necessary to maintain control of essential electrical characteristics, also. These controls would include limits, both for depreciation or change of the average as well as for uniformity about the average determined in much the same manner as before. Here again an examination has been made of available data, and it has been noted, in many instances, that variations remain practically constant even up to several thousand hours. It is suggested, therefore, that initial standard deviation ratings be continued throughout life, or at least until additional data indicates the need for a revision.

As regards the depreciation of transconductance, it appears this follows some form of the exponential law. Therefore, it seems logical to specify the same in terms of the maximum allowable failure rate. This failure rate can be determined on the basis of known history or known equipment requirements, and might be indicated on the tube rating sheet graphically, as shown on Fig. 2, or in the following manner:

Maximum transconductance depreciation rate —0.5 per cent/100 hrs.

In addition to the above, it may be necessary to rate and control other characteristics for various kinds of reliable operation. Such characteristics could include shock, vibration, gas, grid emission, heater cathode leakage, capacitances, and the like. In addition, it may be necessary also to rate and control some of these characteristics during life.

In order to accomplish these objectives, a great many production controls will be required. These must be correlated with typical operating conditions and with the results of tests covering all kinds of operations concerned. It will be necessary to set up different types of tests for disclosing different kinds of defects. In certain instances, large quantities of tubes will be required to determine probabilities when low failure rates are specified. Special requirements will be imposed also by such items as high-voltage operation, intermittent operation, high-

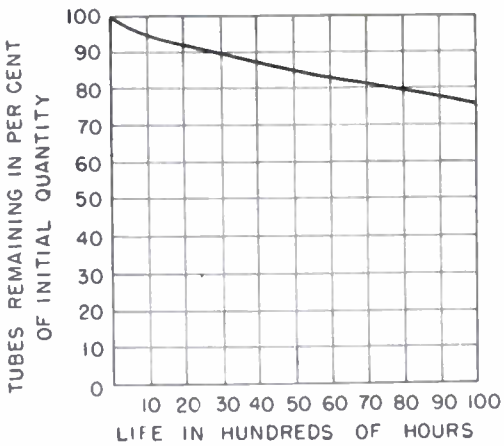

Fig. 1—Maximum tube mortality with life.

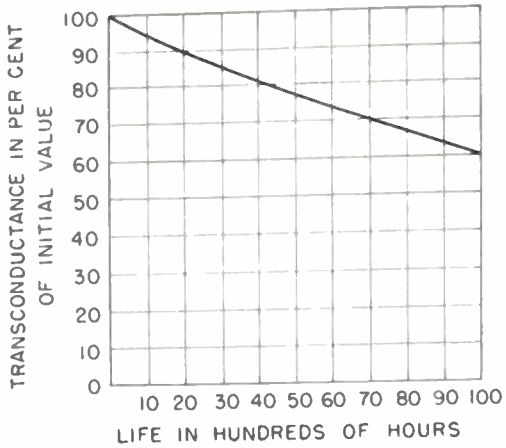

Fig. 2—Maximum transconductance depreciation with life.

temperature operation, and many others too numerous to mention.

In reviewing briefly, therefore, we have said that while much attention has been given the matter of tube reliability a great deal more work will be necessary in order to achieve the degree of reliability demanded. In order to accomplish this the situation should be improved by a more thorough analysis of process capabilities and end-product requirements, by much closer co-operation between the producer and the consumer, and by a better understanding, particularly by the user, of the relationship between a sample and the universe from which it came. The matter of tube-development cost also plays an important part since an outlay of $50,000 to $100,000 does not go far in the development of a new and reliable tube type.

Now that the economics of the situation have been modified to some extent in view of the needs of the military, the matter of providing more reliable tube types is receiving considerable attention. The JETEC Committee on Sampling Procedure has been asked by the Armed Services Committee on Sampling to co-operate in establishing acceptance specifications for certain reliable tube types. As explained previously, this work is going forward. Although many of these comments are the author's, they were prompted by association with members of the Sampling Committee, the JETEC Council, and the ASETC Sampling Committee.

Although it is my feeling that responsibility for more satisfactory tubes rests both with the equipment designer and with the tube maker, I believe that the latter should take the initiative. For who should be better equipped with know-how, facilities, personnel, and the like than the tube manufacturer himself? As the program progresses, therefore, it means that the tube manufacturer is assuming his full responsibility for co-operating with the equipment designer, for teaching and educating him, if necessary, for preparing realistic and objective tube ratings, and for making certain that adequate specifications are assembled and used

The Stability Problem in Feedback Amplifiers*

WILLIAM A. LYNCH,† ASSOCIATE MEMBER, IRE

This paper has been secured by the Tutorial Papers Subcommittee of the IRE Committee on Education as a part of a planned program of publication of valuable tutorial material. It is here presented with the approval of that Subcommittee.—*The Editor.*

Summary—**This paper is written for the engineer or student who has some general knowledge of feedback and who wishes to acquaint himself with the basic problem underlying the design of feedback amplifiers. The concept of complex frequency is introduced as a necessary background for the discussion of the stability problem. The criterion for stability is formulated in terms of fundmental restrictions on amplifier behavior at complex frequencies. From this a simplified criterion placing equivalent restrictions on the behavior at real frequencies leads directly to Nyquist's criterion. The role played by the theory of functions of a complex variable is indicated, but a knowledge of the theory is not required. A survey of certain important relations between gain and phase-shift in minimum phase-shift networks provides the preparation needed for the concluding discussion of the principles by which stability is effected.**

* Decimal classification: R363.23. Original manuscript received by the Institute, June 14, 1951.

† Polytechnic Institute of Brooklyn, Brooklyn, N. Y.

I. Introduction

THE BENEFITS in improved amplifier performance gained through the use of negative feedback are sufficiently well known to make it unnecessary to enumerate them here.[1] In order to exploit the full potentialities of feedback, however, one must be prepared to employ it to whatever extent the application demands. This difficulty is usually experienced, except in a few unimportant instances, because when feedback is applied to it, an amplifier tends at some frequency to satisfy the conditions that permit it to operate as a phase-shift oscillator. This tendency toward instability becomes more pronounced and more difficult to control as the feedback requirement is raised and as one attempts to extend feedback over more and more complicated structures.

Generally speaking, no simple expedient for the solution of the stability problem exists. It becomes necessary, therefore, to apply systematic design methods of a somewhat comprehensive nature that may, in certain problems, reflect upon the design choice of virtually every component. This overburden of design is one of the hidden costs of feedback.

Clearly an amplifier that is not reliably stable, as distinct from barely stable, is useless as such. Hence, the problem of assuring satisfactory stable operation is one of major

[1] See Harold S. Black, "Stabilized feedback amplifiers," *Bell Sys. Tech. Jour.*, vol. 13, pp. 1–18; January, 1934. Also, U. S. Patent No. 2,102,671. For textbook references, see F. E. Terman, "Radio Engineer's Handbook," McGraw-Hill Book Co., Inc., New York, N. Y.; 1943, and H. J. Reich, "Theory and Applications of Electron Tubes," McGraw-Hill Book Co., Inc., New York, N. Y.; 1944.

design importance. Without a working knowledge of the stability problem and of the design limitations it imposes, one is left to deal with a limited group of inherently stable structures, or be forced to resort to trial-and-error methods and the occasional fortuitous solutions arising therefrom.

It is the purpose of this paper to acquaint the reader with the stability problem and, in simple terms, to present the necessary theoretical background for the appreciation of its solution. The solution is offered only in principle, but with the principle understood, a variety of ways of implementing it can be found.

II. A Fundamental View of Amplifier Behavior

In the formulation of the stability problem and its solution, we shall be concerned first with the analysis of amplifier behavior and, later, with methods leading to the synthesis of amplifiers to meet certain prescribed requirements. Accordingly, we might set out by discussing a viewpoint which we shall take in dealing with amplifiers.

It is customary to specify the performance of an amplifier in terms of its steady-state response to a constant-amplitude sinusoidal driving force, or alternatively, in terms of its transient response to a generalized disturbance. Unless the amplifier configuration is fairly simple, it is an easy matter to become so involved in the difficulties of computing the responses as to lose contact with the physical concepts of the problem. Moreover, having at hand, let us say, the steady-state responses expressed by the gain and phase-shift characteristics in the frequency domain, it is not at all an easy matter to judge from them the performance to be expected in the time domain and vice versa. As a consequence, one is led to ask, "Is there not some more fundamental way of characterizing an amplifier so as to avoid dealing with the responses *per se*?" The answer is to be found in the generalization of certain well-known concepts associated with the behavior of pure reactance networks.

A network of pure reactances, when excited by a sinusoidal driving force, exhibits a familiar succession of resonances and anti-resonances as frequency is varied. At the resonance points the reactance vanishes whereas at the anti-resonance points it goes to infinity. These points along the frequency axis are called, respectively, *zeros* and *poles*. The reactance function is expressed mathematically as a quotient of two polynomials in frequency; a form known as a *rational* function. Each of the polynomials is factorable in terms of its roots, the zeros and poles of the function occurring respectively at the root values of the numerator and denominator polynomials. Inasmuch as a polynomial is determined uniquely, except for a constant factor, by its roots, it follows that a reactance function is specified uniquely by its finite zeros and poles together with a constant multiplier in the form of a scale factor.

The foregoing concept may be extended to the general case of networks that are dissipative. The voltage-transfer ratio, (i.e., the complex ratio of output to input voltage), of a linear lumped-constant amplifier network is similarly expressible in the form of a rational function. If we now substitute a new variable s for $j\omega$ and then factor the polynomials with respect to their roots in s, the resulting mathematical form is entirely analogous to that obtained for a reactance function. Examination of the function reveals that it vanishes for values of s corresponding to the roots of the numerator and grows infinite at the roots of the denominator. Hence, in the general case, we have zeros and poles in terms of s rather than frequency.

Before investigating the nature and significance of these general zeros and poles, let us turn our attention to the new variable s. We note that although it is analogous to frequency, it is found in general to be a complex number. It appears that if we are to avail ourselves of this promising analytical tool we must broaden our concept of frequency to include generalized values as well as the positive real values to which we have long been accustomed. The broader concept yields two far-reaching advantages; it affords notably greater freedom of analysis and, after facility with the notion has been acquired, it affords a penetrating insight into network behavior.

We need not regard this concept as a theoretical artifice; in fact it may be instructive to develop the viewpoint that complex frequencies have physical existence. Thus we may view them as being represented typically by sinusoids, the amplitudes of which either decay or grow with time. Then constant-amplitude sinusoids are seen as a subclass. It is also useful to think of complex frequency in terms of its quadrature components. The real component is descriptive of the damping which controls the rate of growth or decay, and the imaginary component corresponds to real frequency. Thus, if we write s as $\sigma+j\omega$, the two components, which together are descriptive of growing or decaying oscillations, combine to give us a single concept of generalized frequency, just as resistance and reactance are combined in a more familiar concept of impedance.

It follows that values of s can be plotted on a complex plane with σ measured along the real axis and ω measured along the imaginary axis.[2] We now have a frame of reference for depicting amplifier behavior in fundamental quantities—the zeros and poles. These can be arrayed on the s plane using small circles to mark the locations of the zeros and crosses to mark the poles. The laws governing physical network behavior limit the occurrence of poles and zeros to either one of two possible forms: they must be real or they must occur in conjugate complex pairs. Accordingly, any zero or pole lying to one side of the real axis must have a paired conjugate. Whereas the zeros and poles of the transfer ratio taken collectively specify the exact time response of an amplifier, the poles have special significance because their locations in the complex plane are associated with certain well-defined types of response. For example, conjugate imaginary poles represent a sinusoidal response of constant amplitude and poles on the real axis represent the limiting condition of responses that are aperiodic, i.e., they exhibit growth or decay, as the case may be, without oscillation.[3] Between these extremes are to be found the conjugate complex poles generally representative of exponentially modulated sinusoids.

It is important to distinguish carefully between the right and left halves of the s plane because of the significance attached to the locations of poles in the two half-planes. Poles in the right-hand half-plane give rise to responses that increase indefinitely with time. Because there is no expedient in linear network theory to check this kind of growth the structures so represented are said to be unstable or without physical realizability. Because of this, our interest will be focused principally upon the problem of seeing to it that the poles are located in the left-hand half-plane, the domain of stable structures.

An example or two will help to fix some of the ideas that have been developed regarding the representation of amplifier behavior by complex-plane patterns. A simple RC coupled amplifier is represented at high frequencies by an equivalent circuit consisting of the parallel combination of the load resistance R and the lumped equivalent shunt capacitance C. Writing the transfer ratio, we have

$$A = g_m R \frac{1}{1+j\omega RC}. \tag{1}$$

Equation (1) has been formulated using conventional steady-state analysis with frequency taken as $\omega/2\pi$. If we substitute s for $j\omega$, (1) becomes

$$A(s) = \frac{g_m}{C} \frac{1}{s+1/RC}. \tag{2}$$

We note that (2) is defined everywhere in the s plane except at the point $s=-1/RC$ where it exhibits a simple pole, which together with the scale factor, g_m/C, uniquely characterizes the amplifier. If we choose to combine the scale factor with the left-hand side of (2), the pole may be said to characterize an entire *family* of RC coupled amplifiers. We should note in passing that the contributions of zeros and poles from the component stages of a multistage amplifier are superposed to form the complex-plane pattern of the composite structure.

Let us take another example. Modifying the simple RC amplifier by adding an inductance in series with the load resistance, converts it to a form of video amplifier. Writing the transfer ratio directly in s, we have at high frequencies

$$A(s) = \frac{g_m}{C} \frac{s+R/L}{(s^2+sR/L+1/LC)}. \tag{3}$$

This function clearly shows a zero at $s=-R/L$ and the quadratic form of the denominator implies that there are two poles. Depending upon the damping, these may be real or conjugate complex.[4] The complex-plane pattern is most readily visualized if we imagine a physically artificial situation wherein L and C remain constant and R is varied. This has the advantage that when

[2] The positive half of the imaginary axis of the s plane will also be referred to as the real-frequency axis.

[3] A pole at the origin represents a constant response or pure dc.

[4] See M. F. Gardner and J. L. Barnes, "Transients in Linear Systems," Chapt. VI, John Wiley and Sons, Inc., New York, N. Y.; 1942.

conjugate poles exist they are restrained to a semicircular locus of radius $(1/LC)^{1/2}$ in the left half-plane. Beginning with the conjugate condition, as R is increased, the poles move along a circular path, finally coalescing into a double real pole as R takes the value $2(L/C)^{1/2}$, known as *critical damping*. Further increase in R causes the two poles to move apart on the negative real axis.

We have had a brief glimpse of the relation that exists between the pattern of zeros and poles in the complex plane and the responses in the time domain. We proceed to show that there exists a simple relation between the complex-plane pattern and the steady-state frequency responses. To illustrate it, let us make further use of the preceding example, that of the video amplifier. The transfer ratio may be rewritten, for our present purpose, in factored form, whence

$$A(s) = \frac{g_m}{C} \frac{(s - s_0)}{(s - s_1)(s - s_2)}, \qquad (4)$$

where s_0 is the zero and s_1 and s_2 are the poles of (3). Each of the factors of (4) represents a vector drawn from the zero or the pole, whichever it may be, to an arbitrary point s in the plane. The magnitude of each factor is given by the length of its vector.

The steady-state gain function $|A(j\omega)|$ is found by permitting the arbitrary point to range over only the positive imaginary axis. At each real frequency thereof, the magnitudes of the separate factors are the measured distances from the zeros and poles to the moving point $s=j\omega$ as it travels along the axis. The gain is evaluated by multiplying the scale factor into the ratio of the zero distance to the product of the two pole distances at each real frequency, as shown in Fig. 1. In general

$$|A(j\omega)| = M \frac{\text{Π Zero distances}}{\text{Π Pole distances}}, \qquad (5)$$

where M is the scale factor.

The steady-state phase function is found by combining the phase contributions of the separate factors. Each is the measured angle of inclination taken with reference to the real axis, as shown in Fig. 1. In general

$$\theta(j\omega) = \Sigma \text{ Zero angles} - \Sigma \text{ Pole angles}. \qquad (6)$$

When the locations of the zeros and poles of an amplifier transfer function are known, they can be plotted on graph paper and the steady-state frequency responses evaluated with the aid of a pair of dividers and a protractor. This method represents a considerable economy of effort compared with a straightforward analytical approach, particularly when the complex-plane pattern is complicated. Moreover, one can soon learn to judge by inspection the effect of the locations of the pattern elements upon the responses. For example, as the moving point $s=j\omega$ passes a closely adjacent pole in its journey along the real frequency axis, the gain can be expected to rise sharply and the phase angle to undergo a rapid change.

III. Nyquist's Criterion for Stability

The concept of generalized frequency can be put to immediate use in the formulation of a criterion for stability. In preparation for this it may be helpful to define somewhat more formally what we mean by stability. An amplifier is said to be stable if its response ultimately decays to zero after it has been subjected to a small impressed disturbance which itself dies out. Conversely, if the response increases until limited by nonlinearity, the amplifier is said to be unstable.

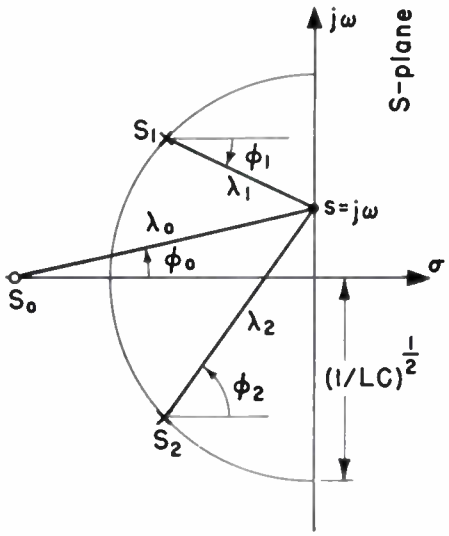

Fig. 1—A typical s-plane pattern consisting of a real zero and a pair of conjugate complex poles. At the point $s=j\omega$, $|A(j\omega)| = gm/C[\lambda_0/(\lambda_1\lambda_2)]$ and $|\theta(j\omega)| = \phi_0 - \phi_1 - \phi_2$.

The foregoing statements can be interpreted more specifically in terms of the possible transient responses of the amplifier. These have been shown previously to be characterized by the locations of the poles of the transfer ratio. If all poles lie within the left-hand half-plane, then all the free modes of response are positively damped and so vanish with time. The presence of a pole in the right-hand half-plane is indicative of a negatively-damped or runaway response.[5]

We can summarize these observations in the form of a theorem:

> *The necessary and sufficient condition that a linear amplifier be stable is that its transfer ratio shall have no poles in the right-hand half of the s-plane.*

Although the theorem affords a fundamental criterion for stability essential to the background of the problem, its utility is quite limited from a practical standpoint. Before it can be applied, all the poles of the transfer function under test must be located. This is likely to involve a long and difficult computation probably requiring that numerical values be assigned to all the amplifier constants. After the poles have been located, if it turns out that some lie in the right-half of the plane, the criterion offers virtually no guidance as to how to modify the structure so as to stabilize it.

What is needed is a simple test to decide at once the question of whether or not there are any poles in the right half-plane. Preferably, its utility should not rest solely upon a numerical process, and, additionally, it should provide a basis for establishing the trend to be taken in modifying the structure in the event instability is indicated.

If the test is indeed to be simple, it would appear that it must be capable of being applied at real rather than complex frequencies. Our quest then narrows down to finding a means by which, at real frequencies, we can examine a transfer function for possible poles lying within the right-half of the complex plane. The solution is to be found in the theory of functions of a complex variable.[6] The integral theory of Cauchy relates the behavior of certain functions of a complex variable, among which are rational functions, in the interior of a closed region to their behavior on the boundary of the region. For our purposes, we identify the right-hand half of the complex plane with the region under scrutiny, and the imaginary axis of the plane with the boundary.[7]

The details of the application of Cauchy's theory will be clarified if the procedure is outlined stepwise.

1. The function $f(s)$ to be examined is evaluated along the entire imaginary axis from $s=-j\infty$ to $s=+j\infty$, giving us $f(j\omega)$.

2. On its own complex plane, the imaginary part of $f(j\omega)$ is plotted against the real part. The resulting contour in the $f(s)$ plane, which we shall refer to as the *transfer locus*, is a polar plot of $f(j\omega)$. It is instructive to think of this step as the mapping of the imaginary axis of the s plane onto the $f(s)$ plane.

3. The transfer locus is inspected for encirclements of the origin. By encirclement we mean a complete revolution of a radius vector drawn from the origin to a moving point describing the curve.

4. The encirclements are interpreted as follows: As a point s moves upward along the imaginary axis of the s plane, a corresponding point on the transfer locus revolves about the origin once in a clockwise direction for each zero and once in a counterclockwise direction for each pole found in the right-hand half of the s plane, the zeros and poles being counted as many times as is indicated by their order.

By way of illustration, let us apply the theory to a known complex-plane pattern. Let us choose the simple configuration of Fig. 2(a), consisting of a first-order real zero in the right half, and a first-order real pole in the left half of the s plane, the two elements being equally spaced from the origin. Since the zero and pole distances are equal at all points along the imaginary axis, the magnitude of the function at real frequencies is unity. After evaluating the phase function $\theta(j\omega)$, using the method outlined in the preceding section, the transfer locus is found to take the form of a circle of unit radius concentric with the origin. As the point s moves upward along the imaginary axis of the s plane, the corresponding point on the $f(s)$ plane travels once around the unit circle in a clockwise direction starting at $\theta=0$, as

[5] The reader may question the fact that we have failed to take into account the possibility that poles may occur exactly on the boundary between the half-planes. The question is academic, for it requires a physically artificial precision of adjustment or a postulate of zero losses.

[6] For textbooks on the theory of functions of a complex variable, see E. J. Townsend, "Functions of a Complex Variable," Henry Holt and Co., New York, N. Y.; 1915; and J. Pierpont, "Functions of a Complex Variable," Ginn and Co., Boston, Mass.; 1914, particularly the chapters dealing with rational functions.

[7] So as to include the entire finite region of the right-hand half of the s plane, the boundary contour extends along the imaginary axis from $-j\omega$ to $+j\omega$, and is closed by a semicircle of infinite radius lying to the right of the axis. The transfer ratio of physical amplifiers vanishes when $|s|$ becomes infinite so that the only values of the transfer ratio on the boundary which differ from zero are those corresponding to the finite portion of the imaginary axis.

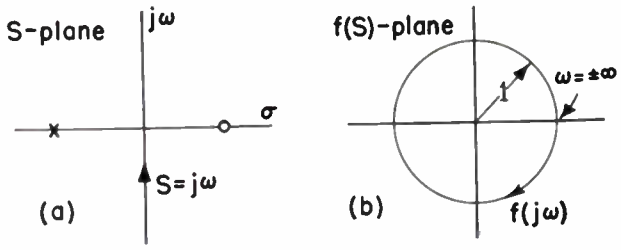

Fig. 2—An elementary *s*-plane pattern and its corresponding transfer locus.

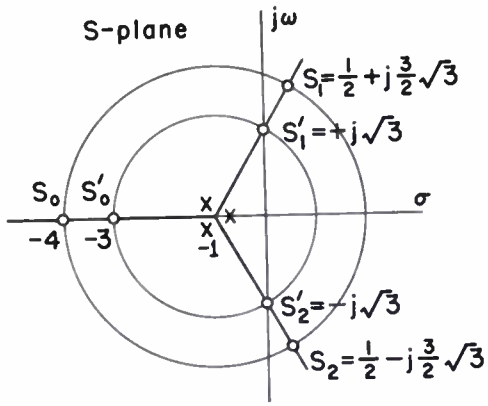

Fig. 3—The complex plane pattern of a three-stage feedback amplifier. The unprimed elements indicate a definitely unstable condition and the primed elements show the amplifier on the threshold of stability.

shown in Fig. 2(b). The reader can readily verify that the converse is true when zero and pole are interchanged.

There is one remaining difficulty to be resolved before we can formulate the simple test that we have been seeking. The stability of an amplifier structure depends upon the locations of only the poles of the transfer function. Therefore, counting encirclements of the origin gives us ambiguous information unless either we know that there are no zeros in the right half-plane, or we know precisely how many there are.

We can profitably explore this aspect of the problem by considering the general expression for the transfer ratio of a single-loop feedback amplifier. With the feedback applied, the transfer ratio takes the well-known form[8]

$$G(s) = \frac{A}{1 - A\beta}, \qquad (7)$$

where A is the transfer ratio of an ordinary nonfeedback amplifier and β is the transfer ratio of the feedback path by which a portion of the output of the A circuit is returned to the input. The sign in the denominator of (7) is a matter of convention. The feedback is negative, by definition, when $|1-A\beta| > 1$ and positive when $|1-A\beta| < 1$.

In examining the zeros and poles of (7), it is helpful to regard each of the quantities G, A, and β as being symbolic of a fractional rational function. From this viewpoint it is readily seen that the poles of $G(s)$ correspond to the poles of $A(s)$ or to the zeros of the function $(1-A\beta)$, which, for convenience, we shall designate as $F(s)$. It is assumed that the A circuit by itself is known to be stable. Therefore none of its poles can appear in the right half-plane. Accordingly, the only poles of $G(s)$ which can possibly be found in the right half-plane are those corresponding to the zeros of $F(s)$.

Inasmuch as the function $A(s)$ contributes nothing to the stability criterion, we may dispense with it and focus our attention exclusively upon $F(s)$, employing it as the critical function. In so doing, we are proposing to test the ultimate stability of $G(s)$ by examining $F(s)$ for possible *zeros* in the right half-plane.[9] First, however, we must verify the fact that there are no poles of $F(s)$ which could lead to ambiguity. This presents no difficulty since the poles of $F(s)$ are the points at which $A(s)$ or $\beta(s)$ becomes infinite. If the β circuit is a passive network, as is usually the case, it is unquestionably stable. If it is an active network, we must assume, as in the case of the A circuit, that it is known to be stable when considered by itself. We conclude then that for single-loop amplifiers, the only elements of the complex-plane pattern characterizing the function $F(s)$ that can possibly be found in the right half-plane, are zeros.

We are now prepared to formulate the criterion for stability for the single-loop case. Having constructed the transfer locus for the function $(1-A\beta)$, we observe the radius vector drawn from the origin to a point moving along the polar diagram. If the net angle swept out by the vector as it traverses the entire transfer locus is zero, the amplifier is stable; otherwise it is not. This is known as *Nyquist's criterion*, and the transfer locus is usually called the *Nyquist diagram*.[10]

An illustrative example will be helpful in crystallizing this concept. In Fig. 3, the unprimed elements in the complex-plane pattern characterize the function $(1-A\beta)$ of an unstable three-stage feedback amplifier. Let us form the Nyquist diagram by evaluating the gain and the phase shift along the imaginary axis. This process is simplified if we make the evaluation at positive frequencies only, thus obtaining one half of the diagram. The other half, contributed by the negative frequencies, is found by reflecting the first half in the real axis of the transfer plane.[11] The total result, shown by Curve I of Fig. 4, encircles the origin twice in a clockwise direction, confirming the known presence in the right half-plane of two zeros of $F(s)$.

Let us now reduce the amount of feedback so that the maximum value is brought down from 29 decibels, as indicated for Curve I, to 19 decibels, as shown for Curve II. This shrinks the entire Nyquist diagram proportionately so that now instead of encircling it the locus twice passes *through* the origin. Evidently, this new diagram of Curve II corresponds to a different *s*-plane pattern, as shown by the primed elements of Fig. 3, the essential feature of which is the pair of conjugate imaginary zeros. This situation, to which we alluded earlier, has no physical significance of any importance, but it does have considerable theoretical utility since we may think of it as representing the *threshold of stability*. We gain from this notion a useful measure of the theoretical limit of feedback from which we must withdraw to insure a margin of safety against instability. The nominal value of the function $|1-A\beta|$ in the useful frequency band which just places an amplifier on the threshold of stability, we shall call the *threshold feedback*.

Reducing the feedback safely below the threshold level, shrinks the Nyquist diagram still more. Now there is no longer any possibility of the origin being encircled and the indication is that the zeros of $(1-A\beta)$ have crossed well into the left-hand half-plane and that the amplifier is now stable by a definite margin.

It may appear to the reader, from the way we have chosen to develop the Nyquist criterion, that we have failed to make a good case for it. It may still appear to hinge upon the complex-plane pattern, which is the very dependence we have sought to avoid. A trivial alteration in the manner of plotting the transfer locus, however, provides the key to transforming the criterion into a powerful tool capable of being applied with great simplicity. Translating the origin one unit to the right converts the diagram from a plot of $(1-A\beta)$ to one of $(-A\beta)$. Revolving the entire plane through 180 degrees converts it to a plot of $A\beta$. This is a measurable quantity representing the transfer ratio of the A circuit and the β circuit arranged in cascade. Hence the quantity $A\beta$ represents the transmission once around the open (but properly terminated) feedback loop.

[8] See Terman, footnote reference 1.

[9] The reader should note that in dropping the function $A(s)$ we have avoided the ambiguity which might have arisen had there been any zeros of $A(s)$ in the right half-plane. It will become apparent later, after minimum phase-shift networks have been discussed, that this would have been an unlikely circumstance.

[10] H. Nyquist, "Regeneration theory," *Bell Sys. Tech. Jour.*, vol. 11, pp. 126–147; January, 1932. Also E. Peterson, J. G. Kreer and L. A. Ware, "Regeneration theory and experiment," *Bell Sys. Tech. Jour.*, vol. 13, pp. 680–700; October, 1934; and F. E. Bothwell, "Nyquist diagrams and the Routh-Hurwitz stability criterion," PROC. I.R.E., vol. 38, pp. 1345–1348; November, 1950.

[11] We may do this because the gain of a physical amplifier is an even function and the phase shift is an odd function of frequency, i.e., $|F(j\omega)| = |F(-j\omega)|$ and $\theta(j\omega) = -\theta(-j\omega)$. We have chosen to depict an amplifier capable of transmission at zero frequency so as to show the details of the Nyquist diagram more clearly. It is much more common, of course, for the transmission of an amplifier to vanish at zero frequency.

In principle then, we may obtain by measurement or calculation, the open-loop transfer ratio $A\beta(j\omega)$, draw the polar diagram, revolve the plane 180 degrees, and, finally, translate the origin back one unit to the left. The result is the Nyquist diagram for $(1-A\beta)$ obtained without prior knowledge of the location of the zeros and poles in the s plane. And so through a relatively simple measurement or computation made on a nonfeedback amplifier network, we are able to predict with certainty the stability status that will obtain upon closing the feedback loop. Actually, of course, we do not have to retrace the various steps indicated above for we may deal directly with the polar plot of $A\beta$. The chief difference is that we count revolutions of a radius vector about the point (1, 0) instead of the origin. It is customary to refer to the particular point about which encirclements are counted as the *critical point*. It is (1,0) for the $A\beta$ plane, $(-1,0)$ for the $(-A\beta)$ plane, and, of course, the origin for the F plane.

IV. Concerning Relations Between Gain and Phase Shift

It is not essential to display the Nyquist diagram exclusively in polar form. As a matter of fact it is generally more desirable, for design purposes, to plot the gain and phase shift as separate functions of frequency instead of combining them in a single curve. In drawing the separate response curves, distinct advantages result from plotting gain and frequency on logarithmic scales. This enables us to combine gain as well as phase-shift contributions by simple addition. Furthermore, a number of symmetries that otherwise would not exist appear when a logarithmic frequency scale is used.

In modifying the manner of plotting the Nyquist diagram, the stability criterion feature is retained and, in addition, we are in a somewhat better position to visualize whatever modifications may be needed to improve the stability situation. In terms of the separate frequency responses, the critical point (1,0) of the $A\beta$ plane is represented by the zero-decibel level of loop gain, and by the locus of 180 degrees of loop phase shift.[12] The frequencies at which these loci are crossed by the response curve are commonly called the *gain crossover* and the *phase crossover*. Threshold feedback is indicated when the gain and phase crossovers coincide.

Inasmuch as we shall be concerned in the design problem with the steady-state frequency responses, we shall need some tools with which to facilitate handling them. In particular, we need a means of obtaining the gain and phase-shift responses directly from given networks, and we need a method of constructing one response if the other is given. A re-examination of the method outlined earlier for obtaining the steady-state responses from the complex-plane pattern reveals that there is a second alternative. Instead of dealing with the entire pattern of zeros and poles, it may be more convenient

[12] The loop phase shift is regarded here as the phase shift resulting from the interstage networks and the β circuit. It does not include the phase reversals normally occurring in the vacuum tubes of the amplifier. If the feedback is nominally negative, it is implied that there is one net phase reversal around the feedback loop in the center of the band of useful frequencies.

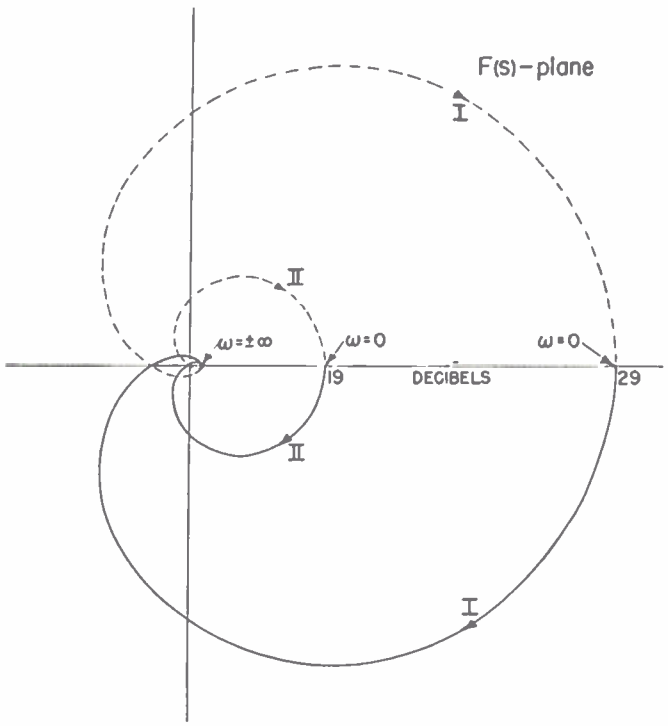

Fig. 4—The corresponding Nyquist diagrams of $(1-A\beta)$ for the patterns of Fig. 3.

to find the componental responses arising from individual zeros and poles. A composite response may then be found by adding component responses. It is frequently possible in simple networks to obtain the location of the zeros and poles without too much difficulty. This is particularly true when we are dealing with the low-frequency circuits of amplifiers. Accordingly, as an example of the principle, let us investigate the componental responses associated with individual real zeros and poles.

Let us begin with a negative real pole and use the equivalent circuit of an RC amplifier at high frequencies as a familiar example of this. Expressing the gain function in normalized form and in decibel units we have

$$\left.\frac{|A(j\omega)|}{g_m R}\right|_{db} = -10\log_{10}[1+(\omega RC)^2].$$

For the corresponding phase shift, we have

$$\theta(j\omega) = -\tan^{-1}(\omega RC).$$

These functions are shown as Curves I of Fig. 5. They are plotted against $\log(\omega/\omega_1)$, where $\omega_1 = 1/RC$ is the *characteristic frequency*. The curves are universal in that they may be applied at low frequencies merely by inverting the normalized frequency variable. It should be noted in passing that this inversion changes the sign of the phase angle.

The reader will observe that the gain response is characterized by two asymptotes, one having zero slope and the other a slope of 6 decibels per octave.[13] The asymptotes intersect at ω_1 and the gain curve lies 3 decibels below the intersection. At an octave above and below ω_1, the curve lies one decibel below its asymptote. Thus, three points define fairly well the transition from one asymptote to the other and this is observed to occupy about 4 octaves. The phase transition, on the other hand, is much broader, occupying roughly two decades (almost 7 octaves).

When the complex-plane element is a zero instead of a pole, Curves I of Fig. 5 still apply provided the decibel scale is read as *loss* instead of gain, and the signs of the phase response are interchanged. In physical amplifiers, real zeros of the transfer ratio are always accompanied by one or more real poles. Since real zeros and poles characterize networks combining resistance and one kind of reactance, we shall refer to the factors of the transfer ratio of such networks as *RX factors* and to the corresponding gain responses as *RX slopes*.

RX factors can often be combined advantageously to form a quotient which is a linear rational function. This form has considerable theoretical utility and we shall name it a *doublet* to denote that it is composed of a negative real zero-pole pair. Obviously there are two kinds of doublets, depending upon whether it is the zero or pole that lies nearer the origin.

The responses of a doublet are determined largely by the spacing of the characteristic frequencies of the component *RX* slopes. The spacing, expressed in octave units (i.e., $\log_2 f_1/f_2$), we shall call the *span* of the doublet. Fig. 7 (see page 1006) shows the gain and phase responses for doublets of various spans. The reader will observe that the responses are symmetrical about the geometric mean of the characteristic frequencies or, in other words, the mid-point

[13] An *octave* is an interval in which frequency changes in the ratio of two-to-one. On a logarithmic scale it represents a constant linear increment. A slope of 6 decibels per octave or 20 decibels per decade is frequently called *unit* slope.

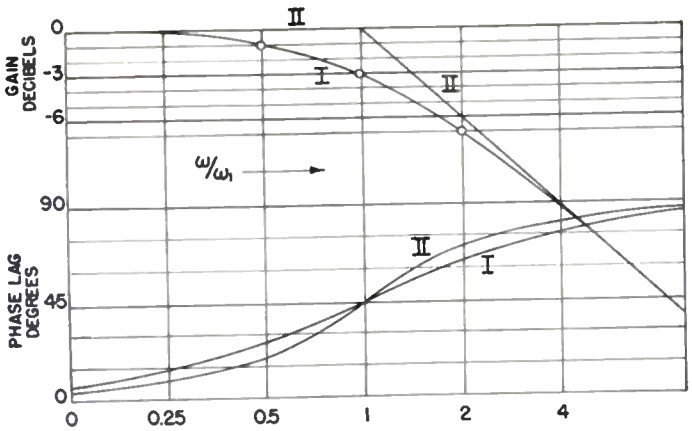

Fig. 5—The frequency characteristics of a simple *RX* factor are shown by Curves I. Curves II are described in a later section of the text.

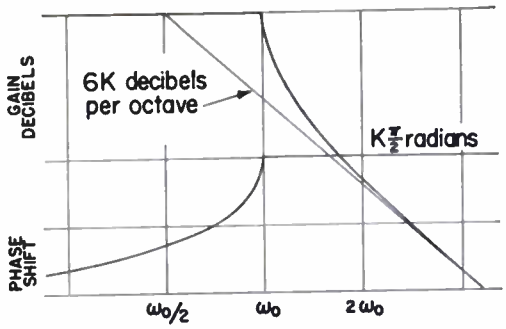

Fig. 6—The frequency responses of the constant-phase cutoff.

of the span. The change in the gain measured at the extremes of frequency is 6 decibels per octave of span. The sign of the phase angle and the direction of the change in gain characterize the doublet. To identify the two kinds we shall refer to them as *leading* or *lagging* doublets; a leading angle being associated with a zero-frequency gain level lying below the high-frequency level, and vice versa.

Occasionally, two simple doublets from different stages of an amplifier exactly coincide. When they are identical they produce zeros and poles of second order, whereas when they are of opposite kinds they annul one another. In higher order doublets both the change in the level of gain and the phase shift are multiplied by the order of the doublet as a scale factor. Instead of finding the phase response by taking the difference of the phase responses of the component *RX* factors, it can be computed directly from the formula

$$|\theta_h| = m \tan^{-1}\left[\frac{2^h(2^\rho - 1)}{(2^{2h}\cdot 2^\rho) + 1}\right],$$

where h refers to an increment in octave units taken above and below the characteristic frequencies, and where m is the order and ρ the span of the doublet. Both h and ρ may be fractional as well as integral and h may be positive or negative. The phase shift at each characteristic frequency is found by placing $h=0$, and the maximum phase shift, occurring at mid-span, is found by placing $h=-\rho/2$.

The problem of finding, let us say, the phase response from a given gain response is easily solved when the gain response is known to be related to a network characterized by negative real zeros and poles. However, when the given gain response is arbitrarily postulated or is possibly a measured response, it may be impossible to ascertain the actual phase response because any number of phase characteristics can correspond to a given gain response. Bode[14] has shown, however, that a definite relation does exist between the gain and phase responses in a restricted class of four-terminal networks known as *minimum phase-shift* networks. These networks, the properties of which are especially well suited to feedback amplifier applications, will be discussed in advance of defining the minimum phase-shift condition.

The determination of the minimum phase-shift response from a given gain response is accomplished conveniently using a method devised by Bode. In this method, the gain response curve is approximated by a series of straight-line segments which follow the major trends of the response. The straight-line approximation has the advantage of reducing the gain function to the sum of elementary straight-line characteristics similar to the *RX* slope. In fact, these elementary characteristics, which Bode calls *semi-infinite slopes*, are the same as the asymptotes of the *RX* slope, except that the inclined portion can be assigned any steepness whatever.

Once having resolved the given gain response into a series of semi-infinite slopes, the minimum phase shift is found for each component slope, and these are summed to obtain the composite response. The phase-shift response corresponding to a semi-infinite *unit* slope has been computed and tabulated.[15] For a semi-infinite slope of any other steepness, say one of k units of 6 decibels per octave, the phase response of the unit slope is simply multiplied by k. Curves II of Fig. 5 show the gain and phase-shift responses of a semi-infinite unit slope, and allow the reader to make a broad comparison between these and the *RX* responses.

A logical extension of the doublet concept leads to an analogous device consisting of two semi-infinite slopes of opposite kinds but of the same order of steepness, k. This device Bode calls a *finite line segment*.[16] Its gain response is that of the asymptotic framework of the doublet. Hence the slope is zero everywhere except between the characteristic frequencies where it is constant. The phase response of the finite line segment is similar in form to that of the doublet and, as in the case of the doublet, it is influenced by the span and by the amount of the change in the level of gain. It rises symmetrically to a maximum at mid-span, and for a given span and change of gain level, the maximum is higher and the rise steeper than that of a doublet. In the limit, if the gain of the finite line segment changes discontinuously, that is, if the span approaches zero and the steepness approaches infinity, the corresponding phase-shift response approaches an infinite peak.

The reader will observe that whereas the *RX* slope and the doublet are physically realizable in terms of very elementary networks, the semi-infinite slope and the finite line segment are not. The latter devices are therefore restricted largely to use in analysis, whereas the former, although limited in application, are valuable tools in both analysis and synthesis problems.

Up to this point, we have specified a gain response throughout the entire spectrum and we have outlined methods whereby the minimum phase-shift response could be determined from it. It is not necessary to be this restrictive. If we choose, we may specify the gain function within selected regions of the spectrum and the phase-shift function in the remainder of the spectrum. This notion leads to a valuable relation of which we shall make future use. We may specify the gain to be constant from zero to a frequency ω_0, and from ω_0 to infinity we may specify the phase shift to be constant. The gain and phase responses so postulated are shown in Fig. 6. The reader will observe that the gain function bears a resemblance to a semi-infinite slope, except that the flat portion extends one octave higher in frequency. This device, which is utilized in the design of the cutoff of the feedback loop, may be specified in terms of either the gain slope or the constant phase value—a slope of $6k$ decibels per octave corresponding to a constant phase shift of $k\pi/2$ radians. For want of a better

[14] H. W. Bode, "Network Analysis and Feedback Amplifier Design," D. Van Nostrand Co., Inc., New York, N. Y.; 1945.

[15] D. E. Thomas, "Tables of phase associated with a semi-infinite unit slope of attenuation," *Bell Sys. Tech. Jour.*, vol. 26, pp. 870–899; October, 1947. See also pp. 346, 347 of footnote reference 14.

[16] See Chapt. 15 of footnote reference 14.

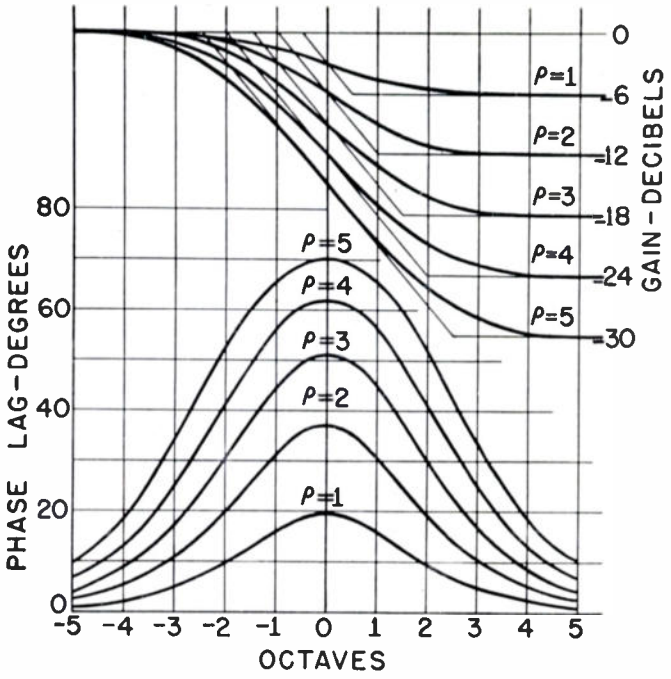

Fig. 7—Gain and phase-shift responses for simple doublets of from one to five octaves span.

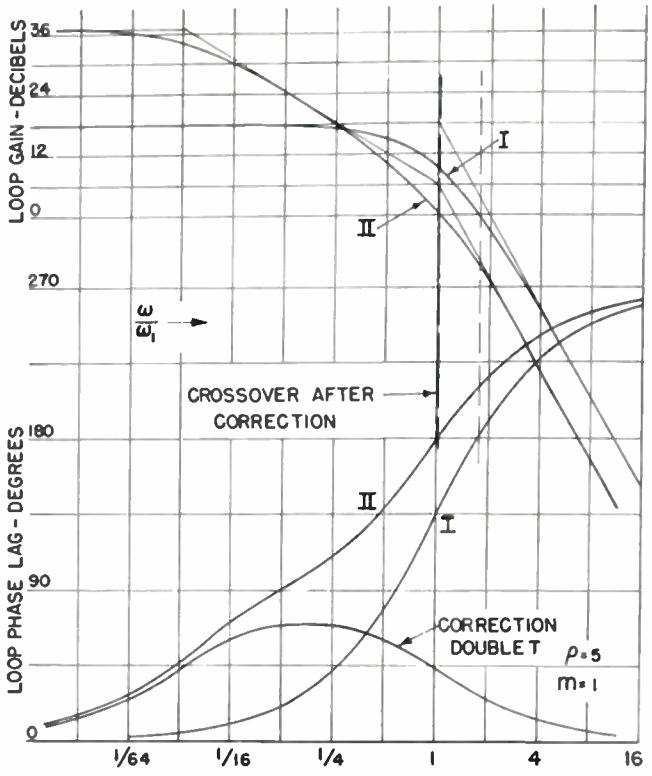

Fig. 8—Showing the effect of applying a simple five-octave correction doublet to the basic three-stage amplifier. Curves I show the frequency responses before correction and Curves II after correction.

name, we shall refer to it as a *constant-phase cutoff*.

Returning now to the minimum phase-shift condition, the most concise definition is one given in terms of the complex-plane pattern. The necessary and sufficient condition that a network be a minimum phase-shift structure is that its transfer ratio shall have zeros and poles only in the left-hand half-plane. Replacing a real zero or a pair of conjugate complex zeros of the transfer ratio by their negatives moves them from their original positions to image positions in the opposite half-plane without affecting the stability status of the structure. In particular, if we suppose them to be transferred from the left to the right half-plane, the change is equivalent to increasing the transfer ratio by the phase shift of an all-pass section.[17] For concreteness, let us suppose that a particular complex-plane pattern includes, among other elements, a negative real zero. Let us add a real zero in the right half-plane which is its negative. Let us also add a real pole which exactly coincides with and neutralizes the original zero. Thus we have effectively moved the original zero to an image position in the opposite half-plane. Since the distance from the zero to the real frequency axis is the same as before, this modification is assumed to leave the gain unchanged. This is indeed the case, for the elements we have added, namely the pole and zero in image relationship in the two halves of the plane, characterize an all-pass section which augments the phase shift without altering the gain.[18]

Ladder networks are always minimum phase-shift structures, but bridge configurations may be nonminimum phase. We shall summarize by saying that a network which does not include an all-pass section or a transmission line, in concealed or explicit form, will have the least phase shift that can possibly be realized physically from a given gain function.

V. Stabilization Principles

It is obvious that an unstable amplifier can be stabilized by utilizing any expedient that will, in effect, alter the course of the Nyquist diagram and so avoid enclosure of the critical point. In the earlier discussion of Nyquist's criterion, it was shown that stabilization was effected by reducing the feedback, thereby changing the scale of the diagram. This is, of course, a trivial solution. It turns out that it is necessary to alter only that part of the curve which lies near the critical point. What is needed, then, is not a change of scale but a change in the actual shape of the transfer locus. Further study of the problem leads to the conclusion that relocation can be confined to the frequencies lying generally outside the useful band of the amplifier. Hence the mechanics of stabilization has to do with the shaping of the cutoff transitions beginning immediately above and below the useful band.

Steering the transfer locus involves changing both the gain and the phase shift in the region where the detour is to be arranged. It is somewhat easier to see what has to be done if we think in terms of the steady-stage frequency functions. As a matter of fact, because of the gain-phase relations existing for minimum phase-shift structures, we can formulate the cutoff-shaping problem with respect to whichever one of the steady-state responses best suits our convenience.

In this concluding section, some of the basic principles of stabilization are demonstrated by way of illustrative examples. So as to provide the reader with a reasonable basis for comparison, several cutoff shaping designs are applied to the same basic amplifier. We have chosen for this purpose a cascade of three identical RC amplifier stages and a feedback circuit such that β can be regarded as a scalar constant. Although the examples relate directly to the high-frequency cutoff, the principles apply at low frequencies as well.

The prototype amplifier we have selected is assumed to tend at sufficiently high frequencies to a final asymptote which is a third-order RX slope. Because the final asymptote is controlled (at high frequencies) by the parasitic shunt capacitances, we assume that it is beyond design control.

In preparation for the examples to follow, let us familiarize ourselves with the frequency functions of the uncorrected amplifier. These are shown as Curves I in Fig. 8. The phase crossover occurs about 0.8 octave

[17] See Chapt. 11, pp. 236 and following, of footnote reference 14.

[18] See Fig. 2

above the characteristic frequency ω_1 (i.e., at $\sqrt{3}\omega_1$), and referring to the gain function, it is seen that 18 decibels of midband loop gain places the amplifier on the threshold of stability. In practice, the loop gain would have to be reduced to something like 10 decibels to assure a satisfactory margin against instability.

The feasibility of increasing the amount of threshold feedback is seen to hinge upon finding a way of reducing the gain in advance of the phase crossover without, at the same time, lowering the crossover frequency materially. We can draw upon the discussion of gain-phase relations for a simple device to serve this purpose—the doublet. Introducing a lagging-angle doublet in the region below ω_1 reduces the gain by an amount dependent upon the span and order. If strategically placed and properly proportioned its phase contribution largely subsides before the original phase crossover is reached. Except for the bandwidth it takes up, the doublet is well suited to the purpose, contributing as it does a permanent gain change and a temporary phase change, viewed frequency-wise.

The reader may agree that the doublet offers an attractive solution, but he may raise the question, "Where is the doublet to come from?" It is true that serious consideration must be given this practical question. Stabilization problems are solved by making advantageous use of the inherent response contributions of the various parts of a given amplifier plus those of auxiliary corrective networks added to enrich the assortment where necessary. It is beyond the scope of this paper to consider corrective circuitry,[19] and so it is assumed that, within reason, circuitry can be improvised to approximate the various cutoff transitions that are proposed.

So as to lead to a simple conclusion in our first example, let us choose, somewhat arbitrarily, a lagging doublet of first order having, say, a five-octave span. And let us locate it by stating that its zero shall coincide with the triple pole of the amplifier at $s=-1/RC$ and that its pole shall lie at $s=-1/32RC$. Curves II of Fig. 8 show the result, and we note that we have partially achieved our goal. Although the phase crossover has been translated downward so that it now lies just above ω_1, the midband loop gain can now be raised to some 37 decibels before the amplifier is placed on the threshold. The improvement in stability has been bought at the expense of loop bandwidth for it is observed that the loop gain is 3 decibels down some four octaves earlier than before.

Closer examination of the example reveals that the zero of the doublet annuls one of the poles of the amplifier, leaving effectively only a double pole at $s=-1/RC$. We may rightly conclude that the remaining pattern differs in no way from that of an amplifier made up of two stages of the original bandwidth and one stage of a bandwidth five octaves narrower. In this example, we have effectively introduced a correction doublet without having employed any additional circuitry, except possibly a shunt capacitor.

A similar result is obtained if we substitute for the simple doublet of the previous example, one of second order. Using the same argument, this case corresponds to specifying two narrow bandwidth stages and one stage of the original bandwidth. The amount of threshold feedback is the same regardless of which of these arrangements is used, but there are differences in loop bandwidth and in the external characteristics.[20] In this version, the loop gain is reduced at a more rapid rate than in the first example. This desirable feature is exactly offset, however, by the fact that the phase crossover occurs earlier. Of the two alternatives, the first is usually to be preferred.

In principle, any amount of feedback can be stabilized using the simple expedient just described. The narrow bandwidth stages presumably correspond to the useful bandwidth of the amplifier, it being generally desirable, except in special circumstances, to maintain the feedback constant throughout the useful band. The amount of feedback required then determines how far above the useful band the characteristic frequency of the broader bandwidth stages must lie. To go beyond the amount chosen in the examples costs about one octave for each additional 6 decibels. The reader can devise examples which will underline the high cost in excess bandwidth of this naïve solution to the stability problem. We wish to emphasize this point because the efficiency of a cutoff transition design is measured largely with respect to how economical it is of excess bandwidth.

In reviewing the foregoing examples, it becomes apparent that we have not hit upon the most effective use of the doublet. Examination of the phase response shows that if the phase of the correction doublet could be given a more steeply rising characteristic, the stability could be improved and perhaps the excess bandwidth reduced as well. A study of doublet phase characteristics reveals that optimum sharpness of phase rise exists when the span is two octaves or less. Let us experiment with this idea, trying a two-octave second-order doublet centered as before. It is found that this arrangement saves almost an octave of loop bandwidth and lowers the threshold loop gain only about 2 decibels as compared with the first example.

Inasmuch as this line of attack looks promising, let us pursue it further. Changing only the order of the correction doublet from second- to third-order, we obtain the results shown in Fig. 9, where the reader will observe that the threshold loop gain is now about 44 decibels and the -3 decibel point is only $3\frac{1}{2}$ octaves below where it originally resided. This is about as far as we can go without centering the doublet at a lower frequency and incurring an attendant loss in loop bandwidth.

It begins to be apparent that we are going to be severely limited in our cutoff designs as long as we restrict ourselves to correction networks characterized by real poles and zeros. It is not possible with such networks to simulate the rapid changes in gain necessary for the production of sharply rising phase responses. The semi-infinite slope and the finite line segment offer much greater versatility in this direction, but at the expense of the handicap that relatively complicated correction networks are then required.[21]

This is a good place to pause and take stock of the situation as we see it. There is evidently more to a good cutoff design than merely effecting stability. A more sophisticated view of the problem takes account of several additional design aims. Among these are provision for (1) including definite margins in gain and phase which are at the designer's disposal, (2) maintaining constant loop gain throughout the useful band, and (3) minimizing the excess bandwidth.

A cutoff transition design due to Bode[22] which cleverly satisfies these requirements, makes use of two elementary devices: the constant-phase cutoff and the semi-infinite slope. The constant-phase cutoff is the foundation of the design, furnishing a flat phase base above the useful band, the level of which can be set a prescribed amount below 180 degrees, thus providing a definite and constant phase margin. The flat portion of the gain response, extending one octave above that of a semi-infinite slope, assures constant loop gain clear to the edge of the useful band and the additional octave appreciably shortens the transition bandwidth. If it were possible to realize it physically, the constant-phase cutoff without modification would afford an ideal cutoff transition. Unfortunately, it is not possible to produce a cutoff slope which is less steep than the final asymptote, except in the range of frequencies below where the parasitic circuit elements take over control from the designer. For this reason, the design of the constant-phase cutoff can be carried only to the point where it intersects the final asymptote of the amplifier.

If the constant-phase cutoff is assumed to merge with the final asymptote at the point where the two loci intersect, the effect is the same as postulating a semi-infinite slope equal to the difference in slope of the two loci and beginning at the intersection frequency. From our knowledge of gain-phase relations, we can foresee the result of this modification. Added to the constant-phase base, we now have the phase contribution of a semi-infinite slope which destroys the constant-phase feature. The effect is indicated by the dashed curve of Fig. 10.

The solution which suggests itself intuitively is to employ a finite line segment for the purpose of introducing a phase contribution capable of cancelling the unwanted phase response at least within a limited frequency range. This is essentially the way Bode met the problem. What we have proposed amounts to designing a minor transition for joining the intersecting slopes. With proper care given to the design of this matching transition between the constant-phase cutoff slope and the final asymptote itself,

[19] See C. R. Burrows and A. Decino, "Ultra-short-wave multiplex," PROC. I.R.E., vol. 33, pp. 84–94; February, 1945; for an excellent discussion of cut-off-shaping problems. See also, V. Learned, "Corrective networks for feedback circuits," PROC. I.R.E., vol. 32, pp. 403–408; July, 1944.

[20] See L. B. Arguimbau, "Vacuum Tube Circuits," John A. Wiley and Sons, Inc. New York, N. Y.; 1948 pp. 384 and following.

[21] See footnote reference 19.

[22] See Chapt. 18, footnote reference 14.

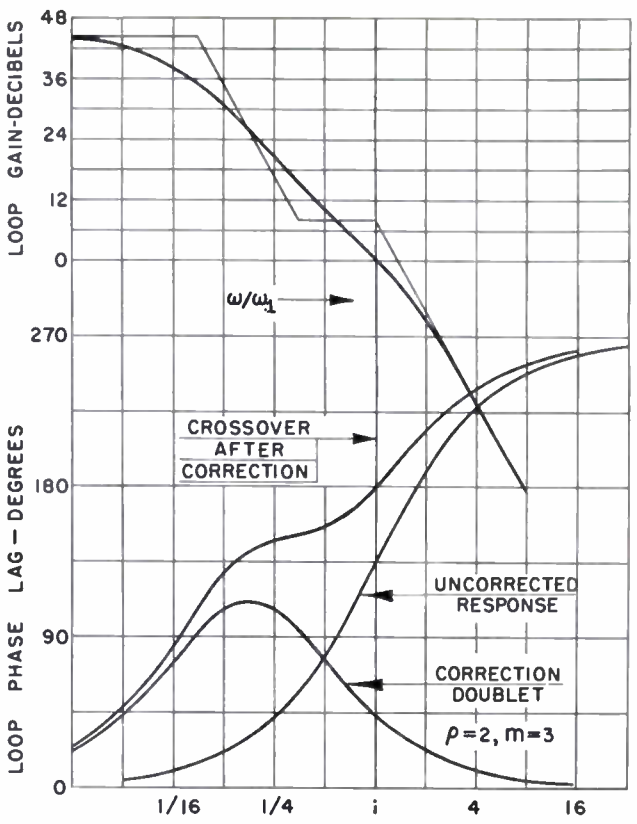

Fig. 9—Showing the improvement effected by using a two-octave third-order correction doublet.

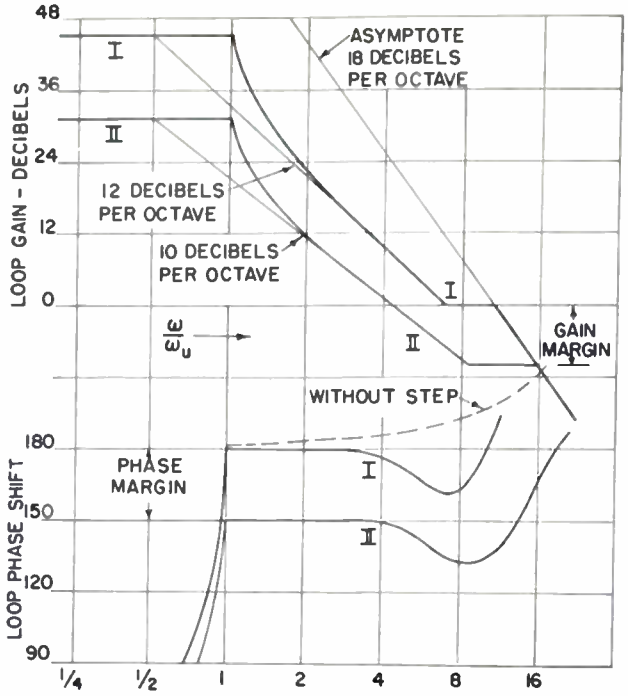

Fig. 10—The step transition cutoff shown without margins in Curves I and with margins of 10 decibels and 30 degrees in Curves II.

the resultant phase response can be made to rise to the desired flat-base level and remain there at least until the loop gain has been reduced to zero or below. In terms of the gain function, this minor transition takes the form of a horizontal step interposed between the intersecting slopes and proportioned in length to their steepness ratio.

Instead of viewing the step transition on the gain diagram as arising from the inclusion of a finite line segment, as first suggested, a more accurate description can be given in terms of two semi-infinite slopes, one of which is located at each of the terminal frequencies of the step. The one placed at the beginning of the step contributes a rising gain characteristic which just cancels the downward trend of the constant-phase cutoff slope. The second, introduced at the end, terminates the step and introduces the slope of the final asymptote. Thus the two semi-infinite slopes are not of the same steepness, in general. The phase response of a semi-infinite slope is closely linear at low frequencies on an arithmetic scale. Therefore the length of the step transition is so proportioned that the linear regions of the two phase characteristics cancel precisely within a range of frequencies just above the useful band, leaving the desired constant phase characteristic unchanged.

As an illustration of the Bode step-transition cutoff design, let us suppose that we have for instance, 45 decibels of open-loop gain incorporated in our basic three-stage amplifier. We shall omit gain and phase margins initially so as to place this example on a comparable basis with preceding ones. This amounts to designing the cutoff transition so as to place the amplifier virtually on the threshold of stability. The gain and phase responses are shown as Curves I in Fig. 10, and the reader will note that the bandwidth given over to the transition is much less than in previous examples in which a comparable amount of feedback was involved.

The details of the transition are of some interest. The reader will observe that the phase response rises sharply to 180 degrees at the top of the useful band, ω_u, and remains at that level until the gain begins to approach zero level. The phase then recedes so that the Nyquist diagram just barely avoids enclosure of the critical point. The corresponding gain response tends above ω_u to a slope of 12 decibels per octave, a limiting steepness corresponding to the limiting phase-shift, both of which are characteristic of threshold conditions. The flat portion of the phase response just above ω_u is the result of the phase cancellation previously described.

Gain and phase margins are easily incorporated into the design. To provide a phase margin of $y\pi$ radian, the constant-phase base is drawn at a level of $\pi(1-y)$ radians instead of π radians. The inclusion of the phase margin affects the slope of the gain response above ω_u reducing it from 12 to $12(1-y)$ decibels per octave. The gain margin is adjusted independently by locating the horizontal step transition x decibels below zero gain. Curves II of Fig. 10 show the changes involved in providing margins of $\pi/6$ radian and 10 decibels. As the figure shows, the inclusion of gain and phase margins reduces the amount of usable feedback considerably below the theoretical maximum obtainable under threshold conditions. Therefore in providing margins to allow for component tolerances and design uncertainties, we must insure as a primary requirement that the amplifier configuration is capable of an amount of threshold feedback sufficient to satisfy the requirement of usable feedback plus the amount needed to be given over to providing margins.

In conclusion, we should like to point out the final simplicity of Bode's solution to the stability problem. It has been formulated in terms of a prescribed gain response so that in making design calculations or in making measurements there is no need to consider the phase response at all, as long as we restrict ourselves to minimum phase-shift structures. The correction or *shaping* networks required to make the gain response conform with the prescribed cutoff design, may be incorporated in the A circuit or the β circuit, and may take any physically realizable form that the ingenuity of the designer can improvise. And if the minimum phase-shift condition is not violated, we are assured that the phase response will automatically conform also to the required pattern.

Analysis and Design of Self-Saturable Magnetic Amplifiers*

SIDNEY B. COHEN†, ASSOCIATE, IRE

Summary—**A self-saturable magnetic amplifier circuit element consisting of a reactor winding in series with a dry-disc rectifier, a resistive load and an ac voltage source is described and analyzed with respect to its operation and design. The results are in the form of curves from which optimum values of power and load resistance can be obtained as a function of the magnetic properties of the core material and the characteristics of the rectifier elements. These curves are used to obtain the best practical design values for complete amplifiers.**

Several magnetic amplifiers made up of a combination of the basic circuit elements are described in this paper with respect to their use as multistage amplifiers in servomechanisms and other applications.

Introduction

MAGNETIC amplifiers have been known for a relatively long time,[1] but only during recent years have great advances been made in their design and application. The development of new magnetic materials and dry-disc rectifiers in Sweden and Germany during World War II led to a renewed interest in this type of amplifier.

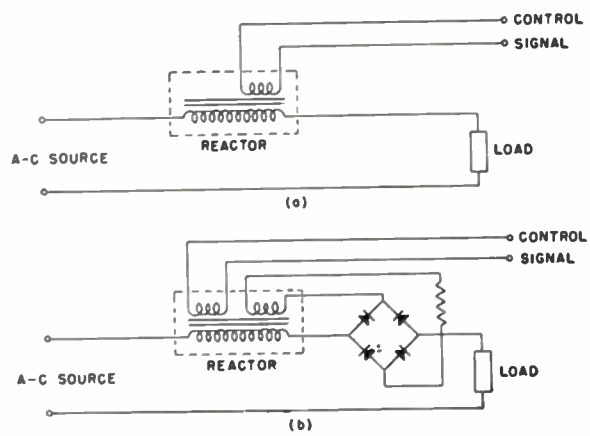

Fig. 1—A saturable-reactor control circuit.

The recent designs of magnetic amplifiers are an outgrowth of the simple type of saturable-reactor control in which a reactor is placed in series with a load across a voltage source (Fig. 1(a)). By controlling the degree of saturation of the reactor by means of a signal into an auxiliary winding, more or less voltage is applied to the load. Balanced and push-pull arrangements can be devised to produce an amplifier which is capable of supplying power to motors and other devices.[2–7]

These amplifiers are generally called *saturable transformers*. In order to obtain more gain, additional windings may be wound on the reactor, through which the output current flows after suitable rectification and phasing, as shown in Fig. 1(b). This essentially applies positive feedback and results in higher gains. In all cases, the amplification is accompanied by a time delay due to the fact that the signal current is applied to a control winding which is inductive.

Other combinations of components have led to circuits with different methods of applying feedback. One of these combinations is the self-saturating type of magnetic amplifier circuit which employs dry-disc rectifiers. Here the feedback is applied to obtain more gain, but without a proportional increase in the time constant. The performance of the self-saturating type of amplifier is superior to the saturable-transformer type, and many circuit combinations are possible by using the self-saturating principle.

Theory of Operation

The basic circuit element in the magnetic amplifier is analagous to the vacuum tube in an electronic amplifier. The element shown in Fig. 2 consists of a reactor the power winding of which is in series with a rectifier, a resistive load, and an ac voltage source. The analysis of the basic element will proceed in the following manner.

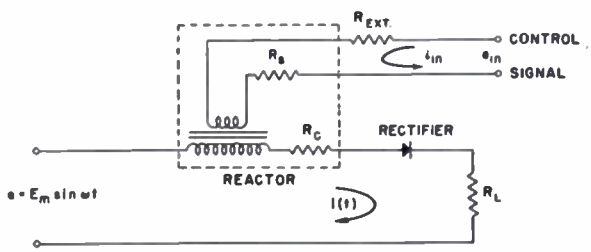

Fig. 2—Self-saturable control element.

* Decimal classification: 538×R363.23. Original manuscript received by the Institute, August 25, 1950; revised manuscript received, January 25, 1951. Presented, 1950 IRE National Convention, March 8, 1950, New York, N. Y.

† Sperry Gyroscope Company, Great Neck, L. I., N. Y.

[1] H. B. Rex, "Bibliography on transductors, magnetic amplifiers, etc.," *Instruments*, vol. XXI, pp. 332, 352–362; April, 1948.

[2] A. S. Fitzgerald, "Magnetic amplifier circuits—neutral type," *Jour. Frank. Inst.*, vol. CCXLIV, pp. 249–265; October, 1947.

[3] A. S. Fitzgerald, "Some notes on the design of magnetic amplifiers," *Jour. Frank. Inst.*, vol. CCXLIV, pp. 323–362; November, 1947.

[4] A. S. Fitzgerald, "Magnetic amplifier characteristics—neutral type," *Jour. Frank. Inst.*, vol. CCXLIV, pp. 415–439; December 1947.

[5] S. Hedstroem and L. F. Borg, "Transductor fundamentals," *Electronics*, vol. XXI, pp. 89–93; September, 1948.

[6] U. Lamm, "The Transductor," Stockholm, Sweden: Esselte Aktiebolag; 1943.

[7] "Magnetic Amplifiers," Vickers, Inc., Bul. No. VT-2000; 1948.

In Part I below, the circuit is analyzed assuming a reactor with constant inductance or permeability, i.e., it does not saturate. This introduces the concept of the extinction angle. Analyses are made for two cases: one in which the rectifiers are assumed to have a constant resistance, and the other in which they are assumed to have a constant voltage drop.

In Part II, the core is assumed to have a realistic characteristic in that the saturation of the core occurs at some value of the field intensity. This introduces the concept of a firing angle.

In Part III, the core is assumed to have the realistic characteristic as described in Part II. The extinction angle is determined as a function of the firing angle. Once this is accomplished, the current and power calculations can be made. All calculations are made for the two cases of the assumed rectifier characteristics.

I. Extinction Angle

The following assumptions are made in the initial analysis.

a. The reactor has a constant value of inductance L, i.e., the *B-H* curve is a straight line.

b. The hysteresis loops of the reactor are narrow. Therefore, the *B-H* curve can be considered as single-valued.

c. The sinusoidal supply voltage, $e = E_m \sin \omega t$, has negligible harmonics.

d. The control winding is electrically isolated from the power winding and merely utilized to apply ampere-turns to the core.

e. The rectifier has a high enough back-resistance to be considered as infinite in this circuit. Forward characteristics may be assumed to be either one of two approximations:

Case 1—Forward resistance a constant value, R_r.

Case 2—Forward voltage drop across the rectifier a constant, e_R.

These assumptions obviously neglect many practical properties of the magnetic amplifier. However, the following analysis aids in the understanding of the actual conditions to be described later.

Case 1—Rectifier forward characteristic is considered a constant resistance.

Considering the circuit of Fig. 2, the differential equation of this circuit is

$$L\frac{di}{dt} + R_T i = E_m \sin \omega t \tag{1}$$

where

$R_T = R_c + R_r + R_L$
R_L = load resistance
R_c = power-winding resistance
R_r = assumed rectifier resistance.

The solution to this equation is

$$i(t) = I_m\left[\sin(\omega t - \theta) + (\sin\theta)\epsilon^{-(R_T/\omega L)\omega t}\right],$$

$$= 0, \qquad \text{for } \theta_1 \leqq \omega t \leqq 2\pi \tag{2}$$

where

θ_1 = extinction angle

$$\theta = \tan^{-1}\frac{\omega L}{R_T}$$

$$I_m = \frac{E_m}{\sqrt{R_T^2 + (\omega L)^2}}$$

$$\sin\theta = \frac{\omega L}{\sqrt{R_T^2 + (\omega L)^2}}$$

$$\cos\theta = \frac{R_T}{\sqrt{R_T^2 + (\omega L)^2}}.$$

The current $i(t)$ is zero at $\omega t = 0$ and at $\omega t = \theta_1$, therefore,

$$\sin\left(\tan^{-1}\frac{\omega L}{R_T} - \theta_1\right) = \sin\left(\tan^{-1}\frac{\omega L}{R_T}\right)\epsilon^{-(R_T/\omega L)\theta_1}.$$

This equation is solved for θ_1, the extinction angle as a function of $\omega L/R_T$.

Where there is no inductance in the circuit, at $\omega L/R_T = 0$, the extinction angle is 180 degrees. As $\omega L/R_T$ increases, the extinction angle increases and may become 360 degrees. Fig. 3[8] is a plot of the current $i(t)$ for various values of $\omega L/R_T$. The effect of increasing the extinction angle can be seen on the over-all current wave form.

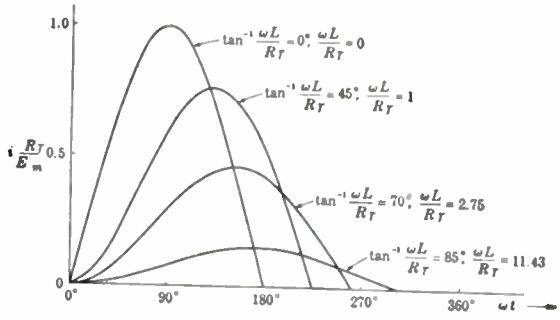

Fig. 3—Current wave forms as a function of $\omega L/R_T$.

Case 2—Rectifier forward characteristic considered as a constant voltage drop, an approximation which is very nearly true for gas rectifiers.

Considering this approximation and the circuit of Fig. 2, the differential equation of the circuit is now

$$L\frac{di}{dt} + R_T i + e_R = E_m \sin \omega t. \tag{3}$$

[8] From "Applied Electronics," edited by the Electrical Engineering Staff, Massachusetts Institute of Technology; The Technology Press, Cambridge, Mass., and John Wiley and Sons, Inc., New York, N. Y., eighth printing; 1946.

The solution is

$$i(t) = I_m\left[\sin(\theta - \omega t) + \frac{\sigma}{\cos\theta} - \left(\sin\theta + \frac{\sigma}{\cos\theta}\right)\epsilon^{-(R_T/\omega L)\omega t}\right] \quad (4)$$

where

$$\sigma = \frac{e_R}{E_m}.$$

θ_i, in this case, solved as a function of $\omega L/R_T$ and σ, is plotted in Fig. 4. If $\sigma = 0$ and R_T includes the rectifier resistance, R_r, the values of θ_i reduce to those which were obtained in Case 1. For other values of σ, the extinction angle varies from values less than 180 up to 360 degrees.

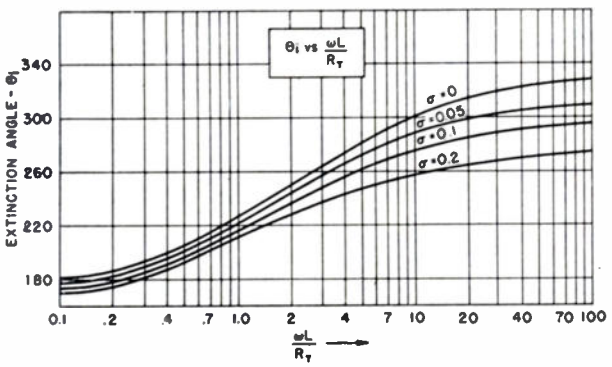

Fig. 4—Plot of the extinction angle versus $\omega L/R_T$ with σ as a parameter.

If L in the preceding analysis is the value at which the core becomes saturated, then the degree of saturation, i.e., the value of L at saturation, determines the extinction angle. In the higher-permeability materials, such as MuMetal, and 4750 Nickel-Iron, saturation is reached faster per unit change in control current, and ωL is very small. Since $\omega L/R_T$ is small, the extinction angle is almost 180 degrees. However, in Silicon-Iron saturation is not sharp, and in many cases the extinction angle may be as large as 240 to 290 degrees.

For the following analysis, an approximation is made to the actual *B-H* curve. This approximation is two straight lines. The first line approximates the initial or unsaturated part of the curve which has a slope or permeability of μ_0. The second line is the saturated part of the curve which has a permeability of μ_1. In many materials μ_1 is very much smaller than μ_0.

II. Firing Angle

Consider the circuit of Fig. 2 operating with a two-line *B-H* curve. The solution for the current would be the same as equation (2) for $L = L_0$, where L_0 is the value of the reactor inductance over that part of the *B-H* curve where $\mu = \mu_0$. However, when the current $i(t)$ reaches the value of i_0, the current at which saturation occurs (Fig. 5), it would begin to change rapidly, since now $L = L_1$ is much smaller than L_0. Because $L_1 \ll L_0$, the current $i(t)$ when $L = L_1$ is much larger than the current $i(t)$ when $L = L_0$. The current waveform is shown in Fig. 5. The current is seen to start out in a

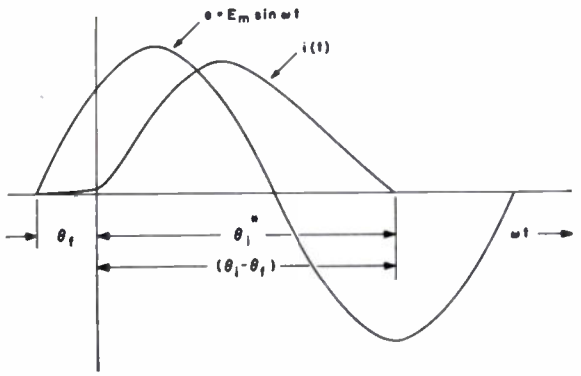

Fig. 5—Current waveforms as a function of the firing angle.

similar manner to the waveform shown in Fig. 3, but is very small in magnitude. At the point θ_f, where the current is equal to i_0, the magnitude of the current increases and continues until θ_i is reached.

It can be seen that the calculation of θ_i, in Part I, was made through that part of the curve where $L = L_1$. This is the case because once the point θ_f is reached, the iron operates in the region of μ_1. The contribution to the total current and power from the region $L = L_0$ can be neglected in most cases.

The point θ_f is called the firing angle and the region $(\theta_i - \theta_f)$ is called the "conduction period." It can be seen this action is analogous to that of thyratron operation.

To calculate the firing angle, refer to Fig. 2. As a first approximation, either *Case 1* or *2* may be assumed for the rectifiers eithout introducing any appreciable error. In either case, the current during the initial period in the region $L = L_0$ is very small, and the effective voltage drop of the rectifier and load is also small at these low values of the current.

Assuming *Case 2*,

$$L_0\frac{di}{dt} + R_T i = E_m \sin\omega t - \sigma E_m. \quad (5)$$

Neglecting the term $(R_T i + \sigma E_m)$ since $i(t)$ and σ are very small during the period 0 to θ_f,

$$di = \frac{E_m}{L_0}\sin\omega t dt.$$

The solution to this equation, obtained by integrating between the time limits of 0 and t, is

$$i(t) - i_i = \frac{E_m}{\omega L_0}(1 - \cos\omega t).$$

To obtain θ_f: when

$$\omega t = \theta_f,$$
$$i(t) = i_0,$$

and since

$$I_m = \frac{E_m}{\sqrt{R_T^2 + (\omega L_0)^2}} \approx \frac{E_m}{\omega L_0}, \quad \text{when} \quad R_T \ll \omega L_0,$$
$$i_0 - i_i = I_m(1 - \cos\theta_f)$$
$$\cos\theta_f = 1 - \frac{(i_0 - i_i)}{I_m},$$

where

i_0 = current at which B-H curve "breaks"

i_i = initial current in the core due to the signal in the control winding and

$$\frac{I_m}{i_0} \propto \frac{E_m}{E_0} \propto \frac{B_m}{B_0}$$

and E_0 has the same relationship to B_0 as E_m has to B_m. E_0 and i_0 are the co-ordinates of the break point in the B-H curve. Since I_m is proportional to E_m and usually, in the design of magnetic amplifiers, E_m/E_0 is made equal to a constant β,

$$\cos\theta_f = 1 - \frac{1}{\beta}\left(1 - \frac{i_i}{i_0}\right). \tag{6}$$

Fig. 6 is a plot of θ_f versus i_i/i_0 for different value of β, where i_i/i_0 is the control-current-to-i_0 ratio. From this

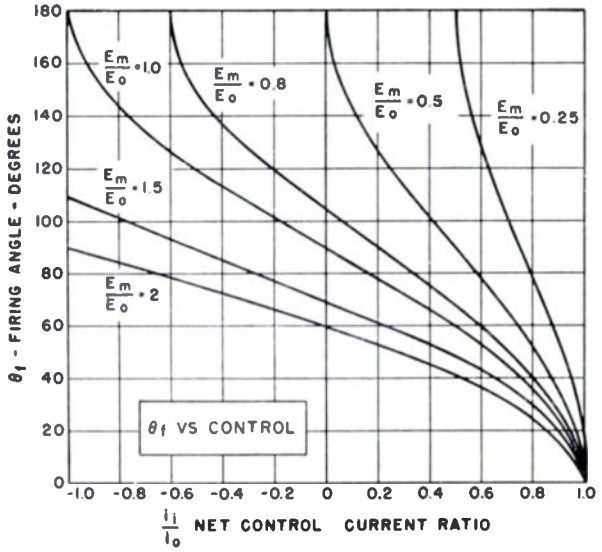

Fig. 6—Plot of firing angle versus control current with E_m/E_0 as a parameter.

family of curves, θ_f can be seen to increase as the control current goes negative. This means that the reactor *fires* later, and thus the conduction period $(\theta_i - \theta_f)$ is smaller. When the control current equals the value i_0, the firing angle is zero degrees and the reactor begins to conduct as soon as the supply voltage goes positive. Once the reactor fires, the control current loses control and the circuit constants then predominate.

The choice of E_m/E_0 depends upon two factors:

a. A value of E_m to be the largest possible so as to obtain more voltage and power across the load.

b. The firing angle θ_f to vary from 0 to 180 degrees with respect to control current so that the amplifier can be cut off.

From Fig. 6, it is obvious that cut-off can be reached with the smallest negative control signal at a value of $E_m/E_0 = 0.5$; the maximum voltage E_m occurs at $E_m/E_0 = 2$. However, for the most practical compromise, E_m/E_0 lies between the values of 0.8 and 1, permitting a variation of θ_f from 0 to 180 degrees, and also giving a reasonably high value of E_m.

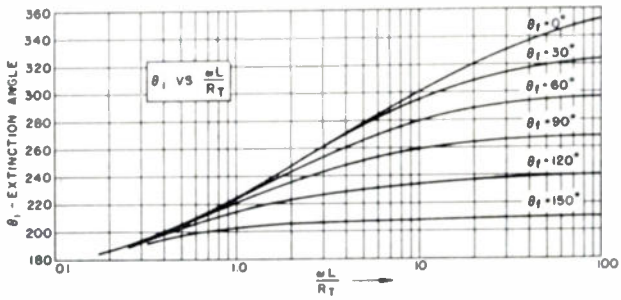

Fig. 7—Extinction angle as a function of $\omega L/R_T$ with θ_f as a parameter.

III. Calculation of Current and Power

The calculation of the dc and power from the basic circuit for various values of control current follows from the previous section with the inclusion of an additional assumption: that at every value of $\omega t = \theta_f$, the current $i(t)$ is zero. This assumption is quite reasonable from the previous discussion.

With this assumption all current and power calculations are made during the period $(\theta_i - \theta_f)$. The circuit equation becomes:

$$L\frac{di}{dt} + R_l i = E_m \sin(\omega t + \theta_f). \tag{7}$$

Here the assumption of *Case 1* is used for the rectifier. The solution of equation (7) is

$$i(t) = I_m\left\{\sin\theta\epsilon^{-(R_T/\omega L)\omega t}\left(\cos\theta_f - \frac{R_T}{\omega L}\sin\theta_f\right) + \sin\left[\omega t - (\theta - \theta_f)\right]\right\}. \tag{8}$$

If $\theta_f = 0$, the solution reduces to the one obtained in equation (2).

To solve for θ_i, the extinction angle, as a function of $\omega L/R_T$ and θ_f, set $i(t) = 0$ as before. The resulting equation is solved for θ_i^* as a function of $\omega L/R_T$ and θ_f, where $\theta_i^* = \theta_i - \theta_f$, the conduction period,

The results are shown in Fig. 7. Note that the values of θ_i plotted are referred to the zero-voltage point of the applied voltage, $E_m \sin \omega t$. For small values of $\omega L/R_T$, the value of θ_i is not changed much by variations of θ_f. However, the change becomes appreciable when con-

sidering the large values of $\omega L/R_T$ used in some applications. Note that the maximum value of θ_i is different for each value of θ_f.

The dc through the circuit as a function of $\omega L/R_T$ and θ_f,

$$I_{DC} = \frac{E_m}{2\pi R_T}\left[\cos\theta_f - \cos\theta_i\right]. \tag{9}$$

The family of transfer curves obtained from this equation by plotting $2\pi I_{DC}\, R_T/E_0$ as a function of i_i/i_0, with β as a parameter and $\omega L/R_T = 0$, is shown in Fig. 8. A similar family of transfer curves for $\omega L/R_T = 2.4$ is also shown in Fig. 8. Note the reduction in sensitivity for this latter set of curves.

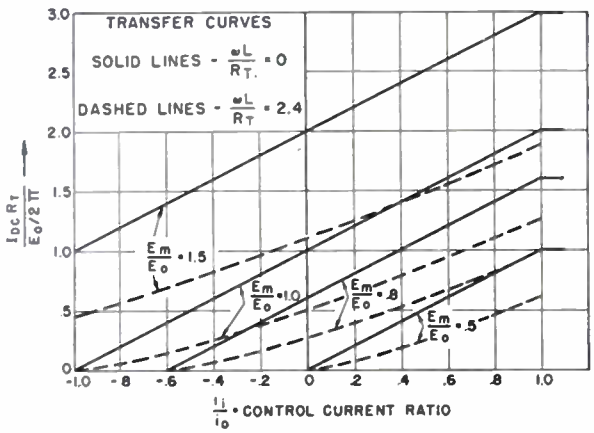

Fig. 8—A plot of the dc output voltage across the load of a basic circuit element versus control current with E_m as a parameter. The solid lines are plotted for $\omega L/R_T = 0$ and dashed linesf or $\omega L/R_T = 2.4$.

The dc power into the load resistance is

$$P_L = \left(\frac{E_m^2}{4\pi^2\omega L}\right)\cdot\left(\frac{R_L}{R_T}\right)\cdot\left(\frac{\omega L}{R_T}\right)\cdot(\cos\theta_f - \cos\theta_i)^2$$

$$= \left(\frac{E_m^2}{4\pi^2\omega L}\right)(\xi) \tag{10}$$

where

$$\xi = \left(\frac{R_L}{R_T}\right)\cdot\left(\frac{\omega L}{R_T}\right)\cdot(\cos\theta_f - \cos\theta_i)^2. \tag{10a}$$

ξ is called the "power coefficient."

The series of graphs, Figs. 9, 10, and 11 show the relationship between ξ and the parameters $\omega L/R_T$, λ, *and* θ_f.

λ is defined as follows:

$$\lambda = \frac{R_r}{R_{OPT}}$$

where R_{OPT} is that value of R_T at which maximum power is delivered.

If λ is equal to zero, i.e., the rectifier assumed to have no power loss, then the expression for ξ is

$$\xi = \left(\frac{\omega L}{R_T}\right)\cdot(\cos\theta_f - \cos\theta_i)^2. \tag{10b}$$

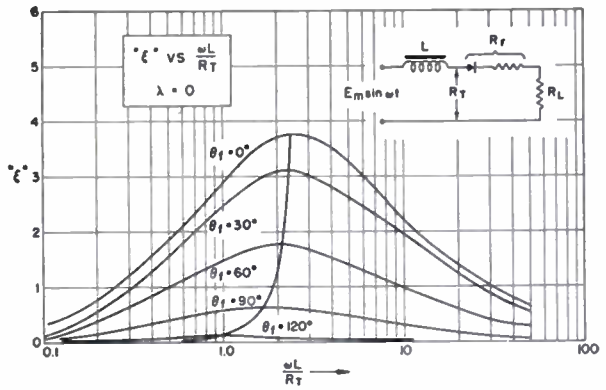

Fig. 9—Power coefficient versus $\omega L/R_T$ with θ_f as a parameter and $\lambda = 0$.

Fig. 9 is a plot of ξ versus $\omega L/R_T$ for equation (10b), with θ_f as the parameter and $\lambda = 0$. (Note that Fig. 7 is used to obtain θ_i as a function of $\omega L/R_T$ and θ_f.) The value at which ξ is a maximum for maximum power delivered to R_L is $\omega L/R_{OPT}$.

The interesting point in this set of curves is the fact that for lower control signals, which means higher values of θ_f, the optimum value of $\omega L/R_T$ decreases. Since all of the curves have been drawn from some finite value of

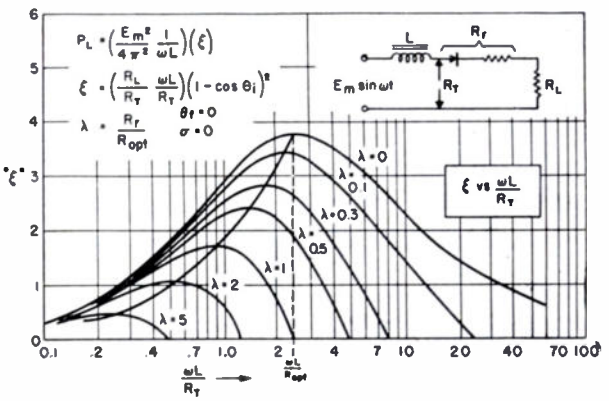

Fig. 10—Power coefficient versus $\omega L/R_T$ with λ as a parameter and $\theta_f = 0$.

ωL, R_{OPT} then increases as θ_f increases. The optimum load varies at different signal levels. This variation is further increased by the fact that the rectifier resistance in the forward direction is not really constant but increases with a reduction in current through it.

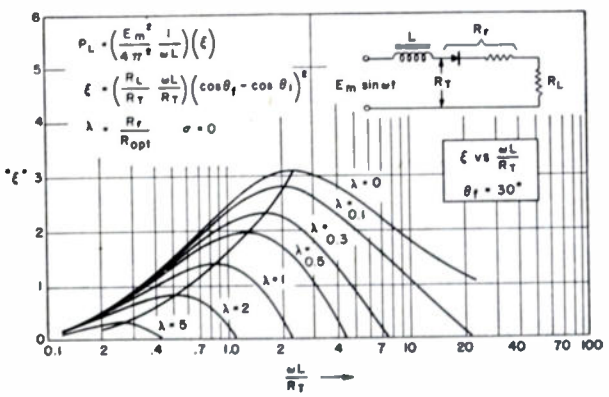

Fig. 11—Power coefficient versus $\omega L/R_T$ with λ as a parameter and $\theta_f = 30°$.

To obtain the power coefficient curves for finite values of λ, i.e., when the rectifier is assumed to have finite power losses, let $y = R_T/R_{OPT}$. Since $R_T = R_r + R_L$,

$$\frac{R_L}{R_T} = \left(1 - \frac{\lambda}{y}\right). \tag{11}$$

For a value of $\theta_f = 0$, $R_{OPT} = \omega L/2.4$ (Fig. 9), then

$$\frac{\omega L}{R_T} = \frac{2.4}{y}. \tag{12}$$

In order to complete the family of curves of $\omega L/R_T$ versus ξ for different values of λ, equation (12) can be used to obtain the values of y for the different values of $\omega L/R_T$ and then substituted in equation (11) to obtain R_L/R_T. The value of ξ can then be obtained as a function of $\omega L/R_T$ with different parametric values of λ by using equation (10a). This has been done in Fig. 10.

The same procedure outlined above can be used to obtain a different set of curves for any value of θ_f. Fig. 11 is plotted for a value of $\theta_f = 30$ degrees.

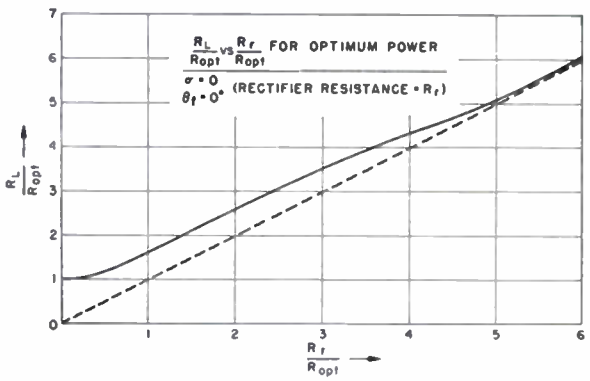

Fig. 12—A relationship between R_L and R_r is obtained by a plot of R_L/R_{OPT} versus R_r/R_{OPT} for optimum power into R_L with $\sigma = 0$ and $\theta_f = 0$.

Examination of Fig. 10 reveals several interesting features:

a. The maximum power for $\omega L/R_T = 2.4$ is obtained at $\lambda = 0$ when $\theta_f = 0$. The maximum power point decreases as λ is increased.

b. Even for small values of λ, i.e., for small values of R_r, the reduction in power becomes appreciable. It is, then, advantageous to have low power-loss rectifiers.

c. ωL at saturation should be small in order to obtain good power transfer. The graphs for other values of θ_f are similar in nature and show the relative decrease in power with increasing firing angle.

As ωL becomes smaller, approaching an ideal type of magnetic material, the problem of matching becomes one of standard circuit analysis in which the internal impedance of the source is the sum of the rectifier impedance and the winding resistance, while the external impedance is the load impedance. Thus as ωL becomes small, R_L should approach R_r for optimum power-transfer. However, if ωL is not negligible, the relationship between R_L and R_r is more complex. From Fig. 10, a relationship can be obtained between R_L and R_r. This relationship is shown in Fig. 12. Here R_L/R_{OPT} is plotted as a function of R_r/R_{OPT}. As R_r/R_{OPT} becomes large, then the circuit analysis mentioned above, in which $R_L = R_r$ for optimum power, is valid. However, if R_r/R_{OPT} is small, then the relationship between R_L and R_r is not linear.

The instantaneous current as a function of $\omega L/R_T$ and θ_f for the assumption that the rectifier is an equivalent constant voltage is

$$i(t) = \left\{ I_m \left[\sin(\theta - \theta_f) + \frac{\sigma}{\cos\theta} \right] \epsilon^{-(R_T/\omega L)\omega t} - \frac{\sigma}{\cos\theta} + \sin(\omega t - \theta + \theta_f) \right\}. \tag{13}$$

Note that ωt is measured as shown in Fig. 5. If $\theta_f = 0$, then the same result is obtained as in equation (4).

A set of power-coefficient curves is obtained similar to that for Fig. 7, except for the fact that the parameter σ would replace λ. Both σ and λ are power-loss coefficients of the rectifier, but based on different assumptions. The curves for θ_i versus $\omega L/R_T$ with σ as the parameter and $\theta_f = 0$, are shown in Fig. 9. For other values of θ_f, a new set of data and curves must be obtained.

The dc power into R_L is expressed by

$$P_L = \frac{E_m^2}{4\pi^2 \omega L}\left(\frac{R_L}{R_T}\right)\left(\frac{\omega L}{R_T}\right)(1 - \cos\theta_i - \sigma\theta_i)^2 = \frac{E_m^2}{4\pi^2\omega L}(\xi') \tag{14}$$

where

$$\xi' = \left(\frac{R_L}{R_T}\right)\left(\frac{\omega_L}{R_T}\right)(1 - \cos\theta_i - \sigma\theta_i)^2.$$

ξ' is a second "power coefficient."

Fig. 13 includes the curves and data obtained from equation (14). Note that for $\sigma = 0$ and $\lambda = 0$ in Figs. 10

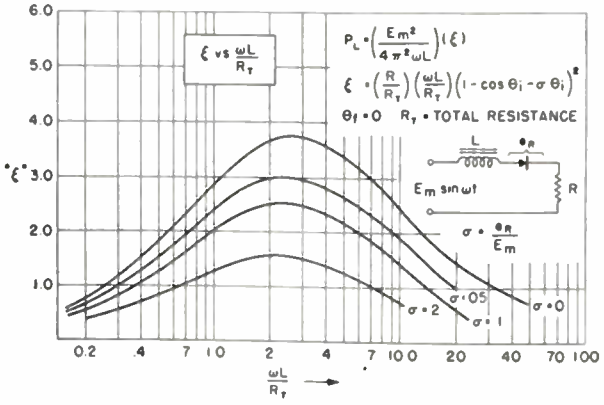

Fig. 13—Power coefficient versus $\omega L/R_T$ with σ as a parameter and $\theta_f = 0$.

and 13 respectively, the curves are the same. In Fig. 13, the optimum load does not seem to vary much with σ. However, even for small values of σ, as was the case with small values of λ, the power available at the load decreases rapidly.

These curves introduced in Parts I, II, and III do not, by any means, represent analytic expressions for output versus input power, as would be the ideal goal. The curves were obtained by solving differential equations empirically, and, as such, represent "end-point" design values, and serve to give a qualitative picture of the operation and performance of the amplifiers.

IV. Gain and Time Response Considerations

The gain of a magnetic amplifier can be expressed in various ways. For the purposes of many applications, the gain expressed as a power ratio is, therefore, the desirable method.

Since $i \propto H$ and $\theta_f = f(i_i)$, it can be seen that the output of the amplifier is a function of the ampere-turns in the control winding. The gain of a particular amplifier depends basically upon the permeability of the core, in that the greatest change in B, the flux density ($\mu = B/H$), is desired for the smallest change in the control ampere-turns. With high values of μ, θ_f is reached faster per unit change in control current.

It is possible to obtain tremendous gains in an amplifier by putting a large number of turns to low resistance in the control winding in order to obtain large values of ampere-turns input without increasing the power dissipation.

The gain can be increased without a theoretical limit except for the fact that *time response* considerations must be taken into account. It is also limited by practical considerations of the core dimensions. The time constant of a magnetic amplifier has many definitions. The most commonly used one is that which defines the time constant as the time for the output to reach 63 per cent of the final value when a unit step voltage is applied to the input.

Referring to the basic circuit, there are two sources for time delay which affect the over-all time constant of the amplifier. One source is the control winding. Since the control winding is inductive, there will be the time delay normally associated with such an R-L circuit.

If, as postulated previously, the number of turns of the control winding were increased to obtain more ampere-turns, the time constant would also increase proportionally. If the total time delay in the amplifier were produced by the control winding, then the *figure of merit A* (also called *performance factor*, A = gain/time constant) would be a constant. It is evident also that by adding external resistance to the control winding, the time response is improved, but the gain is decreased, thus keeping the figure of merit a constant.

The second source of time delay is in the core and main circuit itself.[9,10] The time delays due to the output circuit of the magnetic amplifier have not been studied here in great detail but have been measured experimentally and found to be a function of the various parameters already discussed—the capacitance across the load, E_m, i_i/i_0, and the type of circuit used.

These time delays have been measured to be approximately 0.001 to 0.0035 second (with a 400-cycle carrier), depending upon the conditions of operation. Thus, if for a particular amplifier, a curve of A as a function of the gain or time constant was plotted by varying the control-circuit resistance, a curve as shown in Fig. 14

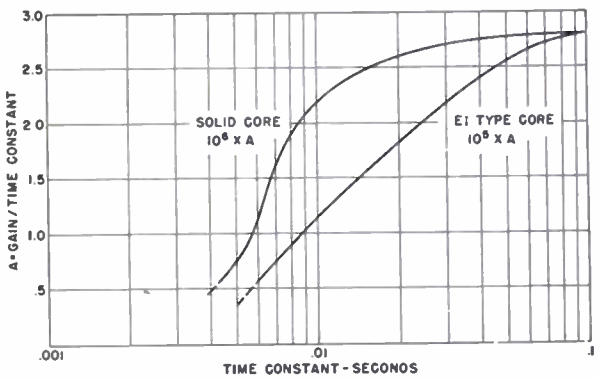

Fig. 14—Performance factor A versus time constant for a gapless core, and an equivalent EI-type core, both of which were used in a 400-cycle double-bridge circuit amplifier capable of 20-watts output power.

would be obtained. At values of the time constant greater than 0.01 second (4 cycles in 400 cycles), the curve for a gapless-core amplifier is fairly flat, since the input control-winding contributes most of the time delay. At the lower values of the time constant, the curve decreases due to the fact that the time delay in the control winding approaches the output time constant and the addition of resistance in the control winding does not affect the output time-delay. It is important to consider the output time-delay when the total time constant in this illustration approaches approximately 0.01 second.

If two stages are cascaded, the total input time-constant is not the sum of the two, but slightly larger. The difference between the sum of the time constants, and the actual time constant is greatest when they are equal. When three or more stages are cascaded, the error in assuming additive time constants does not produce an error greater than the accuracy of the present means of measurement.

If the figure of merit is assumed constant, there is a distinct advantage in cascading stages of magnetic amplifiers. The fact that the gains of each stage are multiplied and the time constants are approximately added, provides the means for improving the over-all figure of merit of a cascaded amplifier. Consider, for example, amplifier stage 1 having time constant T_1, gain K_1, and figure of merit $A_1 = K_1/T_1$; and stage 2 having time constant T_2, gain K_2 and figure of merit $A_2 = K_2/T_2$.

[9] D. W. Ver Planck, L. A. Finzi, and D. C. Beaumariage, "Analysis of transients in magnetic amplifiers," December 1949. *AIEE Technical Paper* 50-76.

[10] H. F. Storm, "Some fundamentals of D-C controlled reactors with resistive loads," *Trans. AIEE.*, vol. LXVIII; 1949 (AIEE Technical Paper 49–55).

The over-all figure of merit is

$$A_T = \frac{K_1 K_2}{T_1 + T_2} .$$

If T_1 and T_2 are equal, and K_1 and K_2 are equal, the resultant figure of merit is

$$A_T = \frac{K_1^2}{2T_1} = \frac{K_1}{T_1}\left(\frac{K_1}{2}\right) = A_1 \frac{K_1}{2} .$$

Thus, the figure of merit of the total amplifier is greater than that of each stage by a factor of $K_1/2$. However, an interesting point is evident when one considers the cascading of many stages of amplification. Since each stage has a minimum time delay ($\approx 1\frac{1}{2}$ cycles out of 400) which is difficult to control, the cascading of stages increases this total minimum time-delay, and as a result may limit the practicability of cascading too many stages.

There is much to be said about improving the time response of amplifiers through the use of feedback.[11] The experimental results indicate that for some types of feedback through shaping networks, an improvement in the figure of merit can be obtained.

V. Lamm Circuit for DC Control

The Lamm circuit shown in Fig. 15 is employed to obtain full-wave operation and is a combination of two basic circuits (Figs. 15(a) and 15(b) are different schematic representations of the same circuit.) Cores 1 and 2 operate on alternate half cycles of a sinusoidal supply voltage to produce a full-wave dc voltage output in a load, and the control windings are so arranged, as to cause identical action in both cores. Qualitatively, the circuit can be thought of as a full-wave bridge rectifier with the cores in the two upper arms (Fig. 15(b). Since the action of the reactors is such as to fire during different portions of the applied line voltage, the cores can be considered as variable switches controlled by a signal in the control winding. The output dc voltage in the load is a function of the *conduction period* of the cores.

In most applications, it is desirable to have balanced amplifiers wherein the net output is zero for zero input signal. Fig. 16(b) shows two sections of a Lamm circuit so arranged that the currents in both loads act in an opposite sense when a control signal is applied, i.e., while each half of the balanced circuit is structurally identical, the control winding is arranged to affect cores 3 and 4 in an opposite sense to that of cores 1 and 2. A control signal which flows through the control winding will cause an effective, positive control signal in cores 1 and 2, and an effective, negative control

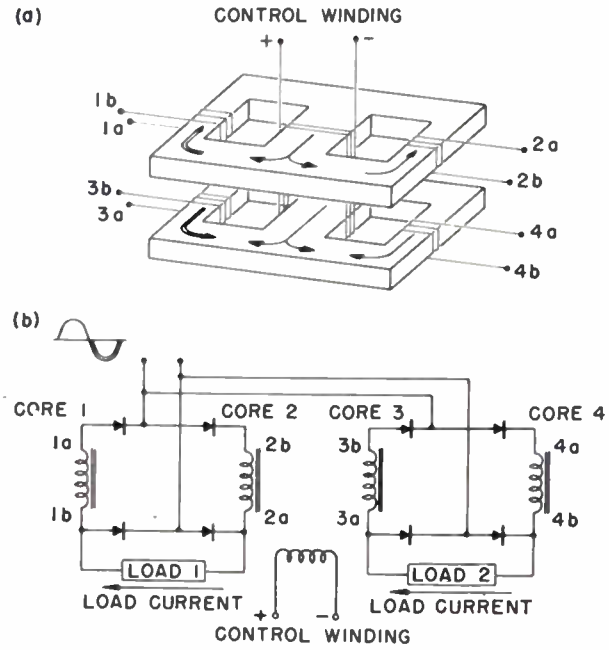

Fig. 16—Lamm circuit with dc control.

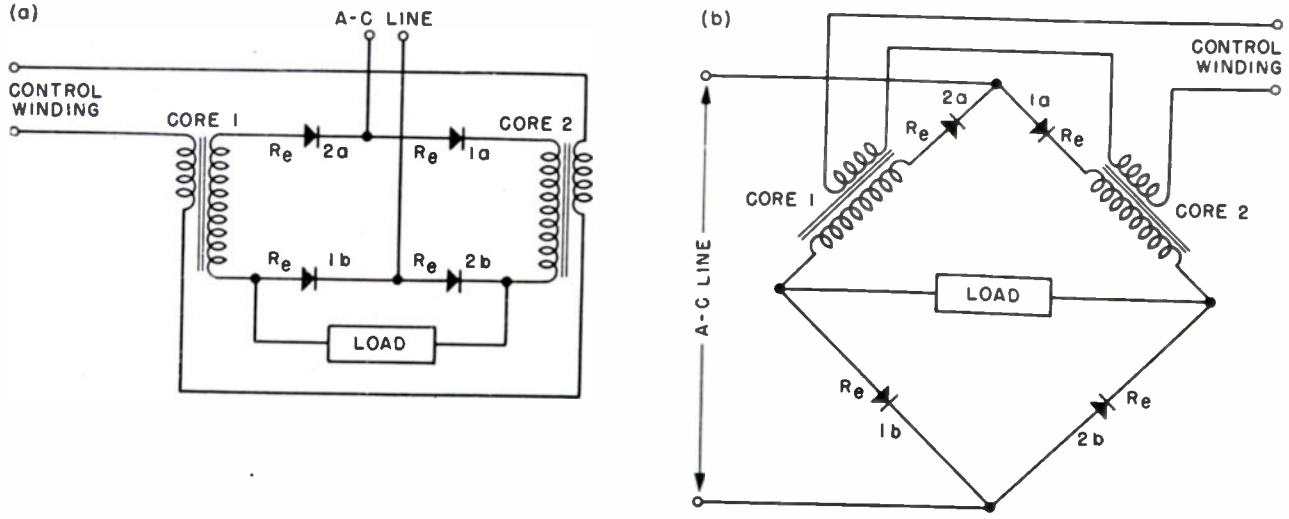

Fig. 15—Single-ended Lamm circuit.

[11] A. O. Black, "Effect of core material on magnetic amplifier design," *Proc. Nat. Elect Conf.*, vol. IV, pp 427–435; November, 1948.

signal in cores 3 and 4. At zero control current, each load current is equal. This type of balanced amplifier is useful in those devices which operate on net ampere turns, such as relays, magnetic amplifier stages, and dc motors with split fields.

Fig. 16(a) is a sketch of a balanced Lamm circuit with a double-core construction using three-legged laminations. The control winding can be seen to encompass both three-legged cores. The direction of the flux for each half-cycle is shown by the arrows: single arrows correspond to operation during the positive part of the cycle and double arrows to operation during the negative cycle. Legs numbered 1 and 2 are equivalent to cores numbered 1 and 2 in Fig. 16(b).

Considering the flux produced by the power windings on the outside legs of the cores with no control signal applied, that flux in the center leg due to the power windings in the upper core is similar in form to a full-wave rectified sinusoidal voltage. This flux does not contain the fundamental frequency, but is rich in second harmonics. In the lower core, the windings are so placed that the direction of the flux in the center leg is opposite to that in the upper core. Since the control winding encompasses both center legs, the net voltage induced in the control winding is zero.

The complete cancellations of the even and odd harmonics in the control winding depends upon the uniformity of the cores and windings. With a control signal, it is possible to have even harmonics in the control winding due to the unequal currents flowing in the power windings of the upper and lower cores. When a control signal is applied, as shown in Fig. 16 the mmf due to this signal aids the power flux in the upper core which is equivalent to cores 1 and 2, and opposes the power flux in the lower core which is equivalent to cores 3 and 4. This action is reversed if the sense of the dc control signal is reversed.

Note: The windings on the core structure and diagram are numbered to enable the tracing of the flux paths as indicated.

VI. Lamm Circuit for AC Control

In the amplifier previously discussed, the control signal was a dc signal which produced a dc mmf in the core. By rearranging the coils of the Lamm circuit, the same core structure can be made to operate with an ac control signal. The arrangement of the coils for ac control operation is shown in Fig. 17 where coils 1 and 4, and coils 2 and 3 act in the same manner respectively. The flux directions due to the power coils are shown as before, the single arrows representing the flux due to the positive half-cycle of the line supply, and the double arrows representing the flux due to the negative half-cycle.

The mmf due to the positive half-cycle of the control signal aids the flux in coil 2 and opposes the flux in coil 4. It has no effect in coils 1 and 3 since the coils are not conducting during the positive half-cycle. During the

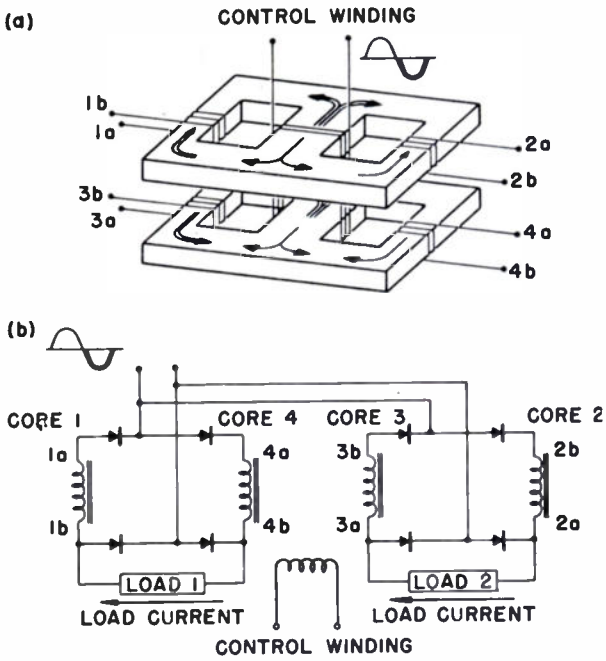

Fig. 17—Lamm circuit with ac control.

negative half-cycle, the control aids coil 3 and opposes coil 1. Coils 2 and 4 are not affected since they are not conducting. Thus coils 1 and 4 respond to the same direction of signal current while 2 and 3 respond to the opposite direction. The pairs of coils are connected as shown in the schematic of the circuit (Fig. 17).

The control signal should be at the correct phase for proper operation. If the control signal were 90 degrees out of the correct phase, the amplifier would not respond to any control voltage. The circuit arrangement can be used to advantage in applications where the control signal has the same frequency as the line voltage.

VII. Double-Bridge Circuit

In many applications, it is desirable to have the current in the load in ac form. The amplifier required for this application, therefore, must of necessity be a balanced ac output type.

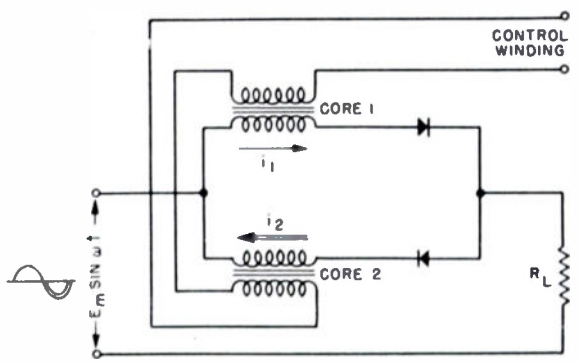

Fig. 18—AC full-wave single-ended circuit.

Consider first the combination shown in Fig. 18. The current in each reactor core is that obtained from

the basic circuit, as shown in Fig. 5. Although dc flows in cores 1 and 2, the current in R_L can be considered to be ac although rich in harmonic content. It is to be noted that at zero control current there is a current through R_L. It is evident that although the output of the circuit of Fig. 18 varies with input signal, there is no reversal of output, either in phase or magnitude, as the input goes through zero.

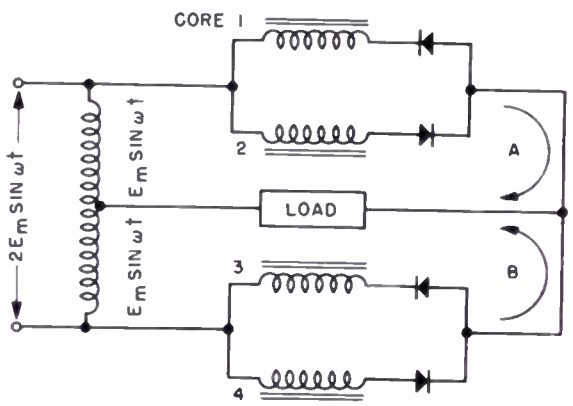

Fig. 19—AC bridge circuit.

In order to obtain a balanced amplier, the circuit of Fig. 19 is used. Each half of Fig. 19 is the same as Fig. 18 except for the fact that the supply voltage is derived from one-half of a center-tapped choke or transformer. The current through R_L from each half of the circuit is ac. However, due to the fact that the voltage supplies to circuits A and B are derived from a center-tapped choke, the voltages in circuits A and B are 180 degrees out of phase. The currents in circuits A and B, are also 180 degrees out of phase. The net voltage across R_L is therefore zero when the control current is zero, and thus θ_f and θ_r for all the cores are identical.

If now the control windings of cores 1 and 2, and cores 3 and 4 are so arranged that, for the same control signal, θ_f in cores 1 and 2 is increased and θ_f in cores 3 and 4 is decreased, a net current will flow in R_L. If the signal is reversed, θ_f in cores 1 and 2 is decreased and θ_f in cores 3 and 4 is increased, and the output current in R_L is reversed in phase.

It is necessary to use a center-tapped choke or transformer in this circuit to obtain the above operation. If now the choke is replaced by another set of reactors as shown in Fig. 20(b), the double-bridge circuit is obtained. The additional reactor windings together with the previous windings form a full-bridge circuit. The control signal now acts to vary θ_f, in cores 1 and 2, in the same sense, and θ_f in cores 3 and 4 in the opposite sense. Thus opposite arms of the bridge are influenced in the same manner by the control signal. It is also possible and practical to wind the additional winding 3(c) on the same leg as 3 and 4(c) on the same leg as 4, since they respond to a control signal in a similar manner. This is also true of windings 1(c) and 2(c) and 1 and 2 respectively. Thus no additional cores are needed besides those shown in the circuit of Fig. 19.

As in the case of the Lamm circuit, the double-bridge circuit can be used with the double-core construction shown in Fig. 20. Each outside leg of the cores has two windings. The flux paths in the cores are shown as single and double arrows. The dc control signal, as before, aids the power flux in the upper core and opposes the flux in the lower core. The windings are arranged so as to unbalance the bridge when a control signal is applied. The fundamental and harmonic voltage in the control winding are also cancelled as in the case of the Lamm circuit.

VIII. Applications to Servo Systems

Any servo system consists of an error detecting device, an amplifier, and a motor or prime driver of some sort. In designing an amplifier for a particular system,

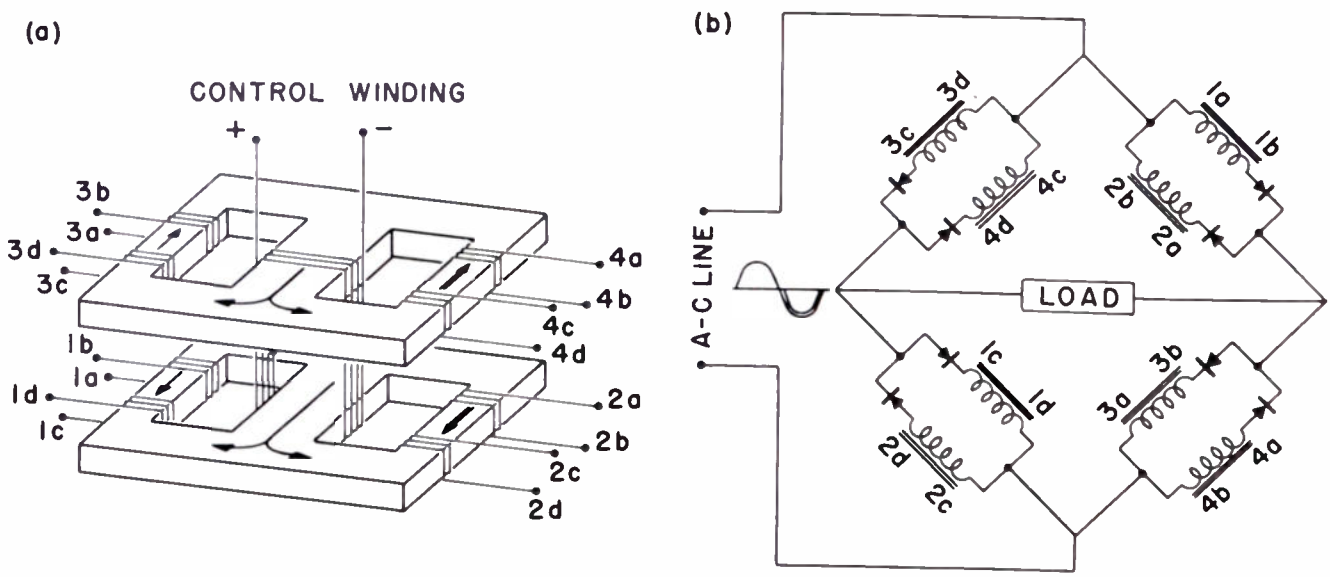

Fig. 20—AC double-bridge circuit with core construction.

the detailed characteristics of each of the components must be known. Since the magnetic amplifier is an impendace-sensitive device, the impedance of the motor must be known in detail. In addition, since the amplifier responds to ampere turns into the control winding, it is necessary to know the detailed characteristics of the error measuring device.

Error Measuring Device

The error measuring device, such as a synchro, magnetic or air-core pickoff, or potentiometer can usually be considered as a generator in series with some internal impedance. As discussed previously, the general idea is to match the input winding impedance of the amplifier to this internal impedance to obtain maximum power transfer, provided a swamping resistor is not used.

In the case of potentiometers, it is most advantageous to use a dc type input amplifier. This requires dc voltages on the potentiometer, but eliminates a demodulator. It is also conceivable that in some applications, it may be desirable to use ac excitation on the potentiometers in combination with either a demodulator and dc control amplifier or with just an ac control amplifier. In any case, the choice of a particular combination will usually depend upon (a) the performance or efficiency of the demodulator in conjunction with the signal device, (b) the performance factor or figure of merit A of the dc control amplifier and the ac control amplifier, and (c) system considerations.

Output Matching to Load

In designing the amplifier output stage, it is necessary to make certain that the stage is stable over the range of impedance variation of the load which is usually a motor in servo applications. In addition to stability, it is also necessary to properly match the load to the amplifier output stage with a matching transformer if the impedances are not originally matched. The point at which it is desirable to make the impedance match, for power considerations, depends upon the servo requirements. It is sometimes desirable to obtain maximum sensitivity about the null in positioning-type servos, whereas in certain tracking servos, it may be desirable to obtain maximum power at some point away from the null.

It is of interest to note that a motor with a fairly constant impedance versus applied-voltage relationship is desirable in these applications.

The Amplifier

As in the case of electronic servo amplifiers, the gain requirement is determined by the system constants. However, the additional problem of time delay in the magnetic amplifier increases the design problems. The gain requirement is determined by the available signal power in the error-measuring device and the power necessary to properly drive the motor. The procedure can be more easily explained by an example.

Consider a servo loop consisting of a motor driving a miniature synchro through a gear train. The control field of the motor must receive 20 watts from the amplifier for one degree of rotation of the miniature synchro. By measurement, the signal power available for one degree movement of the synchro is approximately 100 microwatts of ac power. If a demodulator is used, the efficiency of conversion of ac to dc power is about 25 per cent. The power gain required is, therefore,

$$G = \frac{20}{25 \times 10^{-6}} = 0.8 \times 10^{6}.$$

The time response requirement is also a function of the system. The *largest* time constant permissible is approximately 0.025 second or 10 cycles out of a 400-cycle supply. The required performance factor is, therefore,

$$A = \frac{G}{T} = \frac{0.8 \times 10^{6}}{0.025} = 3.2 \times 10^{7}\ \text{sec}^{-1}.$$

Since a good amplifier stage using a gapless core has a value of A which is approximately 10^{6} second^{-1}, it is evident that at least two stages must be used in even this borderline case.

If the time responses are distributed equally in a two-stage amplifier, and if the values of A for EI-type cores obtainable for Lamm and double-bridge circuits are used, then

A (Lamm circuit) $\approx 5 \times 10^{4}$ sec^{-1}
A (Bridge circuit) $\approx 10^{5}$ sec^{-1}
Required T for total amplifier $= 0.025$ second
Required T_1 for preamplifier $= 0.0125$ second
Required T_2 for output stage $= 0.0125$ second
Gain of preamplifier $= (0.0125)(5 \times 10^{4}) = 0.0625 \times 10^{4} = 625$
Gain of output stage $= (0.0125)(10^{5}) = 1250$
Total gain of amplifier $= G_T = (626)(1250) = 7.8 \times 10^{5}$
Total value of $A = A_T = G_T/T = 7.8 \times 10^{5}/0.025 = 3.12 \times 10^{7}$ sec^{-1}.

Thus, the resultant value of the performance factor obtainable from this two-stage amplifier is just about the value required for the amplifier under discussion. In addition, the fact that A_T is not actually constant was not taken into account. Also, perfect matching was assumed between the preamplifier and output stage. Faced with this preanalysis, the designer would either use a three-stage amplifier or else use a gapless-core type of preamplifier. Using the gapless-core type would increase the gain by a factor of 10 in each stage and therefore meet the requirements with a reasonable safety factor. If EI-type cores were desired, then a third stage would almost be necessary for a proper design. In all, the safety factor necessary for a complete amplifier may be as large as 5 or 10. In cases where negative feedback is used, a larger safety factor must be considered.

Once the required amplifier is obtained, it is necessary

to consider means of stabilizing the servo system. Many of the methods used in electronic servos do not lend themselves to use in this application because low-impedance circuits are prevalent in magnetic amplifiers. The several methods which can be used for stabilization of the magnetic amplifier servo system are:

a. Use of *velocity or acceleration dampers* on the motor. With this type of stabilizer, no additional circuitry is necessary in the amplifier. To use an acceleration damper which has no velocity error, the servo amplifier should have no greater time delay than 10 cycles out of 400. When using a velocity damper, the amplifier time delay may be as high as 15 to 20 cycles out of 400. Use of the velocity damper decreases the maximum speed of the motor.

b. Use of a *generator* or *tachometer feedback*. The use of a velocity signal is very similar to the use of a velocity damper except that the maximum speed of the motor is not decreased, and a regular motor can be used. The delay of the amplifier can be as large as 12 to 15 cycles.

c. Use of a *velocity generator*, but with the output differentiated. This is equivalent to the use of the acceleration damper. The delay of the amplifier can only be as high as 8 cycles out of 400.

d. Use of *rate circuits* on error signal. This type of stabilization is similar to that used in electronic servos in which networks are employed to obtain control functions. For this type of stabilization, the amplifier should have no greater time delay than 4 or 5 cycles out of 400. Also, a loss in gain through the control network of about 10 should be expected.

e. Use of *feedback* in conjunction with networks. This type of stabilization is possible and has been made to work. However, it is difficult to control the feedback for a uniformity of response. At the present time, this type of stabilization is under development.

f. Use of any *combination* of the above five methods. By combining two or more of the above, a realization of the time response and gain requirement may be possible. This method depends a great deal upon experimental technique.

Conclusion

The magnetic amplifier in its present stage of development can by no means be said directly to replace the electronic amplifier. There are advantages and disadvantages associated with each application of a magnetic amplifier The determining factor in the choice of electronic or magnetic amplification will depend upon the over-all performance and operation requirements of the entire project. Table I is a qualitative comparison of magnetic and electronic amplifiers as applied to a low-level (maximum of 50 watts) servo system.

Acknowledgment

The author gratefully acknowledges the cooperation of J. Bentkowsky and A. Levine in the construction of the amplifiers and the accumulation of experimental data.

TABLE I

Qualitative comparison of magnetic and electronic amplifiers as applied to a low-level (maximum of 50 watts) servo system.

Electronic Amplifier	*Magnetic Amplifier*	*Electronic Amplifier*	*Magnetic Amplifier*
1. It is possible to obtain as high a gain as necessary without an appreciable delay.	1. The gain-per-unit-time response is fixed. The time response is not negligible and it increases or decreases as the gain is increased or decreased.	6. The weight of electronic amplifiers can be comparatively small.	6. The weight of equivalent magnetic amplifiers is generally greater than the electronic amplifiers.
2. The amplifier can be made as stable as desired by appropriate feedback networks. Any loss in gain can easily be made up by the addition of a stage of amplification without any time delay.	2. Stability is a serious problem. Since the gain/time constant is fixed, any type feedback used reduces the gain. The loss in gain can be made up by an additional stage but with an increase in the minimum delay.	7. The life of the amplifier depends upon the life of the vacuum tubes. The standard life is about 3,000 hours.	7. The life of a magnetic amplifier system depends upon the rectifier and reactor components. The reactor has the same life as a transformer, while the rectifiers should have a life of about 20,000 hours.
3. Components and vacuum tubes can be obtained to within published tolerances.	3. The rectifiers and magnetic cores have so far been unobtainable to within standard small tolerances. Differences of ±100 per cent in magnetic core properties are not uncommon.	8. The electronic amplifier is sensitive to shock because of vacuum tubes.	8. The magnetic amplifier should be insensitive to shock.
4. The electronic amplifier always has a better figure of merit, i.e., gain/time constant.	4. The magnetic amplifier always has an inferior figure of merit as compared to the electronic amplifier.	9. The electronic amplifier is very versatile in its application.	9. The magnetic amplifier is limited in its versatility, but has the one advantage of being able to add multiple signals easily.
5. The size of an amplifier can be made quite small.	5. The size of an equivalent magnetic amplifier is generally greater than the electronic amplifier, excluding power supply.	10. The warm-up time is usually several minutes.	10. Operation is instantaneous, i.e., within several cycles of the carrier frequency.
		11. Stand-by power is almost as much as full-load power. The heating effect is constant.	11. The stand-by power is low compared to the full-load power. There is no filament and power-supply power. The heating effect is proportional to the duty cycle of the servo system.

Amplitude and Phase Measurements on Loudspeaker Cones*

MURLAN S. CORRINGTON†, SENIOR MEMBER, IRE, AND MARSHALL C. KIDD†,

This paper is published with the approval of the IRE Professional Group on Audio, and has been secured through the co-operation of that Group.—*The Editor.*

Summary—**Amplitude and phase measurements have been made of the mechanical motion of different points on the cone diaphragm for various critical frequencies. From these the cause of various peaks and dips in the sound-pressure curve can be determined. Such information is helpful when making changes to improve the cone design.**

Introduction

LOUDSPEAKER cones are usually designed by means of experimental processes. When a new speaker is to be developed for producing a particular frequency response, it is customary to start with a cone of approximately the desired properties and to modify the shape and paper stock systematically until the response is as close as possible to the desired curve. After this is done, it often happens that there is still something undesirable about the frequency response which is very difficult to correct. We have found that if careful measurements are made of the amplitude and phase of the various parts of the vibrating cone, it becomes possible to visualize the actual mode of vibration leading to the undesired peak or dip in the sound pressure output. This paper will describe some laboratory equipment that can be used to make these measurements, and will show how the results can be used to improve the design of the cone.

A Fairly Common Error

Many acoustical engineers believe that if a small microphone probe is placed close to a vibrating membrane, the sound-pressure variations which are picked up at the tip of the probe will correspond to the actual vibration of the membrane at the point. The theory is as shown by Fig. 1. Let the small area dS on the inner surface of the cone vibrate sinusoidally with a normal velocity u_0. Then the radiation pressure at a point P separated from dS by a distance h is as shown by (1) in the caption to Fig. 1. It should be noted that the quantity h occurs in the denominator. It has been argued in the literature that if h is very small the contribution to the total pressure due to dS will be much greater than that due to the rest of the cone; and therefore, the output of the microphone should be a measure of the motion of dS.

In actual practice, when working inside a loudspeaker cone, this relation does not hold. Even though the distance h for dS is very small, the area of the rest of the

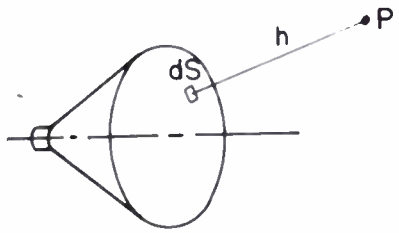

Fig. 1—Radiation pressure at point P due to element of area dS

$$dp = -i(\rho\nu u_0 dS/h)e^{ik(h-ct)} \quad (1)$$

ρ = density of air
ν = frequency
u_0 = velocity of dS
c = velocity of sound
$k = 2\pi\nu/c$.

cone is large in comparison to dS that even though h becomes much greater the contribution to the resultant sound pressure due to the larger area, is much greater than that from the element of area dS.

The curves of Fig. 2 show the phase shift between the current in the voice coil and the sound pressure near the apex of the cone, as measured with a small microphone probe. The cone was 4 inches in diameter with

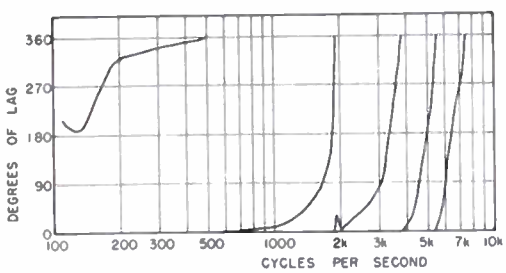

Fig. 2—Phase shift between current in voice coil and sound pressure at center of cone.

an included angle of 118 degrees. At low frequencies, around 100 cps, the sound pressure causes the force on the voice coil to lag by approximately 180 degrees, as shown. At 500 cps the lag is one complete cycle. At 1,900 cps the sound pressure at the apex is 2 cycles behind, at 3,800 cps it is 3 cycles behind, and at 7,400 cps it is

* Decimal classification: R265.2. Original manuscript received by the Institute, April 5, 1951. Presented, 1951 IRE National Convention, March 22, 1951, New York, N. Y.

† RCA Victor Division, Radio Corporation of America, Camden, N. J.

5 cycles behind. Since the voice coil form is only about $\frac{3}{8}$ inch long and since the speaker response drops off rapidly when the voice coil form becomes a quarter-wave transmission line, it is obvious that this curve of degrees of lag has no relation whatever to the actual motion of the cone near the apex. For this reason, the study with the microphone probe was abandoned in favor of the system shown by Fig. 3.

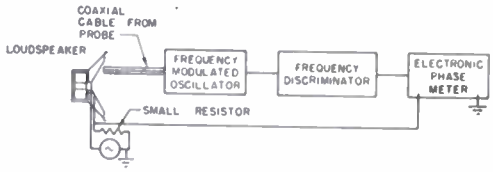

Fig. 3—Capacitor probe circuit.

Measurement of Amplitude and Phase of the Cone

The inner surface of the loudspeaker cone is coated with a thin layer of flexible conducting paint. The paint film is made so thin that there is no noticeable change in the sound-pressure response. A capacitor probe is placed near the cone surface so that the cone motion causes capacitance variations across the probe. A coaxial cable connects the probe to an oscillator tank circuit. As the capacitance varies, the oscillator is frequency modulated in step with the cone motion. The oscillator output is fed into a frequency discriminator to produce a demodulated wave, which represents the cone motion at the probe. This wave is fed into one terminal of the electronic phase meter.

In order to provide a constant and reliable reference for the phase measurements, the voice-coil current is used for comparison. A small resistor is placed in series with the coil, and thus the voltage drop corresponds to the current through the coil and, likewise, to the force on the coil due to the magnetic field. To find the relative phase between two parts of the cone, it is merely necessary to measure the motion of each one with respect to the voice coil and to subtract the two results. This method also corrects for phase shifts in the discriminator and amplifiers.

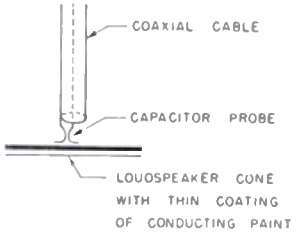

Fig. 4—Capacitor probe details.

The details of the probe are shown by Fig. 4. The diameter of the cable is $\frac{1}{4}$ inch, and the two plates cover an area about 3/16 inch square. The motion of the coating on the cone surface causes capacitance variations in proportion to the motion.

The amplitude measurements are calibrated by operating the loudspeaker at a low frequency so that the cone is moving as a piston at a fixed level. The probe is adjusted to be near the paper, and the gain of the following amplifier is adjusted to give the required output voltage. The actual motion at another frequency is thus referred to the calibration point. It is not necessary to set the levels for the phase measurements since the limiters in the phase meter eliminate variations due to changing amplitudes.

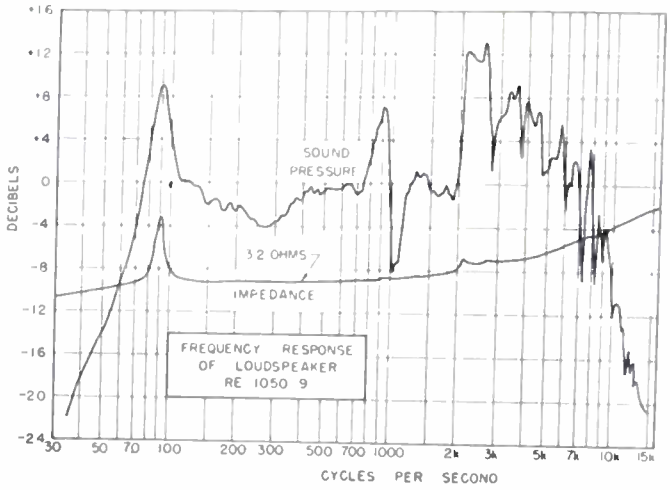

Fig. 5—Frequency response of loud speaker RE1050-9

Application to an 8-Inch Loudspeaker

One of our speakers that had been developed experimentally had the frequency response shown by Fig. 5. It was desired to eliminate the peak near 920 cycles and the hole just past 1,000 cycles. The probe was used to measure the amplitude and phase of the apex of the cone when constant voltage was applied to the voice coil. The results are shown by Fig. 6. Because the voice-coil voltage is proportional to the velocity of motion of the coil in the magnetic field, it is evident that constant voltage tends to give a constant velocity to the cone, and the amplitude will, therefore, fall off at 6 decibels per octave with increasing frequency. Although there is a hole in the response on either side of 950 cps,

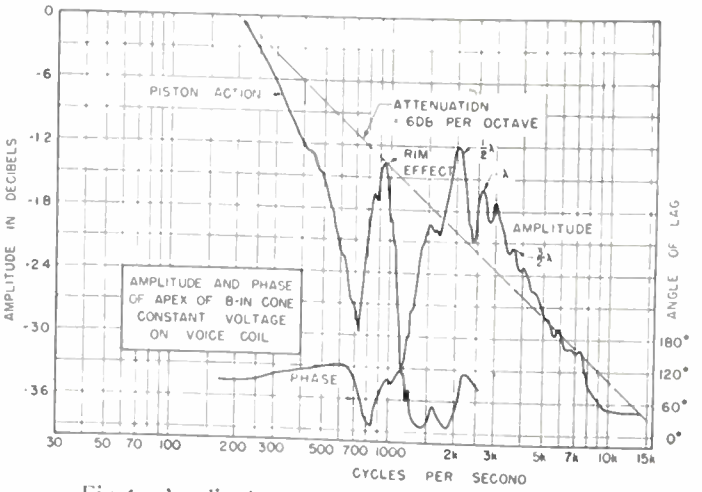

Fig. 6—Amplitude and phase of apex of 8-inch cone.

it is evident that the apex amplitude is not above normal. The phase variations are just what might be expected; as the system falls off at 6 decibels per octave, the phase angle lags approximately 90 degrees throughout the range. Each peak of amplitude corresponds to a rapid increase in phase, as is expected from the well-known relations between the amplitude and phase of such a system.

Since the cause of the trouble was not near the apex, the cone rim was examined next. The amplitude and phase curves for the cone rim are as shown by Fig. 7. This corrugation is oscillating violently at 950 cps, with

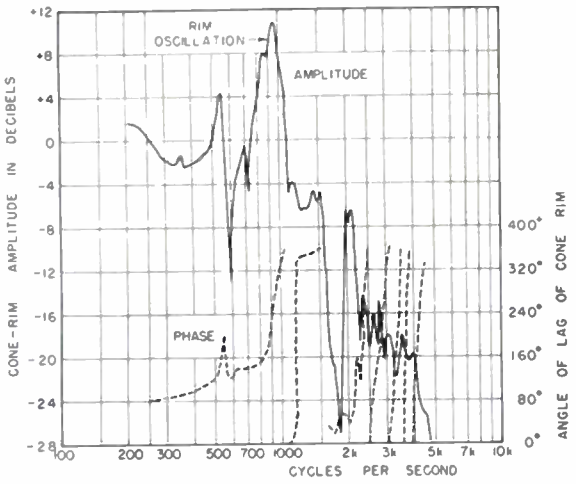

Fig. 7—Cone-rim amplitude and phase, 8-inch cone.

an amplitude at least 14 decibels higher than for frequencies slightly higher or lower. Since the cone rim has a fairly large area and a large amplitude, it causes considerable sound-pressure output near 950 cycles.

The motion of the entire cone was examined at 950 cps to see whether the violent rim resonance produced the peak in response. As shown by the curves of Fig. 8, the amplitude and phase of the cone motion change considerably along a radius. The apex amplitude was

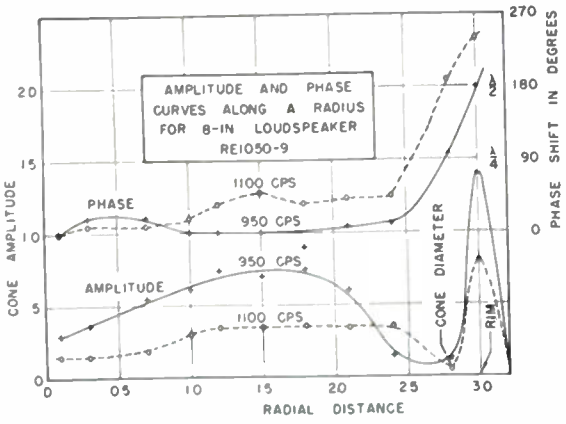

Fig. 8—Amplitude and phase curves along a radius

fairly small, but the central portion of the cone had a large amplitude. There was a node near the cone diameter, and the rim amplitude was large and 180 degrees out of phase, with respect to the central part of the cone. The sound output from the rim canceled part of the sound output from the rest of the cone; however, because the area of the cone was so large, the net result was a peak in output.

When the frequency was increased to 1,100 cycles per second, the rim and cone body were somewhat off resonance, as proved by Figs. 6 and 7. As a result, both amplitudes were reduced, as shown by Fig. 8. The two oscillations were still approximately 180 degrees out of phase over most of the cone, and there was some evidence of two radial nodes at this frequency. Consequently, the sound pressure developed by the rim canceled a considerable part of that developed by the cone, resulting in a hole, about 8 decibels deep, in the sound-pressure curve, as seen in Fig. 5.

These relations are not so simple as they may appear at first glance. The sound pressure at a point in front of the cone is proportional to the integral of the sound pressure generated by each element of the cone, corrected for the phase shift along the cone and for the time required for the sound to be transmitted from the elemental area to the point, in accord with (1).

Since a felted paper cone is not homogeneous and may not be completely symmetrical, the curves of Fig. 8 will be somewhat different along other radii. At certain frequencies, radial modes will also modify the amplitudes considerably. Additional information can be obtained by using lycopodium powder on the cone to produce dust patterns.

Design of the Rim

Examination of the cone rim, shown by Fig. 9, shows that the edge of the cone has a large radius (0.156 inch). As the cone moves along its axis, the paper tends to roll around this curve, and this excites the following 0.094-inch corrugation into violent oscillation at its resonant

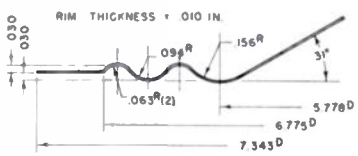

Fig. 9—Rim of 8-inch speaker.

frequency. It is evident that the cone rim and corrugation should be much narrower to reduce the radiating area, and the radius of the cone rim should be much less.

It is sometimes difficult to decide which part of the irregularity in the sound-pressure curve is due to this rim and cone resonance. In most speakers used in commercial radio and television equipment, the effect occurs between 900 and 1,500 cps and usually consists of a peak followed by a hole. In heavy 15-inch woofers the effect may occur as low as 500 cps. If a sine wave is applied to the speaker at this frequency, the violent oscillation can be observed by touching the rim of the cone with the tip of a lead pencil. A sharp buzz will be heard at the resonant frequency.

If the space between the cone rim and the cone housing is packed full of cotton, this oscillation will be damped greatly, as shown by Fig. 10. The peak and hole are much reduced. Because the rim is stiffer than before, the low-frequency resonance occurs at a slightly

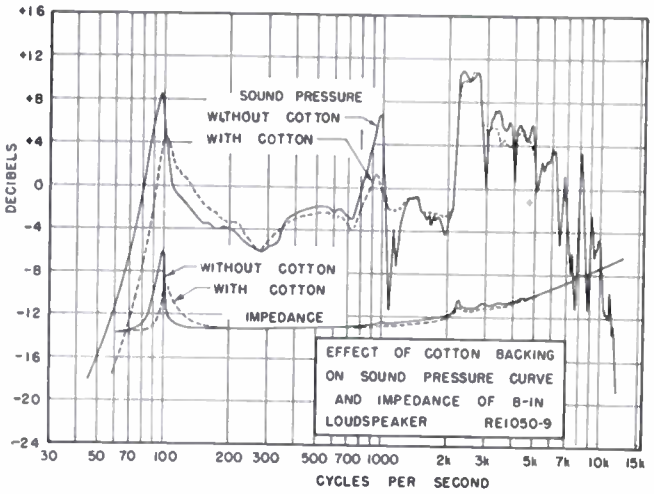

Fig. 10—Effect of cotton backing on sound pressure and impedance.

higher frequency, as shown. It should be noted that rim resonance always causes a small peak in the impedance curve, and this will help identify the effect as it is the first irregularity after the low-frequency resonance. The addition of cotton is not intended to cure the trouble, but it is merely a test to show what the improvement will be if the rim is properly designed.

When the cone rim is narrow and has small radii, the radiating area is reduced and the amplitude of oscillation does not build up to large values. The disadvantage is that the rim may become nonlinear at low frequencies, and the rim may crack at the corrugations when used at high levels. These difficulties can be overcome by felting the rim with a soft paper stock and by adding certain compounds to produce a tough paper having internal friction between the paper fibers. This friction will help to damp out the resonances.

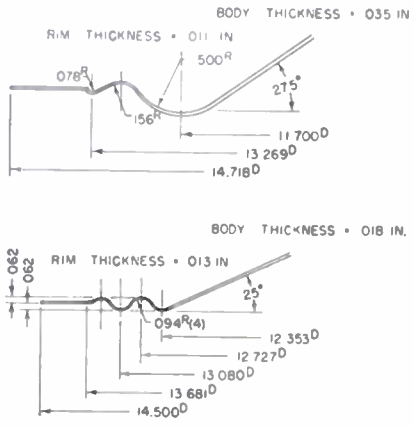

Fig. 11—Cone-rim details.

One of our early models of a 15-inch loudspeaker had a rim and roll, as shown by the upper part of Fig. 11. The rim had an unusually large radius (0.500 inch), and the rim effect caused a peak in response followed by a wide hole. When the rim was redesigned in accord with the lower part of Fig. 11, the response was considerably improved, as shown by Fig. 12. There is still a small cancellation at 720 cycles, but the curve is much smoother than before.

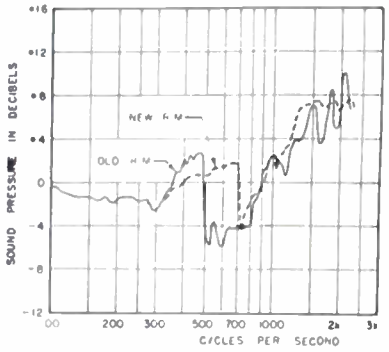

Fig. 12—Variation of sound-pressure response with rim design.

If a rim is made of a very soft, nonresonant material, such as goat-skin, the rim resonance is nearly eliminated. Fig. 13 shows the frequency response of a 10-inch loudspeaker with a leather edge. The curve is quite smooth throughout the range which is usually irregular, due to rim effects.

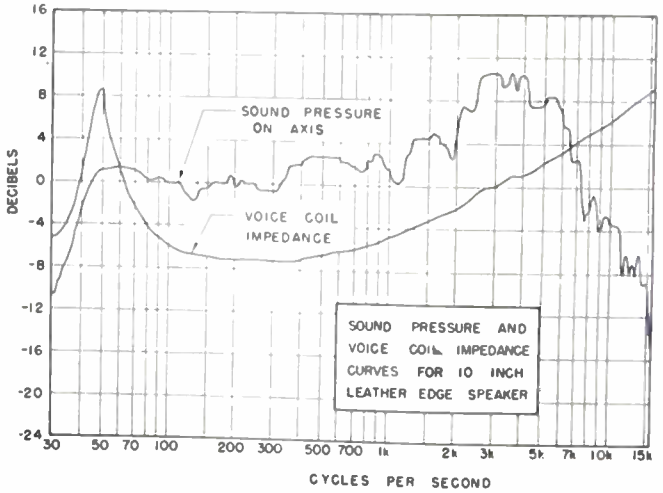

Fig. 13—Sound-pressure and impedance curves for 10-inch leather-edge speaker.

Higher-Order Resonances

Examination of Fig. 5 shows that the next peak occurs at 2,150 cps and is followed by a hole at 2,800 cps. A small peak in the impedance curve occurs at each of these frequencies, indicating that the sound-pressure variations are caused by resonances in the cone. Fig. 14 shows the radial amplitude and phase curves at 2,150 cps. The phase shift from the apex to the cone diameter is 180 degrees, and a circular node occurs at a radial distance of 1.4 as well as at the cone diameter. The portion of the cone near the apex is in phase with the cone rim, but the part of the cone from 1.4 to 2.7 is out of phase with the rest. Because of the large amplitude of

the cone motion, the result is a peak in the sound-pressure curve.

The next resonance occurs at 2,800 cps, and the amplitude and phase curves are shown by Fig. 15. There are circular nodes at radial distances of 1.0, 2.0, and 2.8. The phase shift along the radius is somewhat irregular near the apex, but alternate sections of the cone come in and out of phase. The radiation from the alternate regions tends to cancel out in the resulting sound pressure, and the result is a hole in the response. Each higher peak and hole in the sound-pressure curve corresponds to a similar type of resonance, but, however, with more circular nodes.

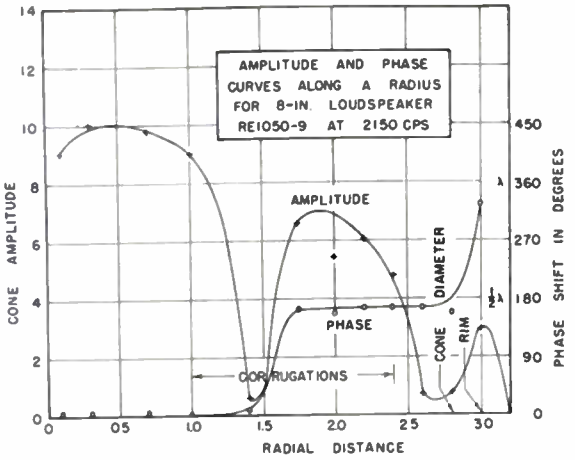

Fig. 14—Amplitude and phase curves along a radius.

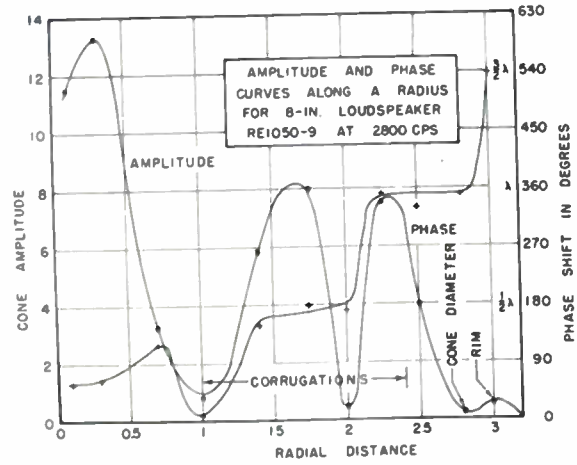

Fig. 15—Amplitude and phase curves along a radius.

Average Velocity in the Cone

If the average radial velocity of transverse wave propagation in a cone is defined as the distance between the apex and the cone diameter divided by the number of wavelengths in that distance, multiplied by the frequency in cycles per second, the measured results are as shown by Fig. 16. For low frequencies the cone behaves as a piston with all parts in phase so that the average transverse velocity can be considered infinite. At higher frequencies the average velocity varies, as shown. It decreases uniformly beyond 1,800 cps and approaches a limiting velocity, which is the same as for a flat sheet of the same material. The phase shift across the cone increases uniformly with frequency.

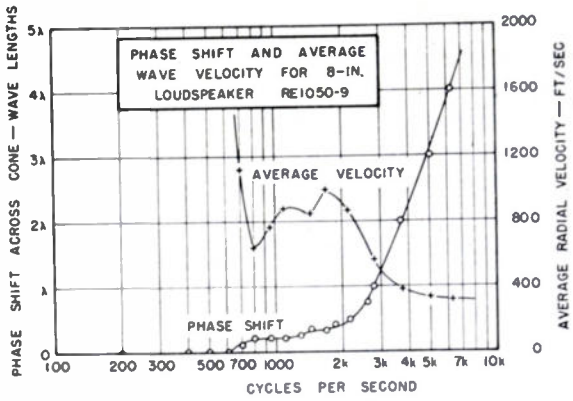

Fig. 16—Phase shift and average wave velocity.

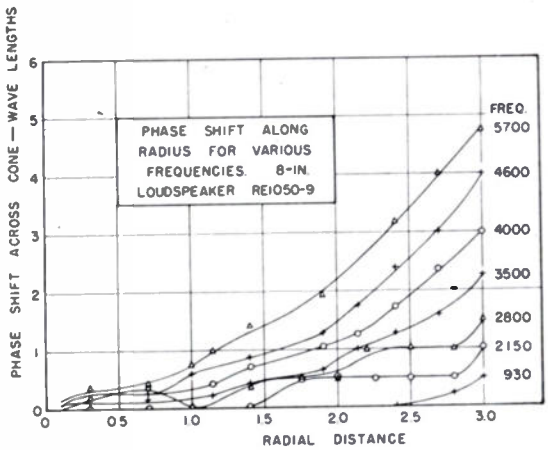

Fig. 17—Phase shift along radius.

The total phase shift along the cone increases fairly uniformly with the distance from the apex, as shown by Fig. 17. There are a few irregularities at certain frequencies, but in general the phase shift increases uniformly with frequency.

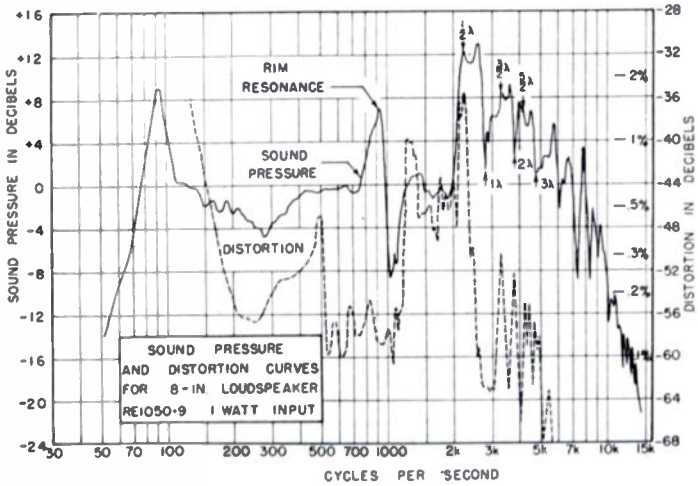

Fig. 18—Sound-pressure and distortion curves.

If the methods described are carried further by analyzing other higher modes, the major peaks and dips in the curve can be interpreted, as shown by Fig. 18.

This drawing also shows the variation of distortion with frequency for the same cone. At an applied frequency of one-half the rim resonance, the rim is excited and produces a peak in the distortion curve. Likewise, when the frequency is one-half of the next resonance (2,150 cps), a second peak occurs. There is a peak in distortion corresponding to each resonance in the cone, except that the one for the resonance at 1λ is apparently missing. The large amplitudes of motion of the cone, at a resonant frequency, lead to nonlinear effects and resulting increases in distortion.

Applications to Other Loudspeakers

The curves of Fig. 19 show that the performance of this 4-inch loud-speaker is very similar to that of the 8-inch cone already described. The irregularities in

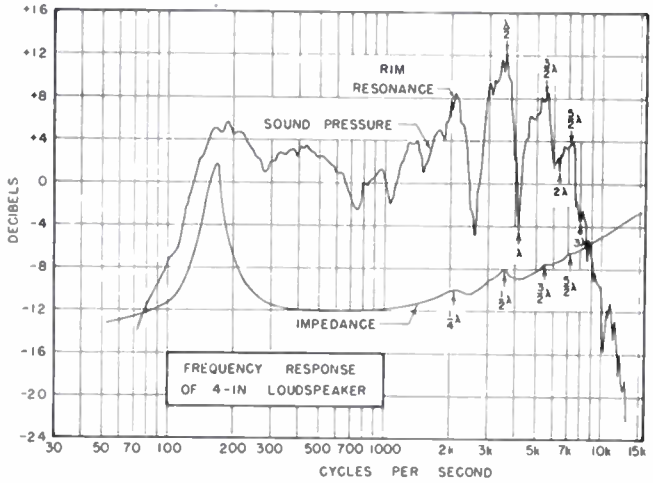

Fig. 19—Frequency response of 4-inch loudspeaker.

the two curves occur at higher frequencies than for an 8-inch cone but are similar otherwise. Each peak in sound pressure coincides with a small peak in the voice-coil impedance.

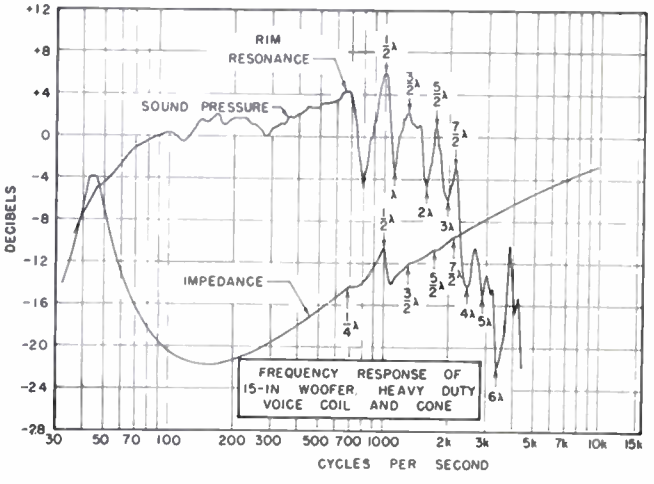

Fig. 20—Frequency response of 15-inch woofer.

When a heavy 15-inch woofer was analyzed, the results were as shown by Fig. 20. The peaks and dips in sound pressure follow the same pattern as before. It is thus evident that the irregularities in the impedance curve are very useful tools for identifying the various resonant modes. These variations in impedance can be made much larger by using a Wheatstone bridge circuit and a duplicate voice coil to balance out the rising electrical impedance. The unbalance then is a measure of the electrical equivalent of the motional impedance.

Conclusions

The illustrations shown are merely a few examples of how this equipment can be used to improve the design of loudspeakers. It has also been used to locate causes of distortion at certain frequencies. Sometimes it is possible to isolate small areas of the cone that put out almost pure second harmonic because of "oilcan" action. In other cases it has been found that the cone rocks back and forth because of an eccentric pole piece or because of dissymmetries in the cone itself. The equipment is a very useful tool for testing the various parts of the cone. Once the physical picture of the motion is obtained, it is usually possible to correct the difficulty.

Acknowledgment

The authors wish to acknowledge the help of H. F. Olson, of the RCA Laboratories, for his help in obtaining the distortion curve of Fig. 18.

Bibliography

1. H. Backhaus, "Über Strahlungs- und Richtwirkungseigenschaften von Schallstrahlern," *Zeit. Tech. Physik.*, vol. 9, pp. 491–495; 1928.
2. A. G. Warren, "The free and forced symmetrical oscillations of thin bars, circular diaphragms, and annuli," *Phil. Mag.*, ser. 7, vol. 9, pp. 881–901; May, 1930.
3. N. W. McLachlan, "The loudspeaker diaphragm," *Wireless World*, vol. 26, pp. 586–588; June 4, 1930.
4. M. J. O. Strutt, "On the amplitude of driven loud speaker cones," Proc. I.R.E., vol. 19, pp. 839–850; May, 1931.
5. N. W. McLachlan, "The lower register in moving coil loud speakers," *Wireless World*, vol. 28, pp. 479–481; May 6, 1931. Also pp. 514–516; May 13, 1931.
6. N. W. McLachlan and G. A. V. Sowter, "The behaviour of conical diaphragms used in acoustic apparatus for the reproduction of speech and music," *Phil. Mag.*, ser. 7, vol. 12, pp. 771–815; October, 1931.
7. N. W. McLachlan, "Additional experiments on moving-coil reproducers and on flexible disks," *Phil. Mag.*, ser. 7, vol. 13, pp. 115–143; January, 1932.
8. N. W. McLachlan, "On the symmetrical modes of vibration of truncated conical shells; with applications to loud-speaker diaphragms," *Proc. Phys. Soc.* (London), vol. 44, pp. 408–420; 1932. Discussion, pp. 420–425.
9. N. W. McLachlan, "The axial sound-pressure due to diaphragms with nodal lines," *Proc. Phys. Soc.* (London), vol. 44, pp. 540–545; 1932.
10. N. W. McLachlan, "Methods of investigating the vibrational frequencies of conical shells and loudspeaker diaphragms," *Wireless Eng. and Experimental Wireless*, vol. 9, p. 626; 1932.
11. H. Benecke, "Über die Schwingungsformen von Konusmembranen," *Zeit, Tech. Physik*, vol. 13, no. 10, pp. 481–483; 1932.
12. M. J. O. Strutt, "Eigenschwingungen einer Kegelschale," *Ann. der Phys.*, ser .5, vol. 17, no. 7, pp. 729–735; August, 1933.
13. Goswin Schaffstein, "Untersuchungen an Konuslautsprechern," *Hochfreq. und Elektroak.*, vol. 45, pp. 204–213; June, 1935.
14. Piero Giorgio Bordoni, "Asymmetrical vibrations of cones," *Jour. Acous. Soc. Amer.*, vol. 19, pp. 146–155; January, 1947.
15. G. L. Beers and C. M. Sinnett, "Some recent developments in record reproducing systems," Proc. I.R.E., vol. 31, pp. 138–146; April, 1943. Also, *Jour. Soc. Mot. Pic. & Telev. Eng.*, vol. 40, pp. 222–241; April, 1943. This paper contains the circuit used for the oscillator and discriminator.

Radio Relay Design Data 60 to 600 MC*

RICHARD GUENTHER†, MEMBER, IRE

Summary—**This paper presents general design data for a complete radio relay transmission system. All parameters are shown in graphs either as gain or attenuation figures (decibels). From these figures, either a level diagram may be plotted or the final signal-to-noise ratio may be obtained by simple addition or subtraction of the respective parameters.**

In order to get realistic figures for various modulation systems, a new parameter has been defined which accounts for the deficiency of the demodulator. Numerical examples are presented to show the convenience in practical use.

I. Introduction

RADIO RELAY circuits today represent an indispensable link in electrical communication networks. The requirements are generally the same as for wire and cable systems within the same network. It is, therefore, desirable to adapt the design data to the common standards in communication circuits. This paper will present all parameters involved in such a manner that communication engineers are enabled to determine the transmission characteristics of each voice channel without specific experience in ratio techniques. For this purpose a level diagram is used to show the signal and noise level in different portions of the system, a procedure commonly used in communication circuits (Fig. 1). By this means, the necessary levels for integration with wire systems may be read directly from the level diagram. Transmitter power and receiver noise will be given as ratios above 1 milliwatt. The transmission characteristics of the radio circuit including the antennas, radio path, transmission cables, and wide-band gain of different modulation systems, will be expressed in terms of attenuation or gain, whichever applies. By this means the design procedure is reduced to the addition and subtraction of the appropriate parameters. The above-mentioned parameters are shown in graphs over a wide range of the respective variables to cover all practical needs. For multichannel systems a correction factor is given to convert the figures for the broad-band output into those for the single voice channel.

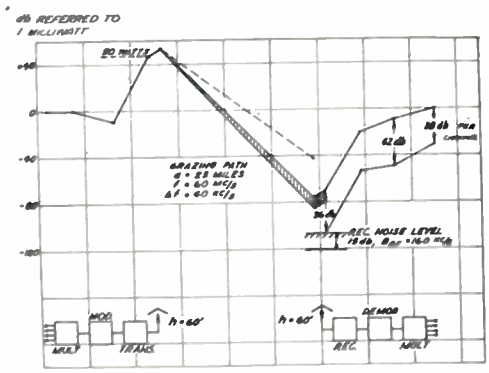

Fig. 1—Level diagram of a multichannel radio circuit.

In wide-band systems it is often overlooked that the practical wide-band gain might be lower than the theoretical. This is caused by a reduced efficiency of the demodulator due to a more or less inefficient detection of the modulated signal. Therefore, a parameter is introduced which represents the deficiency of the demodulator. In connection with the theoretical wide-band gain it yields the practical achieved af signal-to-noise.

II. Transmitter

The output power of the transmitter expressed in db above 1 mw is the starting point, as far as the signal is concerned. After subtracting the attenuation of the transmission line, the antenna gain is then added. The resulting power physically represents the equivalent power which, if applied to the reference dipole, produces the same field strength in the main direction as the transmitter power applied to the actual antenna.

III. Propagation

In some cases, the free-space attenuation can be used for a rough guess. For more realistic figures, the propagation over a spherical earth of finite conductivity has to be considered. Such calculations were carried out by van der Pol and Bremmer[1,2] assuming the earth as a perfect sphere with uniform ground constants, surrounded by a homogeneous atmosphere. Due to the decrease in barometric pressure with increasing elevation, the coefficient of refraction generally decreases according to

$$(n-1)\cdot 10^{-6} = \frac{78.5}{T}\left(p + \frac{4800e}{T}\right) \qquad (1)$$

where

n = index of refraction
P = barometric pressure in millibars
T = absolute temperature
e = partial pressure of water vapor in millibars.

Under average atmospheric conditions (standard atmosphere) the gradient of the index of refraction becomes

* Decimal classification: R480. Original manuscript received by the Institute, October 8, 1950; revised manuscript received, March 19, 1951. Presented, 1950 National IRE Convention, March 7, 1950, New York, N. Y.

† Signal Corps Engineering Laboratories, Fort Monmouth, N. J.

[1] B. van der Pol and H. Bremmer "The diffraction of electromagnetic waves from an electric point source round a finitely conducting sphere, with applications to radio telegraphy and the theory of the rainbow," *Phil. Mag.*, vol. 24, p. 141, Part I, July, 1937; also p. 825, Part II, November, 1937.

[2] H. Bremmer, "Terrestrial Radio Waves," Elsevier Publishing Co., New York; 1949.

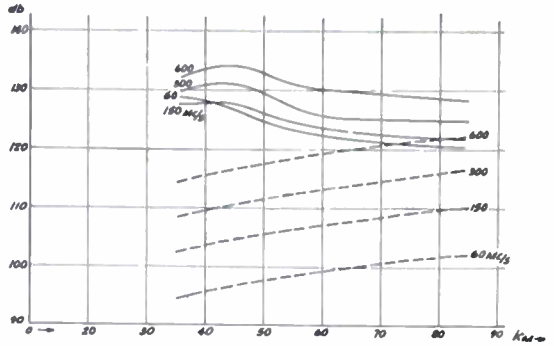

Fig. 2—Attenuation between λ/2 dipoles. Soil $\epsilon = 4$, $\sigma = 5 \times 10^{-6}$ mhos/cm, horizon (grazing path).

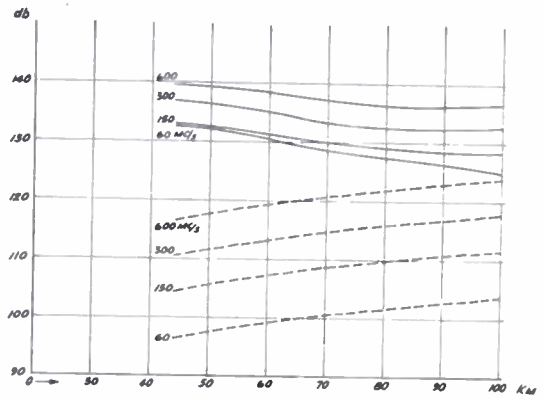

Fig. 3—Attenuation between λ/2 dipoles 20 per cent beyond horizon.

$$-4 \times 10^{-5} \text{ per km} = -1.18 \times 10^{-8} \text{ per foot.}$$

In the case of constant average gradient of refractive index it has been shown by several authors[3-5] that the problem of refraction may be reduced to a problem of diffraction of waves around the earth with an effective radius 4/3 times the actual earth's radius, surrounded by a homogeneous atmosphere. For numerical calculations Norton[6] has published a summary of all the theoretical work done in this direction, giving very useful auxiliary charts to simplify the calculation of field strength. A fairly complete set of graphs from 1.5 to 600 mc was presented by Pfister.[7] For the design of radio relay circuits it is more practical to present the propagation characteristics as attenuation between two half-wave dipoles, because the antenna gain is usually referred to a half-wave dipole. Figs. 2, 3, and 4 show the attenuation for vertically polarized half-wave dipoles over grazing path, and paths 20 and 40 per cent beyond the horizon. For comparison, the free-space attenuation is plotted in dashed lines. The abscissa represents the distance or the corresponding antenna height. Assuming a smooth earth surface, the height for a grazing path

[3] J. C. Schelleng, C. R. Burrows, and F. B. Ferrell, "Ultrashort wave propagation," PROC. I.R.E., vol. 21, p. 427; March, 1933.
[4] T. L. Eckersley, "Ultra-short wave refraction and diffraction," *Jour. IEE* (London), vol. 80, p. 286; March, 1937.
[5] J. E. Freehafer, "The effect of atmospheric refraction on short radio waves," Radiation Laboratory Report 447; 1943.
[6] K. A. Norton "The calculation of ground-wave field intensity over a finitely conducting spherical earth," PROC. I.R.E., vol. 29, p. 623; December, 1941.
[7] W. Pfister "Propagation charts for the entire frequency range," Deutsche Luftfahrtforschung ZWB Research Report 1517; 1941.

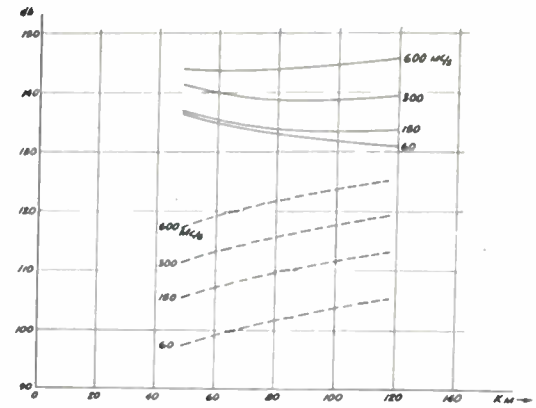

Fig. 4—Attenuation between λ/2 dipoles 40 per cent beyond horizon.

determines the distance, and vice versa. The same applies to a fixed percentage beyond the horizon; the corresponding curves are shown in Fig. 5. From these curves and the available height for the antenna installation, the distance (Fig. 5) for a particular type of path, e.g., grazing path, may be determined. This path distance and the operating frequency are then used in conjunction with the propagation curves (Figs. 2, 3, or 4) to determine the attenuation between the input terminals of the transmitting dipole and the output terminals of the receiving dipole. The gain of the receiving antenna increases the signal level and, therefore, must be added to obtain the signal level at the input to the receiver.

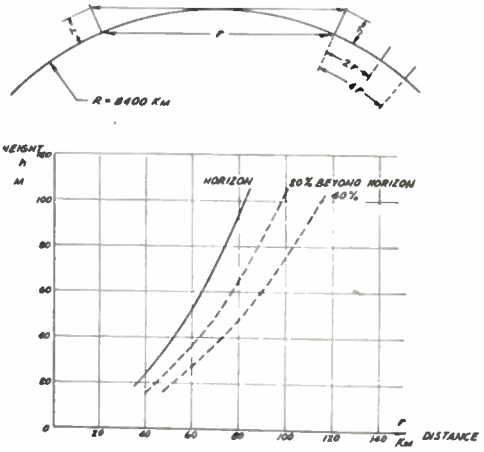

Fig. 5—Relation between antenna height and distance.

It should be recalled that all theoretical propagation figures are derived for average conditions of the atmosphere and assume a uniform smooth earth. They, therefore, represent average values which will deviate more or less from the actual conditions. The deviation from a smooth earth may be taken in account by figuring the elevation of the antennas from the average level of the terrain, instead of using the sea level as a reference. This will give a fairly good approximation to the average signal, but it still does not consider the variation of the atmospheric conditions.

The lower atmosphere, the so-called troposphere, is by no means homogeneous and it varies considerably,

and with it the refraction properties causing variations in the propagation attenuation. Also, multipath propagation, due to tropospheric anomalies, may affect the propagation attenuation. Although many investigations have been carried out in recent years, the physical effects causing anomalies of tropospheric propagation are not yet fully recognized and correlated to the practical observed variations in field strength.

For realistic design data, it is advisable to use experimental results. Due to the lack of satisfactory correlation of present propagation data with meteorological factors, the former have to be evaluated statistically. Based on experience, the following statistics should prove to be satisfactory. The observed normal signal in fading-free periods agrees fairly well with the calculated signal. Due to more or less deep fadings, the signal drops below the normal signal for a certain percentage of time. Evaluating the percentage of time (probability) within which the signal drops below a certain limit, e.g., 10 or 20 db below the normal level, one can find the depth of fading corresponding to a required reliability.

Fig. 6 summarizes in the described manner some of

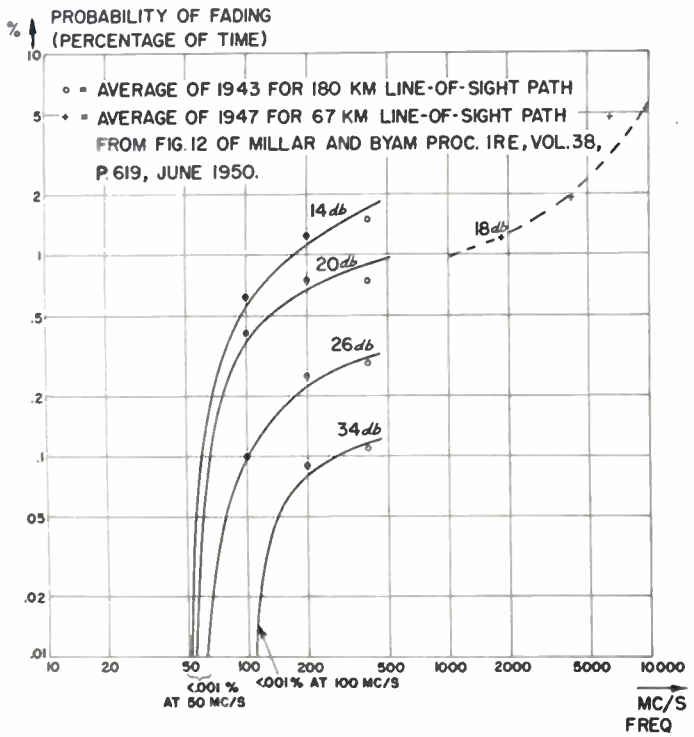

Fig. 6—Percentage of time during which signal fell below indicated amount below normal.
○ average of 1943 for 180-km line-of-sight path
+ average of 1947 for 67-km line-of-sight path from Fig. 12 of Millar and Byam, PROC. I.R.E., vol. 38, p. 619; June, 1950.

the results of extensive propagation tests.[8] The tests were performed over a period of two years and more, on different paths and at frequencies between 60 and 400 mc. Fig. 6 shows the probability for fadings of different depths versus frequency observed on a 110-mile line-of-sight path over a period of one year (1943). The tests were conducted under moderate climatic conditions in Germany along the Rhine River Valley.[9] Below 100 mc the probability drops rapidly to very low figures, making it highly desirable to use frequencies below this cutoff point. These frequencies permit, to a certain extent, operation beyond line-of-sight. Due to the limited rf bandwidth available in this range, however, only a limited number of rf channels are usable within a certain area. It would be wise to restrict operation in this frequency range to circuits where non-line-of-sight operation is unavoidable. The results shown in Fig. 7 seem to support the assumption that the fadings are primarily due to multipath propagation.

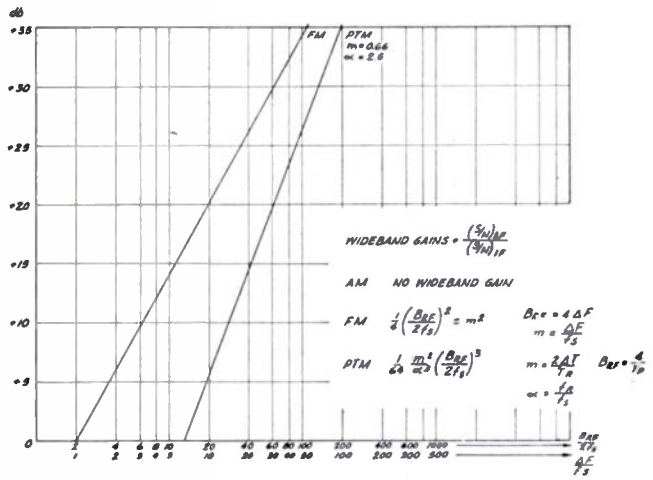

Fig. 7—Wide-band gain of different modulation systems
B_{rf} = rf bandwidth
f_s = maximum signal frequency (modul.)
Δf = frequency deviation (FM)
T_p = pulse width
$f_r = 1/T_r$ pulse repetition frequency.

The discontinuity of the index of refraction in the troposphere due to temperature inversion layers, causes a reflection and the reflected ray meets with the direct ray at the receiving antenna. The latter will be determined by diffraction around the earth and average refractive conditions of the atmosphere below the inversion layer. The superposition of both rays might yield a full addition or subtraction of the amplitude depending upon the difference of path length. Generally, it will vary between both extremes due to variations of the determining parameters. Under fixed topographical conditions, represented by distance and antenna height, and constant refractive index below the inversion layer, only the average elevation of the latter determines the difference in path length. Below a certain frequency, this difference of path length does not produce sufficient phase shift to cause a noticeable fading, which explains

[8] W. Lehfeldt "Die ausbreitung von kurzwellen," *Arch. Elektr. Übertragung*, Vol. 3, p. 137, July 1949, p. 183, August 1949, p. 221, September 1949, p. 265, October 1949, p. 305, November 1949, p. 339, December 1949; (see abstract 982, PROC. I.R.E., Vol. 38, p. 589; May, 1950.

[9] A recent publication by J. Z. Millar and L. A. Byam "A microwave propagation test," PROC. I.R.E., vol. 38, p. 619; June, 1950, deals with propagation under similar conditions at frequencies above 2,000 mc. Statistical values for 18-db fadings taken from Fig. 12 of the paper are marked in Fig. 6 of this paper, and show a remarkable correlation.

the observed drop in probability of fadings. Diversity recordings performed over the same radio path at the same time proved the existence of multipath propagation supporting the above-described explanation of fadings.

In a recent study by Booker and Gordon[10] it has been shown that these propagation effects might also be caused by scattering due to atmospheric turbulence. It will result essentially in the same effect on the radio signal as reflection from inversion layers. Because of the lower energy due to scattering this effect probably will be more serious at larger distances. From the above reasoning it is to be expected that the cutoff frequency of fadings will depend on the distance and antenna heights (topographic constants) as well as the elevation of the reflecting portion of the troposphere (meteorological conditions). In practical application these parameters might vary, but from comparison of results obtained from different radio paths, the graphs shown in Fig. 6 were chosen because they represented the worst case due to the long range and large antenna height.

IV. Receiver

The signal level obtained from the transmitter power, transmitting antenna gain, and propagation data represents the maximum available power from the terminals of a half-wave receiving dipole. After adding the gain of the receiving antenna, the actual signal power at the receiver input is obtained. At this point in the circuit the noise enters into consideration. Physically, the thermal noise is generated in different stages and components of the receiver. For greater convenience, however, the total noise usually is represented by a single noise source at the input terminals of a noiseless receiver. This leads to the common definition of the noise figure[11,12] of a receiver.

$$F = \frac{S_1/N}{S_2/N_2} \tag{2}$$

where S_1 = input signal power
$N_1 = K \cdot T_R \cdot B_{rf}$ = input noise power
S_2 = IF signal output power
N_2 = IF noise output power.

Since the total gain $G = S_2/S_1 = N_2/N_e$ of the receiver holds for the signal as well as for the noise the equivalent noise power N_e at the input terminals of the receiver becomes

$$N_e = F \cdot K \cdot T_R \cdot B, \tag{3}$$

where

$$K = 1.38 \times 10^{-23} \frac{\text{watt sec.}}{^\circ \text{ abs.}} = \text{Boltzmann's constant}$$

$$B_{rf} = \frac{1}{V_{max}^2} \int_{-\infty}^{+\infty} V^2(f)df = \text{integrated bandwidth of the receiver}$$

$V(f)$ = selectivity curve (in voltage) of the receiver.

In the level diagram (see Fig. 1) we may now mark the noise level determined by N_e. The difference between signal input level and the noise level N_e is the signal-to-noise ratio at the input of the receiver. This ratio will remain constant throughout the linear portion of the receiver (G=const.). For this reason, the noise figure measurement of the receiver must be restricted to the linear portion of the IF amplifier. Otherwise the noise figure F and the equivalent input noise power N_e would depend on the amplitude at which the measurement is performed. In discussing the noise N_e represented by (3) it is important to note that it depends on the receiver bandwidth. The noise figure F is independent of bandwidth, since it is determined by the circuit and tube characteristics only. This means that any increase of bandwidth, while the signal input remains constant, increases the receiver noise input power, and by the same rate decreases the signal-to-noise ratio. If in an FM system the frequency deviation is increased with no change in transmitter power, the receiver bandwidth must be increased, and as a result the signal-to-noise ratio at the receiver input decreases.

V. Demodulator

As pointed out before, the measurement of noise figure is restricted to operation in the linear portion of the IF system. It is logical, therefore, to include consideration of the nonlinear portion of the IF system with the demodulator. By this definition the demodulator starts in AM systems with the second detector, in FM systems with the limiter and in pulse modulation systems with the second detector ahead of the video amplifier. The output of the demodulator is the af output; in frequency-division multiplexing systems (conventional carrier systems) it means the broad-band output of the receiver, since the multiplexing system is considered separately. This is reasonable, since the multiplexing system can be also used in connection with other transmission systems, e.g., wire systems. In time-division multiplexing systems, however, the demodulator is combined with the multiplexing unit and the demodulator output will be the af output of the individual voice channel.

Regardless of the modulation system, the problem is to find the relation between signal-to-noise at the output and input of the demodulator. Let the ratio of both be defined as the wide-band gain G_{WB}.

[10] H. G. Booker and W. E. Gordon, "Theory of radio scattering in the troposphere," Proc. I.R.E., vol. 38, p. 401; April, 1950.
[11] D. O. North, "The absolute sensitivity of radio receivers," *RCA Rev.*, vol. 6, p. 332; January, 1942.
[12] E. W. Herold and L. Malter, "Some aspects of radio reception at ultra-high frequency," Proc. I.R.E., vol. 31, p. 423, August, 1943, p. 501, September, 1943; and p. 567, October, 1943.

$$G_{WB} = \frac{(S/N)_{AF}}{(S/N)_{IF}}, \qquad (4)$$

where S denotes always the signal power and N the noise power.

This definition is justified because the signal-to-noise ratio improvement due to the wide-band modulation system becomes effective in the demodulator. At the input to the demodulator, the signal depends only on the average transmitter power and the transmission characteristics of the radio path, including the antennas, irrespective of the modulation characteristics. The af output of the demodulator, however, is determined by the modulation characteristics as well as the rf carrier. Using the definition of the wide-band gain according to (4), the result depends on the modulation characteristics only. Table I shows the theoretical wide-band gain for some typical modulation systems.

TABLE I

WIDE-BAND GAIN G_{WB}

AM	$\frac{B_{rf}}{2f_s}-1$	no wide-band gain
PM or FM	$\frac{1}{4}\left(\frac{B_{rf}}{2f_s}\right)^2=m^2$	$m=\frac{\Delta F_{max}}{f_s}$ deviation ratio (modulation index) $B_{rf}=4\Delta F_{max}$
PTM	$\frac{1}{64}\frac{m^2}{\alpha^3}\left(\frac{B_{rf}}{2f_s}\right)$	$m=\frac{2\Delta T_{max}}{T_r}$ = modulation index ΔT_{max} = maximum pulse shift due to modulation $T_p=\frac{4}{B_{rf}}$ = pulse duration $f_r=\frac{1}{T_r}$ = repetition frequency. $\alpha=\frac{f_r}{f_s}$

where f_s means the maximum signal frequency of the carrier system when frequency division is applied for multiplexing. Using time division $f_s = n \cdot f_{s1}$ where n is the number of voice channels and f_{s1} the maximum signal frequency of the individual voice channel. If a marker pulse of the same duration is used, it should be

$$f_s = (n + 1) \cdot f_{s1}.$$

PM and FM may be treated with the same relations if the maximum deviation ΔF_{max} is used and the maximum signal frequency is substituted for f_s. The result represents then the condition for the highest voice channel in both cases of FM and PM. (For a single modulation frequency, FM and PM are identical.) Lower voice channels in an FM system will differ but the highest voice channel represents the worst case, as far as signal-to-noise is concerned. The same applies to PTM systems where PM or FM of the pulse repetition frequency in conjunction with frequency division may be used. The PTM formula is based on the statistical evaluation of the effect of random noise at the demodulator input on the position of the pulse edge used for the demodulation (see Appendix I).

The rf bandwidth requirements of the FM system are based on the distortion requirement for multichannel operation. For a maximum frequency deviation of ΔF maximum the rf bandwidth B_{rf} has to be approximately four times ΔF maximum, in order to minimize interchannel crosstalk. This is about twice the minimum requirement for single-channel operation. In PTM the minimum required bandwidth is determined by the rise time and decay time of the narrowest pulse. Assuming both equal, and tolerating reasonably rounded edges, the rf bandwidth has to be about four times T_P. These figures are reasonable compromises derived from experience and represent a good average for design purposes, although the actual bandwidth might deviate somewhat. As far as the pulse width is concerned, the calculations are based on the assumption that the pulse duration is not larger than required by the rise and decay time. In the first approximation, such a pulse can be represented by a triangular shape with a width at the half voltage point equal to the rise time T_P. Any larger pulse width would result in wasted power, because the duty cycle T_p/T_r determines the peak power for a given average transmitter power.

Under these assumptions the formulas in Table I are derived, and Fig. 7 shows the wide-band gain versus $B_{rf}/2f_s$ for both modulation systems. The modulation index $m \leqq 1$ for PTM will be limited to about 0.65 or less for practical reasons (linearity of modulation) in the case of frequency division. In time division it changes to $m = n(2\Delta T/T_r)$; however, its numerical value will be practically the same. Once the ratio of rf bandwidth to signal frequency is chosen, Fig. 7 illustrates the corresponding factor by which the af signal-to-noise is increased in comparison to the IF signal-to-noise ratio.

These are the theoretical aspects, while practically speaking there is a deviation from the theoretical figures. Due to the deficiency of conversion of the modulated wave into the intelligence, in comparison to the random noise, the actual wide-band gain will be smaller than the theorectical. In FM demodulators such an effect might be produced by insufficient limiting action; in PTM demodulators, by inevitable tolerances in determining the instantaneous position of the pulse in the presence of noise. The cause, in any case, will be determined by the characteristics of the demodulator used and cannot be expressed in general terms. From experience, however, it is known that in PTM systems for example, an increase of the number of successive clippings and the like increases the efficiency (i.e., the af signal-to-noise) as shown by Moskowitz and Grieg.[13] In some practical sets a difference of 10 to 20 db be-

[13] S. Moskowitz and D. D. Grieg "Noise-suppression characteristics of pulse-time-modulation," PROC. I.R.E., vol. 36, p. 446; April, 1948.

tween the theoretical and practical wide-band gain has been observed. Such discrepancies evidently cannot be neglected. Thus, in all modulation systems under similar conditions, the measured wide-band gain must be used instead of the calculated.

The ratio of theoretical and actual gain shall now be defined as demodulator deficiency.

$$D = \frac{\text{theoretical wide-band gain}}{\text{practical wide-band gain}}. \qquad (5)$$

This factor represents a loss and must be subtracted from the calculated signal-to-noise ratio at the af output, unless the practical wide-band gain directly is used for the calculation. The above-defined deficiency is also a very practical figure for the demodulator design which helps the designer to check how close his demodulator approaches the theoretical limit. It provides an absolute figure similar to the noise figure of the rf receiver for comparing different types of demodulators.

Like the noise figure, the practical wide-band gain has to be determined experimentally. The measurement, however, is somewhat more complicated because the rf carrier has to be present in order to get correct results. Besides, a minimum amplitude of the carrier with respect to the noise is required, because the wide-band gain becomes effective only above this limit, the so-called threshold. The noise level is determined by the receiver noise figure: thus the threshold level is dependent upon it. According to (3a) this threshold becomes:

$$\text{PM or FM threshold} = F \cdot K \cdot T_R \cdot B_{rf} \qquad (6)$$

$$\text{PBM threshold} = 100\alpha \cdot F \cdot K \cdot T_R \cdot f_S.$$

In PM and FM the threshold is equal to the noise level of the receiver. The PTM threshold is based on a noise peak voltage which equals one-half of the pulse peak, the usual clipper limit. The peak voltage of the random noise in this case is defined as 2.5 times the rms value which corresponds to a peak expectation of about 5×10^{-3}. Fig. 8 shows a graph of the threshold power versus

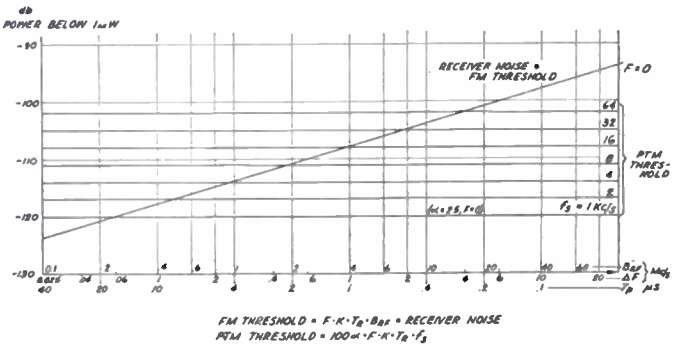

Fig. 8—Receiver noise and threshold power.

rf bandwidth in both modulation systems for 0-db noise figure. For any given noise figure the value (in db) has to be added to the figures on the graph. The two systems behave quite differently, in so far as the PTM threshold is independent of rf bandwidth (B_{rf}) at a given signal frequency f_s. Thus, the wide-band gain can be increased without increasing the threshold. In FM systems, however, the threshold goes up proportionally with the rf bandwidth. In the PTM system this is due to the increase of pulse peak by the same rate as the pulse width is decreased for constant average transmitter power. The PTM system, therefore, becomes superior to FM for greater wide-band gain (see Fig. 8). In PTM systems with time-division multiplexing equipment $f_s = n \cdot f_{s1}$ as has been assumed for the wide-band gain calculation.

For design purposes the threshold is important because it determines the minimum permissible signal. In order to obtain a high degree of reliability, the probability that a signal will fade below the threshold should be as low as possible. Fig. 6 provides the information from which the fade margin at different radio frequencies may be estimated. By this means it is possible to anticipate the reliability of the transmission at a given frequency, or to find the proper operating frequency for a required reliability, after the signal-to-noise ratio at the receiver input has been determined.

VI. Audio System

With the information available from the preceding section, the signal-to-noise ratio at the audio output of the system can be determined. In single-channel transmission it is identical with the signal-to-noise ratio of the voice channel output; in multichannel systems using conventional carrier multiplexing equipment (frequency division multiplexing), it represents the signal-to-noise ratio of the broad-band output. The broad-band terminal output combines the signals of all traffic voice channels. If speech is transmitted over any arbitrary number n of voice channels, the envelope of the common output voltage of the multiplex equipment consists of the linear sum of the instantaneous voltages of the individual channels. Due to the statistical distribution of peaks in the speech voltage of each talker, the peaks of the linear sum are also distributed statistically. The modulation capabilities of the radio transmitter are designed according to the peak expectation at the broad-band terminal. Knowing the ratio of the peaks V_n of n channels to the peak V_1 of one channel the reduction of modulation per channel with respect to full modulation can be established. The problem of determining this ratio V_n/V_1 has been treated by different authors theoretically, as well as experimentally. An excellent and simple theoretical method developed by Jacoby and Spenke[14] has been used to compute the ratio of V_n/V_1. The result is in very good agreement with experimental results obtained in an extensive investigation of the problem by Holbrook and Dixon.[15]

[14] H. Jacoby and F. Spenke, "Ein neuer Beitrag zur Ermittlung der erforderlichen Leistung von Trägerfrequenz-Vielfachverstärkern," Veröffentlichungen a. d. Gebiet d. Nachrichtentechnik, vol. 9, p. 135, No. 1; 1939.

[15] B. D. Holbrook and J. T. Dixon, "Load rating theory for multichannel amplifiers," *Bell. Sys., Tech. Jour.*, vol. 18, p. 624; October, 1939.

Besides the reduction in modulation, the noise level per channel is reduced by the ratio of total bandwidth at the broad-band output to single voice channel bandwidth. The former is usually very close to the maximum signal frequency f_s. Assuming a full utilization of the broad-band, the ratio is equal to n, the number of voice channels. Thus the signal-to-noise per channel may be obtained from the broad-band signal-to-noise ratio by using the following correction factor:

$$\frac{SNR \text{ per channel}}{SNR \text{ broad-band}} = \frac{(V_1)^2}{(V_n)^2} \cdot n \qquad \cdot (7)$$

where

n = number of voice channels
V = peak voltage of n channels
V_1 = peak voltage of one channel.

The ratio V_1/V_n has been computed and the correction factor is shown in Fig. 9 expressed in db. Depending on the sign of the correction factor it has to be added (plus sign) or subtracted (minus sign) from the broad-band signal-to-noise in order to obtain the per channel signal-to-noise ratio.

It should be recalled that in time-division systems this correction factor is unnecessary; the graph in Fig. 7 yields directly the wide-band gain for the per channel signal-to-noise ratio when nf_{s1} is substituted for f_s.

VII. Conclusions

Two typical examples will demonstrate the use of the presented material and how the result may be readily used to derive conclusions as to the choice of appropriate system parameters. In the first section of Table II the given system parameters are listed; in the second, the calculation of the per channel signal-to-noise is carried out. Second column shows which of the graphs is used to obtain value listed in the same line.

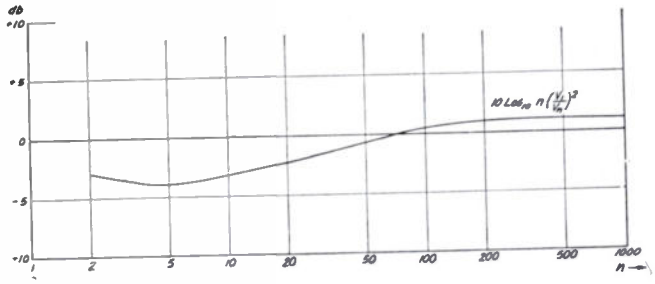

Fig. 9—Correction of broadband S/N for single channel S/N in frequency division multiplex systems.
n = number of voice channels
V_1 = peak voltage of one channel
V_n = peak voltage of n channels
Traffic factor = 0.5.
Peak limiter of the individual channel at 1.5 volts at *Odbm*.

Although the high rf (600 mc) transmission using PTM yields a fairly good af signal-to-noise ratio at average propagation conditions it fails completely in 0.1 per cent of the time, due to the relatively high threshold (−87 db). Using FM instead of PTM, approximately the same af signal-to-noise could be obtained at average conditions. In 0.1 per cent of the time the signal-to-noise ratio will still be 7 db and a

TABLE II

(a) System Characteristics
20 Per Cent Beyond Horizon
$h = 60'$ $r = 27.5$ miles

Transmitter power	50 watts or +47 dbm	50 watts or +47 dbm	
Antenna gain	6 db	15 db	
RF frequency	60 mc	600 mc	
Receiver noise figure	10 db	15 db	
Maximum signal frequency fs	20 kc	60 kc	
Modulation system	FM	PTM	FM
Frequency deviation	40 kc	—	120 kc
Pulse width T_P	—	0.5 μs	—
RF bandwidth B_{rf}	$4\Delta F = 160$ kc	$4/T_P = 8$ mc	$4\Delta F = 480$ kc
Number of voice channels	4	12	
Voice channel band	4 kc	4 kc	

(b) Transmission Parameters, According to the Presented Graphs

	Fig. No.	FM			PTM			FM		
Transmitter Power		+47 dbm			+47 dbm					
Transmitter antenna gain		+6 db			+15 db					
Power radiated		+53 dbm			+62 dbm					
Average propagation attenuation	3	−133 db			−140 db					
Receiver antenna gain		+ 6 db			+ 15 db					
Margin for fadings 0.1 per cent of time	6	Average		−10 db Lowest	Average		−35 db Lowest	Average		−5 db Lowest
Receiver input signal	8	−74 dbm		−84 dbm	−63 dbm		−98 dbm	−63 dbm		−98 dbm
Receiver input noise			−112 dbm			−90 dbm			−102 dbm	
Threshold			−112 dbm			−87 dbm			−102 dbm	
S/N_{IF}		38 db		28 db	27 db			39 db		4 db
Theoretical wide-band gain	7		+ 6 db			+21 db			+ 6 db	
S/N_{AF}		44 db		34 db	43 db		Failure in 0.1 per cent of time	45 db		
Correction per channel	9		− 4 db			− 3 db			− 3 db	
S/N per channel		40 db		30 db	45 db		Signal below threshold	42 db		7 db

complete failure will occur only in about 0.05 per cent of the time. This result shows the advantage of FM in this particular case. Besides this the required rf bandwidth is much smaller (0.48 mc) than for PTM (8 mc). The table shows also how the conditions are improved if one of the parameters is changed in order to find out which one will be the most efficient. Usually the transmitter power and receiver noise figure are fixed by the equipment characteristics determined primarily by the practical limits of the respective tubes. Doubling the antenna size for both transmitter and receiver will give a total increase of +6 db. Approximately the same result can be achieved by raising both antennas from 60 to 90 feet. Another possibility would be an increase of the wide-band gain, e.g., by increasing the frequency deviation from ±120 to ±180 kc. Due to increasing the rf bandwidth to $B_{rf}=720$ kc, the over-all improvement in this case is only 1 db, but the ratio of rf signal input to threshold is reduced by 2 db. This means a reduction in reliability unless the signal input is increased by changing the antenna gain or height at the same time. These figures show that an increase of wide-band gain in FM systems necessarily reduces the margin for fadings. For design purposes it therefore would be advisable to start with the margin which can be tolerated (reliability), and then to calculate the corresponding frequency deviation. If the rf signal input is varied, the frequency deviation can be changed correspondingly. By this means a graph of ΔF versus rf input for different reliability (fade margin) figures can be drawn to help the designer to find the most practical compromise in his specific case. All necessary figures can be obtained from the presented graphs.

The low-frequency example (60 mc) shows a lower average signal because of the small antenna gain, but the reliability is much superior. In 0.1 per cent of the time the signal will drop only 10 db; it practically will never fall below the threshold.

Appendix I

The derivation of the PTM signal-to-noise formula used for the wide-band gain computation of Table I is outlined below:

Provided that the bandwidth is essentially determined by the rise time of the pulse, the slope of the pulse and noise curve at the intersection with the clipper limit is

$$V_S'(t) + V_N'(t) \tag{8}$$

$V_S'(t)$ = 1st derivative of signal (pulse) $V_S(t)$

$V_N'(t)$ = 1st derivative of noise $V_N(t)$

and the shift of the pulse-plus-noise curve against the pulse edge without noise

$$|\tau| = \frac{V_N(t)}{V_S'(t) + V_N'(t)}. \tag{9}$$

The symbol τ represents the instantaneous af noise amplitude. From the probability density function of random noise

$$p(V_N)dV_N = \frac{dV_N}{\sqrt{2\pi}\,V_N}\, e^{-V_N^2/2V_N^2} \tag{10}$$

V_N = noise amplitude at random time

V_N = rms noise voltage,

the probability density $p(\tau)d\tau$ may be obtained, which yields the mean square

$$\overline{\tau^2} = \int_{-\infty}^{+\infty} \tau^2 p(\tau)d\tau = \frac{1}{[V_S'(t)]^2}\int_{-\infty}^{+\infty} V_N^2 p(V_N)dV_N = \frac{V_N^2}{[V_S'(t)]^2}. \tag{11}$$

The term $V_N'(t)$ does not contribute to the noise because the slope of the random noise function is distributed at random from negative to positive values, thus, giving zero for the mean slope.

Equation (11) represents the mean square of the pulse deviation due to the presence of noise at the demodulator (clipper) input. If the modulation amplitude deviates the pulse by ΔT maximum the rms af voltage signal-to-noise becomes

$$\frac{S}{N} = \frac{\Delta T_{max}}{\sqrt{2}}\,\frac{1}{\sqrt{\overline{\tau^2}}} = \frac{\Delta T_{max}}{\sqrt{2}}\,\frac{V_S'(t)}{V_N} = \frac{1}{\sqrt{2}}\,\frac{A_p}{V_N}\,\frac{\Delta T_{max}}{T_p}. \tag{12}$$

where

A_p = pulse peak amplitude

T_p = pulse width = rise time

$V_S'(t) = A_p/T_p$ = slope of pulse edge.

A Spatial Harmonic Traveling-Wave Amplifier for Six Millimeters Wavelength*

S. MILLMAN†, SENIOR MEMBER, IRE

Summary—This paper describes a traveling-wave amplifier in which the electron beam interacts with a spatial harmonic of an electromagnetic wave propagating along an array of resonator slots. The result is a considerable reduction in operating beam voltage for a given physical separation of the circuit elements. This type of amplifier operating at about 1,200 volts has yielded net power gains of about 18 db in the 6-mm wavelength region. A magnetic field of about 1,600 gauss is sufficient for proper beam focusing. Aside from small variations of gain with frequency caused by internal reflections, the bandwidth is of the order of 3 per cent.

I. Introduction

THE TRAVELING-WAVE principle for wide-band amplification has first been applied successfully in the 3,000 to 4,000 mc region by Kompfner[1] and by Pierce and Field,[2] using a helix for the electromagnetic circuit. More recently Field[3] has extended the application of the helix-type tube to 10,000 mc and has obtained second harmonic output in the 20,000-mc region. Other forms have also been employed by Field[3] for the 10,000-mc region. A 3-db gain has been reported for a helix tube at 6 mm by Little.[4] The extension of these techniques to the millimeter range is made difficult by the necessity of building tiny structures for the circuit elements, particularly for moderately low voltages.

In this paper we shall describe the principle of operation and present preliminary results obtained with a traveling-wave amplifier in which the electrons move much slower than the electromagnetic wave in the circuit. Synchronism is maintained between the electron velocity and a spatial harmonic of the wave. This type of amplifier is particularly suited for the operation at wavelengths less than one centimeter. Results obtained with a tube designed for amplifying 6-mm radiation will be described.

II. Principle of Operation

Consider a filter type repetitive structure such as the array of resonator slots shown in Fig. 1. Suppose there is set up in the circuit a traveling electromagnetic wave moving in the z direction with a phase velocity v. Let θ be the phase displacement between the centers of adjacent slots separated by a distance d, so that

$$\theta = \frac{2\pi d}{\lambda_g} \tag{1}$$

where λ_g is the wavelength in this structure. The time taken for the wave to move a distance d is $(\theta/2\pi)T$,

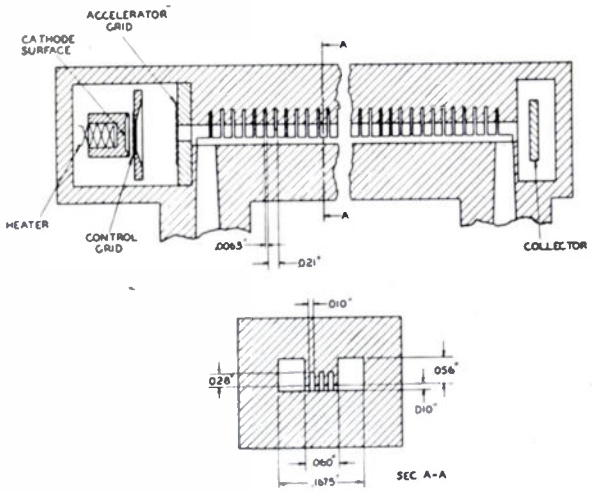

Fig. 1—Schematic diagram of spatial harmonic traveling-wave tube.

where T is the period of oscillation. We have then

$$v = 2\pi \frac{d}{\theta T} = \frac{\omega d}{\theta}. \tag{2}$$

If we were to have a traveling-wave tube in which the electrons are to interact with this wave the electron velocity would have to be approximately equal to v as

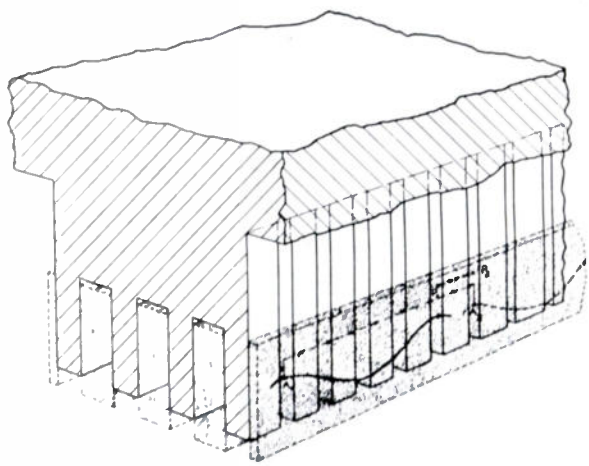

Fig. 2—Portion of interaction region indicating relative speeds of electrons and electromagnetic wave in a spatial harmonic amplifier.

given by (2), and the time taken for an electron to move from one slot to the adjacent slot would be θ/ω.

* Decimal classification: R339.2. Original manuscript received by the Institute, November 22, 1950; revised manuscript received, April 13, 1951.

† Bell Telephone Laboratories, Inc., Murray Hill, N. J.

[1] R. Kompfner, "The traveling-wave tube as an amplifier at microwaves," PROC. I.R.E., vol. 35, pp. 124–127; February, 1947.

[2] J. R. Pierce and L. M. Field, "Traveling-wave tubes," PROC. I.R.E., vol. 35, pp. 108–111; February, 1947.

[3] L. M. Field, "Some slow-wave structures for traveling-wave tubes," PROC. I.R.E., vol. 37, pp. 34–40; January, 1949.

[4] Paper presented at IRE Conference on Electron Devices at Ann Arbor, Michigan, June, 1950.

Suppose, however, that the electron speed is considerably slower than this wave velocity and that the electron traverses a distance d in a time $(\theta/\omega)+T$; it will find the same phase of the electromagnetic wave at P_2 as at P_1, as shown in Fig. 2. If such a phase represents an optimum condition for interaction between the electrons and the wave, such as would be the case when the peaks shown in Fig. 2 represent the maximum retarding force on a bunched electron beam, synchronism is maintained by having a peak of the electromagnetic wave at a slot whenever the bunched electrons pass the slot. The electron speed required for this synchronism is

$$v_e = \frac{d}{T + \frac{\theta}{\omega}} = \frac{\omega d}{2\pi + \theta} \tag{3}$$

instead of $\omega d/\theta$ as for the case when the electrons are in synchronism with the fundamental to the wave. Adverse interaction between the bunched electrons and the wave, during the part of the cycle for which the phase is exactly wrong, is minimized by having the electrons at that part of the cycle close to the metal walls where the axial component of the electric field vanishes.

This type of synchronism between the electron and electromagnetic wave is similar to that present in some early forms of microwave magnetron oscillators having non-π-mode operation. These magnetrons were operating in a Hartree harmonic[5] of one of the modes of the resonant system, in which the synchronism was between the electron bunches having an angular velocity in the opposite direction to that of the electromagnetic wave.

An equivalent analytical expression of the above may be obtained by representing the axial component of the electric field of the traveling wave by the relation

$$E_z = F(z)e^{j\omega t} \tag{4}$$

where

$$F(z) = \sum_{n=0}^{n=\infty} A_n e^{-j(2\pi n+\theta)z/d}. \tag{5}$$

We assume that the amplitude of E_z is constant at the mouth of the slots and denote it by E_0. From (5)

$$A_n = \frac{E_0}{d}\int_{-W/2}^{+W/2} e^{j(2\pi n+\theta)z/d}dz$$

$$= \frac{2E_0}{2\pi n + \theta}\sin\left[(2\pi n + \theta)\frac{W}{2d}\right] \tag{6}$$

where W is the width of the slot.

Combining (4), (5) and (6) gives

$$E_z = E_0\sum_{n=0}^{n=\infty}\frac{2\sin\left[(2\pi n+\theta)\dfrac{W}{2d}\right]}{2\pi n+\theta}e^{j[\omega t-(2\pi n+\theta)z/d]}. \tag{7}$$

Thus E_z is represented as a Fourier sum of traveling waves with different phase velocities. The component wave corresponding to $n=1$ is given by

$$E_{z1} = E_0\frac{2\sin\left[(2\pi+\theta)\dfrac{W}{2d}\right]}{2\pi+\theta}e^{j[\omega t-(2\pi+\theta)z/d]}. \tag{8}$$

This represents a wave moving in the direction of increasing z with a phase velocity $\omega d/(2\pi+\theta)$, which is the same as that given in (3).

Thus for the type of traveling-wave tube considered in this paper the electrons may be said to interact with the first Fourier spatial harmonic of the electromagnetic wave. In operating the amplifier in this harmonic rather than in the fundamental the electron speed is reduced by the factor $(2\pi+\theta)/\theta$, and the beam voltage by the square of this factor. For higher order spatial harmonics the reduction factor in the electron speed is given by $(2\pi n+\theta)/\theta$. However, there is little or no practical advantage in extending the principle of spatial harmonic operation beyond $n=1$, since this would not lead to wider resonator slots for any given beam voltage.

III. Design and Construction

A schematic representation of the essential parts of the 6-mm spatial harmonic traveling-wave tube is shown in Fig. 1. There are 100 transverse slots of approximately $\frac{7}{8}$ of a quarter-wavelength in depth, spaced 0.021 inch between slot centers. The ratio of slot width to the distance between centers, (W/d), is 0.3 and is based on maximizing the electron interaction with the first spatial harmonic of the electromagnetic wave.[6] Three axial slots, 0.010 inch wide, are cut through all of the copper fins to about half the depth of the transverse slots in order to increase the interaction space in which there is an appreciable axial component of the electric field.

The rf input and output to the tube consist of tapered waveguides extending in a direction perpendicular to the tube axis. The narrow ends of the guides open into the wall facing the mouths of the resonators. The appropriate terminating impedance for the resonator structure can be calculated approximately from the equivalent circuit representation given below. The actual dimensions of the narrow end of the waveguide as well as the location of the guide with reference to the last resonator slot have, however, been determined experi-

[5] Microwave Magnetron, MIT Radiation Laboratory Series, p. 32, McGraw Hill Book Co., New York, N. Y., 1948.

[6] See Eq. (46) in the Appendix.

[6] J. R. Pierce, "Theory of the beam-type traveling-wave tube," Proc. I.R.E., vol. 35, pp. 111–123; February, 1947.

mentally, since the simple calculations do not include end-effects near the input and output. An enlarged view of the output end of the tube is shown in Fig. 3. The reflecting properties of this termination are shown in Fig. 4 where the reflection coefficient is plotted as a function of wavelength for one termination when lossy material is introduced in the resonators to eliminate reflection effects of the other end. The data have been obtained with a scaled model at 3.3-cm wavelength region. The appropriate 6-mm wavelengths are also indicated for convenience. The glass output windows are of the same type as used in 1.25-cm magnetrons and klystrons, except that the metal cup used is made of molybdenum instead of kovar. This iron alloy has also been eliminated from all other metal-to-glass seals to facilitate the application of a uniform magnetic field parallel to the axis of the tube. A field strength of about 1,600 gauss is required for the operation of the tube.

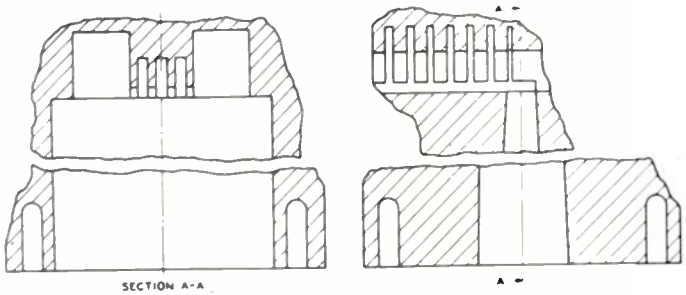

Fig. 3—Sectional views of output end of the amplifier.

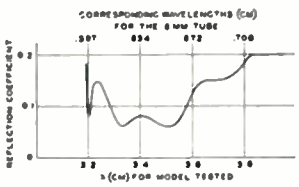

Fig. 4—Reflection introduced by one termination to the circuit shown in Fig. 3.

The requirement that the electrons move in long narrow slots makes it necessary to design the electron gun so that a minimum of transverse motion is imparted to the electrons. Both the control grid and the accelerating grid are wound with closely spaced tungsten wire on molybdenum frames. In the accelerating grid the wires are 0.0008 inch in diameter and 0.004 inch between centers. In the control grid the wires are 0.0004 inch in diameter and the spacing is 0.0033 inch. The two grids are about 0.105 inch apart and the distance between control grid and the planar cathode surface is about 0.020 inch. When the control grid is kept at about +100 volts the electric field is approximately the same on both sides of the grid for the cathode emission densities used (about 1.0 amp/cm^2). This condition reduces the average transverse velocity imparted to the electrons by the control grid.

The cathode is made of oxide-coated nickel and its active area is a rectangle of dimensions large enough to flood the interaction region. No attempt has been made to shape the active area to correspond to the desired cross section of the electron stream. With this arrangement about one half of the electrons leaving the control grid are intercepted by the accelerating grid and the first copper fin. In the operation of the tube about 60 per cent of the electrons entering the interaction space reach the collector plate. The collector is kept at about 50 volts positive with respect to the body of the tube in order to prevent secondary electrons from leaving the collector and thus giving an inaccurate measure of the fraction of electrons that reach it. Photographs of the circuit parts of the amplifier are shown in Fig. 5.

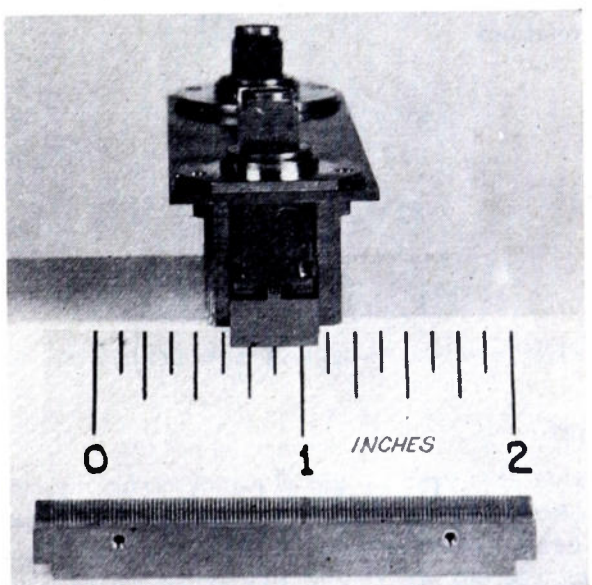

Fig. 5—Photographs of circuit parts of the 6-mm amplifier. The lower photograph shows the array of 100 transverse resonator slots. The upper photograph shows an end view of the assembled circuit, including the 3 longitudinal slots. The four narrow slots shown at the bottom of the waveguide are there for the purpose of inserting copper strips to effect an rf short between the outer wall of the waveguide and the appropriate place of the resonator structure, as shown in Fig. 3.

IV. Equivalent Circuit Representation

The design of the spatial harmonic amplifier is considerably facilitated by setting up an approximate lumped-constants equivalent of the electromagnetic circuit. This is shown in Fig. 6, where the circuit constants associated with each of the slots are denoted by L_s and C_s, the corresponding constants for the shunt impedances by L_p and C_p, and losses have been neglected.

With the aid of this equivalent circuit we can easily calculate the following quantities:

1. θ, the phase displacement per section, from which we determine the operating voltage and its frequency dependence.
2. Z_0, the required terminating impedance for this filter type structure.
3. $|Z_s^2|/Z_0$, a quantity which enters in the calculation of the expected gain of the amplifier.

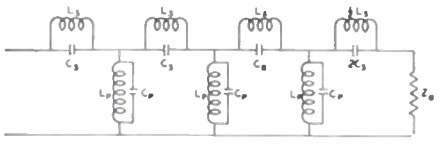

Fig. 6—Lumped constants representation of amplifier circuit.

The phase displacement per section is obtained from the relations

$$\cos\theta = 1 + \frac{Z_s}{2Z_p}$$

$$Z_s = j\frac{r}{C_s\omega_s(1-r^2)} \tag{9}$$

$$Z_p = j\frac{r}{C_p\omega_s\left(\frac{\omega_p^2}{\omega_s^2} - r^2\right)}$$

where

$$\omega_s^2 = \frac{1}{L_sC_s}, \quad \omega_p^2 = \frac{1}{L_pC_p}, \quad \text{and} \quad r = \frac{\omega}{\omega_s}. \tag{10}$$

Combining eqs. (9) we have

$$\cos\theta = 1 - \frac{C_p}{2C_s}\frac{r^2 - \frac{\omega_p^2}{\omega_s^2}}{1-r^2}. \tag{11}$$

A plot of θ as function of r is shown in Fig. 7 for the values $C_p/C_s = 0.8$ and $\omega_p/\omega_s = 0.25$. These parameters correspond very closely to those used in the amplifier here described.

In order to have the operating voltage of the amplifier independent of frequency, at least to a first order, the frequency of the midband should be chosen at a point where the tangent to the curve shown in Fig. 7 intercepts the θ axis at a value $\theta = -2\pi$. Since the phase velocity for the first spatial harmonic is given by $\omega d/\theta + 2\pi$, a fractional change in the phase constant at this point is compensated by an equal fractional change in frequency, i.e.,

$$\frac{\delta\theta}{\theta + 2\pi} = \frac{\delta r}{r} = \frac{\delta f}{f} \tag{12}$$

leaving the phase velocity unchanged.

From (12) and (1) we have

$$\frac{df}{d\left(\frac{1}{\lambda_g}\right)} = \frac{\omega d}{2\pi + \theta}. \tag{13}$$

Since

$$\frac{df}{d\left(\frac{1}{\lambda_g}\right)}$$

is the expression for the group velocity of a wave we see from (13) and (3) that, for the indicated region of operation of the amplifier here described, the phase velocity of the Fourier component wave with which the electrons are interacting is the same as the group velocity of the wave.

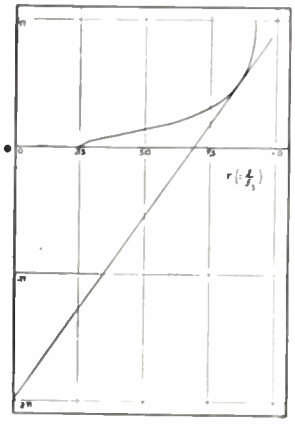

Fig. 7—Phase shift between adjacent resonators as a function of frequency in units of f_s, the resonant frequency of the slots.

The characteristic impedance Z_0 of this filter, when considered as an array of T sections is given by

$$Z_0 = \sqrt{Z_sZ_p + \frac{Z_s^2}{4}}$$

$$= \frac{1}{C_s\omega_s}\frac{r}{1-r^2}\sqrt{\frac{1-r^2}{\frac{C_p}{C}\left(r^2 - \frac{\omega_p^2}{\omega_s^2}\right)} - \frac{1}{4}}. \tag{14}$$

The quantity $|Z_s^2|/Z_0$ is given by

$$\frac{|Z_s^2|}{Z_0} = \frac{1}{C_s\omega_s}\frac{r}{1-r^2}\left[\frac{1-r^2}{\frac{C_p}{C_s}\left(r^2 - \frac{\omega_p^2}{\omega_s^2}\right)} - \frac{1}{4}\right]^{-1/2}. \tag{15}$$

Plots of the quantities $Z_0C_s\omega_s$ and $(|Z_s^2|/Z_0)C_s\omega_s$ as functions of r are shown in Figs. 8 and 9 for the same values of the circuit parameters as used in Fig. 7.

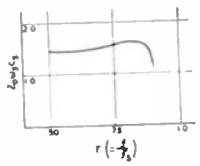

Fig. 8—Characteristic impedance of the circuit, in units of ω_sC_s as a function of frequency.

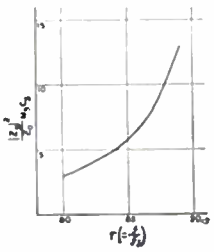

Fig. 9—Plot of the quantity $(|Z_s^2|/Z_0)\omega_sC_s$ as a function of frequency.

V. Performance of Spatial Harmonic Amplifiers

The general performance of the spatial harmonic traveling-wave amplifier is in good agreement with the prediction of the theory. The operating voltage for the tube and the variation of voltage with wavelength, including the voltage maximum at midband, is very closely that predicted by the simple theory given in Section II and by the equivalent circuit calculations. A plot of observed operating voltage at low currents versus wavelength is exhibited in Fig. 10.

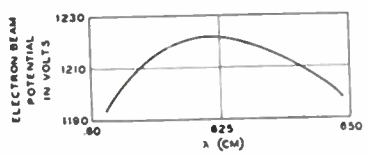

Fig. 10—Operating voltage of amplifier for optimum gain at low currents as a function of wavelength.

The observed net power gain of the amplifier as a function of wavelength is shown in Fig. 11 for several values of the collector current. Although the ripples in the curves are not predicted by the theoretical calculations given in the Appendix, the average values of the observed gain agree very well with those predicted by the theory, particularly when one considers the various approximations involved in the calculations. The rapid variations of gain with wavelength are undoubtedly due to internal reflections arising partly from mismatches at the ends of the circuit and partly from small departures from uniformity of the resonator slots. The reflection coefficient resulting from a small departure ΔZ_s from the average impedance of the slot Z_s is given by

$$\rho = \frac{|\Delta Z_s|}{2Z_0} = \frac{|\Delta Z_s|}{|Z_s|}\,\frac{|Z_s|}{2Z_0}. \tag{16}$$

Using (9), (14) and (16) we find for example that, in the region of operation of the amplifier, a change in slot depths by one per cent introduces a reflection coefficient of about 0.07. A change in slot thickness by one per cent gives rise to a reflection coefficient of only 0.01. On the other hand, the percentage fluctuation in slot width is apt to be considerably greater than in slot depth.

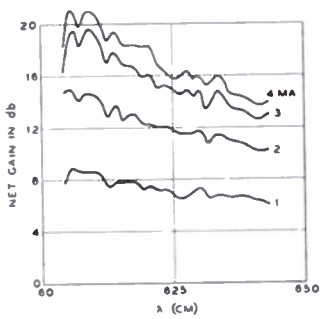

Fig. 11—Net gain of the 6-mm amplifier as a function of wavelength.

The gain curves shown in Fig. 11 have been obtained by adjusting the voltage in each case to obtain the maximum gain for a given wavelength and current. In the wavelength region 0.61 to 0.63 cm, the gain curves are not appreciably affected when the beam voltage is kept constant. Thus, aside from the fluctuations in the gain frequency curves arising from reflections the bandwidth is about 3 per cent.

The power output of the 6 mm amplifier has not been measured. Measurements made on a 1.25-cm scaled version of this amplifier, using a thermistor bridge, gave a maximum output power of about 40 milliwatts for a collector current of 7 ma. From general traveling-wave theory we would expect the output power to be independent of frequency and to depend principally on the current ($\sim I_0^{4/3}$). For a current of 4 ma it should be of the order of 20 milliwatts.

VI. Oscillations

In the helix-type traveling-wave amplifier it is customary to introduce losses in the circuit in order to pre-

vent the tube from oscillating, since it is extremely difficult to effect a good termination of the helix for all frequencies at which it is capable of producing appreciable gain with a given applied beam voltage. In the case of the circuit used for the spatial harmonic tube the amplifier operates with a constant voltage in only a relatively narrow band of frequencies. It was therefore felt that if one can design an output to match the circuit over a bandwidth of about 10 to 15 per cent, one could ignore the termination characteristics at frequencies outside this range, since those would require appreciably different beam voltage for amplification. Actually it was found in the early models of the 1.25-cm version of this amplifier that oscillations in lower frequencies did limit the operation of the tube. Measurement of oscillating frequencies and corresponding beam voltages indicated an amplification in a propagating mode corresponding to a phase displacement per section of θ-2π. This corresponds to a wave propagating in the direction opposite to the electron motion. In Table I we list the long wavelength oscillations, and the corresponding beam voltages observed with one of the 1.25-cm amplifiers.

TABLE I

λ (cm)	Beam Potential (Volts)
1.991	920
1.904	1,020
1.838	1,110
1.780	1,190
1.730	1,270
1.676	1,360

For the same tube the values that correspond to the midband of the amplifying region of interest were 1.24 cm and 1,220 volts, respectively. It is obvious that while it was of interest to measure all of the oscillating frequencies and their corresponding voltages for the purpose of identifying the mode of amplification, only those oscillations that occur at voltages very close to those used in the region of interest need be of any concern. Thus the 1.78-cm oscillation at 1,190 volts was too close for comfort and, indeed, limited the useful operating current to less than 3 ma. It was not surprising to find that the output was very poorly matched to the circuit in that wavelength region. A change in the tapered guide design from one tapered in both dimensions of the guide cross section to one having a taper only in the narrow dimension improved the termination at the 1.78 cm region considerably, without impairing the termination in the amplification region of interest. The dimensions indicated in Fig. 3 correspond to the tube with revised output geometry. With this tube, collector currents as high as 7 ma appeared quite feasible for the 1.25-cm amplifier. There are no losses, other than inherent ohmic losses in the circuit, introduced in the spatial harmonic amplifier. At midband the insertion loss is about 11 db for the 6-mm tube.

VII. Conclusions

The preliminary results reported here point to the feasibility of the spatial harmonic traveling-wave principle for amplification of microwaves up to 50,000 megacycles per second. More gain should be obtainable from this type of amplifier by increasing the length of the tube or by the use of higher density beams. With the development of improved fabricating techniques it should be possible to improve the gain-frequency curve of the 6-mm amplifier and to extend this method to amplifiers of still higher frequencies.

Acknowledgment

The writer wishes to acknowledge his indebtedness to A. M. Clogston, R. C. Fletcher, and J. R. Pierce for stimulating and helpful discussions; to F. H. Best, R. Strnad, R. Azud, and Miss H. Dominguez for assistance in design and construction of the tubes; and to R. F. Heck and G. W. A. Pentico for their assistance in the study of the performance of these amplifiers.

VIII. Appendix

Gain Calculations

We first establish an equivalence between a thick electron beam, as used in the amplifier, and a beam concentrated in a thin sheet. Referring to Fig. 12 we shall require that at $x=b$, the edge of the thick beam, the admittance and its derivative with respect to Γ be the same for the thick beam as the corresponding

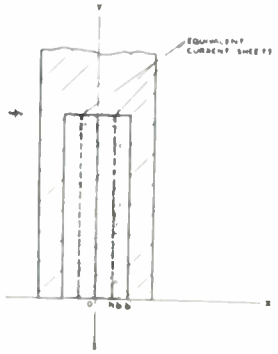

Fig. 12—Cross section of one of the three longitudinal slots showing effective limits of thick beam and equivalent current sheets.

quantities for a current sheet located at $x=h$. The two resulting expressions will locate the position of the current sheet and give the proper current ratio. This is the same as the method followed by Fletcher[7] for the cylindrical case.

[7] R. C. Fletcher, "Helix parameters used in traveling-wave tube theory," Proc. I.R.E., vol. 38, pp. 413–417; April, 1950.

For a thick beam the expression for H_y, corresponding to the axial rf current in the circuit, is given by

$$H_y = A \sinh \alpha' x e^{-\Gamma z}. \tag{17}$$

From Maxwell's equation

$$i\omega\epsilon E_z + J_z = \frac{\partial H_x}{\partial y} - \frac{\partial H_y}{\partial x}$$

we have for $J_z = 0$ and $H_x = 0$

$$E_z = \frac{\Gamma}{j\omega\epsilon} A \sinh \alpha' x e^{-\Gamma z}. \tag{18}$$

Similarly, from the equation

$$i\omega\epsilon E_z + j_z = \frac{\partial H_y}{\partial x} - \frac{\partial H_x}{\partial y}$$

we have

$$j\omega\epsilon E_z + J_z = A\alpha' \cosh \alpha' x e^{-\Gamma z}$$

and since

$$J_z = j \frac{\beta_e J_0}{2V_0(j\beta_e - \Gamma)^2} E_z$$

$$E_z = A \frac{\alpha'}{j\omega\epsilon'} \cosh \alpha' x e^{-\Gamma z} \tag{19}$$

where

$$\epsilon' = \epsilon\left[1 + \frac{J_0\beta_e}{2\epsilon\omega V_0(j\beta_e - \Gamma)^2}\right]. \tag{20}$$

When the expression for H_y, E_x and E_z as given in (17), (18) and (19) are substituted in the Maxwell equation

$$\frac{\partial E_x}{\partial z} - \frac{\partial E_z}{\partial x} = -j\omega\mu H_y$$

we obtain

$$\alpha'^2 = (-\omega^2\mu\epsilon - \Gamma^2)\frac{\epsilon'}{\epsilon} = \alpha^2 \frac{\epsilon'}{\epsilon} \tag{21}$$

where α refers to the free space case.

The admittance at the edge of the beam $x = b$, is given by the expression

$$Y = \frac{H_y}{E} = j \frac{\omega\epsilon'}{\alpha'} \tanh \alpha' b$$

$$= j \frac{\omega\epsilon}{\alpha} \sqrt{\frac{\epsilon'}{\epsilon}} \tanh\left(\sqrt{\frac{\epsilon'}{\epsilon}}\, \alpha b\right). \tag{22}$$

Instead of computing $dY/d\Gamma$ we shall, for the purpose of simplifying the algebra, take derivatives with respect to a quantity proportional to $\beta_e/(j\beta_e - \Gamma)^2$, since it is this quantity rather than Γ that varies rapidly in the region of interest. Let

$$u = \frac{\epsilon'}{\epsilon} - 1 = \frac{J_0}{2\epsilon\omega V_0} \frac{\beta_e}{(j\beta - \Gamma)^2} \text{ from (20).} \tag{23}$$

With this substitution we have at $x = b$, for the case of the thick beam

$$-j \frac{\alpha}{\omega\epsilon} Y = \sqrt{u+1} \tanh (\sqrt{u+1}\, \alpha b) \tag{24}$$

$$-j \frac{\alpha}{\omega\epsilon} \frac{dY}{du} = \frac{\tanh (\sqrt{u+1}\, \alpha b)}{2\sqrt{u+1}} + \frac{\alpha b}{2 \cosh^2 (\sqrt{u+1}\, \alpha b)}. \tag{25}$$

For the equivalent current sheet we assume that the sheet is located at $x = h$. For the region $0 < x < h$ we have

$$H_y = B \sinh \alpha x e^{-\Gamma z} \tag{26}$$

$$E_z = \frac{\alpha}{j\omega\epsilon} B \cosh \alpha x e^{-\Gamma z}. \tag{27}$$

For the region $h < x < b$ we may write

$$H_y = (Ce^{+\alpha x} + De^{-\alpha x})e^{-\Gamma z} \tag{28}$$

and

$$E_z = \frac{\alpha}{j\omega\epsilon} (Ce^{+\alpha x} - De^{-\alpha x})e^{-\Gamma z}. \tag{29}$$

At $x = h$ we require that E_z be continuous and that H_y be discontinuous. We have

$$Ce^{\alpha h} - De^{-\alpha h} = B \cosh \alpha h \tag{30}$$

and

$$(Ce^{\alpha h} + De^{-\alpha h} - B \sinh \alpha h)e^{-\Gamma z} = I_s \tag{31}$$

where I_s is the rf current per unit width of the sheet, and is given by

$$I_s = \frac{I_{s0}}{2V} \frac{\beta_e}{(j\beta - \Gamma)^2} E_z$$

$$= \frac{I_{s0}}{2V} \frac{\beta_e}{(j\beta - \Gamma)^2} \frac{\alpha}{\omega\epsilon} \cosh \alpha x e^{-\Gamma z} \tag{32}$$

making use of (27). Here I_{s0} is the dc current per unit width. We now let

$$I_{s0} = tJ_0 b \tag{33}$$

where t is the ratio of the total current in the sheet to that in the thick beam required to produce equivalent gain. From (31), (32), (33) and (23)

$$Ce^{\alpha h} + De^{-\alpha h} = B[\sinh \alpha h + tb\alpha u \cosh \alpha h]. \tag{34}$$

Combining (30) with (34) gives

$$\frac{C}{D} = e^{-2\alpha h} \frac{\tanh \alpha h + tb\alpha u + 1}{\tanh \alpha h + tb\alpha u - 1}. \tag{35}$$

From (28), (29) and (35) we have at $x = b$ for the case of the current sheet

$$-j \frac{\alpha}{\omega\epsilon} Y = \frac{Ku[e^{2\alpha(b-h)} + 1] + 2(e^{2\alpha b} - 1)}{Ku[e^{2\alpha(b-h)} - 1] + 2(e^{2\alpha b} + 1)} \tag{36}$$

and

$$-j\frac{\alpha}{\omega\epsilon}\frac{dY}{du}=\frac{4Ke^{2ab}[e^{-2ah}+1]}{[Ku[e^{2a(b-h)}-1]+2(e^{2ab}+1)]^2} \tag{37}$$

where

$$K=tb\alpha(e^{2ab}+1). \tag{38}$$

Equating now the expressions for admittance and its derivative for the thick beam to the corresponding expressions for the current sheet, we obtain

$$\sqrt{u+1}\tanh(\sqrt{u+1}\,\alpha b)=\frac{Ku[e^{2a(b-h)}+1]+2(e^{2ab}-1)}{Ku[e^{2a(b-h)}-1]+2(e^{2ab}+1)} \tag{39}$$

per cent of the electrons entering the interaction region reach the collector. When this value of $2b$ is used in (41) and (42) we obtain

$$\alpha h=0.76,\qquad t=0.88.$$

We next calculate the expression $|E_{z1}|^2/\beta^2P^6$ at the position of the current sheet. At the mouth of the resonator, $x=b'$, $|E_{z1}|^2$ is given, from (8), by

$$|E_{z1}|^2=4E_0^2\frac{\sin^2\left[(2\pi+\theta)\frac{W}{2d}\right]}{(2\pi+\theta)^2}.$$

To a sufficient approximation the value of $|E_{z1}|^2$ at $x=h$, is given by

$$|E_{z1}|^2=4E_0^2\frac{\sin^2\left[(2\pi+\theta)\frac{W}{2d}\right]\cosh^2(2\pi+\theta)\frac{h}{d}}{(2\pi+\theta)^2\cosh^2(2\pi+\theta)\frac{b'}{d}}\cos\frac{\pi y}{2l} \tag{43}$$

$$\frac{\tanh(\sqrt{u+1}\,\alpha b)}{2\sqrt{u+1}}+\frac{\alpha b}{2\cosh(\sqrt{u+1}\,\alpha b)}=\frac{4Ke^{2ab}(e^{-2ah}+1)}{[Ku[e^{2a(b-h)}-1]+2(e^{2ab}+1)]}. \tag{40}$$

and from the equivalent circuit considerations

$$\frac{E_0^2}{\beta^2P}=\frac{V_0^2}{\beta^2PW^2}=\frac{2|Z_s^2|}{\beta^2W^2Z_0} \tag{44}$$

since V_0 refers to the peak voltage.

Combining (43) with (44) we obtain

$$\frac{|E_{z1}|^2}{\beta^2P}=\frac{2}{\beta^2W^2}\frac{|Z_s^2|}{Z_0}\frac{4\sin^2\left[(2\pi+\theta)\frac{W}{2d}\right]}{(2\pi+\theta)^2}\frac{\cosh^2(2\pi+\theta)\frac{h}{d}}{\cosh^2(2\pi+\theta)\frac{b'}{d}}\cos^2\frac{\pi y}{2l}. \tag{45}$$

Following the procedure used by Fletcher[7] for the cylindrical case we solve these equations for $\epsilon'=0$, or $u=-1$. It turns out that the results are not very sensitive to the value of u used. For assumed values of $-\frac{1}{2}$ and $-\frac{1}{4}$ for u the results for h and t do not differ from those to be given for $u=-1$ by more than a few per cent.

For $u=-1$, (39) and (40) yield

$$e^{-2ah}=\frac{e^{-2ab}+2\alpha b-1}{e^{2ab}-2\alpha b-1} \tag{41}$$

and

$$t=\frac{2}{\alpha b}\frac{e^{2ab}-1}{(e^{2ah}+1)[e^{2a(b-h)}+1]} \tag{42}$$

where

$$\alpha b=\frac{(2\pi+\theta)b}{d}=2.5\pi\frac{0.003}{0.021}=1.12.$$

This is based on the assumed value of $b=0.6b'$ to correspond to the observed fact that approximately 60

The optimum value for W/d is obtained by maximizing the expression

$$\frac{\sin^2\left[(2\pi+\theta)\frac{W}{2d}\right]}{(2\pi+\theta)\frac{W}{2d}},$$

since $|Z_s^2|/Z_0$ is proportional to W. This yields

$$(2\pi+\theta)\frac{W}{2d}=1.165 \tag{46}$$

or

$$\frac{W}{d}=0.297\quad\text{for}\quad\theta=\frac{\pi}{2}.$$

We may now obtain numerical values for the various factors in (45)

$$\frac{4\sin^2\left[(2\pi+\theta)\frac{W}{2d}\right]}{(2\pi+\theta)^2}=0.055 \tag{47}$$

[7] See footnote, page 1040.

$$\frac{\cosh^2(2\pi+\theta)\frac{h}{d}}{\cosh^2(2\pi+\theta)\frac{b'}{d}} = \frac{\cosh^2 0.76}{\cosh^2 1.87} = 0.154 \quad (48)$$

$$\frac{2}{l}\int_0^{l/2} \cos^2\frac{\pi y}{2l}\,dy = 0.82 \quad (49)$$

where the limits of integration extend over the depth of the longitudinal slots, or half the depth of the resonators.

$$\frac{2}{\beta^2 W^2}\frac{|Z_s^2|}{Z_0} = 2\frac{1}{\beta^2 C_s W}\frac{1}{\omega_s W}\frac{|Z_s^2|}{Z_0}\omega_s C_s = 130 \quad (50)$$

where

$$\beta^2 C_s W = \frac{(2.5\pi)^2}{d^2} A\epsilon_0 = 1.7\times 10^{-9}$$

$$\omega_s W = 5.5\times 10^7, \quad \frac{|Z_s^2|}{Z_0}\omega_s C_s = 6.8 \text{ from curwe in Fig. 7.}$$

Substituting the numerical values given in (47)–(50) in (45) gives

$$\frac{|E_{z1}|^2}{\beta^2 P} \equiv 0.90. \quad (51)$$

We now evaluate the space charge parameter Q as used by Pierce[8] and given by

$$Q = \frac{\beta_e}{\omega C_1}\left[\frac{|E_{z1}|^2}{\beta^2 P}\right]^{-1} \quad (52)$$

where C_1 is essentially a capacity per unit length associated with the rf charge in the current sheet and the voltage difference between the position of the current sheet, $x=h$, and the metal circuit, $x=b'$.

For the current sheet at $x=h$ we may write for the region $h<x<b'$

$$V_1 = A\sinh\alpha(b'-x) \quad (53)$$

in order to satisfy the boundary condition $V_1=0$ at $x=b'$.

For the region $0<x<h$ we have for symmetry reasons

$$V_2 = B\cosh\alpha x. \quad (54)$$

At $x=h$ we must have

$$V_1 = V_2$$

and

$$\left(\frac{\partial V}{\partial x}\right)_1 = \left(\frac{\partial V}{\partial x}\right)_2 = \frac{-\sigma}{\epsilon_0}.$$

From (53) and (54)

$$A\sinh\alpha(b'-h) = B\cosh\alpha h \quad (55)$$

$$-\alpha A\cosh\alpha(b'-h) - \alpha B\sinh\alpha h = \frac{-\sigma}{\epsilon_0}. \quad (56)$$

The difference in potential between $x=h$ and $x=b'$ is given by

$$V = A\sinh\alpha(b'-h)$$

which when combined with (55) and (56) yields

$$V = \frac{\sigma}{2\epsilon}\frac{\sinh\alpha(b'-h)\cosh\alpha h}{\cosh 2b'} \quad (57)$$

and since

$$C_1 = \frac{a\sigma}{V}$$

where a is the width of the current sheet.

$$Q = \frac{1}{a\omega\epsilon_0}\frac{\beta_e}{\alpha}\frac{\beta^2 P}{|E_{z1}|^2}\frac{\sinh\alpha(b'-h)\cosh\alpha h}{\cosh\alpha b'}. \quad (58)$$

In this expression we may set

$$\beta = \beta_e = \alpha = (2.5)\frac{\pi}{d}. \quad (59)$$

In the tube described here $a\omega\epsilon_0 = 1.6\times 10^{-2}$ and with the aid of quantities previously calculated we have

$$Q = 30.$$

The gain parameter C is given by the expression

$$C = \sqrt{\frac{|E_{z1}|^2}{\beta^2 P}\frac{1}{8}\frac{I_0}{V_0}}$$

where I_0 is the effective current in the sheet, which will be assumed to be 0.88 times the collector current, and V_0 is 1,220 volts.

The power gain in db is given by expression

$$G = A + BCN - \alpha L$$

where A is the initial loss in setting up the increasing wave. BCN is the gain of the increasing wave, with N the number of wavelengths. L is the cold loss for the circuit and α is the fraction of cold loss which should be subtracted from the gain. For $QC=0$ and $L=0$, $A=-9.5$ and $B=47.3$. Using the curves published by Pierce[8] one can obtain approximate values for A, B and α for values of QC and L other than zero. In Table II below these values, as well as those for power gain at midband, are listed for various values of collector current. For each case we will assume $L=11$ db, $N=125$ wavelengths and $Q=30$.

TABLE II

Collector Current (ma)	Effective I_0 (ma)	C	QC	B (db)	α	A (db)	Power Gain (db)
1.0	0.88	0.0043	0.13	40	0.43	−8	9
2.0	1.76	0.0055	0.16	39	0.44	−8	14
3.0	2.64	0.0062	0.19	38	0.44	−8	17
4.0	3.52	0.0069	0.21	37	0.45	−8	19

[8] J. R. Pierce, "Traveling-Wave Tubes," Chapts. VII–IX, D. Van Nostrand Co., Inc., New York, N. Y.; 1950.

Traveling-Wave Amplification by Means of Coupled Transmission Lines*

W. E. MATHEWS†, ASSOCIATE, IRE

Summary—**The theory of interaction between coupled transmission lines moving relative to each other is developed, and conditions yielding waves increasing exponentially with distance (amplification) are found. The case of lossless lines, one moving and one stationary, is analyzed in considerable detail, and the results are shown to be applicable to the helix traveling-wave tube. The theory also suggests the possibility of traveling-wave amplification in systems other than electrical, and a mechanical traveling-wave oscillator has been built.**

I. Introduction

THE CONVENTIONAL traveling-wave tube[1,2] may be regarded as a system comprising two coupled wave-propagating media, an electron beam and a passive circuit, each of which has two natural propagation constants.[3–5] The resulting system, therefore, has four propagation constants, at least two of which, under certain conditions, may be complex, implying amplification or attenuation of the respective associated waves with distance. Obviously analogous from this point of view is the double-stream or electron-wave amplifier,[6,7] wherein the passive circuit of the traveling-wave tube is replaced by a second electron beam. We note, however, that the magnetron, induction generator, and many other related devices also involve the same fundamental elements, namely, two continuously coupled media capable of propagating approximately synchronous waves.

Just as a passive waveguide supporting a number of propagating modes may be represented by an equal number of distinct dominant-mode transmission lines, we might expect these active traveling-wave devices also to show equivalence to coupled dominant-mode lines. Now Hahn and Ramo have shown that the space-charge waves which may exist in a cylindrical electron beam occur in pairs, one wave of each pair traveling slightly faster and the other the same amount slower than the average beam velocity.[4,5] A transmission-line model of the traveling-wave tube must therefore involve relative motion between the two coupled equivalent lines,[8] and of course this must be equally true of any active traveling-wave amplifying device since without this relative motion there would be no source of energy for an increasing wave.

In this paper, we examine the behavior of a pair of loosely coupled lossless lines, one assumed stationary and the other moving parallel to the direction of propagation with uniform velocity. The most fundamental qualitative finding is that traveling-wave amplification results from interaction between the *forward* wave on the stationary line and the *backward* wave on the moving line, that is, when the translational velocity of the moving line is sufficiently greater than the natural propagation velocity of that line, the *backward* wave is actually made to move *forward* in approximate synchronism with the forward wave on the stationary line.

Gain is found to exist over a small but finite range of the translational velocity, maximum gain being obtained when the significant waves are very nearly in perfect synchronism. When the coupling is purely capacitive or purely inductive and the natural propagation velocity of the moving line is not too small, the maximum possible fractional deviation from synchronism without complete loss of gain is equal approximately to $\pi\sqrt{\mu\sigma_2}$, where μ measures the degree of coupling between the two lines and σ_2 is the ratio of the natural propagation velocity of the moving line to that of the stationary line. The maximum gain obtainable is equal approximately to $\pi\sqrt{\mu\sigma_2}$ nepers per wavelength.

The results of this new theoretical approach are found to be in agreement with much of the published traveling-wave tube theory and with experimental data on actual tubes. In particular, it is found that under relatively high space-charge conditions Pierce's parameters C and Q[3,9] are related to μ and σ_2 by the simple expressions

* Decimal classification: R142. Original manuscript received by the Institute, August 28, 1950; revised manuscript received, March 9, 1951. Presented, 1949 IRE Conference on Electron Devices, Princeton, N. J., June 20, 1949.

† Formerly, Bell Telephone Laboratories, Inc., Murray Hill, N. J.; now, California Institute of Technology, Pasadena, Calif.

[1] Rudolf Kompfner, "The traveling-wave tube as amplifier at microwaves," PROC. I.R.E., vol. 35, pp. 124–128; February, 1947.

[2] J. R. Pierce and L. M. Field, "Traveling-wave tubes," PROC. I.R.E., vol. 35, pp. 108–111; February, 1947.

[3] J. R. Pierce, "Theory of the beam-type traveling-wave tube," PROC. I.R.E., vol. 35, pp. 111–123; February, 1947.

[4] W. C. Hahn, "Small signal theory of velocity-modulated electron beams," *Gen. Elec. Rev.*, vol. 42, pp. 258–270; June, 1939.

[5] S. Ramo, "The electron-wave theory of velocity-modulated tubes," PROC. I.R.E., vol. 27, pp. 757–763; December, 1939.

[6] J. R. Pierce and W. B. Hebenstreit, "A new type of high-frequency amplifier," *Bell Sys. Tech. Jour.*, vol. 28, pp. 33–51; January, 1949.

[7] A. V. Haeff, "The electron-wave tube," PROC. I.R.E., vol. 37, pp. 4–10; January, 1949.

[8] W. E. Mathews, "Transmission-line equivalent of electronic traveling-wave systems," *Jour. Appl. Phys.*, vol. 22, pp. 310–316; March, 1951.

[9] J. R. Pierce, "Effect of passive modes in traveling-wave tubes," PROC. I.R.E., vol. 36, pp. 993–997; August, 1948.

$$C^3 = \frac{1}{2}\mu\sigma_2^2$$

$$Q = \frac{1}{2\mu}.$$

The theory also suggests the possibility of traveling-wave amplification in systems other than electrical, and a mechanical traveling-wave oscillator has been built.[10]

II. Coupled-Line Equations

Using the subscripts 1 and 2 to refer to the stationary and moving lines, respectively, we assume instantaneous line currents and voltages of the form

$$i_1 = i_{01}e^{j\omega t-\Gamma z} \tag{1}$$

$$i_2 = i_{02}e^{j\omega_2 t-\Gamma z_2}, \tag{2}$$

where z is measured with respect to a fixed origin while z_2 is measured in a reference frame moving with line 2. Assuming line 2 to be moving with a uniform velocity v in the positive (forward) z direction,

$$z = z_2 + vt. \tag{3}$$

Substituting (3) into (1), we obtain

$$i_1 = i_{01}e^{(j\omega-\Gamma v)t-\Gamma z_2}. \tag{4}$$

Now the currents i_1 and i_2 corresponding to any one mode must have the same time and space variation in any one frame of reference. Therefore, from (2) and (4),

$$\Gamma_2 = \Gamma \tag{5}$$

$$j\omega_2 = j\omega - \Gamma v. \tag{6}$$

Representing each transmission line by the parameters that would be measured by an observer stationary with respect to that line, and making use of (5), the behavior of the coupled system at any transverse plane may be described by the equations

$$Z_{11}i_{01} + Z_{1m}i_{02} = \Gamma e_{01}, \tag{7}$$

$$Y_{11}e_{01} + Y_{1m}e_{02} = \Gamma i_{01}, \tag{8}$$

$$Z_{22}i_{02} + Z_{2m}i_{01} = \Gamma e_{02}, \tag{9}$$

$$Y_{22}e_{02} + Y_{2m}e_{01} = \Gamma i_{02}, \tag{10}$$

where the Z's and Y's represent series impedances and shunt admittances, respectively, per unit length of line, distributed either uniformly or in discrete sections short compared to a wavelength, and the subscripts m denote mutual (coupling) elements. Solving (7) through (10) simultaneously, we obtain

$$\Gamma^4 - \Gamma^2(Z_{11}Y_{11} + Z_{22}Y_{22} + Z_{1m}Y_{2m} + Z_{2m}Y_{1m}) + (Z_{11}Z_{22} - Z_{1m}Z_{2m})(Y_{11}Y_{22} - Y_{1m}Y_{2m}) = 0. \tag{11}$$

In the case of conventional lossless series-L shunt-C lines, we may write

$$\begin{aligned} Z_{11} &= j\omega L_1 & Y_{11} &= j\omega C_1, \\ Z_{22} &= j\omega_2 L_2 & Y_{22} &= j\omega_2 C_2, \\ Z_{1m} &= j\omega L_m & Y_{1m} &= j\omega C_m, \\ Z_{2m} &= j\omega_2 L_m & Y_{2m} &= j\omega_2 C_m, \end{aligned} \tag{12}$$

whereupon (11) becomes

$$\Gamma^4 + \Gamma^2(\omega^2 L_1 C_1 + \omega_2^2 L_2 C_2 + 2\omega\omega_2 L_m C_m) + \omega^2\omega_2^2(L_1L_2 - L_m^2)(C_1C_2 - C_m^2) = 0. \tag{13}$$

Introducing the coupling coefficients

$$\mu_L = \frac{L_m^2}{L_1L_2} \qquad \mu_C = \frac{C_m^2}{C_1C_2} \qquad \mu = \mu_L + \mu_C \tag{14}$$

and the uncoupled propagation velocities

$$v_1^2 = \frac{1}{L_1C_1} \qquad v_2^2 = \frac{1}{L_2C_2}, \tag{15}$$

we may rewrite (13) in the form

$$\left(\frac{\Gamma v_1}{\omega}\right)^4 \frac{v_2^2}{v_1^2} + \left(\frac{\Gamma v_1}{\omega}\right)^2 \left(\frac{v_2^2}{v_1^2} + \frac{\omega_2^2}{\omega^2} \pm 2\frac{\omega_2}{\omega}\frac{v_2}{v_1}\sqrt{\mu_L\mu_C}\right) + \frac{\omega_2^2}{\omega^2}(1 - \mu_L)(1 - \mu_C) = 0, \tag{16}$$

where the $\sqrt{\mu_L\mu_C}$ term is to be taken positive when L_m and C_m are of the same sign, and negative when L_m and C_m are of opposite signs. Normalizing the velocities with respect to v_1

$$\sigma = \frac{v}{v_1} \qquad \sigma_2 = \frac{v_2}{v_1}, \tag{17}$$

and the propagation constant Γ with respect to the propagation constant which line 1 would have if uncoupled

$$M = \frac{\Gamma v_1}{j\omega}, \tag{18}$$

and making use of (6) to eliminate the moving frame of reference, we obtain finally

$$\begin{aligned} &M^4(\sigma_2^2 - \sigma^2) \\ &+ M^3 2\sigma(1 \pm \sigma_2\sqrt{\mu_L\mu_C}) \\ &- M^2(1 + \sigma_2^2 \pm 2\sigma_2\sqrt{\mu_L\mu_C} - \sigma^2[1 - \mu_L][1 - \mu_C]) \\ &- M 2\sigma(1 - \mu_L)(1 - \mu_C) \\ &+ (1 - \mu_L)(1 - \mu_C) \\ &= 0. \end{aligned} \tag{19}$$

Neglecting higher-order mixed coupling terms, this may be written in the form

$$F(M) + \mu G(M) = 0, \tag{20}$$

where

$$F(M) = (M^2 - 1)([1 - \sigma M]^2 - \sigma_2^2 M^2) \tag{21}$$

[10] This mechanical traveling-wave oscillator was demonstrated at the IRE Conference on Electron Devices, Princeton, N. J., June, 1949.

$$G(M) = (1 - \sigma M)^2 \pm \frac{\sqrt{\mu_L \mu_C}}{\mu_L + \mu_C} 2\sigma_2 M^2(1 - \sigma M). \quad (22)$$

The four roots of (19) or (20) characterize the four possible transmission modes of the coupled system. If the coupling coefficients are set equal to zero, these four modes are easily recognized as the forward and backward waves on the two independent lines

$$M_1 = 1, \quad (23)$$

$$M_2 = -1, \quad (24)$$

$$M_3 = \frac{1}{\sigma + \sigma_2}, \quad (25)$$

$$M_4 = \frac{1}{\sigma - \sigma_2}. \quad (26)$$

As coupling is introduced the propagation constants become modified slightly, but for small coupling each of the possible modes remains identifiable with one of the uncoupled modes. If the relative velocity is within a certain range, however, one of the coupled modes may exhibit gain (Re Γ opposite in sign to Im Γ), and it is this phenomenon with which the present paper is primarily concerned. A detailed analysis of the characteristic equation (20) is presented in the Appendix; the more important results of this analysis are summarized in the following two sections.

III. Behavior Under Conditions Not Yielding Gain

It is shown in the Appendix that gain may be achieved only when $M_1 \approx M_4$, i.e., when there is approximate synchronism between the forward wave on the stationary line and the backward wave on the moving line. Under all other conditions, the effect of small coupling between the lines is merely to perturb the propagation velocities somewhat, without introducing any gain or loss. If the coupling is purely inductive or purely capacitive and if all of the uncoupled wave velocities are well separated, then the perturbations are given by (62A) through (65A). If the uncoupled velocities of the two forward or two backward waves are nearly equal, then the perturbed velocities of the near-synchronous pair fall outside the interval between the unperturbed velocities, as has been found by Albersheim,[11] and the average velocity of the pair is reduced by an amount proportional to μ.

If the coupling is partly inductive and partly capacitive, instead of wholly one or the other, $\mu G(M)$ is modified by the cross-coupling term $\pm\sqrt{\mu_L \mu_C}\, 2\sigma_2 M^2(1 - \sigma M)$ and (62) through (65) become inaccurate. The analysis of no-gain conditions has not been carried out in detail for this case, but no fundamentally different qualitative behavior would seem to be expected.

[11] W. J. Albersheim, "Propagation of TE_{01} waves in curved wave guides," *Bell Sys. Tech. Jour.*, vol. 28, pp. 1–32; January, 1949

IV. Behavior Under Conditions Yielding Gain

The fundamental condition for gain to be possible is approximate synchronism between the forward wave on the stationary line and the backward wave on the moving line ($M_1 \approx M_4$). This requires in turn that the translational velocity of the moving line must be greater than the natural wave-propagation velocity of either line ($\sigma > \sigma_2$; $\sigma > 1$). Unless σ_2 is very small, the perturbations of M_1 and M_4 are given by (84) and (85) when the coupling is purely inductive or purely capacitive, by (94) when the coupling is equally mixed and L_m and C_m are of like sign, and by (95) when L_m and C_m are of opposite sign. M_{2p} and M_{3p} are given by (63) and (64), respectively. When σ_2 is small, however, the forward wave on the stationary line is also nearly in synchronism with the *forward* wave on the moving line ($M_1 \approx M_3$), and the modifying effect of the latter may have to be taken into account. In this case, the perturbations of the three nearly synchronous waves may be found as the solutions of the cubic equations (101) for pure coupling or (105) for oppositely polarized equally mixed coupling.[12] In general (84), (85), (94), and (95) are reasonably accurate when $\sigma_2 > 4\mu$.

From (84) and (85) we see that in this case, in contrast with the behavior described in the preceding section, the perturbed velocities fall *inside* the interval between the unperturbed velocities, and the average velocity of the pair is *increased* by an amount proportional to μ. If the two lines are considered initially to be uncoupled but with the requisite waves approximately in step, the gradual introduction of coupling serves first to modify the wave velocities so that they approach each other. After the waves have been pulled into perfect synchronism, further increase in coupling yields gain in one and conjugate loss in the other. The wave exhibiting gain is the one associated with the slower unperturbed wave, regardless of which line originally carried it. In the gain-loss region the wave velocity is a linear function both of μ and ϵ, where ϵ is the fractional deviation from synchronism of the unperturbed waves,

$$\epsilon = (\sigma - \sigma_2) - 1. \quad (27)$$

It is shown in the Appendix that maximum gain is obtained when

$$\epsilon = \mu \frac{\sigma}{2}, \quad (28)$$

i.e., when the unperturbed resultant velocity of the backward wave on the moving line is greater than the natural propagation velocity of the stationary line by such an amount that $Re(M_{4p}) = M_4$. The gain-loss region is symmetrical about this optimum value of ϵ and is given by

$$\epsilon_{\text{lim.}} = \mu \frac{\sigma}{2} \pm \sqrt{\mu\sigma_2 + \tfrac{1}{4}\mu^2\sigma^2}. \quad (29)$$

[12] Equally mixed coupling of like polarities cannot yield gain when $\sigma_2 \ll 1$. See (106).

For small μ and $\sigma_2 > 4\mu$, this becomes very nearly

$$\epsilon_{\text{lim.}} = \mu \frac{\sigma}{2} \pm \sqrt{\mu\sigma_2}. \tag{30}$$

When the maximum-gain condition (28) is satisfied, the gain per wavelength is seen from (89) to be approximately

$$G_\lambda = \pi\sqrt{\mu\sigma_2} \text{ nepers} = 27.3\sqrt{\mu\sigma_2} \text{ decibels.} \tag{31}$$

Complete solutions of the cubic equations (101) and (105) have not been worked out. It may be shown, however, that the range of ϵ over which gain and loss is obtained, and the maximum amount of gain or loss obtainable, decrease monotonically with σ_2. It also is found that small values of σ_2 may give rise to a double-peaked curve of gain versus ϵ.

V. Application to Traveling-Wave Tube

Without going into detailed mathematics, we can gain immediately from the coupled-line theory an increased understanding of some well-known characteristics of the traveling-wave tube. For example, we know that four possible waves can exist in the tube, an increasing wave and a decreasing wave of identical velocity, a slightly faster unattenuated wave, and a backward unattenuated wave. We now recognize these respectively as the two significant interacting waves, the relatively unperturbed forward or fast wave of the electron stream, and the even less perturbed backward wave of the helix. Also, we know that increased beam current requires increased beam voltage for maximum gain. One tube that operated at 1,600 volts with a milliampere or less of beam current, required 1,750 volts for maximum gain with 20 milliamperes of beam current. This increase in optimum beam velocity was found to be very nearly equal to the calculated increase in space-charge wave velocity, as would be expected from the present theory.

To apply the theory quantitatively to any particular system, we must first evaluate the parameters σ_2 and μ for that system. In the traveling-wave tube, the moving transmission line takes the form of an electron beam, for which Ramo finds[5]

$$\delta = \frac{\sigma_2}{\sigma} = \sqrt{\frac{-\eta\rho_0}{\pi b^2(\omega^2 + T^2 v_0^2)}}, \tag{32}$$

where η is the ratio of electronic charge to mass, b is the beam radius, T is a function of beam radius, beam velocity, frequency, and shield radius,[13] and Heaviside-Lorentz units are used. This may be written in the form

$$\frac{\sigma_2}{\sigma} = \frac{1.645 \times 10^9 I_0^{1/}}{V_0^{1/4} f b \left(1 + \dfrac{T^2 V_0^2}{\omega^2}\right)^{1/2}}, \tag{33}$$

where I_0 is the beam current in amperes, V_0 the beam voltage in volts, f the frequency in cycles per second, and b the beam radius in centimeters. For the electron beams commonly used in low-power traveling-wave tubes, we may expect σ_2 to be of the order of a few hundredths.

To evaluate μ for the traveling-wave tube, we observe first that the coupling between helix and beam is by means of electric fields, and thus is essentially capacitive. Substituting (12) into (8) and (10), we obtain

$$j\omega C_1 e_{01} + j\omega C_m e_{02} = \Gamma i_{01} \tag{34}$$

$$j\omega_2 C_2 e_{02} + j\omega_2 C_m e_{01} = \Gamma i_{02}. \tag{35}$$

Now for small coupling $C_m \ll C_1$, so (34) becomes approximately

$$j\omega C_1 e_{01} \approx \Gamma i_{01}. \tag{36}$$

Considering i_{02} to consist of two components

$$i_{02} = i_{22} + i_{21}, \tag{37}$$

where i_{22} is the "self-current" of line 2 and i_{21} is the current induced by changing e_1, we see from (35) that

$$j\omega_2 C_m e_{01} = \Gamma i_{21}. \tag{38}$$

Thus, from (14),

$$\mu = \frac{C_m^2}{C_1 C_2} = \frac{C_1 \omega^2 {i_{21}}^2}{C_2 {\omega_2}^2 {i_{01}}^2}. \tag{39}$$

The values of C_1 and C_2 may be determined from the well-known relations

$$C_1 = \frac{1}{v_1 Z_{01}} \qquad C_2 = \frac{1}{v_2 Z_{02}} \tag{40}$$

which yield immediately

$$\frac{C_1}{C_2} = \sigma_2 \frac{Z_{02}}{Z_{01}}, \tag{41}$$

where Z_{01} and Z_{02} are the characteristic impedances of the two transmission lines.

In calculating Z_{02} for the electron beam, we must note carefully the meaning of this parameter. It is *not* simply the *de/di* which would be measured by a stationary observer, and which is equal to $2V_0/I_0$, but rather is the *de/di* which would be measured by an observer *moving with the beam*, and thus with the assumed equivalent wire transmission line. Now this observer sees only the velocity-modulation component of the ac beam current:

$$i_2 = \rho_0 v_e, \tag{42}$$

where v_e is the alternating component of the electron velocity. The equation of motion for an electron gives

[13] Since we assume small coupling between beam and helix, we may to a first approximation assume the shield radius to be infinite. In this case Ramo's equation (25), from which the value of T may be determined, becomes

$$(Tb)\frac{J_1(Tb)}{J_0(Tb)} = \left(\frac{\omega}{v_0} b\right) \frac{K_1\left(\dfrac{\omega}{v_0} b\right)}{K_0\left(\dfrac{\omega}{v_0} b\right)}$$

$T^2 v_0^2/\omega^2$ is plotted as a function of $\omega b/v_0$ in Fig. 1.

$$\frac{dv_e}{dl_2} = \eta \frac{de_2}{dz_2} \tag{43}$$

$$v_e = -\frac{\eta\Gamma}{j\omega_2} e_2. \tag{44}$$

Thus

$$Z_{02} = \frac{e_2}{i_2} = -\frac{j\omega_2}{\eta\rho_0\Gamma} = \frac{\sigma_2}{\sigma}\frac{2V_0}{I_0}. \tag{45}$$

To determine the value of i_{21}, we assume sufficient space-charge density that σ_2 is large compared with the maximum perturbation of the normalized propagation constant M_3. Then under conditions yielding gain, the energy in each line is traveling at very nearly the natural propagation velocity of that line, the energy in line 2 traveling backward, of course. Thus, the induced current i_{21} is related to the potential e_{21} by very nearly the negative of the characteristic impedance Z_{02}, and

$$i_{21} \approx \frac{E}{\Gamma Z_{02}}, \tag{46}$$

where E is the longitudinal component of helix electric field at the position of the beam.

Substituting (41), (45), and (46) into (39), and noting that $\sigma \approx 1$, we obtain

$$= \frac{\omega^2}{\omega_2^2}\frac{I_0}{2V_0}\frac{E^2}{\Gamma^2 i_{01}^2 Z_{01}}. \tag{47}$$

We see from (89) that Γ is very nearly purely imaginary, even under conditions yielding maximum gain. Thus E/i_{01} is also very nearly purely imaginary. Let

$$\Gamma \approx j\beta. \tag{48}$$

Then

$$\frac{E^2}{\Gamma^2 i_{01}^2 Z_{01}} = \frac{EE^*}{\beta^2 i_{01}^2 Z_{01}} = \frac{E_1^2}{2\beta^2 P}, \tag{49}$$

where $E_1 = |E|$ and P is the power transmitted by the forward helix mode for a peak longitudinal field E_1 at the position of the electron beam. Now at the near synchronism required for gain, we have from (80), (6), and (17)

$$\sigma - \sigma_2 \approx 1 \tag{50}$$

$$\frac{\omega_2}{\omega} \approx 1 - \sigma \approx -\sigma_2. \tag{51}$$

Thus (47) yields finally

$$\mu = \frac{1}{\sigma_2^2}\left(\frac{E_1^2}{2\beta^2 P}\frac{I_0}{2V_0}\right). \tag{52}$$

The expression in brackets, which is equal to twice Pierce's C^3,[14] may be recognized as the ratio of the impedance of the active helix mode, as measured at the position of the beam, to the ac impedance of the electron beam as measured by a stationary observer.

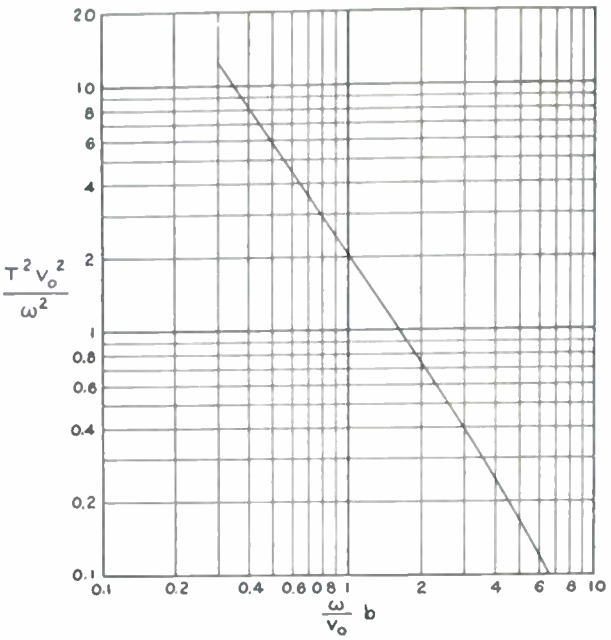

Fig. 1—Curve for approximate determination of the quantity $\Gamma^2 v_0^2/\omega^2$, appearing in the equation for the wave-propagation velocity of an electron beam. b is the beam radius, v_0 the average beam velocity, and ω the signal radian frequency.

It should be noted that this particular calculation of the coupling parameter μ is valid only under relatively high space-charge conditions since for low-current beams, such that $\sigma_2 \ll 4\mu$, the approximation (46) is not justified. When (52) applies, however, we may combine it with Pierce's expression for the unperturbed space-charge wave propagation[15]

$$\sigma_2 = 2\sqrt{QC^3} \tag{53}$$

to obtain the simple relations

$$Q = \frac{1}{2\mu} \qquad \mu = \frac{1}{2Q}$$

$$C^3 = \frac{1}{2}\mu\sigma_2^2 \qquad \sigma_2 = 2\sqrt{QC^3}. \tag{54}$$

Acknowledgments

The writer wishes to express his appreciation to C. C. Cutler, at whose suggestion the investigations leading to this paper were started, and S. P. Morgan, who suggested the perturbation method of analysis used.

Appendix

Analysis of Characteristic Equation and Conditions Yielding Complex Roots for Coupled Lossless Lines

1. Perturbation Method

In the absence of coupling, the characteristic equation (20) may be written in factored form

[14] See footnote 3, equation (19).

[15] See footnote 9, equation (13).

$$F(M) = A(M - M_1)(M - M_2)(M - M_3)(M - M_4) = 0 \quad (55)$$

$$A = \sigma^2 - \sigma_2^2, \quad (56)$$

the roots of which are given by (23) through (26). A small amount of coupling can produce at most a small perturbation in these roots, suggesting that we proceed by first expanding (20) in a Taylor series about each of its unperturbed roots. Suppose we let $a, b, c, d = 1, 2, 3, 4$, not necessarily respectively, and expand about the root M_a

$$\begin{aligned} F(M_a + m) = {} & mA\delta_{ab}\delta_{ac}\delta_{ad} \\ & + m^2A(\delta_{ab}\delta_{ac} + \delta_{ab}\delta_{ad} + \delta_{ac}\delta_{ad}) \\ & + m^3A(\delta_{ab} + \delta_{ac} + \delta_{ad}) + m^4A, \end{aligned} \quad (57)$$

where

$$\delta_{jk} = M_j - M_k. \quad (58)$$

Now for small m, unless $G(M_a) \approx 0$,

$$G(M_a + m) \approx G(M_a). \quad (59)$$

Thus, for small coupling, (20) becomes

$$\begin{aligned} & mA\delta_{ab}\delta_{ac}\delta_{ad} + m^2A(\delta_{ab}\delta_{ac} + \delta_{ab}\delta_{ad} + \delta_{ac}\delta_{ad}) \\ & + m^3A(\delta_{ab} + \delta_{ac} + \delta_{ad}) + m^4A + \mu G(M_a) \approx 0. \end{aligned} \quad (60)$$

The four roots of (55), as given by (23) through (26), may be seen to be real, implying no gain or attenuation. Thus, the conditions yielding gain are precisely the conditions yielding a complex perturbation term m.

2. Case I. Unperturbed Roots Well Separated

In this case none of the δ's are small, and the higher order terms in m may be neglected to yield

$$m \approx -\frac{\mu G(M_a)}{A\delta_{ab}\delta_{ac}\delta_{ad}}. \quad (61)$$

In most cases of practical interest $\mu G(M_a)/A$ is of the order of μ, implying by (61) that m is also of this order and thus that the neglecting of higher powers of m is justified. Since none of the factors of the fraction on the right are complex, m must be real, implying only a slight perturbation of the mode velocities. Making use of (23) through (26), and assuming that the coupling is either purely inductive or purely capacitive ($\mu_C = 0$ or $\mu_L = 0$), we find that

$$M_{1p} = M_1\left(1 - \frac{\mu}{2}\frac{(\sigma - 1)^2}{(\sigma - 1)^2 - \sigma_2^2}\right), \quad (62)$$

$$M_{2p} = M_2\left(1 - \frac{\mu}{2}\frac{(\sigma + 1)^2}{(\sigma + 1)^2 - \sigma_2^2}\right), \quad (63)$$

$$M_{3p} = M_3\left(1 + \frac{\mu}{2}\frac{\sigma_2(\sigma + \sigma_2)}{1 - (\sigma + \sigma_2)^2}\right), \quad (64)$$

$$M_{4p} = M_4\left(1 - \frac{\mu}{2}\frac{\sigma_2(\sigma - \sigma_2)}{1 - (\sigma - \sigma_2)^2}\right), \quad (65)$$

where M_{ap} represents the perturbed value of the root M_a.

3. Case II. Two Unperturbed Roots Nearly Equal

In this case one of the δ's, say δ_{ab}, is small, so that the linear term of (60) is of the *second* order of smallness. Neglecting third- and higher-order infinitesimals, we are left with

$$m(m + \delta_{ab}) + \frac{\mu G(M_a)}{A\delta_{ac}\delta_{ad}} \approx 0 \quad (66)$$

$$m \approx \frac{-\delta_{ab} \pm \sqrt{\delta_{ab}^2 - \dfrac{4\mu G(M_a)}{A\delta_{ac}\delta_{ad}}}}{2}. \quad (67)$$

Thus the necessary and sufficient condition for complex roots, when one δ is considerably smaller than either of the other two, is

$$\frac{4\mu G(M_a)}{A\delta_{ac}\delta_{ad}} > \delta_{ab}^2, \quad (68)$$

where δ_{ab} is the smallest δ. Note that (66) corresponds to (60) with only the two nearly-equal roots retained. The conjugate nature of the two solutions (67) implies that when the perturbation of one of these roots indicates attenuation, the other perturbed root must exhibit gain.

a. Inductive or Capacitive Coupling. We have shown that gain is possible when two of the unperturbed modes have nearly equal velocities. The next step is to determine which pairs of modes in synchronism may yield gain and which may not. Assume first that the coupling is either purely inductive or purely capacitive. From (22)

$$G(M_a) = (1 - \sigma M_a)^2 > 0. \quad (69)$$

Thus in order for (68) to be satisfied, it is necessary at least that

$$A\delta_{ac}\delta_{ad} > 0. \quad (70)$$

Note that

$$\delta_{12} = -\delta_{21} = 2, \quad (71)$$

$$A\delta_{34} = -A\delta_{43} = -2\sigma_2 < 0, \quad (72)$$

$$\delta_{32} = -\delta_{23} > 1 \quad (73)$$

so that

$$A\delta_{32}\delta_{34} < 0 \quad (74)$$

$$\delta_{21}\delta_{23} > 0. \quad (75)$$

Obviously, δ_{12} and δ_{23} cannot be small, and by (74), small δ_{13} cannot yield complex roots. Small δ_{24} implies that $\sigma_2 > \sigma$ so that $A < 0$ and by (75) complex roots are again impossible. If $|\delta_{14}| \ll 1$, $\delta_{42} > 0$ and $A\delta_{42}\delta_{43} > 0$ so that complex roots may be possible. The remaining condition to be examined is $|\delta_{24}| \ll 1$, in which case (68) requires that

$$\frac{4\mu(\sigma-\sigma_2)^2G(M_4)}{1-(\sigma-\sigma_2)^2} > \frac{4\sigma_2^2}{\sigma^2-\sigma_2^2} \approx \frac{4\sigma_2^2}{\sigma^2}. \tag{76}$$

Now

$$G(M_4) = \frac{\sigma_2^2}{(\sigma-\sigma_2)^2}. \tag{77}$$

Thus, for gain,

$$\frac{\mu\sigma^2}{1-(\sigma-\sigma_2)^2} > 1. \tag{78}$$

For small μ, this can be satisfied only when $\sigma-\sigma_2\approx 1$, in which case δ_{41} again is small and the quadratic approximation no longer is valid.

For a more complete analysis of the near-synchronous cases, we may solve the second-order approximate Taylor expansions without making the approximation (59). When $|\delta_{41}|\ll 1$, which we have seen to be necessary for gain, (66) becomes

$$m^2+m\delta_{41}+\mu\frac{G(M_4+m)}{.1\delta_{42}\delta_{43}}=0. \tag{79}$$

We define a parameter ϵ proportional to the difference between the nearly equal unperturbed velocities:

$$\epsilon=(\sigma-\sigma_2)-1 \qquad |\epsilon|\ll 1. \tag{80}$$

Then (79) becomes

$$m^2-m\epsilon+\mu\frac{\sigma_2^2+2\sigma\sigma_2 m+\sigma^2m^2}{4\sigma_2}=0 \tag{81}$$

$$m^2\left(1+\mu\frac{\sigma^2}{4\sigma_2}\right)-m\left(\epsilon-\mu\frac{\sigma}{2}\right)+\mu\frac{\sigma_2}{4}=0. \tag{82}$$

Solving for m

$$m=\frac{\epsilon-\mu\frac{\sigma}{2}\pm\sqrt{\epsilon^2-\epsilon\mu\sigma-\mu\sigma_2}}{2\left(1+\mu\frac{\sigma^2}{4\sigma_2}\right)}. \tag{83}$$

Neglecting the μ term in the denominator, we find that

$$M_{ap}=1-\frac{\epsilon}{2}-\mu\frac{\sigma}{4}+\frac{1}{2}\sqrt{\epsilon^2-\epsilon\mu\sigma-\mu\sigma_2} \tag{84}$$

$$M_{bp}=1-\frac{\epsilon}{2}-\mu\frac{\sigma}{4}-\frac{1}{2}\sqrt{\epsilon^2-\epsilon\mu\sigma-\mu\sigma_2}, \tag{85}$$

where $a, b=1, 4$ if $\epsilon>0$ and vice versa if $\epsilon<0$. Obviously M_{ap} exhibits amplification and M_{bp} attenuation when $\epsilon^2-\epsilon\mu\sigma-\mu\sigma_2<0$. Thus the limiting values of ϵ for gain are given by

$$\epsilon_{\text{lim}}=\mu\frac{\sigma}{2}\pm\sqrt{\mu\sigma_2+\mu^2\frac{\sigma^2}{4}}. \tag{86}$$

For maximum gain

$$2\epsilon-\mu\sigma=0 \tag{87}$$

$$\epsilon=\mu\frac{\sigma}{2}. \tag{88}$$

Substituting (88) into (84),

$$(M_{ap})_{\text{opt.}}=1-\mu\frac{\sigma}{2}+j\frac{1}{2}\sqrt{\mu\sigma_2+\mu^2\frac{\sigma^2}{4}}. \tag{89}$$

b. Mixed Coupling. Purely inductive coupling and purely capacitive coupling have been seen to yield identical expressions for $G(M)$. With a combination of the two, however, the form of $G(M)$ is modified by the cross-coupling term involving $\sqrt{\mu_L\mu_C}$. The effect of this term is greatest when μ_L and μ_C are equal, whereupon we have from (22)

$$G(M)=(1-\sigma M)^2\pm\sigma_2M^2(1-\sigma M). \tag{90}$$

Now

$$(1-\sigma M)^2>0, \tag{91}$$

$$M_2^2(1-\sigma M_2)=(1+\sigma)>0, \tag{92}$$

$$M_3^2(1-\sigma M_3)=\frac{\sigma_2}{(\sigma+\sigma_2)^3}>0. \tag{93}$$

Therefore, when the + sign in (90) applies, $G(M_2)>0$ and $G(M_3)>0$, preserving the validity of the argument of Section 3(a) that a small δ_{13} or δ_{24} cannot yield complex roots. When the − sign applies, however, $G(M_2)\approx 0$ when $|\delta_{24}|\ll 1$ and $G(M_3)\approx 0$ when $|\delta_{13}|\ll 1$ so that (59) becomes unjustified and (68) cannot be used to test these cases. Examination of the appropriate complete second-order Taylor expansions reveals that $|\delta_{41}|\ll 1$ is required for gain as before. Resolving (79) with $G(M_4+m)$ modified in accordance with (90) and noting that $M_4=1-\epsilon$, we find that

$$(M_{1,4})_{p+}\approx 1-\frac{\epsilon}{2}-\mu\frac{1-\sigma_2}{8}\pm\frac{1}{2}\sqrt{\epsilon^2-\mu\epsilon\frac{1+\sigma_2}{2}+\mu^2\frac{(1-\sigma_2)^2}{16}} \tag{94}$$

$$(M_{1,4})_{p-}\approx 1-\frac{\epsilon}{2}-\mu\frac{3+5\sigma_2}{8}\pm\frac{1}{2}\sqrt{\epsilon^2-\mu\epsilon\frac{3+5\sigma_2}{2}-2\mu\sigma_2}. \tag{95}$$

The limiting values of ϵ for gain (complex m) in these cases are

$$\epsilon_+=\mu\frac{1+\sigma_2}{4}\pm\frac{1}{2}\sqrt{\mu^2\sigma_2^2} \tag{96}$$

$$\epsilon_-\approx\mu\frac{3+5\sigma_2}{4}\pm\sqrt{2\mu\sigma_2\left(1+\frac{3\mu\sigma_2}{4}\right)}. \tag{97}$$

4. Case III. Three Unperturbed Roots Nearly Equal

In this case *two* of the δ's of (60), say δ_{ab} and δ_{ac}, are small, so that the linear and quadratic terms of (60) are of the *third* order of smallness. In the physical system under consideration, this can occur only when $\sigma_2\ll 1$ and

$\sigma \approx 1$ so that M_1, M_3, and M_4 are approximately equal. Taking $a=4$ and neglecting fourth-order infinitesimals, we have left

$$m^3 + m^2(\delta_{41} + \delta_{43}) + m\delta_{41}\delta_{43} + \frac{\mu G(M_4 + m)}{A\delta_{42}} \approx 0 \quad (98)$$

$$m^3 - m^2(\epsilon - 2\sigma_2) - m\epsilon 2\sigma_2 + \frac{\mu}{2} G(M_4 + m) \approx 0, \quad (99)$$

where ϵ is defined by (80).

If the coupling is purely inductive or purely capacitive,

$$G(M_4 + m) \approx \sigma_2^2 + 2\sigma_2 m + m^2 \quad (100)$$

$$m^3 - m^2\left(\epsilon - 2\sigma_2 - \frac{\mu}{2}\right) - m2\sigma_2\left(\epsilon - \frac{\mu}{2}\right) + \mu\frac{\sigma_2^2}{2} = 0. \quad (101)$$

If the coupling is equally mixed so that (90) applies,

$$G_+(M_4 + m) \approx \sigma_2^2\epsilon + \sigma_2 m + m^2 \quad (102)$$

$$G_-(M_4 + m) \approx 2\sigma_2^2 + 3\sigma_2 m + m^2. \quad (103)$$

Substituting (102) and (103) into (99), we obtain

$$m_+^3 - m_+^2\left(\epsilon - 2\sigma_2 - \frac{\mu}{2}\right) - m_+2\sigma_2\left(\epsilon - \frac{\mu}{4}\right) + \mu\frac{\sigma_2^2\epsilon}{2} = 0 \quad (104)$$

$$m_-^3 - m_-^2\left(\epsilon - 2\sigma_2 - \frac{\mu}{2}\right) - m_-2\sigma_2\left(\epsilon - \frac{3\mu}{4}\right) + \mu\sigma_2^2 = 0. \quad (105)$$

Now we observe that the fourth term of (104) is an order of magnitude smaller than the other terms. Neglecting this term and solving the remaining quadratic, we obtain

$$m_+ = \frac{\epsilon}{2} - \frac{\mu}{4} - \sigma_2 \pm \frac{1}{2}\sqrt{\epsilon^2 + \epsilon(4\sigma_2 - \mu) + 4\sigma_2^2 + \frac{\mu^2}{4}}. \quad (106)$$

The discriminant of the expression under the radical sign is $-8\mu\sigma_2 < 0$, implying that the expression cannot become negative and thus that m_+ cannot become complex. Gain is possible, however, under the conditions to which (101) or (105) apply. By comparing the discriminants of these equations with those of the quadratic equations (82) and (95), respectively, it may be shown that the quadratic approximations are reasonably accurate when $\sigma_2 > 4\mu$. It also is found that small values of σ_2 may give rise to a double-peaked curve of gain versus ϵ.

A Digital Computer Timing Unit*

R. M. GOODMAN†, ASSOCIATE, IRE

Summary—**In some modern high-speed electronic computers the reference is time. This paper is concerned with the time-reference equipment designed for the EDVAC. The application of electronic matrices to time-pulse production is discussed.**

I. Introduction

THE EDVAC[1] is a serially operated machine with built-in dynamic memories in the form of electrical and acoustic delay lines. The proper operation of these components requires the availability of accurate time information based on the computing cycle. This requirement is one peculiar to a serial machine.

In the course of designing a serial digital computer the logician, the mathematician, and the computer-circuit engineer may tacitly assume the existence of timing marks to initiate circuits or logical arrangements. However, the production of this time information represents a design problem in its own right and must be attacked with the same logical and engineering methods required for the actual computer circuits.

II. The Design Problem

Since time represents the reference system for the machine, it follows that time, or at least certain times relative to a nominal initial time, must be known to a high order of accuracy. The use of quartz-crystal controlled circuits will supply the necessary time precision, but there remains the problem of transforming this readily available accuracy to the particular form required for the successful operation of the EDVAC.

Since the EDVAC is a pulse-operated device, certain pulses must be produced at specific times. The desired characteristics of the pulse are known and are illustrated in Fig. 1. These characteristics are based on the requirements of general EDVAC circuits. All the pulses to be described must conform to them within the specified limits. In addition, each pulse generator must be capable of driving eighteen coaxial cables, each of which is terminated with its characteristic impedance of 93 ohms, or a total load of about 5 ohms.

* Decimal classification: 621.375.2×621.375.618. Original manuscript received by the Institute, May 22, 1950; revised manuscript received, November 8, 1950.

† Moore School of Electrical Engineering, University of Pennsylvania, Philadelphia, Pa.

[1] Electronic Discrete Variable Computer, designed and built at the Moore School of Electrical Engineering, University of Pennsylvania under contract W36-034-ORD-7593 for the Ordinance Department of the Army.

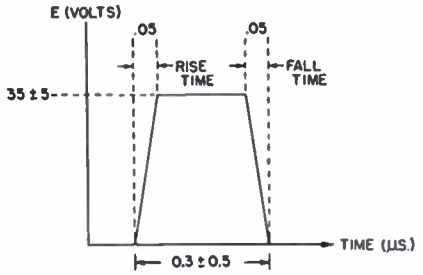

Fig. 1—Characteristic EDVAC timer pulse.

Forty-nine prime pulse sources on a 1-mc time base are required. One of the forty-nine pulse sources must produce an output at a frequency of 1 mc. These pulses, designated "clock pulses," represent the fundamental time marks of the machine. While the machine is in operation, they are produced continuously. Reference to Fig. 2, part A, will illustrate their occurrence.

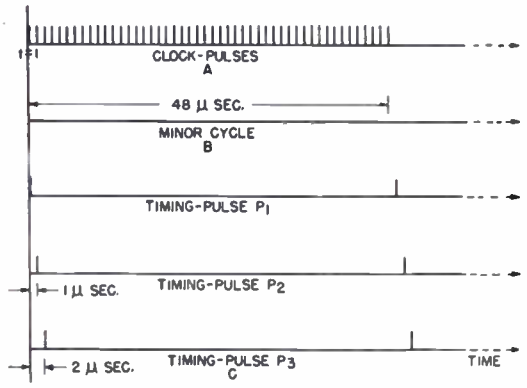

Fig. 2—EDVAC timing pulses.

The fundamental operational time period for the machine is designated the "minor cycle" and is forty-eight microseconds long (see Fig. 2, part B).

The other forty-eight prime pulse sources produce outputs called "timing pulses." They are illustrated in Fig. 2, part C. These pulses are periodic on a 48-microsecond base. Each timing pulse generator is phased with respect to all others such that one timing pulse occurs each microsecond. If the source of timing pulse, say P_n, at $t=1, 2, 3, \cdots$, is observed, the appearance of a pulse at $t=n$, $t=n+48$, $t=n+2(48)$, and so on will be observed. A similar observation at the source of P_{n+1} will indicate pulses at $t=n+1$, $t=n+1+48$, and so forth.

III. Clock-Pulse Generator

Fig. 3 is a simplified illustration of a clock-pulse generator. A sine wave at a 1-mc frequency is produced by a crystal-controlled oscillator. This signal is fed to a tapped delay line terminated in its characteristic impedance and picked off at points A and B. The signals existing at these points differ in phase so that their combination in a diode coincidence gate will result in a signal whose maximum duration ($\frac{1}{2}$ microsecond) occurs when the taps coincide and diminishes as the tapes are moved apart. By changing the relative locations of tap-points A and B, the width of the output pulse and also the phase of its occurrence relative to the 1-mc oscillator can be adjusted. The output of the coincidence circuit is clipped and fed to a power stage

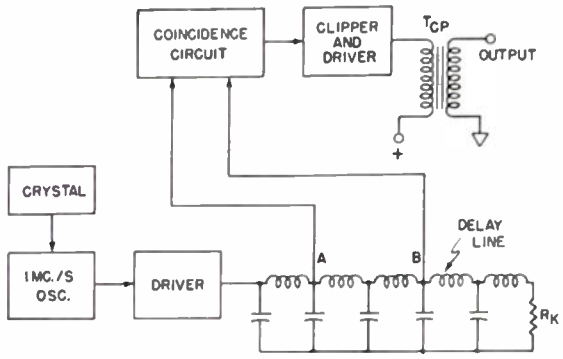

Fig. 3—Clock-pulse generator.

which utilizes a transformer T_{CP} for impedance transformation. The output pulse thus obtained is of desired time and voltage characteristics. The circuit described above involves about ten tube envelopes. Two such circuits supply clock pulses for the EDVAC memory circuits and general machine use. Use of cathode-follower output circuits in place of the pulse-transformer-coupled system would have resulted in marginal operation and much greater power consumption.

IV. Timing-Pulse Generator

A simplified logical diagram illustrated in Fig. 4, shows the method of generating the time pulses by means of a matrix.

The operation of the timing-pulse matrix is as follows: The pulses energizing the entire matrix are designated CPE (clock-pulse early). These pulses are produced in the same manner as the clock pulses described in the preceding section of this paper and differ from them only in that the tap points fed to the CPE coincidence circuit occur at an earlier point on the delay line. This is necessary to correct for delays inherent in the matrix circuits and to allow the output timing pulses to occur in precise synchronization with the clock pulses. Thus the CPE pulses may be considered to be in time with the clock pulses except for a fixed and known time difference.

Six sources of pulses at a frequency of one-sixth of a mc are needed. Each of these is taken from a 6-microsecond delay line (C1F8 and C1G8 of Fig. 4) at 1-microsecond intervals. Each source has its pulse staggered in time by 1 microsecond from adjacent sources. When the inhibiting gate 1H3 has all inputs positive, a CPE will pass into the delay line. However, as this pulse traverses the length of the line it produces five inhibiting pulses, namely those which can be traced as outputs from 1G3, 1H5, and so forth to 1H8, respectively, which find their way back to gate 1H3. These pulses prevent the entrance of another CPE into the 6-microsecond delay line for five pulse periods. Of a

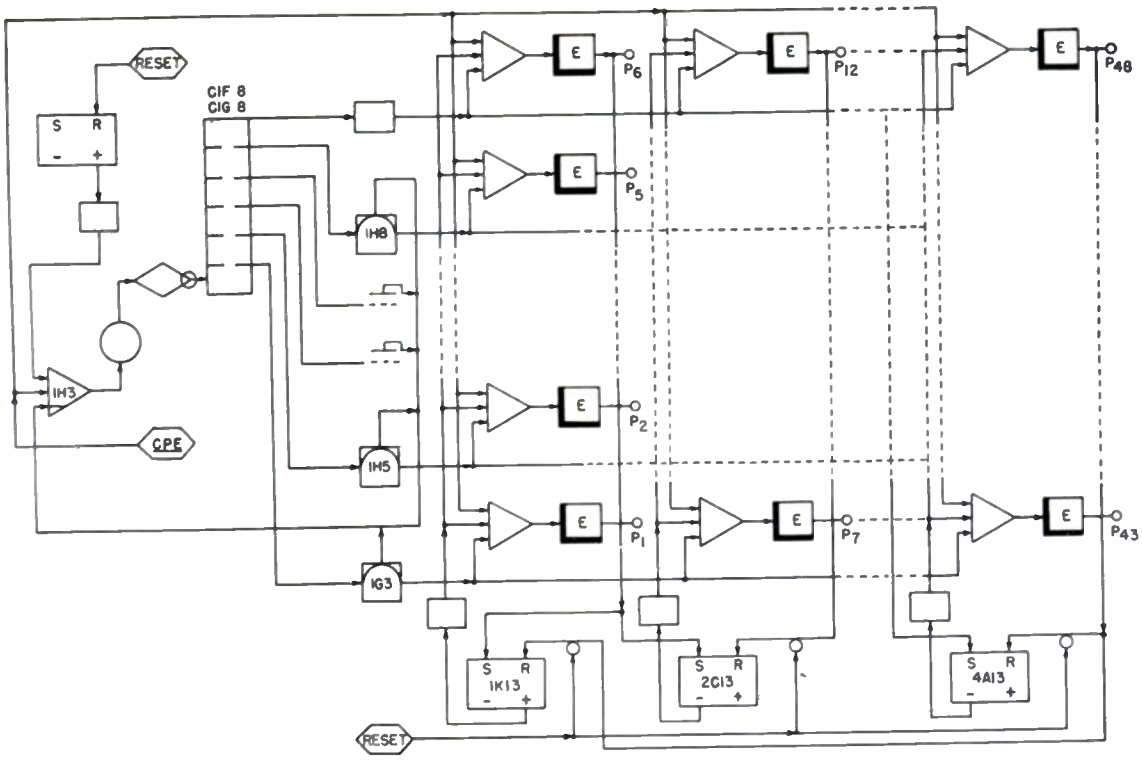

Fig. 4—Timing-pulse source matrix.

continuous series of pulses attempting passage through gate 1H3, only one in every six will be successful. This operation is repetitive and it is seen that six pulse outputs, each stepped in time by 1 microsecond and each occurring at one-sixth mc per second, are produced. The one-sixth mc pulse is common for any row, the dc gating signal for any column, and CPE for all rows and columns. In addition, since the input circuit of any matrix element is an "and" gate, a triple coincidence of positive voltages in time must occur at this gate input if any output from the element is to be realized. The arrangement shown will prevent any matrix element from being energized more or less often than once in a 48-microsecond period.

Assume that all dc gating signals are negative except those of the first column; that is, the outputs of 2C13 and the like to 4A13 are negative, and the output of 1k13 is positive. In the EDVAC this condition is created by the introduction of a single reset-pulse signal. Thus, the earliest of the one-sixth mc pulses produces an output at the matrix element common to row 1, column 1 because a triple coincidence exists at the input of the "and" gate for this element. This output is a pulse designated P_1. The next one-sixth mc pulse (1 microsecond later) generates P_2 by producing a triple coincidence at the element common to row 2, column 1, and so forth, until P_6 is produced.

P_6, in addition to being distributed for use where necessary throughout the machine, is also fed to 1K13 and 2C13 (flip-flops). This pulse causes the "and" input gates of column 1 to be inhibited and those of column 2 to be susceptible to the coincidence effect of one-sixth mc pulses occurring row-wise. This is accomplished by the reversal of output voltages from 1K13 and 2C13. With the advent of the first one-sixth mc pulse (approximately 1 microsecond following P_6), P_7 is produced at the element common to row 1, column 2, and P_1 and P_7 are separated in time by 6 microseconds.

This process continues until P_{48} is produced. P_{48} is the last of the timing pulses and will cause matrix column 8 to be closed and matrix column 1 to be opened to coincidence operation by resetting flip-flops 4A13 and 1K13 simultaneously. This sequence of pulse outputs will continue indefinitely in the order described repeating every 48 microseconds.

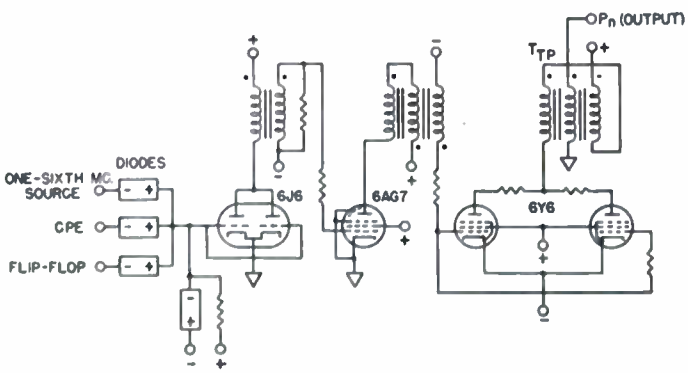

Fig. 5—Timing-pulse generator.

Fig. 5 illustrates the schematic of a particular timing pulse source. It comprises a three-stage amplifier driven

by an "and" gate whose inputs are CPE, one of the six outputs of the one-sixth mc pulse sources, and a dc gate signal generated by a flip-flop circuit. This matrix element is represented in Fig. 4 by the boxes marked E and their associated "and" gates. The input is the "and" gate previously described which is followed by three stages of amplification, shaping, and impedance transfer. The output stage consists of a paralleled 6Y6's feeding a specially designed pulse transformer T_{TP}.

The vital statistics of the complete timer unit follow:

1. Two clock-pulse sources, each with a peak-power output of about 245–320 watts and a duty cycle of about 0.3.
2. One early-pulse generator with a somewhat lower peak-power output and a duty cycle of about 0.3.
3. Forty-eight timing-pulse sources each with nominal peak-power outputs of about 245–320 watts and a duty cycle of approximately 0.006.
4. Tube envelopes total 270, all of which are standard receiver-type tubes with the exception of two 807's.
5. The total power necessary to operate the complete unit is about 2,000 watts. This includes heater power.

Conclusion

The units described represent useful methods for the production of high-frequency pulses capable of feeding low-impedance loads. Variations on and extrapolations of the matrix methods discussed provide a convenient and accurately controlled means for the production of a large variety of pulses in time, each of which is related to all the others by definite logic.

Acknowledgments

The author wishes to express his considerable appreciation to J. Chedaker, T. C. Chen, S. E. Gluck, H. J. Gray, M. Pleasure, and R. L. Snyder, Jr., for their assistance in the design of the circuits described.

Bibliography

EDVAC Staff, "A Functional Description of the EDVAC," vols. I and II, University of Pennsylvania, Moore School of Electrical Engineering Research Division Report 50-9; November 1, 1949.

Glossary

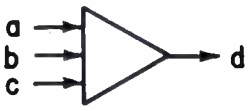

Glossary (a)

"And" gate; an input is required simultaneously at a and b and c in order to produce output at d.

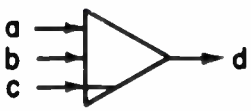

Glossary (b)

Inhibiting "and" gate; an input is required at a and b simultaneously with no input at c in order to produce output d.

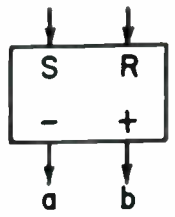

Glossary (c)

Flip-flop or multivibrator with two modes of stability. For a pulse at S input (setting pulse) the output will be positive at a and negative at b. If we now apply a pulse at R input (*resetting* pulse), the outputs will revert to those indicated on illustration.

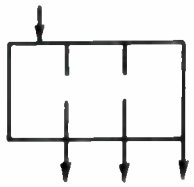

Glossary (d)

Delay line.

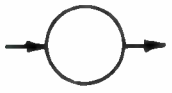

Glossary (e)

Off-tube; a single-stage pulse amplifier biased beyond cutoff, such that only a positive pulse input of sufficient amplitude produces a pulse output, which is negative.

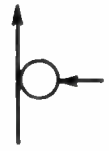

Glossary (f)

Represents dc isolation.

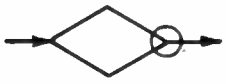

Glossary (g)

Pulse transformer. Circle indicates polarity reversal.

Glossary (h)

Cathode-follower.

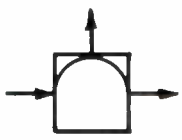

Glossary (i)

Combination cathode-follower and inverter circuit.

Glossary (j)

Input connection; x is designation of input and the inclusion or omission of the underline indicates whether or not the input is produced on the same physical chassis.

Note that numbers or letters placed within or in proximity of symbols described above indicate physical location of circuit elements involved.

Tunable Waveguide Filters*

W. SICHAK†, MEMBER, IRE AND H. AUGENBLICK‡, ASSOCIATE, IRE

Summary—**Heretofore, tunable waveguide filters have consisted of cavities connected with quarter-wavelength coupling lines and tuned by means of a lumped reactance in the cavity. Such filters exhibit asymmetrical frequency response and a bandwidth proportional to the cube of frequency when tuned.**

A different method of tuning is to maintain constant guide wavelength as the filter is tuned. A filter so tuned will exhibit symmetrical pass-band response and essentially constant bandwidth.

Various methods of varying guide wavelength are investigated, including (1) changing the guide width, (2) inserting a dielectric strip in the broad face of the guide, and (3) inserting a metal strip in the broad face of the guide.

Measurements on a three-section filter tuned by a dielectric strip show that almost constant bandwidth with a straight-line frequency tuning curve can be obtained over at least a 12 per cent frequency range.

Introduction

MICROWAVE filters are used to minimize interference from transmissions on unwanted frequencies. The design of microwave filters is covered by Fano and Lawson.[1] A good exposition of the design methods applied to maximally flat band-pass filters and references to other work are given by Mumford.[2] Band-pass filters can be designed and built to give the desired characteristics at one frequency. Mumford,[2] for example, has built a fifteen-cavity fixed-tuned filter that worked very well. Tunable filters, however, that preserve their design characteristics have not been built. This paper gives methods of designing satisfactory tunable filters.

Discussion

Two fundamental methods of changing the resonant frequency of a waveguide cavity have been investigated: (1) The insertion of a lumped susceptance in the cavity, and (2) varying the parameters of the waveguide in such a manner that the guide wavelength at resonance is constant.

Lumped Susceptance

The insertion of a variable lumped susceptance in a cavity will alter the resonant frequency of the cavity.

This method of tuning is subject to several severe limitations. The bandwidth of such a cavity constructed from capacitive or inductive irises is

$$\left.\begin{aligned} BW_{cap} &\doteq \frac{2c}{\pi l}\,\frac{\lambda_0\lambda_{g0}}{X^2}\left(1-\frac{2\lambda_{g0}^2}{X^2}\right) \doteq K/f^2 \\ BW_{ind} &\doteq \frac{2c}{\pi l}\,\frac{\lambda_0}{Y^2\lambda_{g0}^3}\left(1-\frac{2}{Y^2\lambda_g^2}\right) \doteq Kf^4 \end{aligned}\right\}. \quad (1)$$

The superiority of capacitive irises for tunable filters has been demonstrated by Smullin.[3]

A further limitation is that the coupling lines between cavities are not tuned. As a result, the pass-band response becomes more and more asymmetrical as the filter is tuned further from its design frequency.[4]

The limitations on the tuning-post method are such that the filter can only be employed over a narrow frequency range. A three-section inductive-iris filter operating in the 5,000-mc region had a bandwidth that increased 26 per cent for a 4 per cent change in resonant frequency. The percentage change for a filter constructed from capacitive irises is somewhat less but nevertheless sufficient to restrict the operating range of the filter.

Constant Guide Wavelength

Most properties of a dispersive waveguide system depend on the guide wavelength and not on frequency directly. For example, the electrical length of a waveguide line is $2\pi l/\lambda_g$ and not $2\pi l/\lambda$; the susceptance of a capacitive iris varies as $1/\lambda_g$ and not as frequency. This principle can be used in the design of many tunable waveguide systems, but will be applied here only to the design of filters.

The doubly loaded $Q_{\lambda g}$ of a simple cavity is (2)

$$Q_{\lambda g} = \frac{\lambda_{g0}}{\Delta\lambda_g} = \left(\frac{\pi l}{2\lambda_g}\right)(B^4 + 4B^2)^{1/2}. \quad (2)$$

This equation shows that if a cavity has a certain $Q_{\lambda g}$ at one guide wavelength and one frequency it will have the same $Q_{\lambda g}$ at a different frequency if the guide wavelength is the same, provided that B is not changed.

The fact that $Q_{\lambda g}$ is constant over the band unfortunately does not mean that Q on a frequency basis is constant.

* Decimal classification: R143.2×R386. Original manuscript received by the Institute, September 15, 1950; revised manuscript received, January 25, 1951. Presented, 1951 IRE National Convention, March 7, 1950, New York, N. Y. This work was sponsored by the Signal Corps Engineering Laboratories.

† Federal Telecommunication Laboratories, Inc., Nutley, N. J.

‡ Formerly, Federal Telecommunication Laboratories, Inc.; now, Microlab, South Orange, N. J.

[1] G. L. Ragan, "Microwave Transmission Circuits," McGraw-Hill Book Co., Inc., New York, N. Y., chapters 9 and 10; 1948.

[2] W. W. Mumford, "Maximally-flat filters in waveguide," *Bell Sys. Tech. Jour.*, vol. 27, pp. 684–713; October, 1948.

[3] L. D. Smullin, "Design of Tunable Resonant Cavities with Constant Bandwidth," Technical Report No. 106, M.I.T., April 5, 1949. (For abstract, see PROC. I.R.E., vol. 37, p. 1442; December, 1949.)

[4] See page 694 of footnote reference[1].

$$Q_{\lambda_g} = \frac{\lambda_{g0}}{\Delta\lambda_g} = \frac{\lambda_0}{\Delta\lambda}\left(\frac{\lambda}{\lambda_g}\right)^2 = \frac{f_0}{\Delta f}\left(\frac{\lambda}{\lambda_g}\right)^2 = Q_f\left(\frac{\lambda}{\lambda_g}\right)^2. \quad (3)$$

Thus, a system with a constant Q_{λ_g} has a Q that varies as the square of the frequency. Usually a constant bandwidth is desired, which means a Q_f proportional to frequency. This deviation from constant bandwidth is generally not too serious, however.

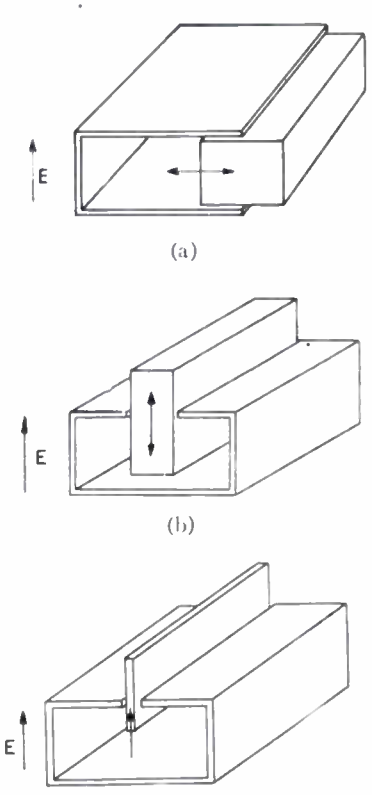

Fig. 1—Methods of changing guide wavelength. (a) Movable wall. (b) Variable-depth dielectric strip. (c) Ridge waveguide.

A further advantage of the constant-guide-wavelength filter is the fact that the coupling lines are exactly tuned over the entire frequency range. Thus, the passband response will not suffer from the asymmetrical response of the tuning-post filter.

Methods of Changing Guide Wavelength

Variable-Width Waveguide

The guide wavelength for the dominant mode in a rectangular waveguide is given by

$$\lambda_g = \frac{\lambda}{[1 - (\lambda/2a)^2]^{1/2}}. \quad (4)$$

Thus, the guide wavelength may be held constant by adjusting the guide width for each resonant frequency. One of the narrow walls of the waveguide is removed and replaced with a movable metal strip that makes good contact with the walls and the irises, (Fig. 1 (a)).

The susceptance of a capacitive iris is not a function of the width of the waveguide. Hence this particular iris may be employed in the variable-width filter. This is not true of other geometries, such as the inductive iris. The end susceptance and impedance mismatch of the tuning section may be minimized by designing the tuning section to have normal guide dimensions in the center of the desired band.

The major limitation of such a filter is the difficulty of making good and uniform contact between the movable wall and the rest of the system.

Dielectric Strip

Another method of changing the guide wavelength is to insert a dielectric strip into a slot cut in the broad face of the guide, Fig. 1(a). The guide wavelength at a fixed frequency is a minimum when the strip extends all the way across the guide, the wavelength increasing as the strip is retracted. The filter is designed to operate properly at the high-frequency end of the band when the strip is completely out of the guide. To tune the filter to a lower frequency, the dielectric strip is inserted to such a depth that the guide wavelength is the same as the design guide wavelength. The dielectric strip is made wide enough so that the guide wavelength with the strip almost all the way across the guide at the lowest desired frequency is the same as the design guide wavelength. The proper width can be determined from an equation derived by Frank.[5]

The end-susceptance and impedance mismatch of the tuning section is low, and matching transformers are quite simple. The filter may suffer from comparatively high losses unless the slot is shielded properly. This particular filter appears to have the most merit of all systems tested.

Ridge Waveguide

Ridge waveguide[6] can be used to change the guide wavelength in the filter, Fig. 1(b). The principle is the same as that discussed above for the dielectric strip. While any width of ridge can be used, a very thin wedge is most suitable because radiation from a narrow slot is small. The characteristic-impedance mismatch between the tuning section and the normal waveguide is high and matching transformers are difficult. Otherwise, the method of tuning is satisfactory.

Constant-Bandwidth Filters

A good approximation to a constant bandwidth can be obtained by using half- or quarter-wavelength transformers between the constant-guide-wavelength filter and the rectangular waveguide.

[5] C. G. Montgomery, R. H. Dicke, and E. N. Purcell, "Principles of Microwave Circuits," McGraw-Hill Book Co., New York, N. Y., page 387; 1948.

[6] S. B. Cohn, "Properties of ridge wave guide," Proc. I.R.E., vol. 35, pp. 783–788; August, 1947.

Fig. 2(a) shows schematically a filter with matching sections between the filter proper and the normal waveguide. Fig. 2(b) is the equivalent circuit of a filter made

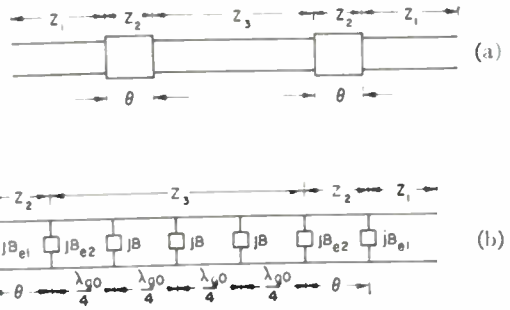

Fig. 2—Filter with matching sections. (a) Schematic of filter. (b) Equivalent circuit.

of three identical sections. B is the equivalent susceptance of each filter section and is given by

$$B \cong 4Q\frac{\Delta\lambda_g}{\lambda_{g0}} \cong 4Q\left(\frac{\lambda_g}{\lambda}\right)^2\frac{df}{f_0}, \tag{5}$$

where

Q = guide wavelength Q of one section

df = deviation from resonant frequency.

For three sections, this becomes

$$B = 1.526\left(\frac{f}{f_0}\right)\left(\frac{2df}{w}\right), \tag{6}$$

where

f_0 = design frequency

w = bandwidth of whole filter at design frequency.

The characteristic impedance of a waveguide is given by

$$Z_0 = K\frac{b}{a}\frac{\lambda_g}{\lambda}. \tag{7}$$

The insertion-loss ratio (LR) at frequencies near the resonant frequency is given in (8), assuming that B_{e_1} and B_{e_2} are equal to zero, that the $\lambda_{g0}/4$ coupling lines and the matching sections are a constant electrical length, and that the susceptances of the irises and the characteristic impedances are constant.

$$LR = 1 + \frac{B^2}{4}\left[\left(\frac{Z_1}{Z_3}\right)^2(B^2 - 2) + \left(\frac{Z_3}{Z_1}\right)^2\right]^2 \tag{8a}$$

$$LR = 1 + \frac{B^2}{4}\left[\left(\frac{Z_2}{Z_1}\right)^2\left(\frac{Z_2}{Z_3}\right)^2(B^2 - 2) + \left(\frac{Z_1}{Z_2}\right)^2\left(\frac{Z_3}{Z_2}\right)^2\right]^2. \tag{8b}$$

Equation (8a) is for matching sections a half-wavelength long and (8b) is for matching sections a quarter-wavelength long. If (Z_3/Z_1) equals the ratio of the guide wavelength in the filter to the guide wavelength in the rectangular guide (as is the case when the filter is tuned with a dielectric strip), (6) and (8a) show that for a 12 per cent shift in the resonant frequency the bandwidth increases 16 per cent. If in addition $Z_2 = (Z_1Z_3)^{1/2}$, (6) and (8b) show that the bandwidth is directly proportional to the ratio of the design frequency to the resonant frequency. If (Z_3/Z_1) equals the ratio of the guide wavelength in the filter to the guide wavelength in the rectangular guide and Z_2 equals Z_3, (6) and (8b) show that almost constant bandwidth can be obtained.

Experimental Results

Movable-Wall Filter

A cavity made of two capacitive irises with half-wavelength transformers on each end was built in a 2- by 1- by 0.064-inch-wall waveguide (RWR 187 or RG-49/U) and tested. The wall of the half-wavelength transformers, as well as the wall of the cavity, was made movable. When the width of the waveguide was 1.872 inches, the center frequency was 4,325 mc and the bandwidth between 3-db points was 91 mc. When the width was 1.42 inches, the center frequency was 5,073 Mc and the bandwidth was 125 mc. The loaded Q is

$$Q_f = Q_{\lambda_g}\frac{a_3}{a_1}\left(\frac{\lambda_{g3}}{\lambda}\right)\left(\frac{\lambda_{g1}}{\lambda}\right). \tag{9}$$

This equation predicts a ratio of bandwidths equal to 1.46, whereas a ratio of 1.37 was obtained experimentally.

Ridge Waveguide

Calculations were made to determine to what depth a metal strip 1/32-inch wide must be inserted to obtain a constant guide wavelength in the ridge guide at frequencies between 4,400 and 5,000 mc. The constant guide wavelength was the same as the guide wavelength in a normal 2- by 1-inch guide at 5,050 mc. The relative characteristic impedance Z_1/Z_3 of the ridge waveguide, determined by measuring the relative impedance (in normal 2- by 1-inch guide) at the face of the ridge, is shown on Fig. 3. Since the large change in characteristic

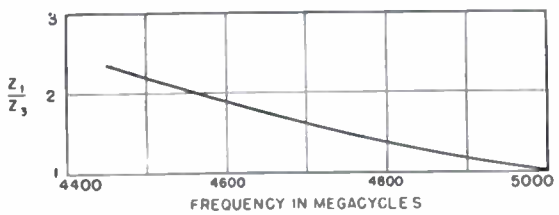

Fig. 3—Mismatch between ridge guide and normal guide.

impedance would make the design of matching sections difficult, no filters were constructed in ridge waveguides.

Dielectric-Strip Filter

Measurements were made to determine to what depth a $\frac{1}{4}$-inch thick polystyrene strip must be inserted to maintain the guide wavelength constant by placing them on the bottom of a slotted section of waveguide, the load end of which was short-circuited. The guide wavelength was determined by measuring the distance

between successive minimums. The depth required to maintain the guide wavelength constant at 7.48 centimeters versus frequency was determined (7.48 centimeters is the guide wavelength at 5,100 Mc in a rectangular waveguide 1.872 inches wide). The depth-versus-frequency curve was essentially a straight line between 4,400 and 5,000 mc.

The relative characteristic impedance Z_1/Z_3 of the partially filled waveguide, determined by measuring the relative impedance at the face of the strip, is shown as circles on Fig. 4. Also shown on Fig. 4 is the variation of Z_1/Z_3 with frequency, assuming that (7) holds.

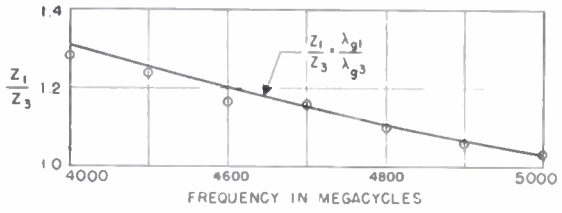

Fig. 4—Mismatch between dielectric-strip guide and normal guide.

A three-element filter, shown in Fig. 5, was designed to resonate at 5,050 mc, with a cavity bandwidth of 84 mc so that the bandwidth of the whole filter would be 65 mc.[7] The measured standing-wave ratio in the pass band with the filter tuned to three different frequencies is shown in Fig. 6. Also shown there is the resonant frequency versus depth of dielectric. For this measurement, a quarter-wavelength transformer with $Z_2 = (Z_1Z_3)^{1/2}$ was used.

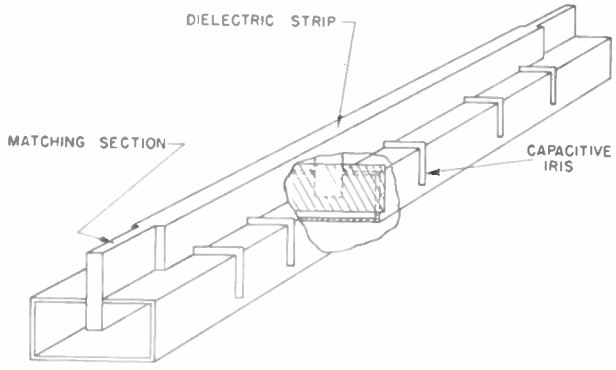

Fig. 5—Tunable three-section filter.

At 4,700 mc, the midband insertion loss was 2 db due to radiation from the poorly shielded slot. At 50 and 100 mc off the resonant frequency, the insertion loss was 21.5 and 42.5 db, respectively. The theoretical insertion losses at these frequencies are 22.5 and 41.5, respectively. These measurements were made with a relatively crude model constructed to test the principle. Separate pieces of dielectric were used in the cavities, quarter-wavelength coupling lines, and matching sections to allow tuning each section to compensate for constructional errors. The shift-of-minimum method[8] was used to align the filter sections at each resonant frequency.

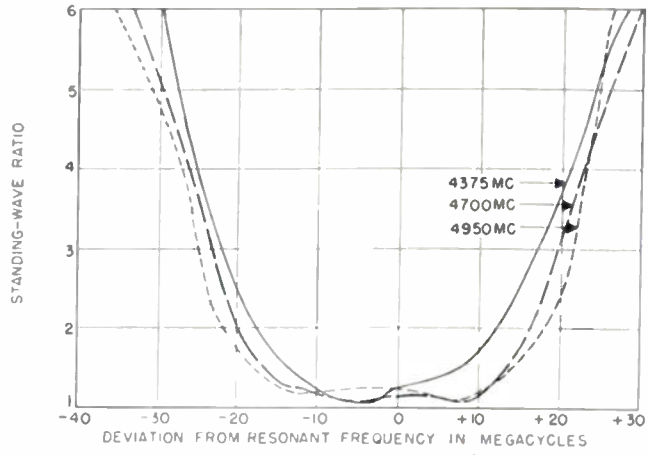

(a)

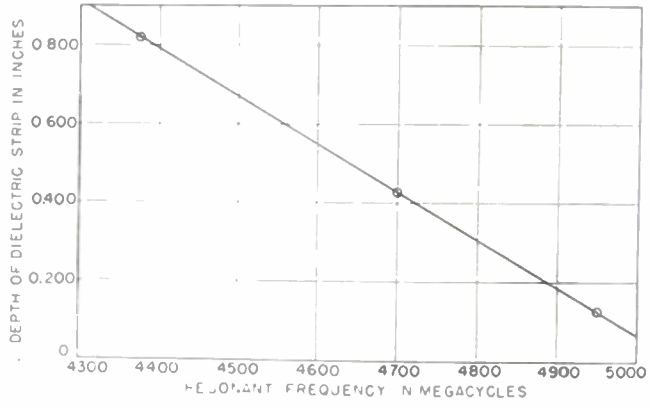

(b)

Fig. 6—Response of three-element filter. The slope of the linear curve is 0.85 Mc per 0.001 inch.

The depth of dielectric in the three cavities varied slightly. The greatest variation, ±0.016 inch from the average, was at 4,375 mc. The depth of dielectric in the quarter-wave coupling lines was consistently less than the depth in the cavities. The greatest variation, 0.083 inch, was at 4,950 mc. It is believed that these variations are due to constructional errors and the method of alignment, and are not inherent in the method of tuning.

Conclusions

The theory and measurements show that a tunable waveguide filter with almost constant bandwidth can be built by using a variable-depth dielectric strip to keep the guide wavelength in the filter constant as the resonant frequency is changed. Single-knob tuning with a linear frequency scale is possible. These features, not possessed by other types, are highly desirable in some systems.

Acknowledgment

Acknowledgment is due to D. J. LeVine and H. Seidel for making some of the measurements reported in this paper.

[7] See page 682 of footnote reference 1.

[8] See page 714 of footnote reference 1.

GLOSSARY

a = waveguide width
a_3 = waveguide width in filter section
b = waveguide height
B = normalized susceptance of iris
B_{e1} = normalized end susceptance between transformer and normal guide
B_{e2} = normalized end susceptance between transformer and filter section
BW = frequency bandwidth
C = velocity of light
K = a constant
l = iris separation
Q_f = loaded Q on a frequency basis
Q_{λ_g} = loaded Q on a guide wavelength basis
Z_1 = characteristic impedance of normal guide
Z_2 = characteristic impedance of matching section
Z_3 = characteristic impedance of filter section
λ = air wavelength
λ_0 = air wavelength at resonance
λ_g = guide wavelength
λ_{g0} = guide wavelength at resonance
λ_{g1} = guide wavelength in normal guide
λ_{g3} = guide wavelength in filter section
$\Delta\lambda_{g0}$ = guide wavelength bandwidth
θ = electrical length, $2\pi l/\lambda_g$.

Induced Grid Noise and Noise Factor*

R. L. BELL†

Summary—**In this paper there is developed an approximate treatment of narrow-band triode noise factor, taking into account induced grid noise by a new method. Minimal values of noise factor predicted theoretically are compared with experimental values, and it is found that from a knowledge of circuit losses, shot noise, mutual conductance, space charge input capacitance, and dc grid current measured on the tube, noise factor, and optimum source conductance can be predicted with accuracy over a wide range of operating conditions.**

It is shown that lead inductance effects and normal induced grid effects (grid noise, space-charge capacitance, transit-time damping) have no influence on noise performance, but merely affect tube admittances. Direct compensation in the grid circuit of components of input admittance to which these effects give rise leads to a deterioration of noise factor usually attributed to grid noise.

It is shown that the optimum grid circuit detuning may be provided automatically by the input space-charge capacitance.

I. INTRODUCTION

THE FLUCTUATIONS induced at a vacuum-tube grid are, as is well known, of considerable importance in the design of low-noise amplifiers for the vhf band. Various attempts have been made to calculate the relation between currents leaving the cathode and currents induced in the grid, the ratio of which two quantities might, by analogy with low-frequency terminology, be termed the "partition coefficient" for the grid. A realistic calculation of this quantity is however in a practical case extremely laborious.

No attempt was made until recently[1,2] to *measure* the partition coefficient and, the cathode fluctuations being known, merely compute the expected grid fluctuations. This, as shown below, is a comparatively simple matter.

The validity of the procedure rests on the assumption that the ratio between the Fourier transform of the current pulse induced in the cathode to that of the current pulse induced in the grid by any given electron is a function of frequency only, and is independent of the energy of emission of the electron, point of emission, and direction of emission. This of course is not in general the case, and the accuracy of the final result is only a measure of the closeness of the approximation. A priori reasons may easily be found for and against the contention that the approximation is likely to be a good one. Justification for its use, however, lies where application, even in unlikely cases, has so far turned out well.

One result of the variation of grid partition coefficient with initial emission conditions is that the behavior of the integrated effect at the grid is similar to that in a tube where the partition coefficient is in fact independent of these conditions, as in our assumption, but additional currents are induced at the grid quite independently of currents induced in the cathode-anode circuit. This fictitious uncorrelated effect has been called the "total emission" component of induced grid noise. Under conditions in which the tube is in no danger of taking direct grid current, the total emission component is small compared with the normal induced component, and our assumption naively applied leads to sufficiently accurate results. In the interest of brevity we shall not consider explicitly all emission effects.

II. GRID NOISE

In terms of the nodal analysis[3] the input admittance at a node (1) of a vacuum-tube circuit is

$$Y_{11} = \frac{\Delta}{\Delta_{11}}, \tag{1}$$

* Decimal classification: R138.6. Original manuscript received by Institute, July 31, 1950; revised manuscript received, February 5, 1951.

† Research Laboratories, The General Electric Company, Ltd., Wembley, England.

[1] R. L. Bell, "Induced grid noise," *Wireless Eng.* vol. 27, p. 86; March, 1950.

[2] A. van der Ziel, "Noise suppression in triode amplifiers," *Canadian Jour. Res.*, p. 189; June, 1950.

[3] N. R. Campbell, V. J. Francis, and E. G. James, "Linear single-stage valve circuits," *Wireless Eng.*, vol. 22, p. 333; July, 1945.

where Δ is the determinant

$$\begin{vmatrix} 11 & 12 & 13 \cdots \\ 21 & 22 & 23 \cdots \\ 31 & 32 & 33 \cdots \\ \cdots & \cdots & \cdots \end{vmatrix} \tag{2}$$

and Δ_{11} the cofactor of the element (11). The elements are

$$\begin{aligned} (xy) &= \alpha_x g_y - Y_{xy} \\ (xx) &= \alpha_x g_x + \sum_0^N Y_{xn}. \end{aligned} \tag{3}$$

α_x is the proportion of cathode current intercepted by electrode x, g_x its conductance with respect to cathode current, Y_{xy} the admittance connected between node x and node y.

$$Y_{1i} = \frac{(11)\Delta_{11} + (12)\Delta_{12} + (13)\Delta_{13} \cdots}{\Delta_{11}}. \tag{4}$$

If all other nodes 2, 3, 4 $\cdots$ are earthed,

$$(22), (33), (44) \cdots \rightarrow \infty$$

and

$$Y_{1i} \rightarrow (11) = \alpha_1 g_1 + Y_{10} + Y_{12} + Y_{13} \cdots. \tag{5}$$

In the absence of the electron stream $\alpha_1 g_1 = 0$ and

$$Y_{1i} = Y_{10} + Y_{12} + Y_{13} \cdots, \tag{6}$$

i.e., the partition coefficient for the electrode (1) is

$$\alpha_1 = \frac{Y_{1i} - Y_{1i(0)}}{g_1} \tag{7}$$

the quantities involved being measured with other electrodes earthed.

In discussing transit-time effects it is convenient to regard "cathode current" as the electron conduction current at the potential minimum, in which case, for reasonable electrode spacings ($d \ll$ free-space wavelength), the conductances g_x of the various electrodes are real quantities.

We are basically interested in the effect of the induced grid effects on the shot effect in the triode valve. The shot noise may be represented in the frequency range $f, f+df$ as a conduction current at the potential minimum of mean-square value

$$d\bar{i}^2 = s_p(f)df \tag{8}$$

where at low frequencies $s_p = 2ei_p\Gamma^2$. Thus, under the assumptions already stated, the fluctuations appearing at say the grid node (1) is

$$\overline{di_1}^2 = s_1(f)df = |\alpha_1^2| s_p(f)df. \tag{9}$$

Similarly, for node (2) $\overline{di_2}^2 = |\alpha_2^2| s_p(f)df$.

The fluctuation $s_1(f)$ gives rise to a further effect at (2)

$$s_2'(f) = s_1(f)\left|\frac{\Delta_{12}}{\Delta_{22}}\right|^2. \tag{10}$$

Bearing in mind that these two fluctuations have the same source, the nett effect at (2) is

$$s_2(f) = s_p(f)\left|\alpha_2 + \alpha_1\frac{\Delta_{12}}{\Delta_{22}}\right|^2. \tag{11}$$

It is now clear that the induced grid noise may be regarded as a manifestation of a kind of feedback effect from the cathode-anode circuit to the grid by the mechanism of electron transit time. It is of interest to inquire whether other feedback effects such as those due to cathode, anode, and grid lead inductances can be taken into account by treating them as internal to the effective tube comprised of anode grid and cathode connecting tags, respectively, without reference to the actual tube elements. Detailed investigation yields the expected result that this is permissible at least so long as the effects of lead inductance on tube admittances remain first order, which is the only case of profitable interest.

Hence where desired at any stage in the analysis, general properties such as admittances, electrode currents and the like, which have been treated as pertaining to the internal tube with zero lead inductances can be transferred to the external tube, bearing in mind that additions and (mostly negligible) transformations of admittance components are thereby effected.

III. Noise Factor

We compute here what has been termed "effective noise figure,"[4] or simply "noise factor."[5] The concept is related in elementary ways to other definitions of amplifier sensitivity such as noise figure referred to a source at standard room temperature[6] and the related "operating noise factor" and "absolute sensitivity."[7] Noise factor as used here is defined by reference to Fig. 1 as follows. One supposes s_r to be the spectrum of an equivalent fluctuation which when injected into node 3 represents the noise output from the whole of the

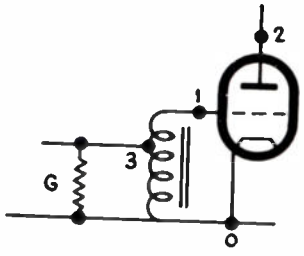

Fig. 1—Node points on the common cathode circuit.

[4] H. Goldberg, "Some notes on noise figures," Proc. I.R.E., vol. 36, p. 1205; October, 1948.
[5] N. R. Campbell, V. J. Francis, and E. G. James, "Noise factor of valve amplifiers," *Wireless Eng.*, vol. 23, p. 74, March, 1946; and p. 116, April, 1946.
[6] H. T. Friis, "Noise figures of radio receivers," Proc. I.R.E., vol. 32, p. 419; June, 1944.
[7] D. O. North, "Absolute sensitivity of radio receivers," *RCA Rev.*, vol. 6, p. 332; January, 1942.

amplifier excluding the source conductor. s_u is the spectrum of the fluctuation current injected into node 3 by the source conductance. Then the noise factor is given by

$$N = \frac{s_u + s_r}{s_u}.$$

Noise factor thus defined is a function of source temperature T_u.

If we now denote by s_1 the spectrum of all current fluctuations injected into the grid node (1) which are uncorrelated with the shot noise in the valve

$$s_1 = 4kT_uG_u + 4kT_{10}G_{10} + 4kT_{10}G_{10} + 2ei_g, \qquad (12)$$

G_u, G_{10} and G_{12} are, respectively, the source conductance viewed from the tube grid, the cutoff grid-earth conductance and the cutoff grid-anode conductance. T_u, T_{10} and T_{12} are the physical temperatures of these conductances. i_g is the direct grid current taken by the tube, which may be shown normally to exhibit full shot effect. Into this term may be lumped all uncorrelated grid noise effects (total emission noise, induced partition noise,[8] anode reflection and secondary emission effects, etc.), by a suitable and normally unimportant modification of the value of i_g.

The total fluctuation injected into the anode node is thus

$$s_2 = s_1\left|\frac{\Delta_{12}}{\Delta_{22}}\right|^2 + s_p\left|\alpha_2 + \alpha_1\frac{\Delta_{12}}{\Delta_{22}}\right|^2, \qquad (13)$$

omitting for simplicity the negligible contribution to anode fluctuations of thermal noise in the anode load and in the grid-anode conductance. The noise factor follows by dividing through by the term in G_u:

$$N = 1 + \frac{G_{10}T_{10} + G_{12}T_{12} + 20i_gT_0}{G_uT_u} + \frac{R_eT_0g_m^2}{G_uT_u}\left|\frac{\alpha_2\Delta_{22} + \alpha_1\Delta_{12}}{\Delta_{12}}\right|^2, \qquad (14)$$

where we have written

$$s_p = 2ei_p\Gamma^2 = 4kT_0R_eg_m^2,$$

and T_0 is standard room temperature (290°K), R_e is the equivalent noise resistance of the triode, g_m its mutual conductance.

$$\frac{2e}{4kT_0} \simeq 20 \text{ volts}^{-1}.$$

One has

$$\Delta_{22} = (11) = \alpha_1g_1 + Y_{10} + Y_{12}$$
$$\Delta_{12} = -(21) = -\alpha_2g_1 + Y_{12} \qquad (15)$$
$$Y_{10} + Y_{12} = G_{10} + G_u + G_{12} + jB_{10} + jB_u + jB_{12}.$$

[8] R. L. Bell, "Negative grid partition noise," *Wireless Eng.*, vol. 25, p. 294; September, 1948.

Since total currents are conserved, for a triode

$$\alpha_1 + \alpha_2 = 1.$$

Thus $\alpha_2g_1 = (1-\alpha_1)g_1$ may be regarded as the high-frequency mutual conductance of the tube.

The factor $|\alpha_2\Delta_{22}+\alpha_1\Delta_{12}|^2$ in the third term of (14) expands to

$$|\alpha_2\alpha_1g_1 + \alpha_2Y_{10} + \alpha_2Y_{12} + \alpha_1Y_{12} - \alpha_1\alpha_2g_1|^2; \qquad (16)$$

(16) becomes simply

$$|\alpha_2Y_{10} + Y_{12}|^2. \qquad (17)$$

The term α_1g_1 representing admittances which appear at the grid due to currents correlated with cathode-anode currents has already disappeared from the noise factor expression. The significance of this is that feedback effects such as the correlated induced grid noise, input admittances due to cathode anode and grid lead inductances, the space-charge susceptance, transit-time damping, and so forth, have no first-order effect on noise factor. This in turn means that the circuit adjusted for optimum noise factor performance under the assumption that such effects do not exist will function optimally when they are present, and will remain unaffected by them. Such phenomena may have their effects on the input and transfer admittances of the stage and in the process of trying to compensate for such admittance components, whether conductive or susceptive, we may find that the noise factor has deteriorated. This however is a property of the circuit maladjustment and not of the effects under discussion. Conditions of optimum adjustment of the external circuit are discussed in Section IV below.

The quantity α_1 is in general complex, $\alpha_1 = \gamma + j\beta$, and normally $\beta \gg \gamma$;

(16) expands to

$$[G_u + G_{10} + G_{12} - \gamma(G_u + G_{10}) + \beta(B_u + B_{10})]^2 + [B_u + B_{10} + B_{12} - \gamma(B_u + B_{10}) - \beta(G_u + G_{10})]^2. \qquad (18)$$

IV. Optimum Circuit Conditions

Writing (18) as

$$(G_u + G)^2 + (B_u + B)^2 \qquad (19)$$

one has approximately

$$N = 1 + \frac{G_{10}T_{10} + G_{12}T_{12} + 20i_gT_0}{G_uT_u} + \frac{R_eT_0g_m^2}{G_uT_u}\left[\frac{(G_u + G)^2 + (B_u + B)^2}{g_m^2 + B_{12}^2}\right]. \qquad (20)$$

The optimum value of source conductance is thus

$$G_{u_0}^2 = G^2 + (B_u + B)^2 + \left[\frac{G_{10}T_{10} + G_{12}T_{12} + 20i_gT_0}{R_eT_0}\right]\left[1 + \frac{B_{12}^2}{g_m^2}\right] \qquad (21)$$

and the minimum noise factor.

$$N_0 = 1 + \frac{2R_s T_0}{T_u}\left[G_{u_0} + G\right]\left[\frac{g_m^2}{g_m^2 + B_{12}^2}\right]. \quad (22)$$

Minimizing with respect to source susceptance, one has simply

$$B_{u_0} + B = 0,$$

i.e., approximately, omitted terms being small.

$$B_{u_0} + B_{10} + B_{12} = 0.$$

This is the condition that the source susceptance shall resonate with the *cold* input susceptance of the tube with the anode earthed. It is clear that this condition implies little or no restriction on the *working* input admittance of the tube as an amplifier, which by suitable choice of circuit components can have any desired value.

It is interesting to note that the optimum source conductance depends on the source susceptance, but not vice versa.

Taking the case of the inductance-neutralized triode with a low anode load (as in the "cascode" arrangement), the input susceptance is simply

$$B_u + B_{10} + \beta g_1,$$

and B_u is normally adjusted for resonance to satisfy

$$B_{u_f} + B_{10} + \beta g_1 = 0.$$

The detuning of the grid circuit required to optimize the noise factor is thus

$$B_{u_0} - B_{u_f} = \beta g_1,$$

which is the value of the total input space-charge susceptance, i.e., the space charge automatically provides the correct value of detuning in this circuit. It is not difficult to show that this detuning remains close to optimum, even for very wide-band operation.

V. Measurements

An experimental check on the above work was carried out by a series of extremely careful measurements at 45 mc on a number of vhf triode and triode-connected tube types employed as first tube in a cascode arrangement. Experience brought to light a large number of necessary techniques and refinements, and the measurements of noise factor quoted are certainly accurate to within 2 per cent. In order to calculate the performance of tubes to this order of accuracy, it is, of course, necessary to substitute carefully determined experimental values of all the various quantities involved. When this is done, it is found that noise factors can be predicted to within 2–3 per cent, an accuracy sufficient for most design purposes. The approximations involved may however be expected to begin to break down for tubes in which the grid winding pitch is much greater than grid-cathode clearance. Further, the treatment is a "first-order" one, and the results cannot be expected to apply near the maximum usable frequency of any particular valve.

The curves of Figs. 2–7 are typical of the agreement found under reasonable conditions between measured and predicted results. Figs. 2 and 3 show the variation of minimum noise factor with bias at fixed anode current (variable anode voltage) for two high-slope E 1714 triodes operating without detuning.

The deterioration in noise factor which may result

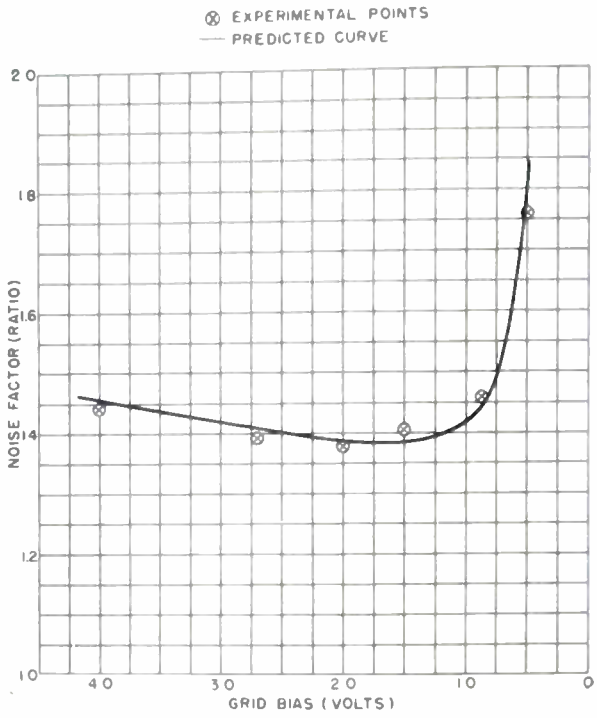

Fig. 2—Minimum noise factor versus grid bias E1714, No. 577, $i_a = 10$ ma, no detuning.

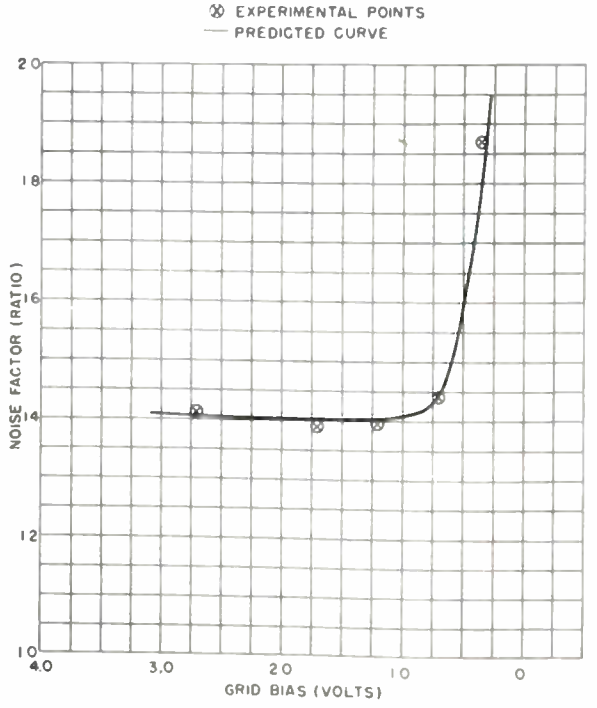

Fig. 3—Minimum noise factor versus grid bias E1714, No. 415, $i_a = 10$ ma, no detuning.

from the flow of a few microamperes of grid current is well illustrated by the characteristic steep rise in the curves at low bias values. A slight elaboration of the algebra of the previous sections shows that the deterioration is due to the shot noise in the grid current, the effect of the grid current-voltage slope being negligible.

Figs. 4 and 5 show the corresponding variation of optimum source conductance with bias for the same tubes. The accuracy in determination of the experimental points is not great, since it involves the estimation of the

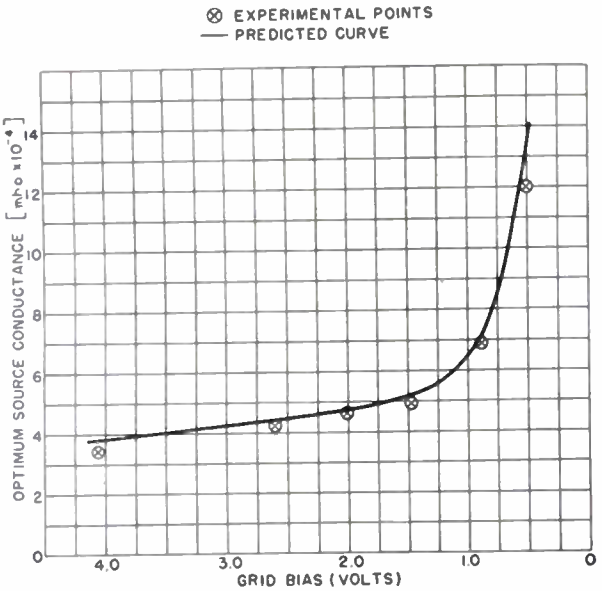

Fig. 4—Optimum source conductance versus grid bias, E1714, No. 577, $i_a = 10$ ma, no detuning.

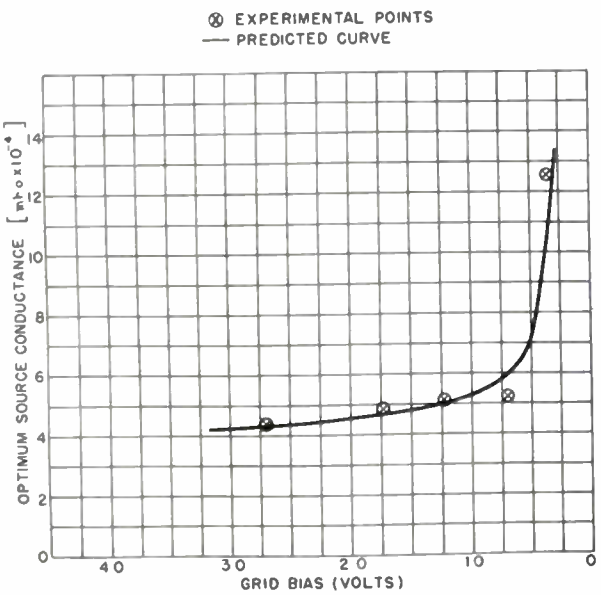

Fig. 5—Optimum source conductance versus grid bias, E1714, No. 415, $i_a = 10$ ma, no detuning.

abscissa of a minimum on an experimental curve. Accuracy of measurement of actual minimum noise factor values may be expected to be of a higher order, however, being the ordinate of the minimum on the same curve.

Measurements were made on special samples of one type of triode in which care had been taken to remove the possibility of reflected or secondary electrons from the anode returning to the region of the grid, and so inducing extra grid noise. No effect on noise factor due to such a phenomenon was in fact detected.

Figs. 6 and 7 show the minimal effect on noise factor of detuning the grid circuit. The theory indicates a minimum value of detuning near to the space-charge capacitance, and this is actually observed. The reduction in noise factor obtained is close to that expected on the basis of the above calculations. While optimum detuning is independent of source conductance, the reverse is not the case; thus, having established optimum detuning, a further reduction in noise factor will in general be obtainable by readjustment of source conductance. The reduction of noise factor on detuning calculated in previous sections is the combined effect of both operations.

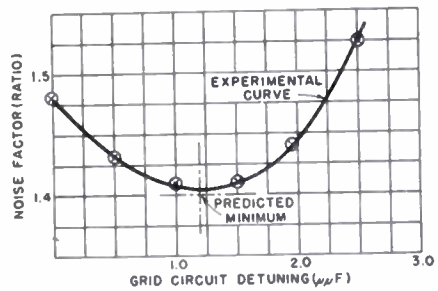

Fig. 6—Grid detuning and noise factor, E1714, No. 577, $i_a = 10$ ma, constant source conductance.

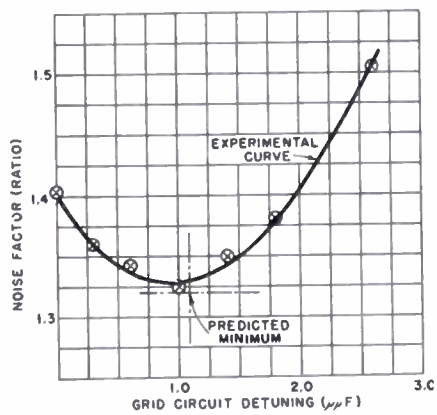

Fig. 7—Grid detuning and noise factor, E1714, No. 415, $i_a = 10$ ma, constant source conductance.

The conclusion that lead inductances have no first-order effect on noise factor is easily verified experimentally. An artificial increase of any of the lead inductances by several times has no detectable effect on measured noise factor.

VI. Acknowledgments

In conclusion, the author desires to tender his acknowledgment to the M. O. Valve Co. Ltd., on whose behalf the work described in this publication was carried out.

Transient Response of Asymmetrical Carrier Systems*

GEORGE M. ANDERSON†, ASSOCIATE, IRE, AND EVERARD M. WILLIAMS†, SENIOR MEMBER, IRE

Summary—**The transient properties of asymmetrical amplitude-modulated carrier systems are studied in the time domain. A vector integral method is given for the determination of system response to arbitrary modulation. Typical nonlinearity of the envelope transfer function is studied as a function of modulation depth. It is found that the time delay associated with a rising response to a step change is always less than the delay associated with a decreasing response to a similar change.**

Transient improvement as a consequence of detuning in asymmetrical systems appears to be accompanied by a decrease in signal-to-noise ratio.

Introduction

AMPLITUDE-MODULATED carrier systems which have asymmetrical amplitude and phase characteristics about the carrier frequency possess a certain type of nonlinearity in the relations between the envelopes of the signal and the response. This nonlinearity, in what is called the envelope transfer function, occurs even though the system is linear in the total signal.

Previous investigators have studied the transient response of asymmetrical carrier systems, particularly in the television field. Their analyses have generally involved the Fourier integral and assumed amplitude and phase characteristics. The physical inconsistencies which often arise from these mathematical methods, such as infinite overshoot, responses existing before the signal is applied, and the like, which cannot in fact exist, have been explained by Guillemin.[1]

Recently Eaglesfield[2] has investigated a specific transient problem in an asymmetrical amplitude-modulated carrier system using Laplace transform methods; results of his study are limited to the case of restricted modulation depth, for which the envelope transfer function becomes linear.

Cherry[3] points out that asymmetric systems may be advantageously analyzed by an extension of the well-known band-pass low-pass analogy.[4]

The paper presents a time-domain study of asymmetrical systems. It is found that account must be taken of the carrier-phase time variation in adding response envelopes and that a vector superposition integral is convenient as a general method of computing transient response. Examples are given of the nonlinearity of the envelope transfer function.

The Vector Integral

In linear systems, it is often convenient to solve the system differential equations for a particular input and thereafter to make use of the superposition integral. In the case of asymmetrical systems, the envelope response to a given input envelope is not sufficient, of itself, to determine the envelope response to any arbitrary input. However, it is possible to derive an integral, analogous to the ordinary superposition integral, which relates the response envelope to any signal envelope in terms of the envelope and phase response to a given signal envelope.

The Heaviside unit step function is often chosen as an appropriate test signal for video systems. For band-pass, amplitude-modulated systems, the unit step function of carrier plays a role analogous to that of the unit step function in video systems.

Fig. 1 is a block diagram of a typical amplitude-modulated carrier system. The modulated stage is

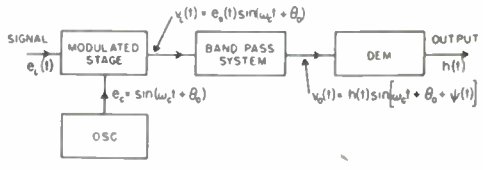

Fig. 1—Block diagram of a typical amplitude-modulated carrier system.

linear, i.e., its output contains an envelope component linearly related to the input. The band-pass system is assumed to be linear. Its output is fed to a detector which produces a response proportional to the envelope.

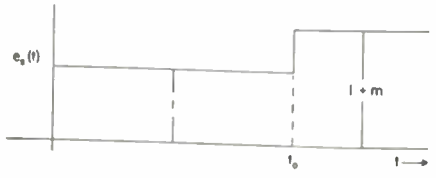

Fig. 2—Unit step function at time zero followed by a step function of depth m at time t_0.

The superposition integral applicable to asymmetrical systems is derived by considering the effect on the response envelope of the composite signal envelope, $e_s(t)$, of Fig. 2. Here $e_s(t)$ consists of a unit step function and

* Decimal classification: R148.1. Original manuscript received by the Institute, September 14, 1950; revised manuscript received, December 11, 1950. This paper is part of a dissertation submitted by George M. Anderson in partial fulfillment of the requirements for the degree of Doctor of Science at Carnegie Institute of Technology.

† Carnegie Institute of Technology, Pittsburgh 13, Pa.

[1] E. A. Guillemin, "Communication Networks," vol. 2, John Wiley and Sons, New York, N. Y., p. 480; 1935.

[2] C. C. Eaglesfield, "Carrier-frequency amplifiers, transient response with de-tuned carrier," *Wireless Eng.*, vol. 23, pp. 67–74; March, 1946.

[3] E. C. Cherry, "The transmission characteristics of asymmetric-sideband communication networks," in two parts, Pt. I, *Jour. IEE* (London), vol. 89, pt. III, pp. 19–42; March, 1942; and Pt. II, *Jour. IEE* (London), vol. 90, pt. III, pp. 75–88; June, 1943.

[4] P. R. Aigrain, B. R. Teare, Jr., and E. M. Williams, "Generalized theory of the band-pass low-pass analogy," PROC. I.R.E., vol. 37, pp. 1152–1155; October, 1949.

a displaced step function of depth m.

$$e_s(t) = u(t) + mu(t - t_0), \tag{1}$$

where

$$u(t) = 0; \quad t < 0$$
$$= 1; \quad t \geqq 0$$

and

$$-1 \leqq m \leqq +\infty.$$

The total input to the band-pass system, $v_{i_1}(t)$, attributable to $u(t)$ is

$$v_{i_1}(t) = u(t) \sin(\omega_c t + \theta_0). \tag{2}$$

The response $v_{0_1}(t)$ to $u(t)$ may be written as

$$v_{0_1}(t) = A(\omega_c)a(t, \omega_c) \sin[\omega_c t + \theta_0 + \psi(t, \omega_c)], \tag{3}$$

where

$$a(t, \omega_c) = 0; \quad \psi(t, \omega_o) = 0 \quad \text{for} \quad t \leqq 0$$
$$a(\infty, \omega_c) = 1; \quad \psi(\infty, \omega_c) = \delta(\omega_c).$$

$A(\omega_c)$ and $\delta(\omega_c)$ are the steady-state gain and phase shift, respectively; $a(t, \omega_c)$ and $\psi(t, \omega_c)$ represent the envelope and phase response to $u(t)$. It is assumed that the system bandwidth is small enough so that $a(t, \omega_c)$ and $\psi(t, \omega_c)$ are not functions of θ_0.

To determine the system response, $v_{0_2}(t)$ attributable to $mu(t-t_0)$, write the input $v_{i_2}(t)$

$$v_{i_2}(t) = mu(t - t_0) \sin(\omega_c t + \theta_0) \tag{4}$$

as

$$v_{i_2}(t) = mu(t - t_0) \sin[\omega_c(t - t_0) + \theta_0 + \omega_c t_0]. \tag{5}$$

$v_{i_2}(t)$ is the same function of $(t-t_0)$ as $v_{i_1}(t)$ is of t with the exception of the additional constant phase $\omega_c t_0$. Since $a(t, \omega_c)$ and $\psi(t, \omega_c)$ are independent of the initial carrier phase, $v_{0_2}(t)$ may be obtained from $v_{0_1}(t)$ by replacing t by $(t-t_0)$ and substituting $(\theta_0+\omega_c t_0)$ for θ_0.

$$v_{0_2}(t) = A(\omega_c)ma(t - t_0, \omega_c) \sin[\omega_c(t - t_0) + \theta_0 + \omega_c t_0 + \psi(t - t_0, \omega_c)] \tag{6}$$
$$= A(\omega_c)ma(t - t_0, \omega_c) \sin[\omega_c t + \theta_0 + \psi(t - t_0, \omega_c)].$$

The response to the composite signal of (1) is given by

$$v_0(t) = v_{0_1}(t) + v_{0_2}(t)$$
$$= IA(\omega_c)\{a(t, \omega_c)e^{i\psi(t,\omega_c)} + ma(t - t_0, \omega_c)e^{i\psi(t-t_0,\omega_c)}\}e^{i(\omega_c t+\theta_0)}, \tag{7}$$

where I indicates the imaginary part is to be taken. The envelope associated with (7) is simply the absolute value of the last expression

$$h(t, \omega_c) = A(\omega_c)\left| a(t, \omega_c)e^{i\psi(t,\omega_c)} + ma(t - t_0, \omega_c)e^{i\psi(t-t_0,\omega_c)} \right|. \tag{8}$$

It is evident from (8) that the effects of different signals on the response envelope may be determined by considering the individual envelopes as vector quantities with associated variable (in time) phase angles.

Equation (7) may be employed for determining the output $v_0(t)$, attributable to any input envelope $f(t)$, in terms of $a(t, \omega_c)$ and $\psi(t, \omega_c)$. The input envelope is approximated by a series of step functions. By letting the number of steps go to infinity, the sum which represents $v_0(t)$ becomes an integral.

$$v_0(t) = IA(\omega_c)\left\{f(0)a(t, \omega_c)e^{i\psi(t,\omega_c)} + \int_0^t f'(\tau)a(t - \tau, \omega_c)e^{i\psi(t-\tau,\omega_c)}d\tau\right\}e^{i(\omega_c t+\theta_0)}. \tag{9}$$

The response envelope $h(t, \omega_c)$ is the absolute value of $v_0(t)$

$$h(t, \omega_c) = A(\omega_c)\left| f(0)a(t, \omega_c)e^{i\psi(t,\omega_c)} + \int_0^t f'(\tau)a(t - \tau, \omega_c)e^{i\psi(t-\tau,\omega_c)}d\tau \right|. \tag{10}$$

This is the vector, or complex, form of the superposition integral. It provides a method for determining the envelope response to any signal envelope provided that $a(t, \omega_c)$ and $\psi(t, \omega_c)$ are known. The advantage lies in the fact that the method leads directly to the desired envelope response, and further it is applicable to those problems for which $f(t)$ cannot be expressed in a convenient analytical form and graphical methods must be employed.

Typical Nonlinearity as Function of Modulation Depth

The nonlinear character of the envelope transfer function can be conveniently investigated for the case of step function modulation. In this study, the system of Fig. 1 is presumed to have reached steady-state conditions and subsequently a change in $e_s(t)$ occurs. The system envelope response can be determined from (8) by letting t_0 become very large. For convenience, shift the time axis so that time is computed from t_0 as zero. This gives

$$h(t, \omega_c) = A(\omega_c)\left| e^{i\delta(\omega_c)} + ma(t, \omega_c)e^{i\psi(t,\omega_c)} \right|$$
$$= A(\omega_c)\left| 1 + ma(t, \omega_c)e^{i\phi(t,\omega_c)} \right|$$
$$= A(\omega_c)\sqrt{1 + m^2a^2(t, \omega_c) + 2ma(t, \omega_c)\cos\phi(t, \omega_c)}, \tag{11}$$

where

$$\phi(t, \omega_c) = \psi(t, \omega_c) - \delta(\omega_c).$$

In order to study the differences in the response envelope as a function of m, a new function $b_m(t, \omega_c)$ is defined as the normalized difference of $h(t, \omega_c)$ and the initial value $h(0, \omega_c)$.

$$b_m(t, \omega_c) = \frac{h(t, \omega_c) - h(0, \omega_c)}{h(\infty, \omega_c) - h(0, \omega_c)}$$

$$= \frac{1}{m}\left[\sqrt{1+m^2a^2(t,\omega_c)+2ma(t,\omega_c)\cos\phi(t,\omega_c)}-1\right] \quad (12)$$

since $h(0, \omega_c) = A(\omega_c)$ and $h(\infty, \omega_c) = A(\omega_c)(1+m)$.

This has the effect of plotting all changes whatever m may be, on a scale from 0 to 1, and is useful for comparison purposes.

Examination of the partial derivative of $b_m(t, \omega_c)$ with respect to m shows

$$\frac{\partial b_m(t,\omega_c)}{\partial m} \geqq 0 \quad \text{for} \quad t > 0 \quad (13)$$

and

$$\cos^2\phi(t,\omega_c) \not\equiv 1.$$

Except for the excluded points, relation (13) shows that $b_m(t, \omega_c)$ is monotonic, increasing in m, and satisfies

$$b_{-1}(t,\omega_c) < b_m(t,\omega_c) < b_\infty(t,\omega_c) = a(t,\omega_c). \quad (14)$$

At the excluded points, $\cos^2\phi(t, \omega_c) = 1$, some of the $b_m(t, \omega_c)$ curves have a common point and tangent while the remaining curves again satisfy (13).

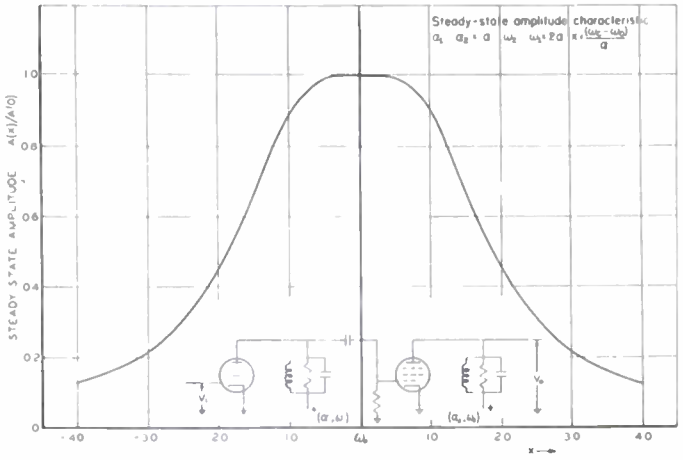

Fig. 3—Steady-state amplitude characteristic of the amplifier shown in the inset.

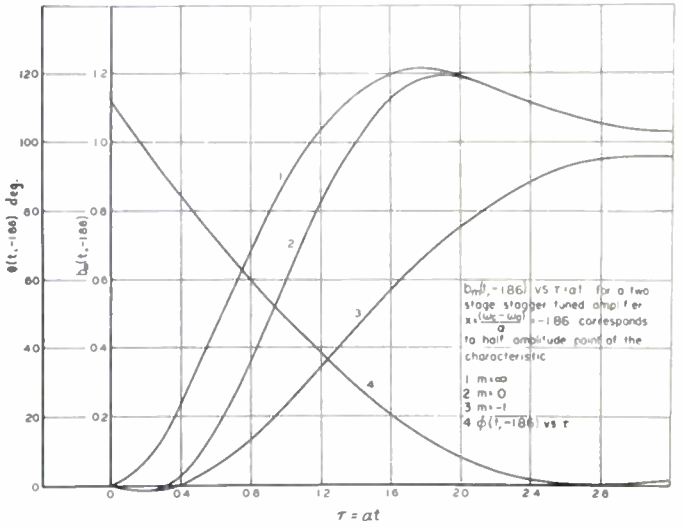

Fig. 4—Normalized envelope response of the amplifier of Fig. 4 to step-function change of modulation for three values of modulation depth m.

Relation (14) is illustrated in Fig. 4, which shows the normalized envelope response $b_m(t, \omega_c)$ for the two-stage amplifier of Fig. 3. The frequency parameter, $x = (\omega_c - \omega_0)/a$ corresponds to the half amplitude point of the steady-state characteristic. Also shown is $\phi(t, \omega_c)$. It is clear from Fig. 4 that the time delay associated with a decay is always greater than the time delay of a rise.

An interesting singularity is evident in the normalized envelope response curves $b_m(t, \omega)$ in Fig. 4 for $m = 0$, and -1. The curves swing negative before beginning to rise. The actual envelope response will therefore rise before decaying in the $m = -1$ case. Since

$$b_0(t,\omega_c) = a(t,\omega_c)\cos\phi(t,\omega_c) \geqq b_{-1}(t,\omega_c), \quad (15)$$

and from (3) and (11)

$$\phi(0,\omega_c) = -\hat{o}(\omega_c),$$

a sufficient condition for this effect to occur is that the steady-state phase shift exceed 90 degrees.

Signal-to-Noise Ratio

The chief advantage of detuning the carrier to produce an asymmetric system is an improvement in system transient response without an attendant increase in bandwidth. Because of mathematical difficulties, an investigation of transient response as a function of carrier frequency must be carried out, point by point, by actually computing the response at a number of frequencies. Results for a limited number of systems appear to show that the transient improvement does not come about until the carrier is detuned down the sides of the steady-state characteristic. The build up of the response in time proceeds at a maximum rate determined by the system bandwidth and not by the position of the carrier frequency. The principal reason for the transient improvement is that while the maximum rate of rise is essentially constant, the response is rising to a smaller final value, and thus reaches a higher percentage of that final value in a shorter time. Fig. 5 illustrates these effects in the case of the two-stage amplifier of Fig. 3 for two values of carrier frequency.

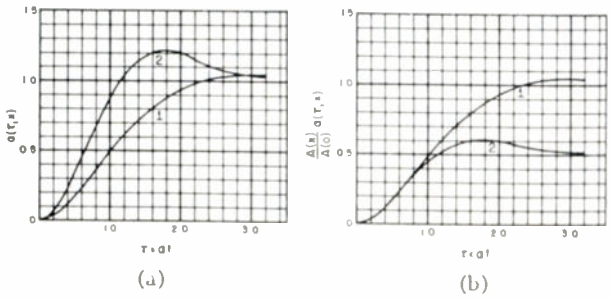

Fig. 5—(a) Normalized envelope response of the amplifier of Fig. 4. to a unit step modulation for two values of carrier frequency 1. $x = 0$, the symmetrical case 2. $x = -1.86$, the half-amplitude case. (b) The response curves of Fig. 5(a) are shown multiplied by the ratio of steady-state amplitude at frequency x, to the amplitude at the center frequency, $x = 0$.

Since the transient improvement comes about by decreasing the steady-state amplitude, it would appear that such improvement is accompanied by a decrease in signal-to-noise ratio.

Analysis of Audio-Frequency Atmospherics*

RALPH K. POTTER†, FELLOW, IRE

Summary—**Sound portrayal techniques used in studies of speech and noise reveal the structure of atmospheric disturbances well known to long-wave radio and ocean-cable engineers as "whistlers," "swishes," and "tweeks." It is suggested that renewed investigation of these effects, using modern analyzing tools, might yield information of considerable scientific interest.**

AUDIO-FREQUENCY atmospherics of a special type recorded during the period 1930–1933 by Burton and Boardman[1] were recently analyzed by the sound spectrograph. These atmospherics, thought to be a result of electrical reverberation within the ionosphere, are heard at times against the background noise on ocean cables and long wire lines. The sound spectrograph used for their analysis is an instrument developed in Bell Telephone Laboratories for research on speech, noise, and other sounds.[2] This instrument literally takes a sound sample to pieces and spreads its components out as a pattern, with frequency in the vertical dimension and time extending from left to right. The disposition of frequency and time is similar to that in the familiar musical staff. In the spectrogram random noise is revealed as a mottled, black-and-white surface. Steady tone becomes a horizontal black line and a clicking sound forms a vertical spike. The Burton-Boardman recordings of audio atmospherics included at least four kinds that have been called "whistlers," "swishes," "tweeks," and "rumblers."

Whistlers

Whistlers are whistling sounds that start at a high frequency, sweep downward in frequency at a more or less constant rate, and then tend to rise again. According to the Burton-Boardman article, "These types of atmospherics appear to have no connection with the time of day or with local weather conditions, and there is no indication of any correlation with the time of year. During some periods they have been observed frequently during days and nights for possibly 48 hours or longer. They have been found at times to persist steadily through the early morning, bridging the transition period when the more common forms of atmospherics rapidly change character."

Examples of whistlers are shown in Fig. 1. A frequency scale is included at the left of (a) and time is marked off along the top. Note that depth of frequency penetration varies and that the tonal quality becomes indefinite on the rise at the right as indicated by broadening of the trace. When frequency penetration is curtailed, the downward sweep of tone is lost in noise, as illustrated by the slanting traces at either end of Fig. 1(c). In all three of the spectrograms of Fig. 1 faint horizontal, harmonically spaced traces of uncertain origin may be seen in the lower half against the background noise.

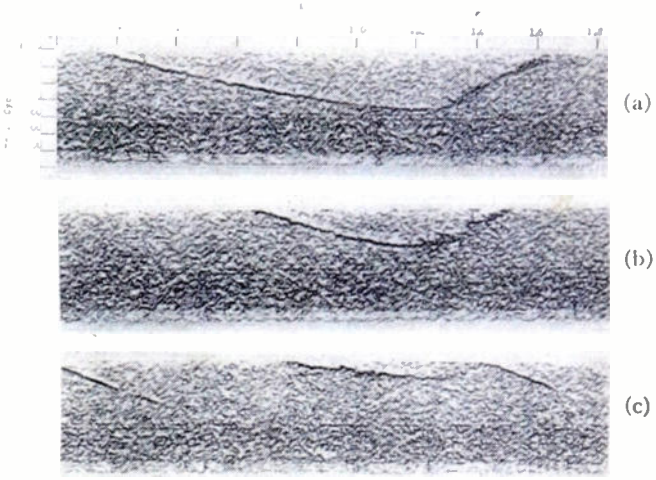

Fig. 1—Examples of "whistlers."

Swishes

Swishes are hissing sounds with a broad tonal quality, but no distinct pitch. Burton and Boardman compare them with the sounds "made by thin whips when lashed through the air." These sounds follow the same downward frequency sweep as the whistlers and seem in some way related to them. As to their occurrence, the Burton-Boardman report states, "Our observations have shown these often to appear during periods when the whistling tones are frequent, to correspond approximately to the length of the whistles, and at times to appear in regularly spaced trains." While the spectrographic patterns of available recordings seem to indicate that whistlers and swishes are distinctively different, Mr. Burton has expressed an opinion that they are perhaps of the same origin, differing only in the amount of irregularity introduced by some variability in the transmission medium. He believes all degrees of irregularity were heard during the course of the aural observations.

Examples of the swishes appear in Fig. 2 as the shadowy bands sloping toward the right. Their frequency-time slopes are similar to those of the whistlers as may be seen in (a) and (b). Faint remnants of what might be individual whistler traces are evident here and there throughout the shadowy bands. These suggest the swish could be a whistler that has been subjected to strong reverberation.

* Decimal classification: R114×R272. Original manuscript received by the Institute, October 31, 1950.
This discussion is part of a presentation by the author at a meeting of URSI in Washington, D. C., on April 18, 1950.
† Bell Telephone Laboratories, Inc., New York, N. Y.
[1] E. T. Burton and E. M. Boardman, "Audio frequency atmospherics," PROC. I.R.E., vol. 21, pp. 1476–1494; October, 1933. Also *Bell Sys. Tech. Jour.*, vol. XII, pp. 498–516; October, 1933.
[2] R. K. Potter, "Visible patterns of sound," *Science*, vol. 102, pp. 463–470; November 9, 1945.

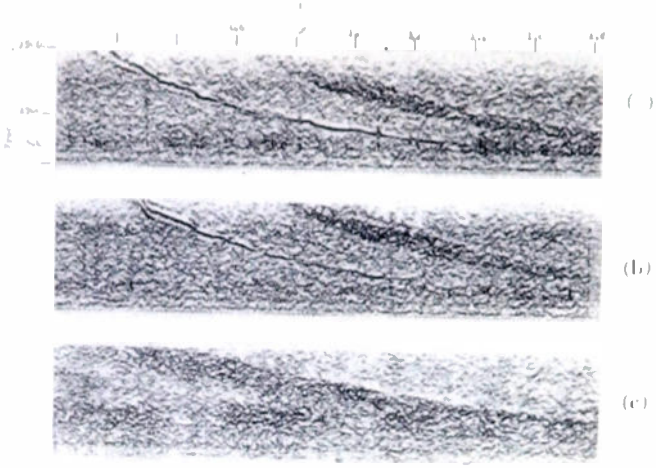

Fig. 2—Examples of "whistlers" and "swishes."

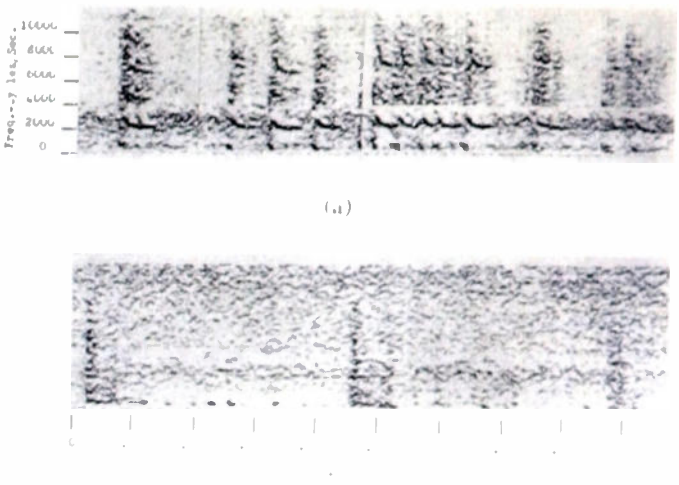

Fig. 3—Examples of "tweeks" and "rumblers."

Burton and Boardman state that, "Series of swishes have been observed following each other with almost perfectly regular spacing of a few seconds, the train persisting on occasion for as long as a few minutes." One group analyzed with the spectrograph consisted of four swishes that followed a regular sequence very near to three seconds apart. In this foursome each successive swish became fainter, and penetration leveled off at a progressively higher frequency.

The whistlers at the left in Figs. 2(a) and 2(b) display a peculiar "sideband" structure that deserves mention. It could be suspected some overload characteristic of the equipment was responsible, but harmonics, which almost invariably accompany overload, were absent or too weak to be recorded. There is also some evidence in (a) that the sideband spacing decreases as the tone sweeps downward, meaning that the wave train contains equally numbered groups regardless of frequency.

The Burton-Boardman report explains that the whistlers "sometimes swept upward or downward." In a recent elaboration of this statement Mr. Burton says that they often heard the rapid upward progressions, sometimes several in a closely spaced group, with no obvious evidence of a preceding downward sweep.

Tweeks

Examples of tweeks appear in (a) of Fig. 3. Incidentally, in the spectrograms of Fig. 3 the frequency range is extended about threefold, as indicated by the vertical scale at the left of (a). Simultaneously the time scale was expanded as shown at the bottom of (b). The horizontal light streak near the middle of both spectrograms in Fig. 3 was caused by an abrupt manual change in the spectrograph adjustment to bring out the weaker high-frequency components.

The tweeks are the small sled-shaped traces that curve downward and flatten out at a common level. The duration of these is much shorter than that of the whistler by a ratio of fifty or more to one.

The Burton-Boardman paper explains that tweeks are first heard around sunset and continue through to sunrise. They normally trail static impulses. The frequency of leveling off, they report, varies over the night period. One representative series of observations showed a sunset shift from about 2,300 cps down to some 1,650 cps within about three hours, and in the morning a return to 2,300 cps within about two hours.

Second and third harmonics of the tweeks are clearly evident at the left end of Fig. 3(a) and third harmonic patterns may be seen throughout the spectrograms. The slopes in these harmonic traces are steeper because all frequencies are multiplied. Whether the harmonics were present in the original signals is uncertain. Quite possibly they are caused by receiving and recording equipment nonlinearities.

Dark spots near the bottom of Fig. 3(a) are believed to be low-frequency "static" bursts. Their appearance seems to coincide closely with the beginning of each tweek and coincidentally a splash of random noise spreads upward through the frequency spectrum. This is in agreement with the theory that the tweeks are an aftermath of the potential release. Burton and Boardman suggest that they are explainable by multiple reflections between the ionosphere and earth as proposed by Barkhausen[3] for the swish and whistler.

Rumblers

Three examples of rumblers may be seen in Fig. 3(b). They appear as dark upright forms, one far to the left, another at the middle, and the third near the right end of the spectrogram. Close examination reveals that they start rather abruptly and consist of many closely spaced,

[3] H. Barkhausen, Proc. I.R.E., vol. 18, p. 1155; July, 1930. (Note Figs. 1, 2, and 3.)

horizontal traces that are overtones of a low frequency. A count of the overtones within a given frequency interval shows that the fundamental tone of these samples is around 600 cps. Along the bottom edge may be seen dark spots of faint tone at about this fundamental frequency.

The purpose of describing the above spectrograms of audio atmospherics is not to support any theory as to their cause. It is rather to suggest that a critical study of these natural audio-frequency signals with some of the analyzing tools now available might yield results of considerable scientific interest. The spectrographic display of oscillation intensity in relation to frequency and time affords a form of visual correlation that has proven to be highly effective in the study of such signals as these.

The Realization of a Transfer Ratio by Means of a Resistor-Capacitor Ladder Network*

JOHN T. FLECK† AND PHILIP F. ORDUNG‡, SENIOR MEMBER, IRE

Summary—**A method is offered for the exact realization with a ladder network containing only resistors and capacitors of a transfer ratio subject to the following three conditions:**

1. **Poles of $H(p)$ occur at real, negative values of p and are simple.**
2. **Zeros of $H(p)$ occur at real, negative values of p, but may be multiple.**
3. **$H(p)$ is finite for $p=j\omega$, $-\infty \leqq \omega \leqq \infty$.**

This type of network frequently has gain factors considerably greater than that allowed for an equivalent network synthesized on the lattice basis.

Introduction

THE PROBLEM considered in this paper is that of the realization of a transfer ratio, E_{output}/E_{input}, with a ladder-type network containing only resistors and capacitors. In the synthesis method to be described, the transfer ratio is used to establish the driving-point and transfer admittances of the ladder, then the ladder is synthesized. However, in order that the relationship of the transfer ratio to the driving-point and transfer admittances of the ladder be established and in order that the necessary conditions for realization of the transfer ratio be obtained, the properties of the RC ladder must first be carefully examined.

Properties of the Resistor-Capacitor Ladder Network

The type of ladder network considered in this paper is shown in Fig. 1. This ladder has n meshes, and the output voltage appears across the impedance Z_{2n}. In determinant notation, the driving-point admittance of the filter offered to E_{input} can be expressed as

$$Y_{11} = \frac{I_1}{E_{input}} = \frac{\Delta_{11}}{\Delta}, \tag{1}$$

where

$$\Delta = \begin{vmatrix} Z_{11} & Z_{12} & 0 & 0 & 0 & 0 \\ Z_{21} & Z_{22} & Z_{23} & 0 & 0 & 0 \\ 0 & Z_{32} & Z_{33} & Z_{34} & 0 & 0 \\ \cdot & & \cdot & & & \\ & & \cdot & & & \\ & & & \cdot & & \\ & & & & \cdot & \\ 0 & 0 & \cdot & \cdot & \cdot & Z_{n,n-1}\ Z_{nn} \end{vmatrix} \tag{2}$$

and where Δ_{11} is the cofactor of the element in the first row and first column of Δ. The elements of Δ are the respective contour and mutual impedances in the ladder. Since the expansion of Δ as well as Δ_{11} leads to a polynomial of the form

$$\Delta = a_0 + \frac{a_1}{p} + \cdots + \frac{a_s}{p^s}, \tag{3}$$

Y_{11} can be converted to a ratio of two rational polynomials in p by multiplying numerator and denominator, respectively, by an appropriate power of p, p^s.

$$Y_{11} = \frac{p^s\Delta_{11}}{p^s\Delta} = \frac{f(p)}{g(p)}. \tag{4}$$

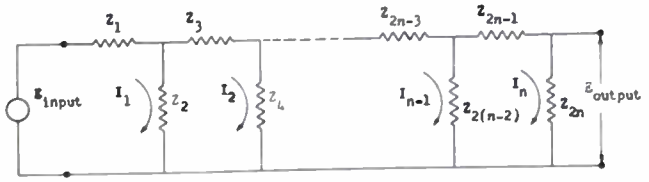

Fig. 1—The ladder network constructed with elements of the form

$$Z_j = R_j + \frac{1}{pC_j}.$$

The driving-point admittance[1] of an RC network has the property that when expressed in factored form

$$Y_{11} = \frac{f(p)}{g(p)} = h\frac{(p+\alpha_1)(p+\alpha_2)\cdots}{(p+\gamma_1)(p+\gamma_2)\cdots} \tag{5}$$

the zeros and poles are simple, occur at negative real

* Decimal classification: R143. Original manuscript received by the Institute, May 12, 1950; revised manuscript received, December 26, 1950. Presented, 1951 IRE National Convention, New York, N. Y., March 20, 1951.

The major part of the material in this paper was developed by John T. Fleck in a thesis entitled "Network Synthesis," which was submitted to Yale University in partial fulfillment of the requirements for the Ph.D. degree in electrical engineering.

† Cornell Aeronautical Laboratories, Ithaca, N. Y.

‡ Yale University, New Haven, Conn.

[1] E. A. Guillemin, "Communication Networks," John Wiley and Sons, Inc., New York, N. Y., vol. 2, pp. 208–215; 1935.

values of p, and satisfy the separation requirement

$$0 \leqq \alpha_1 < \gamma_1 < \alpha_2 \cdots . \tag{6}$$

The transfer ratio $H(p)$ can also be expressed in determinant notation as

$$H(p) = \frac{E_{\text{output}}}{E_{\text{input}}} = \frac{I_n Z_{2n}}{E_{\text{input}}} = \frac{\Delta_{1n} Z_{2n}}{\Delta} \tag{7}$$

or as the ratio of two rational polynomials

$$H(p) = \frac{p^s \Delta_{1n} Z_{2n}}{p^s \Delta} = \frac{h(p)}{g(p)} . \tag{8}$$

The cofactor Δ_{1n} can easily be shown by expansion to be the product of the mutual impedances between meshes of the ladder; hence

$$Z_{2n}\Delta_{1n} = Z_2 Z_4 Z_6 \cdots Z_{2(n-1)} Z_{2n}. \tag{9}$$

Furthermore, as the element Z_j is restricted to the form

$$Z_j = R_j + \frac{1}{pC_j} = \frac{R_j}{p}\left(p + \frac{1}{R_j C_j}\right), \tag{10}$$

the zeros of $H(p)$ are zeros of the shunt impedances in the ladder, and these zeros necessarily occur at real negative values of p. As any number of the shunt impedances may be alike, the zeros of $H(p)$ can have any desired multiplicity.

The poles of $H(p)$, on the other hand, must be simple. It can readily be shown with the residue criterion that if a root of multiplicity r occurs in the Δ of a resistor-capacitor network, the first-order cofactors each contain the root with multiplicity $r-1$. Therefore, the ratio Δ_{ij}/Δ has only simple poles; consequently $H(p)$ *has only simple poles.*

In the synthesis method to be offered, each pole of $H(p)$ requires a mesh in the network. If $H(p)$ has n poles, the network will have n meshes. With n meshes, a resistor-capacitor network has a maximum of n transient modes; thus, $p^s\Delta$ has n factors. Since $H(p)$ has n simple poles; $p^s\Delta$ must have all simple factors. This is a sufficient condition for the poles of $H(p)$ to also be the poles of Y_{11}.

The necessary conditions that $H(p)$ must satisfy in order that it may be realized with a network of the form of Fig. 1 may now be summarized as follows:

1. Poles of $H(p)$ must occur at real negative values of p, and must be simple. The poles of $H(p)$ are also the poles of Y_{11}.
2. Zeros of $H(p)$ must occur at real negative values of p, but may be multiple. The zeros of $H(p)$ are the zeros of $Z_2 Z_4 \cdots Z_{2n}$.
3. The transfer ratio must be finite at all points on the ω axis; hence $H(p)$ necessarily has no poles at zero or infinity.

Approximation to the Realization of the Transfer Ratio

It is assumed that a transfer ratio $H(p)$ that satisfies the preceding conditions is given and that it is desired that this transfer ratio be realized with the ladder type of network shown in Fig. 1. The general method of realizing a ladder network is to synthesize the driving-point admittance or impedance of the structure. The problem then is to determine a driving-point admittance which can be realized with a ladder in which the shunt elements have zeros at the zeros of $H(p)$. The solution to this problem hinges upon obtaining a polynomial $f(p)$ such that $f(p)/g(p)$ satisfies condition (6) and such that the resultant Y_{11} can be realized with a ladder that has shunt elements which have zeros at the zeros of $H(p)$. There is an infinite set of polynomials $f(p)$ that will satisfy condition (6); however, the set of polynomials that allows Y_{11} to be synthesized with the proper form is much more restricted. Unfortunately, no test has been discovered by which Y_{11} may be examined in order to predetermine that it can be realized in ladder form with the proper shunt elements; therefore, a process of approximation is used to ascertain $f(p)$. There is no guarantee then that the $f(p)$ so determined necessarily allows Y_{11} to be realized in the desired form.

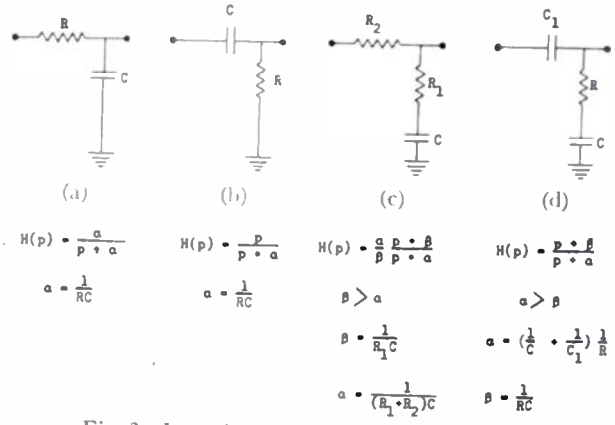

Fig. 2—L sections used to approximate $H(p)$.

The first step in approximating Y_{11} is to approximate the network that realizes $H(p)$.[2] Any $H(p)$ subject to the conditions in the preceding section can be approximated with cascaded L sections appropriately chosen from those shown in Fig. 2. The procedure is to choose the types of L sections and their order in the network. Then the impedance level of each L section is chosen in such a way that its loading upon its predecessor is sufficiently small so that the over-all transfer ratio of the network is approximately the product of the transfer ratios of the individual L sections.

The input admittance to the network so obtained is very nearly that of the first L section because the loading of each successive section on its predecessor is assumed small. This means that of the zeros and poles of Y_{11}, that zero and pole representative of the input admittance of the first L section in the network have predominant influence on the driving-point admittance of the network at real frequencies. Furthermore, those zeros and poles representative of the input admittance

[2] J. L. Bower, J. T. Fleck, and P. F. Ordung, "The Synthesis of Resistor-Capacitor Networks," chapt. 2. This is an unpublished report to the General Electric Company on research conducted at Yale University on the design of resistor-capacitor networks.

of each of the successive following sections have progressively less influence upon the driving-point admittance of the filter. This suggests the way in which $f(p)$ is to be chosen. The polynomial $f(p)$ shall be chosen from the set of $f(p)$'s that yield zeros of Y_{11} which satisfy condition (6) on the basis that successive L sections will have progressively less effect upon the driving-point admittance of the filter at real frequencies. That is, the zeros of Y_{11} will be located so that the pole of each L section further removed from the input is more nearly cancelled by a zero placed near it than is the pole of its predecessor. How this is done will be clarified by example.

Choice of $f(p)$

Suppose a transfer ratio

$$H(p) = H\frac{p(p+10)(p+20)(p+40)}{(p+1)(p+3)(p+5)(p+80)} \tag{11}$$

is to be realized with a ladder network. The first step is to choose sections from Fig. 2 with which $H(p)$ might be approximated. Although there is a considerable latitude in choice, at least one section of type (d) and one section of type (a) are required. Usually it is desirable to associate the factors in (11) with L sections chosen from Fig. 2 in such a way that the largest value of H, the level of the transfer ratio, is obtained. The association of the factors in (11) with L sections in order to obtain greatest H is that given in the following equation.

$$H(p) = \underbrace{\left[\frac{p}{p+1}\right]}_{\text{section type (b)}} \underbrace{\left[\frac{3}{10}\ \frac{p+10}{p+3}\right]\left[\frac{5}{20}\ \frac{p+20}{p+5}\right]}_{\text{sections type (c)}} \underbrace{\left[\frac{p+40}{p+80}\right]}_{\text{section type (d)}}. \tag{12}$$

The value of the level of the transfer ratio of the filter is then

$$H = \left(\frac{3}{10}\right)\left(\frac{5}{20}\right) = 0.075. \tag{13}$$

The order in which the section of type (b), the two sections of type (c), and the section of type (d) will be cascaded must now be chosen. Without discussion of this point, suppose the order that has been arbitrarily selected is that shown in Fig. 3.

The driving-point admittance Y_{11} of the network shown in Fig. 3 has poles at the poles of $H(p)$; i.e., the $-\alpha$'s shown in the figure. One of the zeros of Y_{11} is at the origin because the input current to the network at $p=0$ is zero. The other zeros of Y_{11} are yet to be chosen. Because each successive L section in Fig. 3 is not to load its predecessor, Y_{11} at real frequencies is predominantly influenced by the input admittance of the first section and to a progressively lesser degree by that of each of the succeeding sections. The zero at $p=0$ and the pole at $p=-80$ are the most important of the zeros and poles in governing Y_{11}. In the choice of $f(p)$ the other poles of Y_{11} shall then be assigned less influence through placement of a zero near each of them, as will be shown. The zeros of Y_{11} shall therefore be chosen in accordance with the diagram shown in Fig. 4.

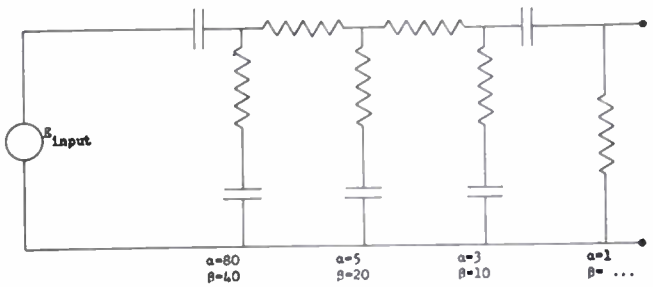

Fig. 3—A possible arrangement of the L sections in (12) in order to realize $H(p)$ of (11).

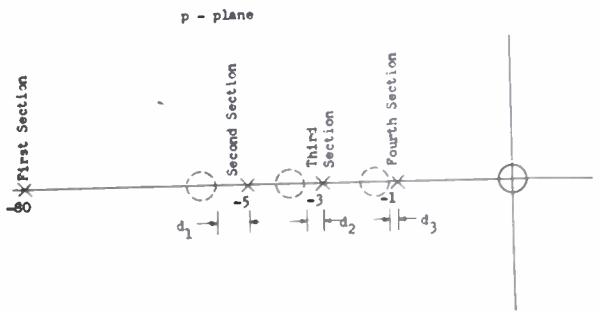

Fig. 4—Allocation of the zeros of Y_{11}. Dotted circles indicate approximate location of the zeros of Y_{11} that are yet to be chosen.

The effects on Y_{11} of a pole in Fig. 4 due to an L section within the network is controlled by adjustment of the spacing between it and its companion zero. How should this spacing be adjusted? In order to answer this question, let the effects of a pole and its companion

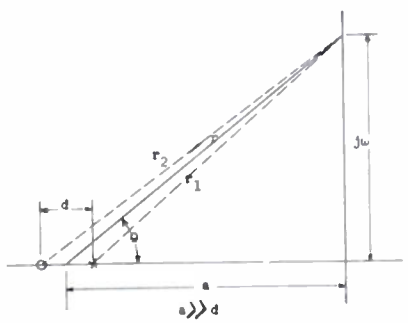

Fig. 5—Zero-pole diagram for a pole-zero pair.

zero on Y_{11} be examined for real frequencies. The zero-pole diagram for such a pole-zero pair is shown in Fig. 5.[3] This pole-zero pair would be contained in Y_{11} as a factor of the form

[3] P. F. Ordung, and H. L. Krauss, "The frequency-coordinate vector diagram," *Jour. Frank. Inst.*, vol. 251; 1951.

$$\frac{p+a+\frac{d}{2}}{p+a-\frac{d}{2}}. \tag{14}$$

The magnitude of (14) for a frequency $p=j\omega$ can be expressed in terms of the geometry of Fig. 5 as

$$\left|\frac{r^2+\frac{d^2}{4}+rd\cos\theta}{r^2+\frac{d^2}{4}-rd\cos\theta}\right|^{1/2} \leqq 1+\frac{d}{r}\cos\theta \quad r\gg d. \tag{15}$$

The approximation in (15) is everywhere valid on the real frequency axis since $a\gg d$. This approximation shows how to choose d so that the effects of a pole-zero pair on Y_{11} at real frequencies may be limited to any desired degree. The greatest effect of the pair on Y_{11} occurs at $p=0$, where $\cos\theta=1$ and $r=a$. If the effects on Y_{11} at real frequencies of a pole-zero pair are to be limited to δ per cent of Y_{11}, then

$$\frac{d}{a} \leqq \frac{\frac{\delta}{100}}{1+\frac{\delta}{100}} \rightarrow \frac{\delta}{100}. \tag{16}$$

Since a is known, d may be computed from (16); hence the location of a zero with respect to a pole may be specified for any desired degree of effect of the pair on Y_{11}. Usually the equality in (16) is chosen for the calculation because the use of the inequality means that the impedance of the L section in the network that is responsible for the pole-zero pair becomes unduly large.

Now the remaining zeros in Fig. 4 can be allocated. Suppose the second L section in Fig. 3 is to be chosen arbitrarily so as not to have an effect of more than 25 per cent on Y_{11}. Then according to (16) and to Fig. 4,

$$\frac{d_1}{5} \leqq 0.25$$
$$d_1 \leqq 1.25. \tag{17}$$

Therefore, let the zero of the pole-zero pair being considered be located at $p=-6.25$. Since the third section must effect Y_{11} less than the second section, suppose the effects of the third section upon Y_{11} are not more than 10 per cent. Then

$$\frac{d_2}{3} \leqq 0.10$$
$$d_2 \leqq 0.30. \tag{18}$$

Thus let the zero be located at $p=-3.3$. Suppose the fourth section is not to effect Y_{11} by more than 3 per cent. Then

$$\frac{d_3}{1} \leqq 0.03. \tag{19}$$

Thus let the last zero be located at $p=-1.03$.

Now the Y_{11} that will be used to realize the $H(p)$ of this example can be expressed as to within an unknown constant multiplier h, as

$$Y_{11}=h\frac{p(p+1.03)(p+3.3)(p+6.25)}{(p+1)(p+3)(p+5)(p+80)}. \tag{20}$$

The constant h is merely an impedance-level determining factor, and has no bearing upon the synthesis procedure. There is no guarantee that $H(p)$ can be realized with this Y_{11}; however, as the zeros of Y_{11} have been chosen in a realistic fashion, it appears likely that $H(p)$ will be realized with this Y_{11}. In the event that $H(p)$ cannot be realized in the synthesis, the zeros of Y_{11} must be recalculated using smaller percentages to express the loading effects of the L sections upon the driving-point admittance. Ultimately, a Y_{11} is obtained that necessarily may be synthesized in such a way as to *exactly* realize $H(p)$.

Synthesis of Y_{11}

The synthesis of the network is accomplished by expanding the driving-point admittance function into a continued fraction expansion in such a way that the elements of the expansion represent the impedances of the ladder structure that realizes $H(p)$. For the realization of (12) as a network of the form of Fig. 3, the continued fraction expansion of (20) is

$$\frac{h}{Y_{11}}=\frac{1}{pC_1}+\cfrac{1}{\cfrac{p}{R_{12}}+\cfrac{1}{p+\cfrac{1}{R_{12}C_{12}}}+\cfrac{1}{R_2+\cfrac{1}{\cfrac{p}{R_{23}}+\cfrac{1}{p+\cfrac{1}{R_{23}C_{23}}}+\cfrac{1}{R_3+\cfrac{1}{\cfrac{p}{R_{34}}+\cfrac{1}{p+\cfrac{1}{R_{34}C_{34}}}+\cfrac{1}{\cfrac{1}{pC_2}+R_4}}}}}}}, \tag{21}$$

where

$$\frac{1}{R_{12}C_{12}} = 40$$
$$\frac{1}{R_{23}C_{23}} = 20$$
$$\frac{1}{R_{34}C_{34}} = 10.$$

Thus, in the synthesis the terms in (21) must be evaluated. The driving-point impedance of Fig. 3 is exactly equal to $1/pC_1$ when $p=-40$ because the first shunt branch has zero impedance at this frequency. Thus C_1 can be computed as

$$C_1 = \left.\frac{Y_{11}}{hp}\right|_{p=-40} = 0.023893 \text{ farads.} \tag{22}$$

The admittance $Y^{(1)}$,

$$Y^{(1)} = \frac{1}{\left(\frac{h}{Y^{11}} - \frac{1}{pC_1}\right)} \tag{23}$$

of the network to the right of the capacitor C_1 in Fig. 3 has a pole at $p=-40$, and it is to be realizable with resistors and capacitors. For $Y^{(1)}$ to be realizable the reactance $1/pC_1$ extracted from h/Y_{11} must be equal to or less than the largest series capacitive reactance that can be extracted from $1/Y_{11}$. This largest value is that which would be obtained from one of the canonical expansions;[1] therefore, it is ascertained from h/Y_{11} by allowing p to approach zero frequency. The largest reactance is therefore

$$\lim_{p\to 0} \frac{h}{Y_{11}} \to \frac{1}{0.017703p}. \tag{24}$$

Since $C_1 > 0.017703$, the reactance of C_1 is less than the limiting value and $Y^{(1)}$ is realizable.

The term

$$\frac{\frac{p}{R_{12}}}{p + \frac{1}{R_{12}C_{12}}}$$

in (21) represents the admittance of the first shunt branch in Fig. 3, and it is obtained by expanding $Y^{(1)}/p$ into a partial fraction expansion and then multiplying the expansion by p. This yields

$$Y^{(1)} = \frac{p}{1.10068}$$
$$Y^{(1)} = \frac{}{p + 40}$$
$$+ \frac{0.0914709p^3 + 0.427685p^2 + 0.354659p}{p^3 + 7.14724p^2 + 14.3082p + 7.7703}. \tag{25}$$

By continuing through to completion the process of expansion in the foregoing manner the desired continued fraction expansion of h/Y_{11} is obtained as follows:

$$\frac{h}{Y_{11}} = \frac{1}{0.023893p} + \cfrac{1}{\cfrac{p}{\cfrac{1.10068}{+40}} + \cfrac{1}{9.54496} + \cfrac{1}{\cfrac{p}{\cfrac{1.43082}{p+20}} + \cfrac{1}{33.1695} + \cfrac{1}{\cfrac{p}{\cfrac{13.1926}{p+10}} + \cfrac{1}{\cfrac{1}{0.0031p} + 290}}}}} \tag{26}$$

If at any step in the process, a series impedance larger than the largest permissible value is to be extracted, the resultant network function will become unrealizable and it will be necessary to go back and reassign all of the zeros of Y_{11} on the basis of reduced loading.

The network that is realized by the expansion in (26) is shown in Fig. 6. That this network realizes $H(p)$ can be shown by straightforward analysis. The size of the components in the network are stated to two significant figures. It will be observed that throughout the computations in the example, six significant figures have been carried. This is necessary because the errors in making the expansion accumulate. Since the zeros of Y_{11} are very close to its poles, it is necessary that considerable accuracy in the calculations be maintained in order to limit the error; otherwise, sufficient error may accumulate in the process of expansion so as to make the derived impedance functions unrealizable. The tolerances on the elements, however, are not so severe as on the mathematical processes; therefore 1 per cent tolerance on the elements is usually acceptable.

The level of the transfer ratio H for the network of Fig. 6 can be obtained easily if one recognizes that H for this particular network is

$$H = \lim_{p\to\infty} \frac{\Delta_{12}}{\Delta} Z_{2n} = 0.0354. \tag{27}$$

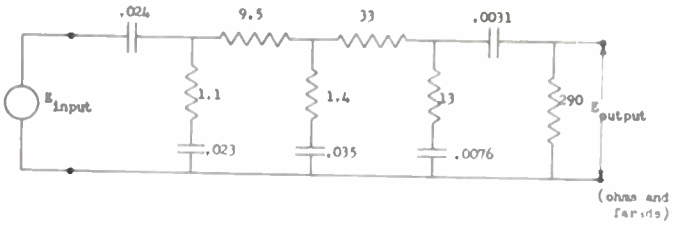

Fig. 6—The network synthesized to realize $H(p)$.

As to be expected, it is somewhat less than that predicted from the approximate structure because of the loading of an L section upon its predecessor. On the other hand, the H obtained with the network in Fig. 6 is considerably greater than that which would be obtained if $H(p)$ were realized with a lattice network. In an earlier paper[4] the $H(p)$ chosen as an example in this paper was realized with a lattice structure, and the maximum value for H which could be obtained with the lattice was shown to be $H=0.0165$.

[4] J. L. Bower, and P. F. Ordung, "The synthesis of resistor-capacitor networks, PROC. I.R.E., vol. 38, pp. 263–269; March, 1950.

Conclusions

A method has been offered for the realization of a transfer ratio with a ladder network containing only resistors and capacitors subject to the conditions: (a) zeros of $H(p)$ of any multiplicity that occur at negative real values of p; (b) poles that are simple and that occur at real negative values of p; and (c) a finite transfer ratio of all real frequencies including zero and infinity. The method requires the synthesis of an approximate network, which is then used as a guide to the synthesis of the exact network and which moreover allows the maximum value of H to be estimated. The level of the transfer ratio H, achieved with networks synthesized by the method offered in this paper, is usually greater than that which can be achieved with networks designed on the lattice basis.

Radiation Patterns of Arrays on a Reflecting Cylinder*

JOHN E. WALSH†, MEMBER, IRE

Summary—**Simple approximate formulas are derived for the horizontal and vertical patterns of directional arrays of dipoles arranged on an arc of a circle or on the surface of a right circular cylindrical segment and backed by a reflecting cylinder. The dipoles may be aligned axially or circumferentially and the amplitude distribution on them may be uniform or cosinusoidal. The results are valid in the vicinity of the radiation maximum, but are less certain at wide angles unless the dipole spacing is substantially less than a half wavelength.**

It is found that the array patterns compare favorably with those of linear arrays of comparable dimensions and similar amplitude distributions, and that there exists, in certain cases, an increase in gain over the linear array brought about by the end-fire effect inherent in the geometry of the circle.

Introduction

THIS paper treats semicircular and semicylindrical arrays of dipoles on a reflecting cylinder whose radius is greater than five wavelengths. Consideration is also given to arrays covering something less than a semicircle. In all instances, the phasing of the elements will be such as to produce a constant phase front lying in a plane normal to that radius of the cylinder which passes through the midpoint of the array. Antennas of this type find application in direction finding and present possibilities for rapid scanning of a radar beam because of their symmetry.

The radiation patterns of cylindrical arrays, variously phased, have been discussed by Carter,[1] Sinclair,[2] Lucke,[3] a group at Syracuse University,[4] and others. The solutions are in series form, involving some labor in getting numerical values. It is proposed here to derive simple approximate pattern equations sufficiently accurate to allow predictions of side lobes and beamwidths. The fundamental assumption will be that the pattern of an array of discrete dipoles spaced not more than a half wavelength apart can be computed (at least in the neighborhood of the principal beam) with a fair degree of accuracy by mathematically substituting a continuous current distribution and by inserting directivity factors to account for the patterns of the individual dipoles. For a confirmation of the validity of this assumption, the reader is referred to the report by LePage, Harrington, and Schlecht.[4]

Geometry of the System

Only the two principal patterns will be considered, that is, the patterns, both horizontally and vertically polarized, taken (a) in the plane containing the axis of the cylinder and the midpoint of the array; and (b) the pattern taken in the plane normal to the plane of (a)

* Decimal classification: R120.1×R125.1×R325.11. Original manuscript received by the Institute, June 27, 1950; revised manuscript received, December 4, 1950.

This paper was condensed from a paper of the same title published as Report No. E5061 by the Air Force Cambridge Research Laboratories, Cambridge, Mass.; October, 1950.

† Air Force Cambridge Research Laboratories, Cambridge, Mass.

[1] P. S. Carter, "Antenna arrays around cylinders," PROC. I.R.E., vol. 31, pp. 671–693; December, 1943.

[2] G. Sinclair, "The Patterns of Simple Antennas Mounted on Cylinders of Elliptical Cross-Section," Report 301-10, Ohio State University Research Foundation; September 1, 1948.

[3] W. S. Lucke, "Electric Dipoles in the Presence of Elliptic and Circular Cylinders," Report No. 1, Project No. 188, Stanford Research Institute; September 26, 1949.

[4] W. R. LePage, R. F. Harrington, and M. F. Schlecht, "A Study of Directional Antenna Systems for Radio D/F Purposes," Report Institute of Industrial Research, Department of Electrical Engineering, Syracuse University; September 15, 1949.

and containing the midpoint of the array. Patterns included under (a) will hereafter be called "vertical patterns," those under (b), "horizontal."

A. Horizontal Patterns

(See Fig. 1.) We assume elementary infinitesimal radiators (in place of actual dipoles) distributed on an arc of a circle or segment of a cylinder which is concentric with an infinite, perfectly reflecting cylinder of radius r at a distance a inside the dipoles. The height of the antenna measured parallel to the Z axis is not relevant to the pattern in this plane; i.e., the pattern is

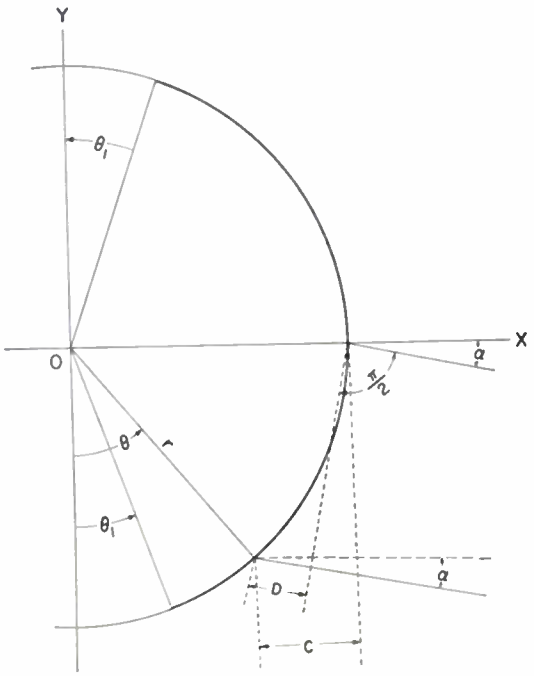

Fig. 1—Array geometry.

the same whether we speak of a circular arc or a cylindrical segment. The angular location of an arbitrary point on the arc is given by θ, which is measured from the negative Y axis. The limits of the arc have the angular co-ordinates θ_1 and $\pi-\theta_1$. The radiators are presumed to be so phased that a linear phase front is obtained perpendicular to the line $\alpha=0$, where α is the angle of observation measured from the X axis. The radiation pattern of such an arrangement will be given by

$$E_n = \int_{\theta_1}^{\pi-\theta_1} \exp\left[-i\frac{2\pi}{\lambda}(C-D)\right] f_n(\alpha,\theta) g_n(\theta)\, d\theta, \qquad (1)$$

where, from trigonometrical considerations,

$$C - D = r[\sin\alpha\cos\theta + (\cos\alpha - 1)\sin\theta]$$
$$= 2r\sin\frac{\alpha}{2}\cos\left[\theta + \frac{\alpha}{2}\right].$$

The patterns of the individual radiators which would actually be used in place of the theoretical infinitesimal elements are represented by $f_n(\alpha, \theta)$, while $g_n(\theta)$ is the amplitude distribution around the periphery. The subscripts will be used to distinguish the various cases to be treated.

Factors in (1) not involving θ have been dropped, as they will be throughout, since they disappear in the normalized version of either the voltage or intensity patterns. The range of values of θ_1 which is allowed by the integration methods to be used will be discussed later.

B. Vertical Patterns

For the vertical patterns the array of Fig. 1 is extended a distance $w/2$ above and below the XY plane. The radiation pattern can then be shown without difficulty to be

$$E_n = \int_{\theta_1}^{\pi-\theta_1}\int_{-w/2}^{w/2} \exp\left(iB\sin\theta + \frac{2\pi i}{\lambda} z\sin\beta\right)$$
$$\cdot F_n(\beta,\theta) g_n(\theta) G_n(z)\, dz\, d\theta, \qquad (2)$$

where β is the angle of elevation of the observation point measured from the horizontal, B is $(2\pi r/\lambda)(1-\cos\beta)$, $F_n(\beta, \theta)$ represents the pattern of the individual dipole, $g_n(\theta)$ is defined as in (1), $G_n(z)$ is the vertical amplitude distribution, and w is the height of the array.

The Weighting Functions

The individual dipole patterns f_n and F_n have been evaluated in the literature[1–4] and by Moullin,[5] but the series converge quite slowly for cylinder radii even of the order of 5λ so that not much is known about the patterns for large cylinders. It will be assumed here that they can be represented by the simple trigonometric functions given below. That the assumed horizontal pattern for the vertical (axial) dipole is not entirely unreasonable has been shown by Lel'age, Harrington, and Schlecht, both experimentally and by calculations based on Carter's solution. They use $\cos^2\phi/2$ for rough pattern calculations if the dipole-to-cylinder spacing is a quarter wavelength, and $\cos\phi$ if it is an eighth wavelength.

Reference to Fig. 1 makes it clear that when α exceeds θ_1, some of the dipoles lie in a shadow area. These dipoles, on the basis of geometric optics, contribute nothing to the pattern and therefore when we come to write the simplified horizontal pattern of a vertical dipole in terms of the co-ordinate system used in this paper, it becomes

$$\text{for } \alpha \geqq \theta_1,\ f_n(\alpha,\theta) = \sin(\theta+\alpha),\ \theta_1 \leqq \theta \leqq \pi-\alpha$$
$$= 0 \text{ otherwise,}$$
$$\text{for } \alpha < \theta_1,\ f_n(\alpha,\theta) = \sin(\theta+\alpha),\ \theta_1 \leqq \theta \leqq \pi-\theta_1$$
$$= 0 \text{ otherwise.}$$

The same kind of formulation is used for the horizontal pattern of the horizontal (circumferential)

[5] E. B. Moullin, "Radio Aerials," Oxford University Press, Oxford, England; 1949.

dipole, except that the sine is squared.

The discontinuities in the dipole patterns are taken care of by merely changing the upper limit of integration in (1) from $\pi-\theta_1$ to $\pi-\xi$, where we define ξ as follows: F for $\alpha \geqq \theta_1$, $\xi=\alpha$; for $\alpha<\theta_1$, $\xi=\theta_1$.

It is worthy of note that these same approximations could have been arrived at by an extreme simplification of the pattern of a dipole on an infinite plane. It will be recalled that the relevant formula is[6]

$$E = k\frac{\cos\left(\frac{\pi}{2}\cos\chi\right)}{\sin\chi}\sin\left(\frac{\pi b}{\lambda}\sin\chi\sin\psi\right),$$

where χ and ψ, are, respectively, the colatitude and longitude ($\psi=0$ at the reflector surface) of the field point, and the dipole is parallel to the Z axis. The dipole-to-reflector spacing is b. The factor $\cos(\pi/2\cos\chi)/\sin\chi$ is well approximated by $\sin\chi$, and if b is presumed small, the formula can be written very approximately

$$E \approx \sin^2\chi\sin\psi,$$

where the constants are dropped since they would disappear on normalization of an array pattern. When this formula is converted to our co-ordinate system, the simple dipole patterns above result immediately.

We are, therefore, emboldened to approximate the vertical patterns of the dipoles, $F_n(\beta,\theta)$, in precisely the same manner for insertion in the integral of (2). The result is

for vertical dipoles,

$$F_n(\beta,\theta) = \cos^2\beta\sin\theta, \qquad \theta_1 \leqq \theta \leqq \pi-\theta_1$$
$$= 0 \text{ otherwise,}$$

for horizontal dipoles,

$$F_n(\beta,\theta) = \cos\beta\sin^2\theta, \qquad \theta_1 \leqq \theta \leqq \pi-\theta_1$$
$$= 0 \text{ otherwise.}$$

In addition to the patterns of the individual radiators, the amplitude distribution factors, $g_n(\theta)$ and $G_n(z)$, have to be considered. For the former we shall treat two cases, namely, a uniform amplitude distribution and a cosinusoidal distribution. When $g_n(\theta)=\sin\theta$, the amplitude will not go to zero at the edge of the energized sector of the array unless $\theta_1=0$, that is, unless the entire semicircle is illuminated. In order to accommodate an illumination which actually goes to zero when less than a semicircle is energized it would be necessary to use a $g_n(\theta)$ somewhat more complicated than $\sin\theta$, and this complexity would make the simple integration of (1) impossible. Because of the somewhat artificial restrictions thus imposed on the illumination when we have $\theta_1\neq 0$ and $g_n(\theta)=\sin\theta$, we shall omit a discussion of arrays covering less than a semicircle when the illumination is not uniform.

[6] See, for example, R. W. King, H. R. Mimno, and A. H. Wing, "Transmission Lines, Antennas, and Waveguides," McGraw-Hill Book Co., New York, N. Y.; 1945.

The z amplitude distribution $G_n(z)$ will be considered uniform; it will be apparent, however, that a nonuniform vertical distribution can readily be treated by a simple extension of the formulas to be derived.

Table I identifies the eight cases that will be treated in this paper, and summarizes the weighting functions to be inserted in (1) and (2).

TABLE I

DIPOLE AND ILLUMINATION FUNCTIONS

E_n	Dipole Orientation	Energy Distribution	f_n or F_n	g_n
		Horizontal Pattern (1)		
E_1	Vertical	Uniform	$\sin(\theta+\alpha)$	1
E_2	Vertical	Cosinusoidal	$\sin(\theta+\alpha)$	$\sin\theta$
E_3	Horizontal	Uniform	$\sin^2(\theta+\alpha)$	1
E_4	Horizontal	Cosinusoidal	$\sin^2(\theta+\alpha)$	$\sin\theta$
		Vertical Pattern (2)		
E_5	Vertical	Uniform	$\cos^2\beta\sin\theta$	1
E_6	Vertical	Cosinusoidal	$\cos^2\beta\sin\theta$	$\sin\theta$
E_7	Horizontal	Uniform	$\cos\beta\sin^2\theta$	1
E_8	Horizontal	Cosinusoidal	$\cos\beta\sin^2\theta$	$\sin\theta$

Evaluation of the Horizontal Patterns

In the various integrals represented by (1), we put $\phi=\theta+(\alpha/2)$ and $k=2\pi d/\lambda$, d being $2r$. Let $\chi=\alpha/2$ for $\alpha\geqq\theta_1$ and let $\chi=\theta_1-(\alpha/2)$ for $\alpha<\theta_1$. Furthermore, to save space, put $\psi=\exp(-ik\cos\phi\sin\alpha/2)$. We introduce the following notation:

$$P=\int\psi\sin\phi d\phi, \qquad Q=\int\psi d\phi, \quad R=\int\psi\cos\phi d\phi,$$

$$T=\int\psi\sin^2\phi d\phi, \qquad U=\int\psi\sin\phi\cos\phi d\phi,$$

$$V=\int\psi\sin^3\phi d\phi, \text{ and } W=\int\psi\sin^2\phi\cos\phi d\phi.$$

The limits of integration in all cases are from $\theta_1+(\alpha/2)$ to $\pi-\chi$. Then, on expanding the functions of sums of angles in (1), we have

$$2\cos\theta_1 E_1 = P\cos\frac{\alpha}{2}+R\sin\frac{\alpha}{2} \tag{3}$$

$$\left(\frac{\pi}{2}-\theta_1+\frac{1}{2}\sin 2\theta_1\right)E_2 = T-Q\sin^2\frac{\alpha}{2} \tag{4}$$

$$\left(\frac{\pi}{2}-\theta_1+\frac{1}{2}\sin 2\theta_1\right)E_3$$
$$= T\cos\alpha+U\sin\alpha+Q\sin^2\frac{\alpha}{2}, \tag{5}$$

$$\frac{2}{3}\cos\theta_1(\sin^2\theta_1+2)E_4 = V\cos\frac{\alpha}{2}+W\sin\frac{\alpha}{2}$$
$$-P\sin^2\frac{\alpha}{2}\cos\frac{\alpha}{2}-R\sin^3\frac{\alpha}{2}, \tag{6}$$

where for convenience we have put the normalizing factors on the left.

All the integrals in (3) through (6) can readily be evaluated in terms of Q, R, and the trigonometric functions. It is shown in Appendix I that to a good order of approximation

$$Q \approx \pi J_0\left(k \sin\frac{\alpha}{2}\right) - \exp\left[-ik\sin\frac{\alpha}{2}\right](M_1 + iN_1) - \exp\left[ik\sin\frac{\alpha}{2}\right](M_2 - iN_2),$$

$$R \approx -\pi i J_1\left(k\sin\frac{\alpha}{2}\right) - \frac{i\left(\theta_1 + \frac{\alpha}{2}\right)}{2k\sin\frac{\alpha}{2}} \cdot \exp\left[-ik\sin\frac{\alpha}{2}\cos\left(\theta_1 + \frac{\alpha}{2}\right)\right] - \frac{i\chi}{2k\sin\frac{\alpha}{2}}\exp\left[ik\sin\frac{\alpha}{2}\cos\chi\right] - \exp\left[-ik\sin\frac{\alpha}{2}\right]\left(1 - \frac{i}{2k\sin\frac{\alpha}{2}}\right)(M_1 + iN_1) + \exp\left[ik\sin\frac{\alpha}{2}\right]\left(1 + \frac{i}{2k\sin\frac{\alpha}{2}}\right)(M_2 - iN_2),$$

where

$$M_1 = \frac{C(p_1)}{p_1}\left(\theta_1 + \frac{\alpha}{2}\right), \qquad M_2 = \frac{C(p_2)}{p_2}(\chi),$$

$$N_1 = \frac{S(p_1)}{p_1}\left(\theta_1 + \frac{\alpha}{2}\right), \qquad N_2 = \frac{S(p_2)}{p_2}(\chi).$$

C and S represent the Fresnel integrals, and

$$p_1 = 2\frac{\sqrt{k\sin\frac{\alpha}{2}}}{\sqrt{\pi}}\sin\frac{1}{2}\left(\theta_1 + \frac{\alpha}{2}\right),$$

$$p_2 = 2\frac{\sqrt{k\sin\frac{\alpha}{2}}}{\sqrt{\pi}}\sin\frac{1}{2}\chi.$$

Equations (3) through (6), with the approximations for Q and R, are good representations of the integrals out to $(\theta_1 + \alpha/2) = \pi/4$. They are used as the basis of greatly simplified forms of the patterns suitable for easy analysis in the vicinity of the main beam. It must be noted that, owing to the phasing and orientation of the dipoles in a circular array, there exists the possibility of high, far-out side lobes because of possible end-fire effects along a line to a given field point. Their amplitude cannot be computed by the methods used in this paper because end-fire arrays are much more sensitive to the spacing of discrete elements than are broadside arrays. It can be proved, however, that for a *continuous* distribution of current elements, each element having assigned to it the pattern of a dipole, there are no side lobes higher than the first. The conclusion implied is that if the distant lobes are high for half-wave spacing of the dipoles, one way of reducing them is to space the elements closer together. (If the dipoles are horizontal, they must be staggered.)

Simplified Formulas, Horizontal Patterns, $\theta_1 = 0$

When θ_1 is put equal to zero (i.e., when we speak of the complete semicircular or semicylindrical array), we find at once that

$$p_1 = p_2 = 2\frac{\sqrt{k\sin\frac{\alpha}{2}}}{\sqrt{\pi}}\sin\frac{\alpha}{4}$$

and that $M_1 = M_2$. We denote these values by M and p.

As a starting point for deriving approximations, note that when M and p are inserted in (3) through (6), the dominant terms after normalization are approximately of the forms

$$\frac{\sin x}{x} \quad \text{for (3)},$$

$$\frac{2J_1(x)}{x} \quad \text{for (4) and (5)},$$

$$\frac{-3g^1(x)}{x} \quad \text{for (6)}.$$

Here x is $(k/2)\sin\alpha$ and $g^1(x)$ is the first derivative of $\sin x/x$. (The form for (6) is not immediately obvious, but will become so in the sequel.)

The function having the widest half-power beamwidth is the last of these, and its width is about 1.2 (λ/d). The first side lobe occurs at a value of α, which is roughly 3.2 times its value at half power; therefore, to include all of the pattern out to the first side lobe in all four equations, we must take α out to 1.92 (λ/d). For a margin of safety, we take $\alpha < (9/4)\lambda/d$. We have confined this discussion to radii greater than five wavelengths so that a top numerical limit on α is set.

An approximation for the Fresnel integrals in M and N is readily obtained by expanding the integrands, yielding

$$\frac{C(p)}{p} \approx \left(1 - \frac{\pi^2 p^4}{40}\right); \qquad \frac{S(p)}{p} \approx \frac{\pi p^2}{6}.$$

Now

$$p^2 \approx \frac{2d}{\lambda}\sin^2\frac{\alpha}{2},$$

and hence, for $\alpha < (9/4)\lambda/d$, p is less than $\sqrt{3/10}$. For

values of p up to 0.25 the approximations given above for $C(p)/p$ and $S(p)/p$ are exact to at least four decimal places.

It can now be seen that if we approximate $M = C(p)/p \cdot \alpha/2$ by $\alpha/2$, the error is of the order of $\alpha/2 \cdot (\pi^2 p^4/40) < 0.00003$. Similarly, the error in calling $N = 0$ is less than 0.0018. Hence, we can assign an upper limit on the errors made in these approximations in the various combinations in which M and N appear. For example, the error made in considering the term $N/k \sin(\alpha/2)$ as equal to zero is

$$\frac{\alpha}{2} \cdot \frac{\pi p^2}{6} \cdot \frac{1}{k \sin \frac{\alpha}{2}} \approx \frac{1}{6} \sin^3 \frac{\alpha}{2} < 0.00025.$$

Furthermore,

$$\frac{\sin\left(\frac{k}{2} \sin \alpha\right)}{k \sin \frac{\alpha}{2}} \approx \frac{\sin\left(k \sin \frac{\alpha}{2}\right)}{k \sin \frac{\alpha}{2}},$$

with an error which can be shown to be less than 0.0064 and,

$$\cos\left(k \sin \frac{\alpha}{2}\right) \approx \cos\left(\frac{k}{2} \sin \alpha\right),$$

with an error less than 0.045. These substitutions can be used wherever the multiplying factors are sufficiently small.

The complete process of simplification for all four formulas will not be shown here. In Appendix II it is carried out for E_4, the most complicated case.

The results are that the normalized patterns out to and including the first side lobe can be expressed as follows:

$$E_1 = \frac{\sin\left(\frac{k}{2} \sin \alpha\right)}{k \sin \frac{\alpha}{2}} - \frac{\pi i}{2} \sin \frac{\alpha}{2} J_1\left(k \sin \frac{\alpha}{2}\right), \tag{7}$$

$$E_2 = \Lambda_1\left(k \sin \frac{\alpha}{2}\right) - 2 \sin^2 \frac{\alpha}{2} J_0\left(k \sin \frac{\alpha}{2}\right). \tag{8}$$

$$E_3 = \cos \alpha \cdot \Lambda_1\left(k \sin \frac{\alpha}{2}\right) + \frac{4i}{\pi} \sin \alpha \cos^2 \frac{\alpha}{2} g^1\left(\frac{k}{2} \sin \alpha\right) + 2 \sin^2 \frac{\alpha}{2} J_0\left(k \sin \frac{\alpha}{2}\right), \tag{9}$$

$$E_4 = -\frac{3 \cos^3 \frac{\alpha}{2}}{k \sin \frac{\alpha}{2}} g^1\left(\frac{k}{2} \sin \alpha\right) - \frac{3\pi i}{4k} J_2\left(k \sin \frac{\alpha}{2}\right), \tag{10}$$

where $\Lambda_1(x)$ is $2J_1(x)/x$ and is tabulated in Jahnke and Emde.[7] The derivative $g^1(x)$ is also tabulated.[8]

The errors which have been introduced by the simplifications given in this section decrease with increasing radius. For a radius of five wavelengths these errors are as follows (except near the first minima, where the errors have not been computed): for E_1, not more than $\frac{1}{2}$ db at a level 13 db down; for E_2, not more than $\frac{1}{4}$ db at the 17 db level; for E_3 and E_4, not more than $\frac{1}{3}$ db at the 20 db level. The errors are referred to the normalized values of the integrals at $\alpha = 0$, and it has been assumed that all errors are at their worst and are adding in the same direction. The probable error is, of course, considerably less.

It is evident that terms other than the first in each of these formulas contribute little even for arrays with $r = 5\lambda$; on this basis, the summary in the first part of Table II was prepared. Equivalent data for linear arrays of length $a = 2r$ are included for comparison.

TABLE II

HORIZONTAL PATTERNS

Dipole Orientation	Energy Distribution	Half-Power Beamwidth in Terms of λ/d or λ/a		First Side Lobe, db Down from Peak	
		Circular Array	Linear Array	Circular Array	Linear Array
$\theta_1 = 0$ (Semicircular Array)					
Vertical	Uniform	0.88	0.88	13.2	13.2
Vertical	Cosinusoidal	1.02	1.2	17.6	23
Horizontal	Uniform	1.02	0.88	17.6	13.2
Horizontal	Cosinusoidal	1.14	1.2	21.3	23
$\theta_1 \neq 0$ (Less than Semicircular Array)					
Vertical	Uniform	$0.88/\cos\theta_1$		13.2	
Horizontal	Uniform	See Fig. 2		See Fig. 2	

Note—The figures for $\theta_1 = 0$ are based on the approximations $\sin x/x$, $\Lambda_1(x)$, and $-3g^1(x)/x$ for E_1, E_2, and E_3, and E_4, respectively.

HORIZONTAL PATTERNS FOR $\theta_1 \neq 0$

The formulas for the horizontal patterns when $\theta_1 \neq 0$ are sufficiently complicated to prevent an accurate, detailed treatment without actual computation of the patterns. However, a rough analysis can be made which will yield estimates (somewhat less accurate than those of the preceding section) of the beamwidths and the heights of the first side lobes when the illumination is uniform. It will be recalled that for $\theta_1 \neq 0$ it is not possible to treat E_2 and E_4 because of the form of the integral in (1).

[7] E. Jahnke and T. Emde, "Tables of Functions," Dover Publications, New York, N. Y., p. 181; 1943.

[8] Annals of the Computation Laboratory of Harvard University, "Tables of the Function $(\sin \phi)/\phi$ and of its First Eleven Derivatives," vol. XXII, Harvard University Press, Cambridge, Mass.; 1949.

Only the results are presented here; they are shown in Table II and in Fig. 2.

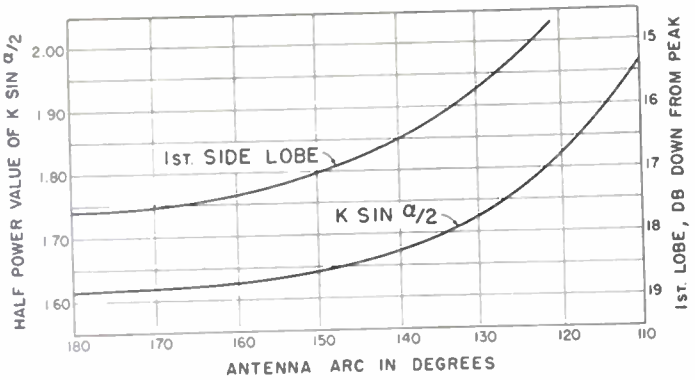

Fig. 2—Beamwidth and first side lobe for E_3.

Vertical Patterns for $\theta_1 = 0$

Equation (2) for $\theta_1 = 0$ integrates directly into combinations of Bessel, Lommel-Weber, and Struve functions:[9,10]

$$E_5 = g\left(\frac{\pi w}{\lambda}\sin\beta\right)\cos^2\beta\cdot\frac{\pi}{2}\left[-\Omega_1(B) + iJ_1(B)\right], \quad (11)$$

$$E_6 = g\left(\frac{\pi w}{\lambda}\sin\beta\right)\cos^2\beta\cdot 2\left\{\left[J_0(B) - \frac{J_1(B)}{B}\right] + i\left[S_0(B) - \frac{S_1(B)}{B}\right]\right\}, \quad (12)$$

$$E_7 = g\left(\frac{\pi w}{\lambda}\sin\beta\right)\cos\beta\cdot 2\left\{\left[J_0(B) - \frac{J_1(B)}{B}\right] + i\left[S_0(B) - \frac{S_1(B)}{B}\right]\right\}, \quad (13)$$

$$E_8 = g\left(\frac{\pi w}{\lambda}\sin\beta\right)\cos\beta\cdot\frac{3\pi}{4}\left\{i\left[J_1(B) - \frac{J_2(B)}{B}\right] - \left[\Omega_1(B) + \frac{S_0(B)}{B} - 2\frac{S_1(B)}{B^2}\right]\right\}, \quad (14)$$

where $g(x) = \sin x/x$.

The factors to the right of the multiplication signs in these formulas are functions of $B = (2\pi r/\lambda)(1-\cos\beta)$ only, and are plotted against that quantity in Fig. 3. It will be seen that in all cases they operate to reduce the vertical beamwidths and the side lobes of the arrays as compared with those for plane arrays of the same height. If the array consists of a single layer of dipoles ($w = 0$), then the power patterns consist only of the plotted factors multiplied by either $\cos^2\beta$ or $\cos^4\beta$. In this case the effect on the vertical patterns is the most pronounced; Fig. 4 shows the resulting beamwidths. Note that if we consider the gain of an array to be, very roughly, inversely proportional to the product of the horizontal and vertical beamwidths, the semicircular array one dipole high will, in general, have a higher gain than the corresponding linear array with a reflector a quarter wavelength behind it. The latter will have a

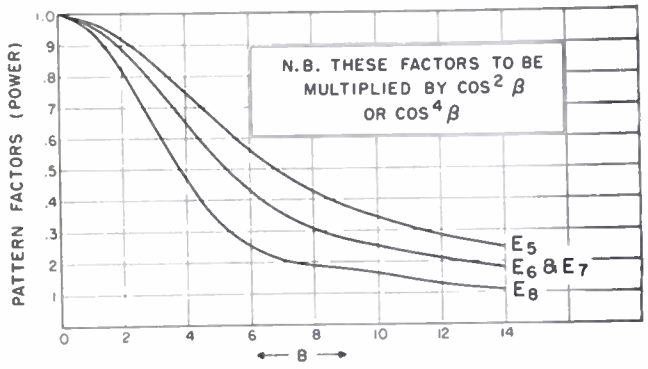

Fig. 3—Array factors for vertical patterns.

vertical beamwidth of approximately 72 or 120 degrees, depending on whether the dipoles are vertical or horizontal. This increase in gain for the semicircle is, of course, caused by the end-fire effect which resides in the geometry of the circle. The advantage becomes smaller as the array is extended in height or as the diameter is decreased.

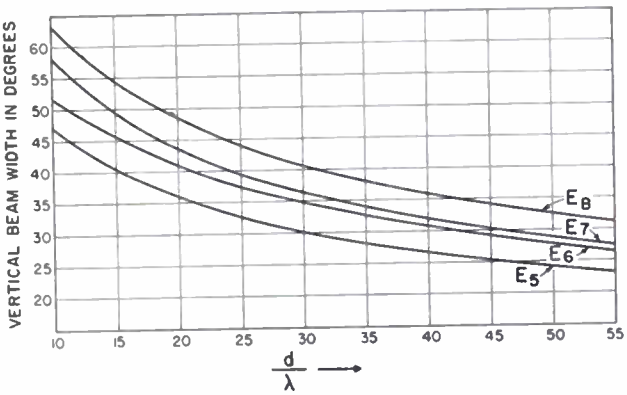

Fig. 4—Vertical beamwidths.

Note also that if the semicircular array is several dipoles high, a vertical amplitude distribution $G_n(z)$, other than uniform, will affect only the integration with respect to z in (2). Hence, to the extent that a fictitious continuous vertical distribution represents the actual situation, the only major changes introduced into (11) through (14) will be in the sin x/x factor, and these changes are well known.[11]

Conclusion

The principal results derived in this report are contained in (7) through (14) and in Table II and Figs. 3 and 4. Unfortunately, experimental data on arrays conforming to the conditions posited in this paper are not yet available.

It is fairly clear, especially in the treatment of the semicircular arrays, that the purely mathematical approximations introduce negligible errors, and that the validity of the analysis depends chiefly on the validity

[9] G. N. Watson, "A Treatise on the Theory of Bessel Functions," Cambridge University Press, New York, N. Y., 2nd ed., chapt. X; 1944.

[10] See p. 211 ff. of footnote reference 7.

[11] See, for example, S. Silver, "Microwave Antenna Theory and Design," Radiation Laboratory Series, McGraw-Hill Book Co., New York, N. Y., vol. 12, p. 180 ff.; 1949.

of the patterns assumed for the individual dipoles. If the element pattern were changed, say, from $\cos\phi$ to $\cos^2(\phi/2)$, a significant change would be introduced into (3) through (6), resulting, in general, in an increase in side-lobe level. This points up a need for further investigation of the problem of the single dipole on a cylinder and emphasizes the important conclusion that for good patterns the dipoles should be kept as close to the reflector as the impedance conditions will allow.

The close similarity between the horizontal patterns of the semicircular and the linear array is noteworthy, and confirms the intuitive view that near the main beam one might almost predict the results for the semicircular array by considering the pattern produced by the projection of the dipole directivity factor f_n and the amplitude distribution factor g_n upon a straight line tangent to the semicircle at its midpoint.

Acknowledgements

The writer wishes to express his appreciation for assistance and valuable suggestions to R. C. Spencer, J. Ruze, R. M. Barrett, F. J. Zucker, and W. Rotman, and other members of the staff of the Antenna Laboratory, Air Force Cambridge Research Laboratories, and to M. Barnes, of the same organization, who did the computations.

Appendix I

Approximations for Q and R

The quantity Q can be broken up as follows:

$$Q = \int_{\theta_1+\alpha/2}^{\pi-\chi} \psi d\phi = \left[\int_0^{\pi} - \int_0^{\theta_1+\alpha/2} - \int_{\pi-\chi}^{\pi}\right]\psi d\phi$$

$$= \pi J_0\left(k\sin\frac{\alpha}{2}\right) - \int_0^{\theta_1+\alpha/2} \exp\left[-ik\sin\frac{\alpha}{2}\cos\phi\right]d\phi - \int_0^{\chi} \exp\left[ik\sin\frac{\alpha}{2}\cos\phi\right]d\phi.$$

The integrals here are of the form

$$\int_0^{\gamma} \exp\left[-iA\cos\phi\right]d\phi, \qquad \gamma > 0.$$

Put $\cos\phi \approx 1-\mu\phi^2$, where $\mu = (1-\cos\gamma)/\gamma^2$. This gives an approximation for $\cos\phi$ which is perfect at $\phi=0$ and $\phi=\gamma$, and is sufficiently good, as it turns out, in the intermediate range.[12] The expression can now be integrated in terms of Fresnel integrals. The same procedure is followed in breaking up R, yielding integrals of the form

$$\int_0^{\gamma} \exp\left[-iA\cos\phi\right]\cos\phi d\phi,$$

which can be integrated by parts when the cosine approximation is inserted.

By expanding the original integrands into series of Bessel functions, it can be shown that the errors in the approximate integrations are completely negligible for $\gamma=\theta_1+(\alpha/2)$ as large as $\pi/4$, and for $k\sin\alpha/2$ as large as 100, in view of the fact that the strongest appearance of Q and R in (3) through (6) is in

$$Q\sin^2\frac{\alpha}{2}, \quad \frac{R}{k\sin\frac{\alpha}{2}}, \quad \text{and} \quad R\sin\frac{\alpha}{2}.$$

Hence θ_1 can be allowed to go as high as 30 degrees.

Appendix II

Simplification of the Pattern E_4

If (6) is completely expanded with θ_1 put equal to zero, an equation with nineteen terms results. If we drop at once the five terms which contain as factors

$$\frac{2N}{k}, \quad \frac{4N}{k^2\sin\frac{\alpha}{2}}, \quad \frac{2N}{k^3\sin^2\frac{\alpha}{2}}, \quad 2N\sin^3\frac{\alpha}{2}, \quad \text{and} \quad \frac{N\sin^2\frac{\alpha}{2}}{k}$$

and if we call

$$\frac{\frac{\alpha}{2}\sin^2\frac{\alpha}{2}}{k} = \frac{M}{k}\sin^2\frac{\alpha}{2}, \qquad \frac{\alpha}{k^3\sin^2\frac{\alpha}{2}} = \frac{2M}{k^3\sin^2\frac{\alpha}{2}},$$

we make by actual computations of the kind shown in the text an error not greater than 0.0001. This leaves us with

$$E_4 \approx \frac{3i}{4}\frac{\sin\alpha}{k}\cos\left(\frac{k}{2}\sin\alpha\right) - 3\cos^2\frac{\alpha}{2}\frac{\cos\left(\frac{k}{2}\sin\alpha\right)}{\left(k\sin\frac{\alpha}{2}\right)^2} + 3\cos\frac{\alpha}{2}\frac{\sin\left(\frac{k}{2}\sin\alpha\right)}{\left(k\sin\frac{\alpha}{2}\right)^3} + \frac{3\pi i}{4k}J_0\left(k\sin\frac{\alpha}{2}\right) - \frac{3i}{2k}M\cos\left(k\sin\frac{\alpha}{2}\right) - \frac{3i}{k^2}\sin\left(\frac{k}{2}\sin\alpha\right)$$

[12] Integrals of the form

$$\int_0^{\gamma} \exp\left[-iA\cos(\phi-\theta)\right]\cos m\phi d\phi$$

occur in the paper "Theory of the electromagnetic horn," by W. L. Barrow and L. J. Chu, Proc. I.R.E., vol. 27, pp. 51–64; January, 1939. The process of approximate evaluation used is given by Dr. Chu in his doctoral thesis for the electrical engineering department of the Massachusetts Institute of Technology, "Transmission and Radiation of Electromagnetic Waves in Hollow Pipes and Horns;" 1938. It consists of using the first two terms of the infinite product which represents $\cos(\phi-\theta)$, neglecting fourth-order terms, and also including in the exponential the exponential form of $\cos m\phi$.

$$-\frac{3\pi i}{2}\frac{J_1\left(k\sin\frac{\alpha}{2}\right)}{k^2\sin\frac{\alpha}{2}}+3iM\frac{\sin\left(k\sin\frac{\alpha}{2}\right)}{k^2\sin\frac{\alpha}{2}}$$
$$+\frac{3\pi i}{4}\sin^3\frac{\alpha}{2}J_1\left(k\sin\frac{\alpha}{2}\right)$$
$$-\frac{3i}{2}M\sin^3\frac{\alpha}{2}\sin\left(k\sin\frac{\alpha}{2}\right).$$

Combine the first and fifth terms; their absolute value is approximately equal to

$$\frac{3}{4}\frac{\alpha}{k}\left[\cos\left(\frac{k}{2}\sin\alpha\right)-\cos\left(k\sin\frac{\alpha}{2}\right)\right]<0.00007,$$

which we drop. The same can be done with terms six and eight, which are less than 0.00004. Dropping term nine introduces a maximum error of 0.0035 (in view of the maximum value of the Bessel function after its first minimum and in view of the maximum value of α), and term ten is less than 0.0002 so that it also can be dropped.

Terms two and three combine, with no error, to form

$$\frac{-3\cos^3\frac{\alpha}{2}}{k\sin\frac{\alpha}{2}}g^1\left(\frac{k}{2}\sin\alpha\right)$$

if we note that the first derivative of $\sin x/x$ is

$$g^1(x)=\frac{1}{x}\left(\cos x-\frac{\sin x}{x}\right).$$

Terms four and seven combine by the recurrence formula for the Bessel functions.

The maximum error is certainly not greater than the numerical sum of all the errors listed, viz., 0.004 ($\frac{1}{3}$ db at 20 db down).

A Note on Super-Gain Antenna Arrays*

NICHOLAS YARU†, STUDENT, IRE

Summary—**Numerical calculations have been made for linear broadside super-gain arrays. Using arrays having an over-all length of a quarter wavelength as an example, it is shown that as the required directive gain is increased, tremendous currents are required to produce only a small radiated field. For a 9-element array which produces a power gain of 8.5, the currents must be adjusted to their correct value to an accuracy of better than 1 part in 10^{11}. The efficiency is less than 10^{-14} per cent.**

THE THEORETICAL POSSIBILITY of obtaining arbitrarily high directivity from an array of given over-all length appears to have been pointed out first in 1943 by Schelkunoff[1] in connection with end-fire arrays. In 1946, Bowkamp and de Bruijn,[2] discussing the problem of optimum current distribution on an antenna, concluded that there was no limit to the directivity obtainable from an antenna of given length (or broadside array). In 1947, Laemmel[3] gave source-distribution functions for small high-gain antennas. The extension of the results of Bowkamp and de Bruijn to a two-dimensional current distribution was considered by Riblet.[4] In a discussion of Dolph's[5] paper on an optimum current distribution for broadside arrays, Riblet[6] showed that if spacings less than one-half wavelength were considered, the Tchebyscheff distribution used by Dolph could be made to yield an array having as great a directivity as might be desired.

Arrays which are capable of producing arbitrarily sharp directive patterns for a given aperture or over-all length have become known as super-gain arrays. That such arrays might be possible in theory but quite impractical to build is almost to be expected. The papers mentioned above do not concern themselves with this aspect of the problem, but several other authors[7–9] have indicated some of the practical limitations. Wilmotte[8] pointed out the low radiation resistance and efficiency of such arrays, and later Chu[9] gave a completely general answer to the problem in terms of the maximum gain-Q ratio obtainable from a system of given size.

It is the purpose of this paper to carry through a typical super-gain array design in order to obtain numerical answers for some actual cases. These will serve to demonstrate the rapidity with which the design becomes impractical as the directivity is increased. Schelkunoff's method for the analysis of linear arrays is employed with the arrangement of nulls being made in accordance with the Tchebyscheff distribution as suggested by Riblet. The numerical results are rather sur-

* Decimal classification: R125.1×R325.112. Original manuscript received by the Institute, March 7, 1950; revised manuscript received, December 29, 1950.

† University of Illinois, Urbana, Ill.

[1] S. A. Schelkunoff, "A mathematical theory of linear arrays," *Bell Sys. Tech. Jour.*, vol. 22 ,pp. 80–107; January, 1943.

[2] C. J. Bowkamp and N. G. de Bruijn, "The problem of optimum antenna current distribution," *Philips Res. Rep.*, vol. 1, pp. 135–158; January, 1946.

[3] A. Laemmel, "Source Distribution Functions for Small High-Gain Antennas," Microwave Research Institute, Polytechnic Institute of Brooklyn, Report R-137-47, PIB-88; April 4, 1947.

[4] H. J. Riblet, "Note on the maximum directivity of an antenna," PROC. I.R.E., vol. 36, pp. 620–624; May, 1948.

[5] C. L. Dolph "A current distribution for broadside arrays which optimizes the relationship between beam width and side-lobe level," PROC. I.R.E., vol. 34, pp. 335–348; June, 1946.

[6] H. J. Riblet, Discussion on "A current distribution for broadside arrays which optimizes the relationship between beam width and side-lobel level," PROC. I.R.E., vol. 35, pp. 489–492; May, 1947.

[7] C. E. Smith, "A critical study of two broadcast antennas," PROC. I.R.E., vol. 24, pp. 1329–1341; October, 1936.

[8] R. M. Wilmotte, "Note on practical limitations in the directivity of antennas," PROC. I.R.E., vol. 36, p. 878; July, 1948.

[9] L. J. Chu, "The physical limitations of directive radiating systems," *Jour. Appl. Phys.*, p. 1163; December, 1948.

prising and point up some interesting facts concerning such arrays.

It will be recalled that the basis of Schelkunoff's analysis is his fundamental theorem that every linear array with commensurable separation between its elements may be represented by a polynomial, and, conversely, every polynomial can be interpreted as a linear array. Furthermore, a recognition of the correspondence between the nulls of the array pattern and the roots of a complex polynomial on a unit circle in the complex plane leads to a combination analytical-graphical technique for determining antenna current amplitudes and phases and for obtaining a detailed plot of the directive field pattern.

In this analysis the relative amplitude of the electric field intensity for a linear array of n equispaced elements is represented by

$$E = \left| a_0 e^{j\alpha_0} + a_1 e^{j\psi + j\alpha_1} + a_2 e^{j2\psi + j\alpha_2} + \cdots + a_{n-2} e^{j(n-2)\psi + j\alpha_{n-2}} + e^{j(n-1)\psi} \right|, \quad (1)$$

where $\psi = \beta d \cos\phi + \alpha$ and $\beta = 2\pi/\lambda$.

In the above expression, d is the spacing between elements. The coefficients a_0, a_1, a_2, and so forth are proportional to the current amplitudes in the respective elements. The factor α is the progressive phase shift (lead) from left to right between successive elements; α_1, α_2, and so forth are the deviations from this progressive phase shift.

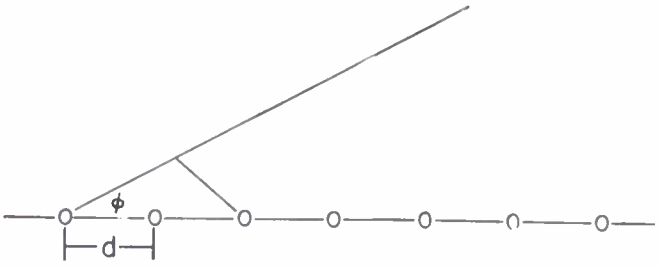

Fig. 1—λ linear array.

By substituting $Z = e^{j\psi}$ and $A_m = a_m e^{j\alpha_m}$, (1) becomes

$$E = \left| A_0 + A_1 Z + A_2 Z^2 + \cdots + A_{n-2} Z^{n-2} + Z^{n-1} \right|. \quad (2)$$

The transform $Z = e^{j\psi}$ is a complex quantity whose modulus is one and whose argument ψ is real and a function of ϕ (the angle between the line of arrival of the signal and the line of the array). Hence, the plot of Z in the complex plane is always on the circumference of a unit circle. Each multiplication by $z = e^{j\psi}$ represents a displacement through an arc of ψ radians.

The polynomial (2) may be written also in the form of the product of $(n-1)$ binomials; thus,

$$E = \left| (Z - t_1)(Z - t_2) \cdots (Z - t_{n-1}) \right|, \quad (3)$$

where $t_1, t_2, \cdots, t_{n-1}$ are the zeros of the polynomial and correspond to the null points of the array. Accordingly, by (3), the relative amplitude of the radiated field intensity in any direction is given by the product of the distances from the null points on the unit circle to the point Z which corresponds to the chosen direction.

As a consequence of this correspondence between the nulls of an array and the roots of a complex polynomial, it is possible to obtain a relative field-strength plot and antenna-current ratios for a specified radiator spacing, and an arbitrary location of the nulls on the unit circle. The graphical-mathematical method involves the expansion of $(n-1)$ binomials.

In the expression $\psi = \beta d \cos\phi + \alpha$, ψ varies from $(\beta d + \alpha)$ to $(-\beta d + \alpha)$ as ϕ ranges from 0 to 180 degrees, and the range described by ψ is $(\beta d + \alpha) - (-\beta d + \alpha) = 2\beta d$. It is apparent that the current ratios and array pattern will vary with different location of the nulls in the range of ψ. For spacings less than a half wavelength, Schelkunoff has shown that an end-fire array with its null points equispaced in the range of ψ on the unit circle, has a narrower principle lobe and smaller secondary lobes than a uniform array (one whose null points are equispaced over the entire unit circle). If the current distribution of the array is always made to be that which corresponds to equispaced nulls in the range of ψ, it appears possible to increase indefinitely the directivity of an end-fire array of given length by increasing the number of elements and decreasing the spacing between them.

When this same technique of equispacing the nulls in the range of ψ is applied to a broadside array of given length, the pattern does not improve as the number of elements is increased, but, instead, deteriorates for spacings less than $\lambda/2$. However, if the nulls on the unit circle are spaced in the range of ψ according to a "Tchebyscheff distribution," a super-gain pattern results when a large number of elements at small spacings is used.

The properties of the Tchebyscheff polynomials[10] were used by Dolph[5] to obtain the optimum pattern of a broadside array for which the spacing between elements is equal to or greater than $\lambda/2$. The Tchebyscheff polynomials are defined by

$$T_n(Z) = \cos\left[n \cos^{-1} Z\right] \quad \text{for} \quad -1 < Z < +1$$
$$T_n(Z) = \cosh\left[n \cosh^{-1} Z\right] \quad \text{for} \quad |Z| > 1.$$

Graphically all the roots of $T_n(Z)$ occur between $Z = \pm 1$ and the maximum and minimum values of $T_n(Z)$ lying between $Z = \pm 1$ are alternately $T_n(Z) = \pm 1$ (see Fig. 2). For $|Z| > 1$, it can be shown that $|T_n(Z)|$ increases as $|Z|^n$. Derivations from the definition of the Tchebyscheff polynomials show that $T_0(x) = 1$; $T_1(x) = x$; $T_2(x) = 2x^2 - 1$, and so forth. Higher-order polynomials may be derived from the following equation:

$$T_{m+1}(x) = 2T_m(x)T_1(x) - T_{m-1}(x).$$

It is evident from an inspection of Fig. 2 that a pat-

[10] Courant and Hilbert, "Methoden der Mathematischen Physik," Julius Springer, Berlin, Germany, vol. 1, p. 75; 1931.

tern may be obtained whose side lobes are all down an equal amount from the main lobe and that the ratio of the main lobe to the subordinate lobes may be determined by using the proper portion of the Tchebyscheff function.

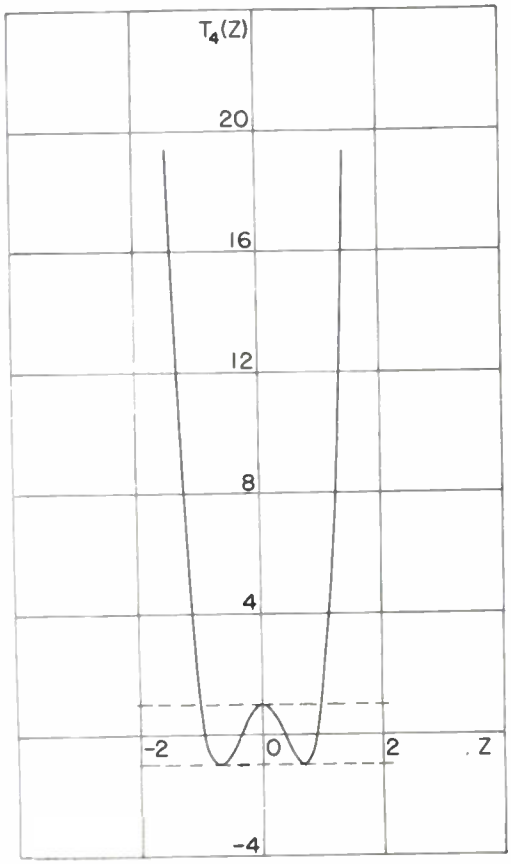

Fig. 2—Fourth-degree Tchebyscheff polynomial.

For $2n+1$ elements, symmetrical in spacing and current about the center element, the expression for the

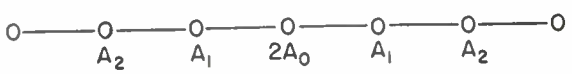

Fig. 3—Symmetrical linear array.

relative field strength can be found directly from (2). It is

$$|E| = A_0 + A_1 \cos\psi + A_2 \cos 2\psi + \cdots + A_n \cos n\psi, \quad (4)$$

with $\psi = \beta d \cos\phi$ since $\alpha = 0$ for broadside arrays. Substituting $x = \cos\psi$ in the above expression yields the polynomial

$$|E| = A_0 + A_1 x + A_2(2x^2 - 1) + \cdots + A_n T_n(x). \quad (5)$$

Expression (5) is a summation of polynomials, and it appears feasible, therefore, to design an array pattern exhibiting the useful properties of a Tchebyscheff plot. A linear shifting of the desired portion of the Tchebyscheff polynomial of correct degree into the range defined by $x = \cos\psi$ for the given array, and the equating of coefficients of (5) to those of the transformed Tchebyscheff function, permits the determination of the relative current distribution (A_1, A_2, A_3, A_n). Knowing the positions of the nulls, the Tchebyscheff pattern is obtained from (3) by the method previously indicated.

As an example, consider a nine-element broadside array whose total length is $\lambda/4$ (spacing between elements $d = \lambda/32$). The side-lobe level is to be 1/19.5 of the main lobe. Since there are nine elements, the array should have 8 nulls on the unit circle within the range of ψ, and 8 nulls in the range of the Tchebyscheff pattern which is used. It is possible to select the polynomial $T_4(x)$ (see Fig. 2) and use the whole range from $x = -1$ to x_0 (point at which $T_4(x) = 19.5$) and back to -1. With $d = \lambda .32$, $\psi = \beta d \cos\phi = \pi/16 \cos\phi$; $x = \cos\psi = \cos(\pi/16 \cos\phi)$.

When

$$\phi = 0°, \quad x = \cos \pi/16$$
$$\phi = 90°, \quad x = 1$$
$$\phi = 180°, \quad x = \cos \pi/16.$$

Hence, the desired portion ($x = -1$ to x_0) of $T_4(x)$ must be shifted into the array range of $\cos \pi/16$ to 1. The point x_0 may be calculated from

$$T_4(x_0) = 8x_0^4 - 8x_0^2 + 1 = 19.5$$
$$x_0 \cong 1.449.$$

The shift of $T_4(x)$ is accomplished by the linear transform $x' = ax + b$.

Therefore, (5) for a nine-element array becomes

$$\begin{aligned} |E_R| &= A_0 + A_1 x + A_2(2x^2 - 1) + A_3(4x^3 - 3x) \\ &\quad + A_4(8x^4 - 8x^2 + 1) \\ &= 8(x')^4 - 8(x')^2 + 1 \\ &= 8(ax + b)^4 - 8(ax + b)^2 + 1. \end{aligned} \quad (6)$$

At this point the question arises as to what accuracy is required in the computations in order to achieve a reasonably accurate result. By using the general error formula,[11] it is shown below that the error in coefficients a and b must be less than 10^{-9} in order that current distribution A_1, A_2, A_3, A_4 be accurate to one decimal place.

In (6), $8(x')^4 = 8a^4x^4 + 32a^3x^3b + 48a^2x^2b^2 + 32axb^3 + 8b^4$ and $8(x')^2 = 8a^2x^2 + 16axb + 8b^2$. An error δa in a would have its greatest effect in the $8a^4x^4$ term ($a > 1$). Neglecting high-order infinitesimals

$$\delta N = \frac{\partial N}{\partial u_1}\delta u_1 + \frac{\partial N}{\partial u_2}\delta u_2 + \cdots + \frac{\partial N}{\partial u_n}\delta u_n,$$

where N denotes a function of several independent variables (u_1, u_2, u_n). Using the above expression, where $N = 8a^4$, for a variation in a, δN is $32a^3 \cdot \delta a$. For the example chosen, the approximate values of a and b determined from substitution in $x' = ax + b$ are 126.9 and 125.5, respectively. Hence, if the figures A_1, A_2, A_3, and

[11] J. B. Scarborough, "Numerical Mathematical Analysis," Johns Hopkins Press, Baltimore, Md., p. 7; 1946.

A_4 are to be accurate to 1 decimal place, $32a^3 \cdot \delta a < 0.1$ and

$$\delta a < \frac{0.1}{(32)(126.9)^3} \cong 10^{-9}.$$

Consequently, the first requirement is to determine a and b to this accuracy; $x = \cos \pi/16$ must therefore be found to this same degree of exactness. After carrying out the computation of (6) to this degree of accuracy, the current distribution (A_1, A_2, A_3, and A_4) may be considered to be accurate to one decimal place. Any numerical calculations not maintaining this degree of accuracy are worthless, as may be seen from the following calculations for the example. For this particular array of nine elements, the current ratios are as follows:

$$\begin{aligned} A_0 &= 8,893,659,368.7, \\ A_1 &= -14,253,059,703.2, \\ A_2 &= 7,161,483,126.6, \\ A_3 &= -2,062,922,999.4, \\ A_4 &= 260,840,226.8, \end{aligned}$$

and (4) becomes

$$\begin{aligned} E_R = {} & 8,893,659,368.7 \\ & - 14,253,059,703.2 \cos\left(\frac{\pi}{16}\cos\phi\right) \\ & + 7,161,483,126.6 \cos\left(\frac{\pi}{8}\cos\phi\right) \\ & - 2,062,922,999.4 \cos\left(\frac{3\pi}{16}\cos\phi\right) \\ & + 260,840,226.8 \cos\left(\frac{\pi}{4}\cos\phi\right). \end{aligned} \tag{7}$$

The antenna pattern (portion of $T_4(x)$) is available from direct substitution of ϕ in the above expression. The accuracy requirements in the computations can now be demonstrated. Broadside to the array (direction of maximum radiation) where $\phi = 90$ degrees, (7) is evaluated as

$$\begin{aligned} E_R = {} & 8,893,659,368.7 - 14,253,059,703.2 \\ & + 7,161,483,126.6 - 2,062,922,999.4 \\ & + 260,840,226.8. \end{aligned}$$

The sum of the positive terms is 16,315,982,722.1 and the sum of the negative terms is $-16,315,982,702.6$. The resultant $|E_R|$ is 19.5, the value specified for the ratio of the major lobe to the side lobes. End-fire to the array $\phi = 0$ or 180 degrees, and (7) takes the form

$$\begin{aligned} |E_R| = {} & 8,893,659,368.7 - 14,253,059,703.2 \cos\frac{\pi}{16} \\ & + 7,161,483,126.6 \cos\frac{\pi}{8} \\ & - 2,062,922,999.4 \cos\frac{3\pi}{16} \\ & + 260,840,226.8 \cos\frac{\pi}{4}. \end{aligned}$$

The numerical values for the trigonometric functions must be accurate to the same number of significant figures as are the coefficients. The resultant $|E_R|$ for the end-fire direction is 1.0. Calculations having an accuracy that would normally be considered adequate—four or five significant figures—cannot be used to obtain the correct current distribution and array pattern from (7). The resultant $|E_R|$ in (7) is the difference between large numbers, nearly equal, such that significant figures (to the left) are lost. In this example, 12-figure accuracy was necessary at the start in order to end up with only 2 or 3 figures.

It is interesting to note that the pattern obtained by the graphical method from the location of the nulls on the unit circle does not require this high degree of accuracy. Solution of (6) maintaining accuracy to 4 significant figures, and the determination of the nulls from the roots of (6) affords sufficient information to plot a fairly accurate pattern. This is because this method involves the product of the lengths from the $(n-1)$ null points on the unit circle to the point Z corresponding to a chosen direction. The final result is as exact in significant figures as are contained in the least accurate factor. In Fig. 4 there is shown the pattern for the nine-element array of this example as calculated (graphically) from (3), using 4 figures, or alternatively from (7) using 12 figures.

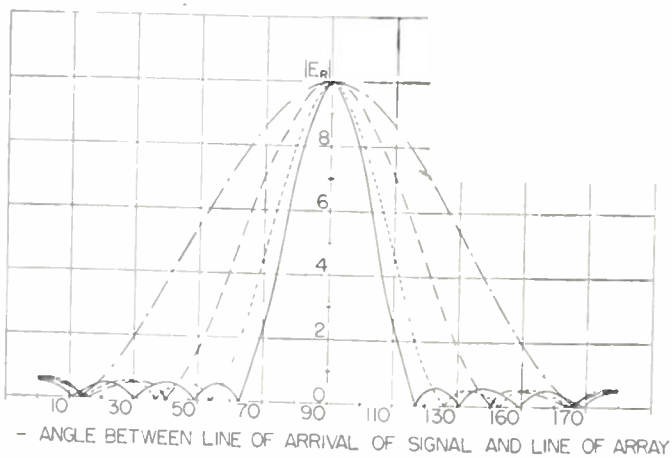

Fig. 4—Broadside "super-gain" patterns for three-, five-, seven-, and nine-element arrays with an over-all array length of quarter wavelength.

- Three elements, $d = \lambda/8$
- Five elements, $d = \lambda/16$
- Seven elements, $d = \lambda/24$
- Nine elements, $d = \lambda/32$

Examination of the numerical results for the 9-element example indicates some of the practical shortcomings of super-gain arrays. In this example, currents of the order of 14 million amperes are required in the individual elements in order to produce in the direction of

maximum radiation a field intensity equivalent to that which would be produced by 19.5 milliamperes flowing in a single element. Moreover, it would be necessary to maintain these currents, as well as the spacing between antenna elements, to an accuracy of about 1 part in 10^{11} if the super-gain pattern is to be obtained.

In order to illustrate the rapidity with which the design becomes impractical, the curves of Figures 4, 5, 6, and 7 have been drawn. Fig. 4 shows the directivities obtainable from an array that has an over-all length of one-quarter wavelength when the number of elements used is 3, 5, 7, and 9, respectively. In Fig. 5 these directivities are expressed in terms of directive gain over a single element. As the number of elements is increased

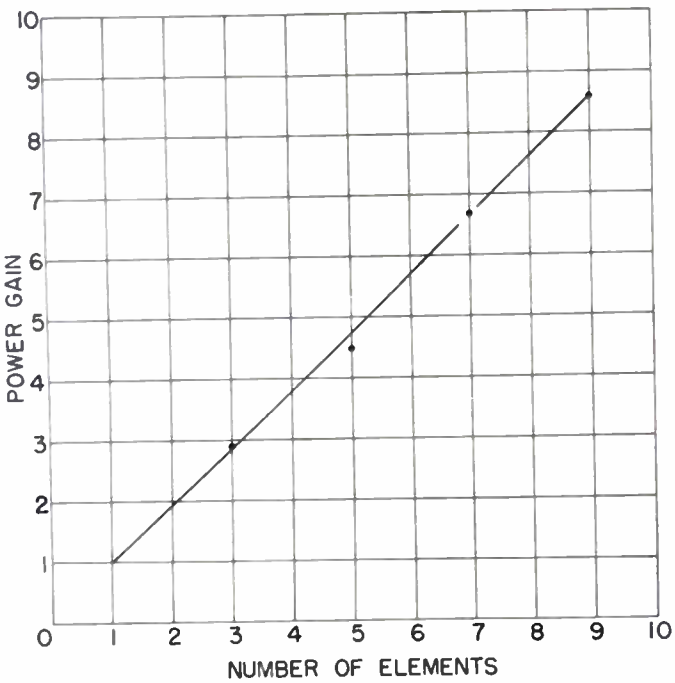

Fig. 5—Power gain of Tchebyscheff arrays over a single element. The array length is $\lambda/4$ in each case.

and the spacing between elements is correspondingly decreased, the required currents become very large for any appreciable radiation. The accuracy with which these currents must be adjusted in order to obtain the calculated super-gain patterns within 0.5 per cent is shown in Fig. 6.

The exceedingly large currents required cause large ohmic losses with resultant low efficiencies. In general, most of these losses will occur in the coupling and matching networks (and in the ground system if monopole antennas erected on a finitely conducting earth are being considered). However, for the efficiency calculations, the results of which are shown in Fig. 7, only the ohmic losses in the antenna elements themselves have been considered. For the purpose of illustration, the antennas have been assumed to be half-wave dipoles at 10 mc, constructed of copper with a diameter of 1 cm. The resultant efficiencies under the assumptions are shown in Fig. 7. When matching network losses are considered, the actual efficiencies would be much lower.

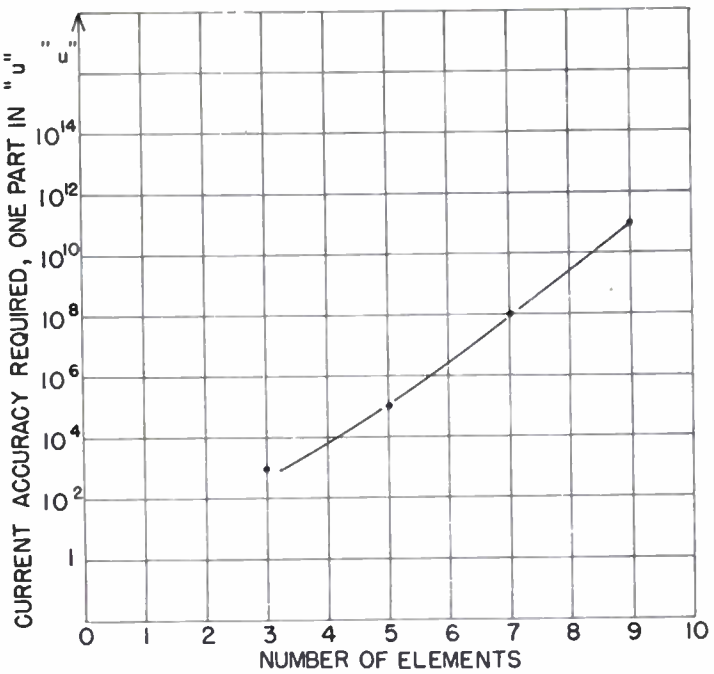

Fig. 6—Current accuracy required to obtain Tchebyscheff super-gain patterns correct to 0.5 per cent.

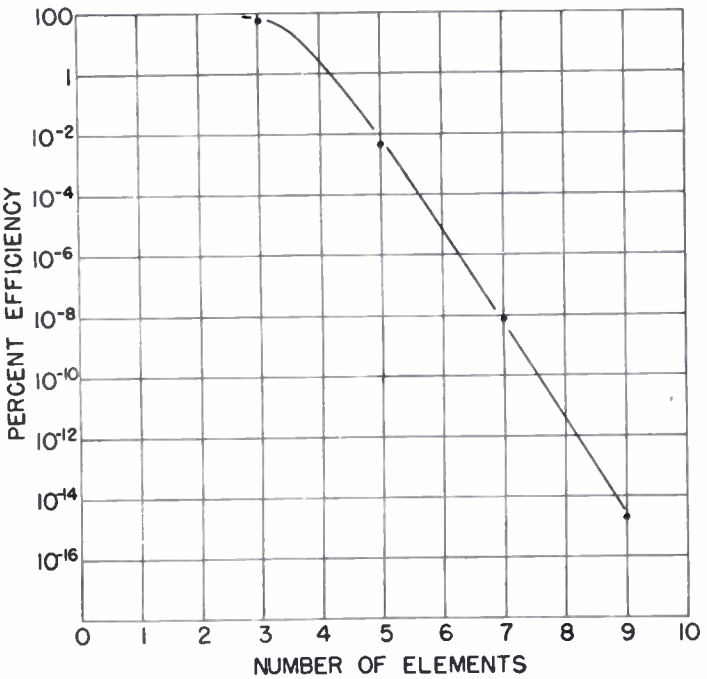

Fig. 7—Per cent efficiency of Tchebyscheff arrays versus number of elements in a quarter-wavelength array.

Acknowledgments

Acknowledgments are due H. A. Elliott of McGill University for his observance of the accuracy requirements in the computations, and G. A. Miller of National Research Council, Ottawa, Ont., Canada, for comments and suggestions. The writer is indebted to E. C. Jordan of the University of Illinois for his guidance on this problem which arose in connection with an investigation of antenna systems suitable for radio direction finding. The radio direction-finding research program at the University of Illinois is sponsored by the Office of Naval Research under Contract No. N6ori-71-Task XV.

Crystal-Plates Without Overtones*

J. J. VORMER†

Summary—**By using a special electrode form or a special field distribution, overtones in lengthwise vibrating crystal plates or bars can be suppressed to any amount.**

IT IS A WELL-KNOWN fact that in different types of piezoelectric elements overtones can be excited, a phenomenon made use of for various practical purposes. Thus, e.g., *BT*-cut quartz oscillator plates may be excited in a harmonic shear mode, so that very high frequencies can directly be generated in an appropriate oscillator. Moreover, for filter crystals of quartz, use is sometimes made of long plates or bars in which a harmonic of the lengthwise fundamental is excited. In the last-mentioned case preference is mostly given to rotated *X* cuts in which the *Y'* wave is excited. A special electrode arrangement is necessary to obtain the desired mode of vibration. Here the aim is not so much to get a high frequency, but to obtain quartz plates with a low impedance, because this last item is decreased by a factor equal to the ordinal number of the harmonic.[1]

In other purposes overtones merely cause the same kind of difficulties as unwanted spurious resonances. For instance, in some types of radar-receivers resonators are used for time or distance marking, and in these not only can spurious frequencies not be tolerated, but harmonics of the wanted frequency must be suppressed at the same time. The main resonance in this case is of the order of 150 kc.

The first requirement can be fulfilled by choosing for the resonator a rotated *X*-cut quartz plate, with a sufficiently low ratio of width to length, in which the *Y'* wave is excited. In such a crystal plate all unwanted resonances in the neighborhood of the main resonance are extremely weak; it is possible, however, to excite all odd and even harmonics.

Normally, electrodes cover the *Y'Z'* plane of the plate. Whenever electrodes are placed symmetrically with respect to the nodal line, all even harmonics are suppressed; this follows directly from considerations of symmetry. By giving the electrodes a special form or special dimensions, one or more odd harmonics may be suppressed as well as all odd harmonics, with the exception of the main resonance.

To illustrate the way in which a selected harmonic may be suppressed, let us first study the way in which it may be excited. If we want the third *Y'* harmonic in a rotated *X*-cut plate, an electrode arrangement as shown in Fig. 1(a) is indicated. As two subsequent sections of the vibrating crystal plate have opposite phases the corresponding electric fields must also have a phase difference of π, and this is achieved by the indicated electrode arrangement. The electric fields at a certain time in each of the three parts of the crystal plate are indicated by the arrows.

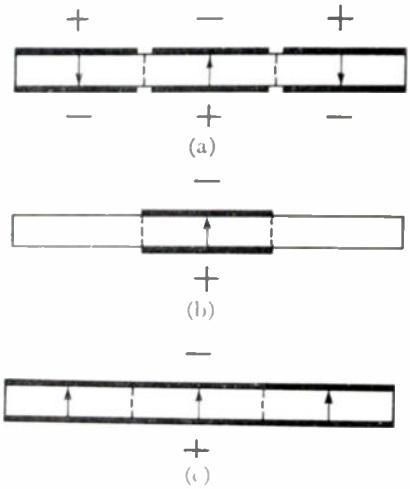

Fig. 1—Electrode arrangements for exciting the third overtone.

If now the first and third pairs of electrodes are omitted and a voltage with a frequency corresponding to the third harmonic is applied to the middle electrodes only (Fig. 1(b)), the resonator is once more excited in its third harmonic. The excitation is however weaker now, due to the fact that only one-third of the plate is excited.

Weak excitation of the third overtone is also possible if the voltage is applied to the three pairs of electrodes in phase, or if the plate is completely covered by one large electrode (Fig. 1(c)). In the latter case, the influence of the first and the third part prevail over that of the middle part.

If, however, an electrode arrangement is made as indicated in Fig. 2, when the electrode covers two-thirds of the crystal surface, the effects of the first and the third part just balance out that of the middle part, and the result is that no third harmonic can be excited. In a similar way the fifth harmonic may be suppressed by choosing the electrode length 2/5 or 4/5 of the crystal length; and so on.[2]

Fig. 2—Electrode arrangement for suppressing the third overtone.

* Decimal classification: R214.22. Original manuscript received by the Institute, August 10, 1950; revised manuscript received, December 27, 1950.

† Radio Laboratory of the Netherlands Postal and Telegraph Services, s'-Gravenhage, Netherlands.

[1] J. J. Vormer, "Quartz filter crystals with low inductance," PROC. I.R.E., vol. 36, pp. 802–804; June, 1948.

[2] Partly electroded crystal plates (for other purposes) are discussed in W. G. Cady, "Piezoelectricity," McGraw-Hill Book Co., Inc.; 1946, p. 301.

If the length of the electrode is chosen somewhere between 2/3 and 4/5 (e.g., about 8/11) the third and fifth harmonic are both more or less suppressed, but, of course, it is impossible to do so completely in this way. It can be shown, however, that if the part of the crystal covered by the electrodes varies sinusoidally with the length, the desired compensation may be obtained for all harmonics with the exception of the main resonance. The same result can be obtained by varying the exciting electric field sinusoidally with the length.[3]

If the principle of shaped electrodes is applied to filter crystal-plates with four electrodes, the unwanted capacitances between the electrode-pairs are incidentally appreciably diminished. (See Fig. 3.)

Experiments were carried out with electrodes of the sine-shape and with rectangular electrodes of the type indicated in Fig. 2. The amount of overtone suppression depends, of course, on the precision of the dimensions; moreover, the fact that no correction is applied for the edges of the electrodes is of influence. Nevertheless, it is quite simple to get without special precautions such an overtone suppression that the response of any overtone is less than 1 per cent of the main resonance.

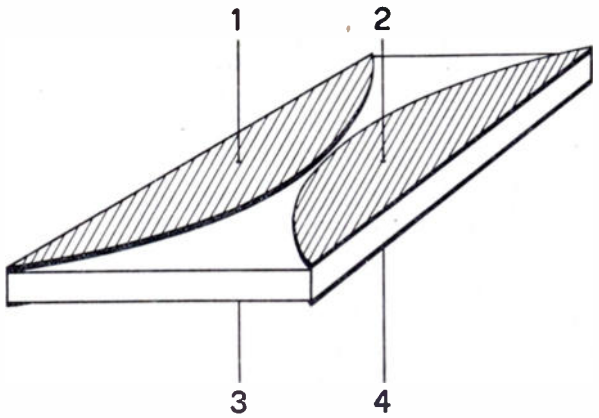

Fig. 3—Electrode arrangement for suppressing all overtones, applied to a crystal plate with four electrodes.

ACKNOWLEDGMENT

The author is indebted to J. Oortgijsen and E. J. Post for their useful suggestions in regard to the preparation of this paper.

[3] If the form of the electrode is a sine function ($\sin \pi x/l$) and the piezoelectric reaction of the bar for the kth harmonic is given by $\sin k(\pi x/l)$ the total response of the crystal disappears if:

$$\int_0^l \sin \frac{\pi x}{l} \sin k \frac{\pi x}{l} \, dx = 0.$$

This is true if $k \neq 1$, according to the orthogonality theorem of Fourier series.

A Series Expansion of the Fourier Integral*

WILLIAM A. WHITCRAFT, JR.†, ASSOCIATE, IRE

Summary—**Evaluation of the Fourier integral by parts leads to two different series representations of a time function in the frequency domain. These series involve powers of the frequency variable and either derivatives or integrals of the function, evaluated at the upper time limit only.**

It is necessary that the function so treated be analytic between the time limits imposed. The convenience of the formulation then follows from choosing the time limits symmetrically.

The method is presented as a mathematical experiment rather than a rigorous formulation.

THIS PAPER is intended to outline a series expansion of the Fourier integral, which method has been used successfully in studies of bandwidth requirements for pulsed transmissions.

If we define the Fourier integral of a time function $f(t)$ by

$$g(w) = \int_{-\infty}^{\infty} f(t) \exp(-iwt)dt \tag{1}$$

and limit the function to the time interval $-D/2$ to $D/2$ we will have

$$g(w) = \int_{-D/2}^{D/2} f(t) \exp(-iwt)dt. \tag{2}$$

Providing the function $f(t)$ is analytic within these limits, consider integrating (2) by parts, choosing

$$u = f(t) \tag{3}$$

$$dv = \exp(-iwt)dt. \tag{4}$$

The first integration yields

$$g(w) = \frac{1}{-iw}\left[f(t) \exp(-iwt) - \int f'(t) \exp(-iwt)dt\right]_{-D/2}^{D/2} \tag{5}$$

where the prime indicates the time derivative. Continuing the integration by parts, we find

$$g(w) = \frac{1}{-iw} \sum_{m=0}^{\infty} \left[\frac{1}{(iw)^m} f^m(t) \exp(-iwt)\right]_{-D/2}^{D/2} \tag{6}$$

Ignoring for a moment the question of convergence, divide the summation into two parts and change limits to obtain

* Decimal classification: 510. Original manuscript received by the Institute, June 21, 1950; revised manuscript received, October 30, 1950.

† Raytheon Manufacturing Co., Waltham 54, Mass.

$$g(w) = \frac{1}{iw}\left[\sum_{m=0,2,4,\cdots}^{\infty}\left\{\frac{1}{(iw)^m}f^m(t)\exp(-iwt)\right\}_{D/2}^{-D/2} + \sum_{n=1,3,5,\cdots}^{\infty}\left\{\frac{1}{(iw)^n}f^n(t)\exp(-iwt)\right\}_{D/2}^{-D/2}\right]. \quad (7)$$

If the function is even, or cosine symmetrical, the even-ordered derivatives will be even functions and the odd-ordered derivatives odd. Factoring (7) and making use of the substitution

$$\exp\left(iw\frac{D}{2}\right) - \exp\left(-iw\frac{D}{2}\right) = 2i\sin w\frac{D}{2} \quad (8)$$

we obtain

$$g(w) = \left(\frac{2}{w}\sin\frac{wD}{2}\right)\left\{f\left(\frac{D}{2}\right) - \frac{f''\left(\frac{D}{2}\right)}{w^2} + \cdots\right\} + \left(\frac{2}{w}\cos\frac{wD}{2}\right)\left\{\frac{f'\left(\frac{D}{2}\right)}{w} - \frac{f'''\left(\frac{D}{2}\right)}{w^3} + \cdots\right\} \quad (9)$$

for an even time function. Note that the derivatives are evaluated at the upper limit only. For an odd function, similar reasoning leads to

$$g(w) = \left(\frac{2i}{w}\cos\frac{wD}{2}\right)\left\{f\left(\frac{D}{2}\right) - \frac{f''\left(\frac{D}{2}\right)}{w^2} + \cdots\right\} - \left(\frac{2i}{w}\sin\frac{wD}{2}\right)\left\{\frac{f'\left(\frac{D}{2}\right)}{w} - \frac{f'''\left(\frac{D}{2}\right)}{w^3} + \cdots\right\}. \quad (10)$$

If, instead of the relations (3) and (4), we choose

$$u = \exp(-iwt) \quad (11)$$

$$dv = f(t)dt \quad (12)$$

we obtain, for an even function

$$g(w) = \left(\frac{2}{w}\cos\frac{wD}{2}\right)\left\{wf_1\left(\frac{D}{2}\right) - w^3f_3\left(\frac{D}{2}\right) + \cdots\right\} + \left(\frac{2}{w}\sin\frac{wD}{2}\right)\left\{w^2f_2\left(\frac{D}{2}\right) - w^4f_4\left(\frac{D}{2}\right) + \cdots\right\} \quad (13)$$

where the subscripts give the order of the time integration of $f(t)$, the integrals being evaluated at the upper limit only.

If the function is odd, the result is

$$g(w) = \left(\frac{2i}{w}\sin\frac{wD}{2}\right)\left\{wf_1\left(\frac{D}{2}\right) - w^3f_3\left(\frac{D}{2}\right) + \cdots\right\} + \left(\frac{2i}{w}\cos\frac{wD}{2}\right)\left\{w^2f_2\left(\frac{D}{2}\right) - w^4f_4\left(\frac{D}{2}\right) + \cdots\right\}. \quad (14)$$

In practical examples studied it has been found that the series obtained from (9) and from (13) converge in mutually exclusive regions but that whenever one of the series can be recognized as representing a function in closed form within a given radius of convergence, the other series represents the same function but does so everywhere outside the radius of convergence of the first. If neither of the series (9) or (13) can be recognized as an expansion of a function of closed form, the method loses most of its usefulness. If, in this case, it is still desired to use the method, careful attention must be paid to the convergence of the series before any assumptions are made concerning the possibility of curtailing or otherwise altering it for the purpose of obtaining an approximation. These matters are not within the scope of the present paper.

A brief example will demonstrate the use of the method and clarify some of the above statements.

Given a pulse consisting of a single positive half cycle of a cosine wave with unit amplitude and radian frequency w_0: required, the Fourier spectrum $g(w)$.

We have

$$f(t) = \cos w_0 t \quad \text{for} \quad -\frac{\pi}{2w_0} < t < \frac{\pi}{2w_0}$$
$$= 0 \text{ for all other } t. \quad (15)$$

The function (15) is even and is analytic within the limits shown. It is zero at the limits, and its derivatives are discontinuous there. The even-ordered derivatives vanish at the limits (since they involve $\cos(w_0 t)$) and the values of the first, third, fifth, . . . derivatives at the upper limit are respectively

$$-w_0,\ w_0^3,\ -w_0^5,\ w_0^7,\ \cdots.$$

Substituting in (9),

$$g(w) = \left(\frac{2}{w}\cos\frac{wD}{2}\right)\left\{-\frac{w_0}{w} - \left(\frac{w_0}{w}\right)^3 - \left(\frac{w_0}{w}\right)^5 - \cdots\right\} \quad (16)$$

The expression in braces can be put into closed form by considering the following Maclaurin expansion:

$$\frac{1}{1-y} = 1 + y + y^2 + \cdots \text{ for } y < 1. \quad (17)$$

Factoring a minus w_0/w and setting its square equal to y,

$$g(w) = \left(\frac{2}{w}\cos\frac{wD}{2}\right)\left(-\frac{w_0}{w}\right)\left(\frac{1}{1-y}\right) \quad \text{for } y = \left(\frac{w_0}{w}\right)^2 < 1. \quad (18)$$

Substituting and rearranging,

$$g(w) = \frac{2w_0}{w_0^2 - w^2} \cos \frac{\pi w}{2w_0} \tag{19}$$

$$= \pi \frac{D}{2} \frac{\cos w \frac{D}{2}}{\left(\frac{\pi}{2}\right)^2 - \left(w \frac{D}{2}\right)^2} \quad \text{where } D = \frac{\pi}{w_0} \cdot \tag{20}$$

This result is the same as that obtained by formally evaluating the Fourier integral (1) for the given time function (15).

It will be found that the integral formulation (13) leads to exactly the same final answer but that it involves a Maclaurin series which converges only for $(w_0/w)^2 > 1$ in contrast with the restriction $(w_0/w)^2 < 1$ of (18). This behavior has been observed in examples tried thus far but is not here stated as a general theorem; it is considered merely an experimental fact, subject to verification or modification by rigorous mathematical methods not yet successfully applied.

Finally it should be pointed out that time functions possessing no symmetry can be separated into even and odd parts by well-known methods and (9) and (10) or (13) and (14) applied separately.

ACKNOWLEDGMENT

This work was done in connection with Contract AF28-099-182 with Watson Laboratories, AMC, USAF.

The Design of Transmission-Line Tuning Elements for Mininum Dissipation*

R. W. KLOPFENSTEIN†, MEMBER, IRE

Summary—**A design procedure is described by which a coaxial transmission line tuning stub may be designed for minimum energy dissipation when the input susceptance or reactance is specified. The problem has been formulated for air dielectric only where dielectric losses are ordinarily small compared to copper losses. The results are presented in curve form.**

I. INTRODUCTION

IN CONNECTION with coaxial transmission lines, the selection of the diameter of the inner conductor so that some property of the transmission line is optimized has been a topic of considerable interest.[1-4,6-9] A recent paper[7] gives a good summary of work done in this connection to date. It is a fairly common situation in the design of radio-frequency filters that the reactance or susceptance of a filter element is fixed by the response requirements of the filter. It is the object of this paper to devise a design procedure by which transmission-line tuning elements may be designed for minimum dissipation when the input reactance or susceptance is specified. The results of the analysis of the problem will be presented in curve form so that the technique may be easily applied in design problems. Section III *B* of the paper discusses the curves and how they are used.

* Decimal classification: R117.2. Original manuscript received by the Institute, June 8, 1950; revised manuscript received, November 27, 1950.

† RCA Victor Division, Camden, N. J.

[1] A. Russel, "Effective resistance and inductance of concentric mains," *Philosophical Mag.*, 6th Ser., vol. 17, p. 524; April, 1909.

[2] E. J. Sterba and C. B. Feldman, "Transmission lines for short-wave radio systems," PROC. I.R.E., vol. 20, pp. 1163–1202; July, 1932.

[3] B. J. Witt, "Concentric tube lines," *Marconi Rev.*, pp. 20–25; January–February, 1936.

[4] L. S. Nergaard and Bernard Salzberg, "Resonant impedance of transmission lines," PROC. I.R.E., vol. 27, pp. 579–584; September, 1939.

[6] R. P. King, "Transmission line theory and its application," *Journ. Appl. Phys.*, vol. 14, pp. 577–600; November, 1943.

[8] C. R. Cox, "Design data for beaded coaxial lines," *Electronics*, vol. 19, pp. 130–135; May, 1946.

[7] P. H. Smith, "Optimum coax diameters," *Electronics*, vol. 23, pp. 111–114; February, 1950.

[8] F. E. Terman, "Resonant lines in radio circuits," *Elect. Eng.*, vol. 53, pp. 1046–1053; July, 1934.

[9] J. A. Stratton, "Electromagnetic Theory," McGraw Hill Book Co. Inc., New York, N. Y., pp. 545–554; 1941.

II. LIST OF SYMBOLS TO BE USED

Y = Input admittance of a transmission line section
Z = Input impedance of a transmission line section
R = Input resistance of a transmission line section
G = Input conductance of a transmission line section
X = Input reactance of a transmission line section
B = Input susceptance of a transmission line section
l = Length of transmission line section in units of length
α = Attenuation constant of transmission line section in nepers per unit length
β = Phase constant for transmission line section in radians per unit length
Y_0 = Characteristic admittance for transmission line section under the assumption that the line is lossless
Z_0 = Characteristic impedance for transmission line section under the assumption that the line is lossless
P_D = Power dissipated in a transmission line tuning element in watts
V = Voltage at the input to a transmission line section in volts rms
I = Current flowing into a transmission line tuning element in amperes rms
B_1 = Specified value of B
θ = Ratio of inside diameter of outer conductor to

outside diameter of inner conductor of a coaxial transmission line section
D = Inside diameter of outer conductor in units of length
d = Outside diameter of inner conductor in units of length
$j = \sqrt{-1}$
k_1 = Constant
k_2 = Constant.

III. Theory

A. *Design of Open-Circuit Terminated Coaxial Transmission-Line Tuning Stub for Minimum Input Conductance when the Input Susceptance Is Specified.*

The power loss in a coaxial transmission line tuning stub in shunt with a transmission line is expressed by the following equation:

$$P_D = V^2 G. \tag{1}$$

From this, it is seen that if the input conductance is minimized, the power dissipated in the stub will be minimized.

The input susceptance and conductance of an open-circuit terminated coaxial transmission-line section operated off resonance is expressed by the equation

$$Y = G + jB = Y_0 \left\{ \alpha l \left[\sec^2 \beta l - \frac{\tan \beta l}{\beta l} \right] + j \tan \beta l \right\}. \tag{2}$$

The origin of this equation is discussed in Appendix I. If the input susceptance is specified,

$$B = B_1, \tag{3}$$

then l must obey the following relation:

$$l = \frac{1}{\beta} \arctan \left(\frac{B_1}{Y_0} \right). \tag{4}$$

Under the above conditions by substitution into equation (2)

$$G = Y_0 \frac{\alpha}{\beta} \left\{ \frac{\arctan \left(\frac{B_1}{Y_0} \right)}{\cos^2 \left[\arctan \left(\frac{B_1}{Y_0} \right) \right]} - \frac{B_1}{Y_0} \right\}. \tag{5}$$

This expression for G may be expressed entirely in terms of the diameter ratio of the coaxial transmission line if the inside diameter of the outer conductor is considered fixed since for air dielectric, low loss transmission lines[10]

$$Y_0 = \frac{1}{60 \log \theta}, \tag{6}$$

and

$$\alpha = k_1 \frac{1 + \theta}{\log \theta}. \tag{7}$$

When (6) and (7) are substituted into (5) it reduces to

$$G = k_2 (1 + \theta) \log^{-2} \theta \left\{ (1 + 3600 B_1^2 \log^2 \theta) \arctan (60 B_1 \log \theta) - 60 B_1 \log \theta \right\}. \tag{8}$$

Values of $\arctan (60 B_1 \log \theta)$ are taken in accordance with the electrical length of the line being considered. Note that the same expression for the first derivative of G with respect to θ will result for all values of line length. All of the angles in the foregoing are expressed in radians, and the indicated logarithms are natural logarithms.

When the first derivative of G, as expressed by equation (8), with respect to θ is taken and equated to zero, the following transcendental equation is obtained:

$$\frac{\theta \log \theta}{1 + \theta} = 2 \left\{ \frac{\arctan (60 B_1 \log \theta) - 60 B_1 \log \theta}{(1 + 3600 B_1^2 \log^2 \theta) \arctan (60 B_1 \log \theta) - 60 B_1 \log \theta} \right\}. \tag{9}$$

The finite root of (9) greater than unity may be obtained by successive approximations. That this root represents a minimum value of G can be determined by examination of the limiting cases. $\theta = 1$ and $\theta \to \infty$ are always roots of (9), but they are of no practical interest. In fact, they represent limiting cases for which the input conductance is indefinitely large. Therefore, the value of θ for minimum input conductance has been determined. The length of the tuning stub corresponding to this value of θ may be determined from (4). Note that no minimum value for G exists for open-circuit terminated coaxial transmission-line sections less than one-quarter wavelength long [$\beta l < (\pi/2)$]. In this region, the diameter ratio is made as nearly unity as possible, and design is usually limited by voltage gradient considerations. Minimum values for G do exist in all other quadrants of βl for open-circuit terminated coaxial transmission-line sections, however.

A similar analysis may be carried out for short-circuit terminated coaxial transmission-line sections. This analysis will not be carried out in detail here because of its similarity to the foregoing. The relation that must be satisfied for θ in order that minimum input conductance be obtained when the input susceptance is specified is shown in (10).

[10] T. Moreno, "Microwave Transmission Design Data," McGraw-Hill Book Co. Inc., New York, N. Y., p. 1–110; 1948.

$$\frac{\theta \log \theta}{1+\theta} = 2\left\{\frac{\text{arc cot}\,(-60B_1 \log\theta) - 60B_1 \log\theta}{(1+3600B_1^2\log^2\theta)\,\text{arc cot}\,(-60B_1\log\theta) - 60B_1\log\theta}\right\}. \quad (10)$$

Solutions of this equation exist in all quadrants for βl. It is often desirable to place a tuning stub in series with a coaxial transmission line. In this case, the power dissipated in the tuning stub is expressed by:

$$P_D = I^2R. \quad (11)$$

If the reactance of the tuning stub is specified, the power dissipated in the stub will be minimized when R has its least value. For low-loss coaxial transmission-line tuning stubs, the results expressed by (9) and (10) can be directly applied to this case since

$$R + jX = \frac{1}{G + jB},$$

which is

$$= \frac{G}{G^2+B^2} - j\frac{B}{G^2+B^2}. \quad (12)$$

For $G \ll B$,

$$R + jX \simeq \frac{G}{B^2} - j\frac{1}{B}. \quad (13)$$

It is seen that R is directly proportional to G if B is fixed. Therefore, the conditions under which G will be a minimum when B is specified as B_1 are the same, for low loss lines, as those for which R will be a minimum when X is specified as $-1/B_1$.

B. *Presentation of Results*

A set of four curves are presented with which one may design an open circuit terminated or short circuit terminated coaxial line tuning stub for minimum conductance with specified susceptances from -1.0 mhos to -0.001 mhos and from 0.001 mhos to 1.0 mhos or for minimum resistance with specified reactances from $-1{,}000$ ohms to -1.0 ohms and from 1.0 ohms to 1,000 ohms. These curves show, graphically, solutions of (4), (8), (9), and (10), and they make it needless to seek solutions of these equations for the more common situations for which the curve sheets have been plotted.

Figs. 1 through 4 may be used in designing coaxial line tuning stubs for minimum conductance or resistance when the susceptance or reactance has been specified. It will be noted that the curves are useful for open-circuit terminated and short-circuit terminated lines up to one-half wavelength long. For a particular specified susceptance value, the diameter ratio and electrical length of the tuning stub are found from Figs. 1, 2, or 3, depending upon what stub configuration has been chosen. From Fig. 4, a factor which will permit the determination of the minimum value of conductance can be obtained. From this, the losses in the stub may be evaluated.

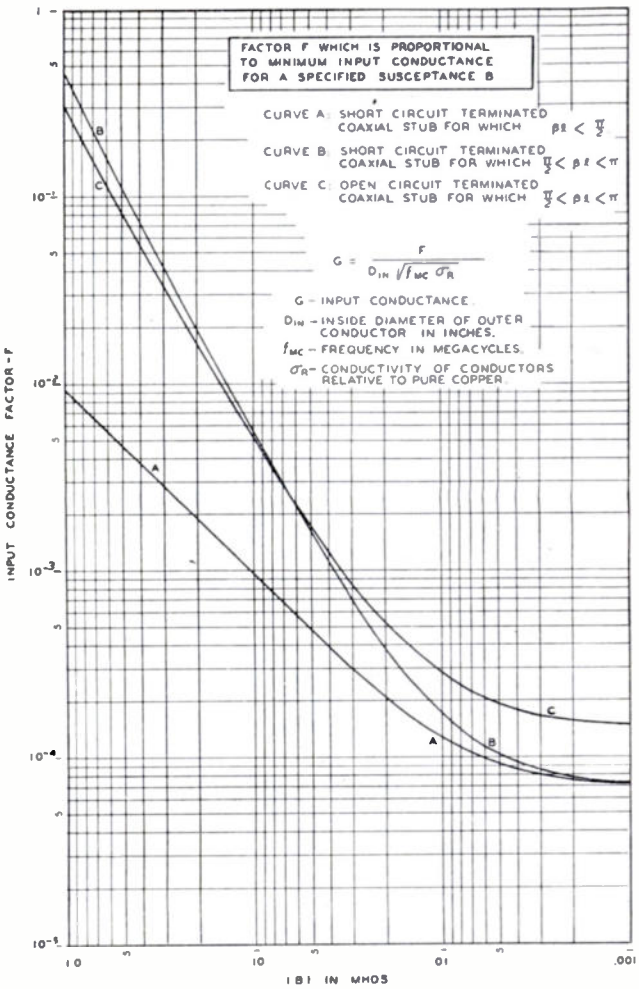

Fig. 1—Diameter ratio and effective length of short-circuit terminated coaxial stub having minimum conductance for a specified susceptance. $\beta l < (\frac{\pi}{2})$.

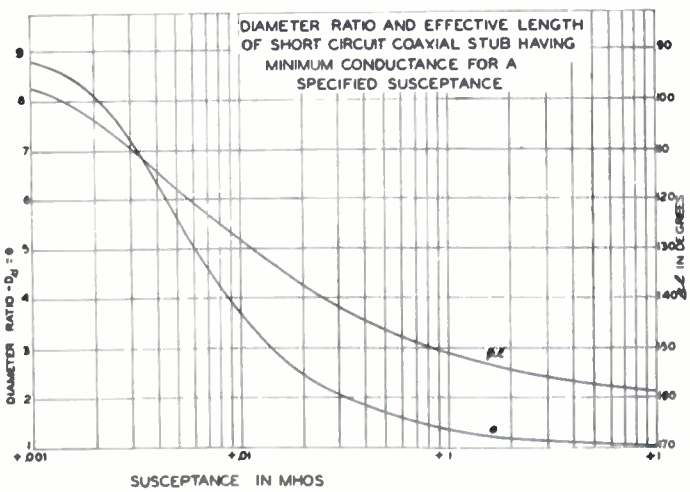

Fig. 2—Diameter ratio and effective length of short-circuit terminated coaxial stub having minimum conductance for a specified susceptance. $(\pi/2) < \beta l < \pi$.

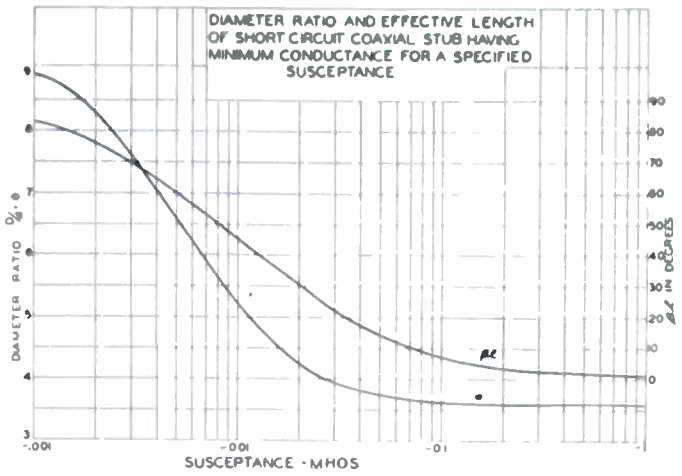

Fig. 3—Diameter ratio and effective length of open-circuit terminated coaxial stub having minimum conductance for a specified susceptance, $(\pi/2) < \beta l < \pi$.

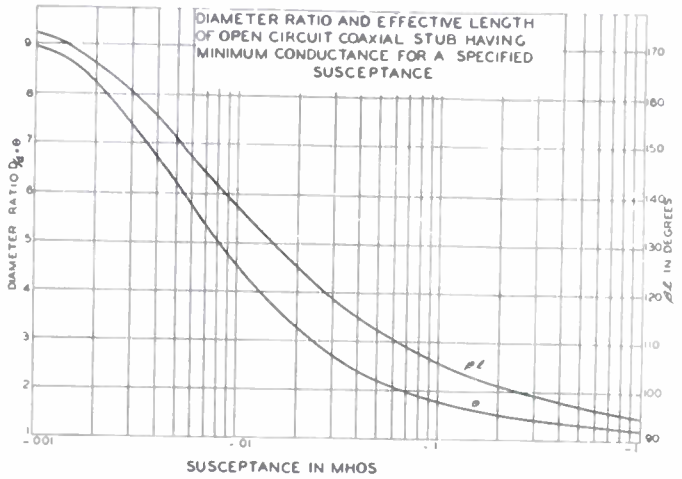

Fig. 4—Factor F which is proportional to the minimum conductance of a short- or open-circuit terminated coaxial line stub when the input susceptance B is specified.

It will be noticed that no curves are shown for open circuit terminated tuning stubs less than a quarter wavelength long. In this case, the losses can be made as small as desired by letting the diameter ratio approach unity. This process is usually limited by voltage gradient considerations or mechanical considerations. This is the only situation in which no minimum value for the loss will be found.

In order to make the use of these curves more clear, two examples involving their use will be worked out here.

Example 1: It is desired to construct a short circuit terminated coaxial line tuning stub having an input reactance of 100 ohms so that it shall have the least input resistance possible. It is desired further that this stub be less than one-quarter wavelength long. The operating frequency is to be 100 mc per second, and the conductors will be constructed of copper, the inside diameter of the outer conductor being 1.527 inches. Referring to Fig. 1, it is seen that the diameter ratio of the stub should be 5.23 and that the electrical length of the stub should be 45.2 degrees. Therefore, the outer diameter of the inner conductor should be 0.292 inches, and the length of the stub should be 14.83 inches since a wavelength at a frequency of 100 mc is equal to 118 inches.

In order to evaluate the losses of this stub, the input resistance may be found from the curve in Fig. 4. In referring to this figure, it is found that F is equal to 1.26×10^{-4} for this case, and when the formula shown in Fig. 4 is applied, it is found that the resistance is equal to 0.083 ohms. The energy dissipated in the stub may be found directly by multiplying the resistance by the square of the current flowing into the stub.

It might be of interest to know just how large an increase in losses might be incurred if some other diameter ratio than the optimum value were to be chosen. In order to show this, the curve of Fig. 5 has been plotted showing the input resistance of a coaxial line tuning stub with a reactance of 100 ohms as a function of the diameter ratio. As may be seen, the curve is quite sharp, and if for any reason the diameter ratio is decreased to as low a value as 2.0, the losses in the stub will be doubled.

Example 2: It is desired to construct an open-circuit terminated coaxial-line tuning stub having an input susceptance of -0.1 mhos, so that it shall have the least input conductance possible. It is desired further that this stub be greater than one-quarter wavelength long but that it be less than one-half wavelength long. The operating frequency will be 100 mc per second, and the conductors will be constructed of copper, the inside diameter of the outer conductor being 1.527 inches.

Referring to Fig. 3, it is seen that the correct diameter ratio is 1.78 and that the electrical length of the stub should be 106.1 degrees. Therefore, the outer diameter of the inner conductor should be 0.858 inches, and the length of the stub should be 34.8 inches since a wavelength is equal to 118 inches at this frequency. The actual length will be somewhat less than this figure due to capacity end loading of the stub.[11] In this case, capacity end loading will serve to decrease the length by about 0.26 inches.

In Fig. 4, it is seen that the factor F is equal to 0.0051 so that using the formula shown on the figure, the input conductance of this stub is 334 micromhos. The loss can be easily calculated from this by multiplying the input conductance by the square of the applied voltage.

The behavior of the input conductance of a stub of this type for other diameter ratios is shown in Fig. 6 where the input conductance of an open-circuit terminated coaxial-line tuning stub is plotted for various diameter ratios under the conditions stated for this example. It is seen that the minimum in this case is much broader than that shown in Fig. 5.

C. *Limitations Imposed by Non-zero Impedance Metal Short Circuiting Disks and by End Loading of Open-Circuit Terminated Transmission Lines.*

As was mentioned above, when it is attempted to

[11] J. R. Whinnery, H. W. Jamieson, and T. E. Robbins, "Coaxial-Line Discontinities," PROC. I.R.E., vol 32, pp 695–709; November, 1944.

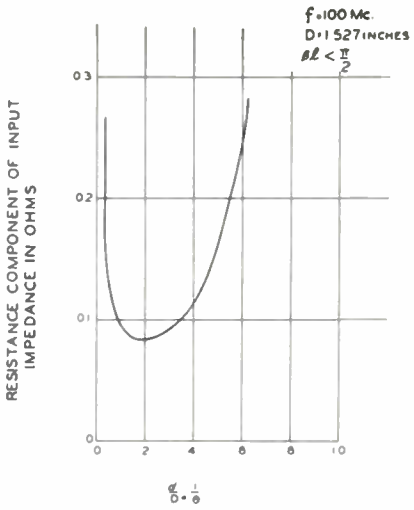

Fig. 5—Input resistance of coaxial line short-circuit terminated having an input reactance of 100 ohms plotted against diameter ratio.

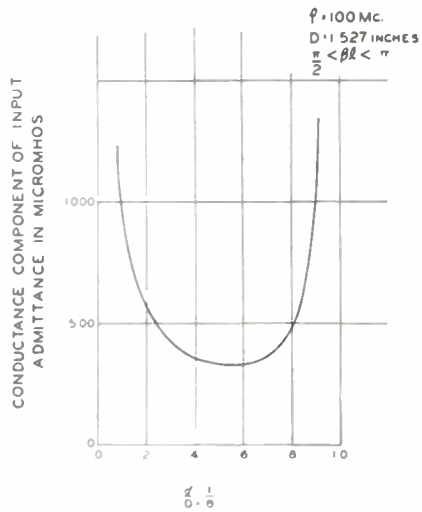

Fig. 6—Input conductance of coaxial line open-circuit terminated having an input susceptance of −0.1 mhos plotted against diameter ratio.

open circuit a length of coaxial transmission line by simply terminating the inner conductor it is found that an end capacity of the inner conductor exists and this operates to reduce the length of inner conductor necessary for a specified susceptance or reactance. This end capacity is due to the fact that it is impossible to satisfy the boundary conditions in the neighborhood of a discontinuous inner conductor in a coaxial transmission line with the TEM mode alone. This problem has been successfully solved.[11] It was found that the effect of a discontinuous inner conductor could be represented by a capacity termination at the plane of the discontinuity, and values of this discontinuity capacity have been tabulated. At first thought, it might seem that this shortening of the inner conductor would appreciably affect the accuracy of (2). It will affect the imaginary term of this equation as pointed out above, but the real term will be affected only in a minor way. This is due to the fact that the currents in the neighborhood of an open-circuit termination of the inner conductor are very small so that the losses associated with these currents are also small, and the change of length of the inner conductor by a small amount will not affect the total losses an appreciable amount in most practical cases.

In the case of short-circuit terminated coaxial tuning stubs, a different type of effect operates to make equations derived on the basis of lossless shorting disks not exactly correct. A short-circuiting plug in a coaxial line must always have some finite nonzero impedance. In the case of shorting plugs constructed of good conductors, this impedance will be very small and will consist of equal parts of resistance and inductive reactance.[12] Analysis shows that the effect of the reactive component is extremely small, and may be neglected for most purposes. The effect of the resistance component on the other hand is appreciable, but in most cases, it is small enough to be neglected.[5] In the case of Example 1 previously worked out, the losses with a copper shorting plug are about 2.3 per cent greater than those with a fictitious perfectly conducting shorting plug.

IV. Conclusion

A design procedure has been devised by which it is possible to design a coaxial transmission-line tuning stub for minimum energy dissipation when the reactance or the susceptance is specified. The results have been presented in curve form in order that they may be easily utilized in design. Although the design procedure has been discussed in detail only for coaxial transmission-line tuning stubs, a similar procedure could be carried out for any transmission system in which an analytical expression for the input admittance or impedance was available.

By the use of this design procedure, filter elements constructed of coaxial transmission-line sections are designed for maximum efficiency. This is an important consideration in present-day applications at very-high frequencies and ultra-high frequencies where high continuous powers are being used.

V. Acknowledgment

The author wishes to express his appreciation to Owen O. Fiet of the Broadcast Engineering Section, RCA Victor Division, for his suggestion of the topic of this paper, and for his advice and criticism. He also wishes to acknowledge with thanks the suggestions of other associates at the RCA Victor Division.

VI. Appendix

Since (2) is at odds with some equations for the same quantity that have previously appeared in the literature, some comment may be called for. It was at one time common practice to assume the characteristic impedance of low-loss high-frequency transmission lines a completely real number for the purpose of computing losses. That this assumption leads to erroneous results has recently been pointed out by Nergaard and Salz-

[12] Simon Ramo and J. R. Whinnery, "Fields and Waves in Modern Radio," John Wiley & Sons, Inc., New York, N. Y., pp. 248–254, 270–273, 332; 1944.

berg.[4] Their experimental results are of particular interest. Equation (2) was derived without assuming the characteristic impedance real.[4,5] Following is a list of approximate equations for the input admittance of open-circuit terminated and short-circuit terminated transmission-line sections which are valid when the dielectric loss is small compared to the copper loss. These equations may be derived from the general expressions for the input admittance of a transmission-line section, or, alternately, they may be derived by computing the currents flowing on the transmission-line section under the assumption of no losses and then finding the losses by integration.

For a short-circuit terminated transmission line off resonance,

$$Y = Y_0\left\{\alpha l\left[\csc^2\beta l + \frac{\cot\beta l}{\beta l}\right] - j\cot\beta l\right\}. \qquad (14)$$

For an open-circuit terminated transmission line off resonance,

$$Y = Y_0\left\{\alpha l\left[\sec^2\beta l - \frac{\tan\beta l}{\beta l}\right] + j\tan\beta l\right\}. \qquad (2)$$

For a short-circuit terminated transmission line at series resonance

$$Y = \frac{Y_0}{\alpha l}, \qquad (15)$$

while at antiresonance

$$Y = Y_0\alpha l. \qquad (16)$$

For an open-circuit terminated transmission line at series resonance and antiresonance, the same equations apply as for the short-circuit terminated transmission line.

"Application of Correlation Analysis to the Detection of Periodic Signals in Noise"*

Y. W. LEE, T. P. CHEATHAM, JR., AND J. B. WIESNER

N. Marchand,[1] M. Leifer,[2] and H. R. Holloway:[3] In the recent timely paper entitled "Application of correlation analysis to the detection of periodic signals in noise," by Y. W. Lee, T. P. Cheatham, Jr., and J. B. Wiesner, several controvertible statements appeared. Because of the importance of this subject and the consequent possibility that the reader might easily arrive at erroneous conclusions, we feel that these several statements should be amplified.

The statement was made that "Theoretical considerations show that a periodic signal masked by random noise can be detected by autocorrelation however small the signal may be." The paper continued to say (and truly so) that this possibility requires an infinite amount of observation time, among other things. But this is hardly enough! Actually, the noise power per unit bandwidth should be less than the total received energy, and, unless merely a negligible amount of information is to be obtained from the system, the total received energy should be large compared with the noise power per unit bandwidth.[4]

In Section IV of the paper, "Remarks," this statement is made: "It is well to emphasize that theoretically no claim can be made that the method of correlation is superior to conventional filtering in the frequency domain in the sense of accomplishing in the time domain what is impossible in the frequency domain." The reader is led to believe that the phrase "conventional filtering" actually means filtering a signal function by means of a truly conventional low-pass filter, or band-pass filter, or high-pass filter. The phrase "conventional filter" as used by the authors is not the correct term. It refers, actually, to the particular, special filter of D. O. North[5] which was further shown by Van Vleck and Middleton[6] to be a comb filter whose amplitude variation is equivalent to that of the signal spectrum, and whose phase characteristic is the conjugate of the signal spectrum line phase. This is by no means a conventional

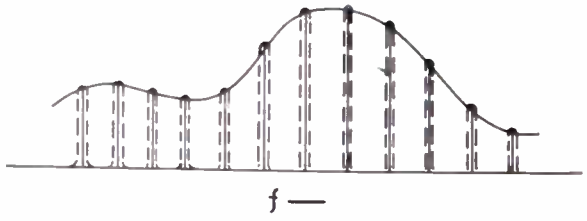

filter! Referring to Fig. 1, this comb filter must separate each spectrum line individually, while leaving all the other spectrum components completely undisturbed. In other words, for each spectrum line, the filter must have a gain of cA_k and a phase response $j(\phi - \phi_k)$, where c is a constant, A_k represents the amplitude of the spectrum line, ϕ_k represents the phase of this spectrum line which in the general case is different for each spectrum line, and ϕ represents a delay factor common to all the filters. No means is known to us of designing and building such

* Proc. I.R.E., vol. 38, pp. 1165–1171; October, 1950.
[1–3] Sylvania Electric Products Inc., Bayside, L. I., N. Y.
[4] P. M. Woodward and I. L. Davies, "Theory of radar information," *Phil. Mag.*, vol. 41, pp. 1008–1009; October, 1950.
[5] D. O. North, "Analysis of Factors which Determine Signal-Noise Discrimination in Pulsed Carrier Systems," unpublished report PTR-6C, RCA, Princeton, N. J.; June 25, 1943.
[6] J. H. Van Vleck and David Middleton, "A theoretical comparison of the visual, aural and meter reception of pulsed signals in the presence of noise," *Jour. of Appl. Phys.*, vol. 17, pp. 940–971; November, 1946.

a filter, and a little reflection will show that such a filter would present extreme difficulty for conventional signals. The term "conventional filtering" should not have been used here, since correlation methods do give superior results to those obtainable by truly conventional filtering in the frequency domain.

Further, in order to make this work useful for a communications system, one must take due regard of the modified Hartley law. It seems quite evident that the sampling method of correlation does not make efficient use of the time parameter, and therefore the gain in signal-to-noise ratio is not efficiently achieved.

The exact gain using cross correlation when the frequency of the signal is known may be given quantitatively in a form which has more direct physical meaning than the forms previously presented. This will be done in a paper that has been submitted for presentation to the 1951 IRE National Convention. It can be shown that efficient use of the cross correlation approach gives a signal-to-noise ratio equivalent to that obtainable with a continuous-wave nonmodulated signal of equivalent noise bandwidth and signal power input to the receiver.

Y. W. Lee,[7] T. P. Cheatham, Jr.,[8] and J. B. Wiesner:[9] The discussion of Marchand, Leifer, and Holloway first concerns our statement: "Theoretical considerations show that a periodic signal masked by random noise can be detected by autocorrelation however small the signal may be. However, the theoretical possibility requires, among other things, an infinite time for observation." Marchand, Leifer, and Holloway agree that an infinite amount of observation time is necessary but say that "this is hardly enough!" It should be noted that, as quoted above, we do not even imply that it is enough. The statement of Woodward and Davies cited by Marchand, Leifer, and Holloway to the effect that "noise power per unit bandwidth should be less than the total received energy . . ." is amplification of our statement but does not contradict it, since noise power per unit bandwidth is independent of time, while energy received increases with time of observation. We fail to see that the statement concerned is "controvertible."

The discussion then concerns the use of the phrase "conventional filtering" in the statement: "It is well to emphasize that theoretically no claim can be made that the method of correlation is superior to conventional filtering in the frequency domain in the sense of accomplishing in the time domain what is impossible in the frequency domain." The phrase "conventional filtering" refers to filtering on the basis of the spectrum concept as it is done in classical wave-filter theory; it does not include the special filter of North, which is however a special form of a frequency domain filter.

The special filter is the result of maximization of the ratio of the square of the magnitude of *a single pulse* which has passed through the filter to the mean square value of a white noise through the same filter. Since the spectrum of a single pulse is *continuous* and overlaps the *continuous* noise spectrum, a maximization problem exists. The result of the problem is that the filter should have an amplitude spectrum the same as that of the pulse and a phase spectrum equal to the conjugate of that of the pulse. All spectrums are continuous. This is the North filter.

It is not known to us how the maximization problem may be extended to the case of a *periodic* signal with a *discrete* spectrum corrupted by a random noise with a *continuous* spectrum with the result that the filter should have the comb shape as illustrated in Fig. 1. Even if this is the correct extension, it does not seem to be a unique solution. For while the pulse-to-noise ratio is finite in the North filter, the periodic-signal-to-noise ratio in the present case has a theoretical maximum of infinity which may be achieved by a theoretical filter of the conventional type. The filter is a multiband-pass filter with an amplitude characteristic in the shape of a comb of *uniform* height (unity) for preserving uniformly the harmonics of the signal. Each band is centered about a harmonic of the signal and the bandwidth may be made negligibly small. Obviously any finite rms signal-to-noise ratio, however large, may be attained by narrowing the bandwidths. This theoretical filter is of the conventional type, quite different from the North filter for a different situation whose theory involves the use of calculus of variations or of the Schwarz inequality in a maximization problem, which does not lead to a trivial solution.

The remainder of the remarks of Marchand, Leifer, and Holloway primarily concerns work to be presented at the 1951 IRE National Convention. In our opinion the discussion of this work should take place when it is presented.

N. Marchand,[1] M. Leifer,[2] and H. R. Holloway:[3] Inasmuch as the principal issue of these discussions is the comparative use of "conventional filters" as opposed to statistical methods for the recognition of periodic radio signals, the following will confine itself to the second part of the reply by Lee, Cheatham, and Wiesner. We agree with their description of the *special filter* of North and Van Vleck and Middleton, but we cannot follow the distinction which is made between this filter and a conventional filter in the penultimate paragraph of the reply. It may clarify matters if now it is noted that no realizable periodic signal is truly periodic nor does it have a discrete line spectrum. The uncertainty in the phase of the signal ordinarily represents the information which is sought in periodic radio systems, which might therefore make it more appropriate to refer to such systems as "almost periodic." Further, no practical system will permit of an infinite time for observation, which means that the signal spectrum cannot be of the *line* type. From these two statements we have the conclusions that neither the receiver nor the signal will permit consideration of an infinitely narrow bandwidth, and

[7-9] Massachusetts Institute of Technology, Cambridge, Mass.

that such simplification, even for theoretical purposes, is questionable. Accordingly, it would appear that the maximization procedure is the same for both the single pulse or the *almost-periodic* signal, resulting in a filter of the form described in our previous discussion. Finally, it seems to be agreed that such a filter is not of the conventional type.

Y. W. Lee,[7] T. P. Cheatham, Jr.,[8] and J. B. Wiesner:[9] To keep the main issue in the foreground, let it be emphasized that these discussions primarily concern two statements of ours (as quoted in our reply) which Marchand, Leifer, and Holloway claim to be the "several controvertible statements" appearing in the paper.

The validity of the first statement is not challenged after our reply. We conclude, therefore, that it is not controvertible.

With respect to the second statement, Marchand, Leifer, and Holloway do not disagree that the conventional filter described in the penultimate paragraph of our reply will theoretically achieve as much as a correlator in signal-to-noise ratio improvement. However, they do not follow the distinction between this filter and the North filter. We believe that the distinction between them has been made clear in our reply. To repeat for their benefit, the comb-shaped filter with teeth of *uniform* height (the reason for this shape has been given) has been conceived solely through the spectrum concept of classical wave filter theory which we have referred to as conventional filter theory. The theory of the North filter involves a maximization problem, and, in its original form, does not include a periodic signal. Furthermore, the amplitude characteristic of such a filter is not the same as that of the conventional filter we have described. In view of these facts, we believe that the second statement under discussion holds true, and that it has not been shown to be controvertible.

Having justified the statements with which these discussions are primarily concerned, we should like to comment on the latter part of the second discussion of Marchand, Liefer, and Holloway. This part of the discussion relates to the derivation of the comb filter characteristic they gave in the figure. They state that "no realizable periodic signal is truly periodic nor does it have a discrete line spectrum" and that since "no practical system will permit of an infinite time for observation . . . the signal spectrum cannot be of the line type." They further state that the assumption of infinitely narrow bandwidth "even for theoretical purposes is questionable." Accordingly, they say that by application of the North filter theory, the comb filter characteristic, as illustrated, is obtained for use with "almost-periodic" signals.

But, turning back to their original description of the same filter characteristic, we find several statements in which the term "spectrum line" is used. For instance, they say "Referring to Fig. 1, this comb filter must separate each spectrum line individually. . . . In other words, for each spectrum line, ..." There are other references to spectrum lines in the same paragraph.

From these statements of Marchand, Leifer, and Holloway, it is clear that in describing their comb filter for the first time they accepted the line spectrum concept, but later in the second discussion of the same filter they rejected this concept "even for theoretical purposes." The apparent self-contradiction has thrown their explanation of the illustrated comb filter into utter confusion. These observations are actually of no great importance as far as the main issue is concerned, but we feel that in the interest of fruitful discussion, one should avoid vacillating between acceptance and rejection of a given concept.

Contributors to Proceedings of the I.R.E.

George M. Anderson (A'45) was born in Rochester, Pa. in 1921. He received the B.S. degree in electrical engineering in 1942 from Carnegie Institute of Technology.

G. M. Anderson

From 1943 to 1946, he served as an officer in the Signal Corps. He returned to Carnegie Tech in 1946 and completed the work toward the Doctor of Science degree in 1948.

Dr. Anderson is at present assistant professor of electrical engineering at Carnegie Tech.

Dr. Anderson, in addition to his affiliation with I.R.E., is a member of Eta Kappa Nu and Sigma Xi.

❖

Harry A. Augenblick, Jr. (A'48) was born on July 21, 1926, at South Orange, N. J. He received the B.S. degree in electrical engineering from Massachusetts Institute of Technology in 1946.

H. Augenblick, Jr.

On graduation, he joined Federal Telephone and Radio Corporation, transferring later to Federal Telecommunication Laboratories, where he worked on microwave antennas and components. In 1950, he founded the firm Microlab, where he is presently engaged in the design and production of microwave components and test equipment.

Mr. Augenblick is a member of Sigma Xi.

R. L. Bell was born on September 5, 1924, in Alnwick, England. He received the B.Sc. and Ph.D. degrees at Durham University in electrical engineering in 1945 and 1948, respectively. He was associated with the Research Laboratories, General Electric Company, Ltd. Wembley, England, engaged in research on receiving-tube development, during the period from 1948 to 1950.

R. L. Bell

Dr. Bell is presently in the Services Electronics Research Laboratory, Baldock, England, where he is devoting his time to work on microwave gas discharge and noise problems.

Contributors to Proceedings of the I.R.E.

Sidney B. Cohen (A'47) was born in New York, N. Y., in 1922. He received the B.S. degree in electrical engineering from the College of the City of New York in January, 1943. From 1943 to 1945, he was a staff member at the Radiation Laboratory of the Massachusetts Institute of Technology, engaged in development of electronic circuitry and computers.

SIDNEY B. COHEN

In 1945 Mr. Cohen joined the Sperry Gyroscope Company. From 1947 to 1949, he was the recipient of a Sperry Graduate Scholarship award which enabled him to pursue daytime studies toward the D.E.E. degree, after having completed the requirements for the M.E.E. degree.

At Sperry, Mr. Cohen has been engaged in the development of electronic circuitry and magnetic amplifiers in automatic-control systems. He is a member of Eta Kappa Nu.

❖

Murlan S. Corrington (SM'49) was born on May 26, 1913, in Bristol, S. D. He received the B.S. degree in electrical engineering in 1934, from the South Dakota School of Mines and Technology, and the M.Sc. degree in 1936, from Ohio State University. From 1935 to 1937, he was a graduate assistant in the physics department of Ohio State University. In 1937 he joined the Rochester Institute of Technology, where he taught mathematics, mechanics, and related subjects.

M. S. CORRINGTON

Since 1942, Mr. Corrington has been engaged in mathematical engineering in the advanced development section of the RCA Victor Division, Radio Corporation of America, at Camden, N. J. Mr. Corrington is a member of Sigma Pi Sigma, the Acoustical Society of America, and is on the Sound Recording and Reproducing Committee.

❖

No material on JOHN T. FLECK was available. Therefore, his biography does not appear.

Robert M. Goodman (S'42–A'45) was born in Philadelphia, Pa., on November 21, 1920. He received the B.S. degree in electrical engineering from the Moore School of Electrical Engineering, University of Pennsylvania, in 1943. He joined the Hazeltine Electronics Corporation the same year, where he was engaged in the development of IFF equipment and special instrumentation. In 1947 Mr. Goodman returned to the University of Pennsylvania as a graduate student and a member of the research division of the Moore School. He has been associated with guided missile research and digital and analog computer design. Since 1949, he has been associated with the development of special computer devices.

R. M. GOODMAN

❖

Richard Guenther (M'49) was born in Lodz, Poland, on September 9, 1910. He received his higher education from the Technische Hochschule in Danzig, specializing in electrical communications, and graduating in 1934 with the degree of Dipl. Ing. From 1934 to 1937, he served as research assistant at the same institution and was awarded the degree of Dr. Ing. in 1937. He then joined the Central Laboratory of Siemens and Halske Company, in Berlin, Germany, where he was first in charge of the development of carrier telephone equipment for radio links.

RICHARD GUENTHER

In 1941 Dr. Guenther was placed in charge of the engineering department for radio communication and remote control systems of the Siemens and Halske Company. He did consulting work for various institutions in Berlin during the period 1945 until 1947, when he came to the United States. At that time he was invited to enter into a contract with the U. S. Signal Corps, attached to the Signal Corps Engineering Laboratories at Fort Monmouth, N. J. In this capacity he acts as consultant to various branches of this agency.

❖

Marshall C. Kidd was born on April 11, 1923, in Columbus, Ohio. He received the B.Ch.E. degree from Ohio State University in 1944. He worked at the Bakelite Corporation from 1944 to 1945, and in 1945 entered the electronics field with the Allen B. DuMont Laboratories.

MARSHALL C. KIDD

In 1946 Mr. Kidd returned to Ohio State University and received the B.E.E. degree in 1948. Since then, he has been in the advanced development section of the home instrument department of the RCA Victor Division at Camden, N. J. Mr. Kidd is currently engaged in work with loudspeakers and high-fidelity audio systems.

❖

Ralph W. Klopfenstein (S'44–A'46–M '50) was born on June 3, 1923, in Aberdeen, S. Dak. He was graduated from the University of Washington in 1944, with the B.S. degree in electrical engineering. He served with the United States Navy from July, 1943, through July, 1946 as a radio materiel officer aboard the U.S.S. *Henry W. Tucker*.

R. W. KLOPFENSTEIN

Mr. Klopfenstein pursued graduate study in physics at the South Dakota School of Mines during 1946, remaining as an instructor for the term 1947–1948. Following this, he was employed by the RCA Victor division, in Camden, N. J., in 1948, where he worked in advanced development of television and FM transmitting antennas and filters, continuously, until September, 1950. He is now on leave of absense from RCA Victor Division in order to engage in graduate study in mathematics at the Iowa State College. He is an associate member of Sigma Xi.

❖

William A. Lynch (A'44) was born in Brooklyn, N. Y., on July 11, 1904. He received his undergraduate degree at the Polytechnic Institute of Brooklyn in 1925. After a brief association with the Long Lines Division of the American Telephone and Telegraph Company, he joined Alonzo K. Lynch, Inc., a Brooklyn corporation. Upon the death of his father in 1929, he became its president.

W. A. LYNCH

Contributors to Proceedings of the I.R.E.

In 1942, after completing the radio and television technology courses at the RCA Institutes, Mr. Lynch joined the staff of the Department of Electrical Engineering of the Polytechnic Institute of Brooklyn. In 1944 he was appointed technical manager of the newly-formed P. I. B. Products Inc., of Brooklyn. This company was established to produce precision microwave measurement equipment, which had been developed by the research group of the Microwave Research Institute, under the direction of Dr. Ernst Weber.

At the close of the war, the company became the Polytechnic Research and Development Corp., where Mr. Lynch remained for two years as a staff member. In 1947 he rejoined the faculty of the Polytechnic. In 1948 he received his M.E.E. and later that year was appointed associate professor of electrical engineering. He currently directs the curriculum in communications and electronics.

Professor Lynch is a member of Sigma Xi and Eta Kappa Nu.

❖

Warren E. Mathews (S'43–A'46) was born in Osborne, Kan., on November 10, 1921. He received the B.A. degree from Ohio Wesleyan University in 1942, and the B.S. and M.S. degrees in electrical engineering from the Massachusetts Institute of Technology in 1944. He served overseas with the Signal Corps during the following two years. From 1946 to 1948, he was a member of the technical staff of the Bell Telephone Laboratories, Inc., engaged in research work on broad-band microwave amplifiers. It was during this time that the study described in this issue was carried out. Since 1949, Mr. Mathews has been engaged in graduate work toward the Ph.D. degree in physics, as a Howard Hughes Fellow at the California Institute of Technology.

W. E. Mathews

Mr. Mathews is a member of the American Physical Society, Tau Beta Pi, Phi Beta Kappa, Sigma Pi Sigma, and Pi Mu Epsilon, and also holds associate membership in Sigma Xi.

❖

Sidney Millman (A'48–SM'48) was born on March 15, 1908, in Russia. Fourteen years later he came to the United States and became a naturalized citizen. In 1931 he was graduated from City College of New York with the B.S. degree in physics. He received A.M. and Ph.D. degrees from Columbia University, 1932 and 1935, respectively. Holding the Tyndall Fellowship in 1935–1936, and the Barnard Fellowship the following year. Dr. Millman spent most of his time in research at Columbia, his special interests being nuclear spins and magnetic moments, using molecular beam methods. In 1939 he taught at the College of the City of New York, and two years later at Queens College in New York. From 1942 to 1945, he was associated with the Columbia Radiation Laboratory, under the auspices of the Office of Scientific Research and Development. He joined the staff of Bell Telephone Laboratories, Inc., in 1945, where he engaged in electron dynamics research. Currently, he is studying traveling-wave amplifiers for millimeter waves.

Sidney Millman

Dr. Millman was elected to Phi Beta Kappa and Sigma Xi. He is a member of a subpanel on rf tubes for the Government Research and Development Board, and he is a Fellow of the American Physical Society.

❖

Philip F. Ordung (S'40–A'43–M'48–SM'49) was born on August 12, 1919, in Luverne, Minn. He received the B.S. degree in electrical engineering from South Dakota State School of Agriculture and Mechanic Arts in 1940, and the degrees of M.Eng. and D.Eng. from Yale University in 1942 and 1949, respectively.

Philip F. Ordung

Dr. Ordung has been on the electrical engineering staff at Yale since 1942, with the exception of the period 1944–1945 when he was employed by the Naval Research Laboratory in connection with the development of radar modulators. He has the rank of assistant professor at Yale and is currently engaged in undergraduate instruction, graduate instruction in network synthesis, and in research in pulse communications for the U. S. Signal Corps. Dr. Ordung has been the author of numerous papers in network synthesis, pulse communications, and power machinery.

He is a member of the Circuits Committee of the IRE and a member of the American Institute of Electrical Engineers.

❖

R. K. Potter (A'25–M'26–F'41) was born in Elgin, Ill., on October 1, 1894. He was graduated from Whitman College in 1917, with the B.Sc. degree. The next two years were spent with the Artillery Corps of the United States Army, after which he attended Columbia University, receiving the E.E. degree in 1923. He then joined the development and research department of American Telephone and Telegraph Company, where his work concerned the field of radio transmission. He transferred with this department to the Bell Telephone Laboratories, Inc., in 1934, where studies of distortion in radio transmission and of speech "secrecy" methods led to an interest in the structure of speech itself. Mr. Potter has originated various sound portrayal techniques, one product of which is the Visible Speech device.

R. K. Potter

In his present position, Mr. Potter has, under his supervision, acoustics research and studies of modulating systems, including pulse-code modulation.

❖

William Sichak (M'46) was born on January 7, 1916, at Lyndora, Pa. He received the B.S. degree in physics from Allegheny College in 1942.

From graduation until near the end of 1945, he was with the Radiation Laboratory at Massachusetts Institute of Technology. He then joined the staff of Federal Telecommunication Laboratories, where he is now a department head in the radio and radar components division, and has been active in the microwave field.

William Sichak

Mr. Sichak is a member of the American Physical Society.

❖

Contributors to Proceedings of the I.R.E.

Jerome R. Steen (A'24–M'36–SM'43–F'50) was born on June 29, 1901, at West Bloomfield, New York. He attended the University of Wisconsin, where he received the B.S. degree in electrical engineering in 1923. Mr. Steen was connected with the General Electric Company, the Grigs-by-Grunow Company, and Bell Telephone Laboratories, Inc., before joining Sylvania Electric Products, Inc., in 1931, as supervisor in charge of finished-tube quality control at the Emporium, Pennsylvania, radio-tube plant. In 1936, his work was expanded to include similar activities at the Salem, Massachusetts radio-tube plant. In 1942, he was transferred to the commercial engineering department, and in 1944, was appointed manager of the quality control engineering department of the radio-tube division. On September 1, 1946, Mr. Steen was appointed to the newly created position of director of quality control for Sylvania Electric Products, Inc., the position he now holds.

JEROME R. STEEN

Mr. Steen is a fellow of the American Society for Quality Control and a member of the American Institute of Electric Engineers, the Illuminating Engineering Society, the Institute of Mathematical Statistics, the American Statistical Association, and the Radio Club of America.

❖

Jan J. Vormer was born in The Hague, Holland, on October 24, 1901. He received the degree of electrotechnical engineer from the Technical University at Delft, Holland, in 1925. In the same year, he was appointed an engineer of the Netherlands Postal and Telecommunication Services at the Radio Laboratory in The Hague.

JAN J. VORMER

Mr. Vormer was named chief engineer of the Radio Laboratory in 1941, and in 1943 he was made Chief, which is his present position.

John E. Walsh (M'50) was born in Lenox, Mass., on November 14, 1917. He received the A.B. degree from Saint Michael's College in Vermont in 1938, and the M.A. degree from Boston University in 1940. After further graduate study, he taught mathematics at Northeastern University. He left in 1943 for service in the Navy as a navigation instructor and as an electronics officer, until the beginning of 1946. Mr. Walsh then joined the staff of the Antenna Laboratory at the Air Force Cambridge Research Laboratories, where he has been since that time. He is also an instructor in mathematics at Lincoln Technical Institute.

JOHN E. WALSH

❖

Alvin M. Weinberg was born in Chicago, Ill., on April 20, 1915. He received the A.B. degree in 1935, the M.S. in 1936, and the Ph.D. in 1939, all from the University of Chicago. During the period 1939 to 1941, he was an assistant in mathematical biophysics at Chicago, until his appointment as a physicist at the Metallurgical Laboratory of the University, from 1941 until 1945.

A. M. WEINBERG

Dr. Weinberg was made a member of the staff of the Clinton Laboratories at Oak Ridge, Tenn., in 1945, and became acting Director of the Physics Division of the Oak Ridge National Laboratory in 1947. On March 1, 1948, he was appointed full-time Director, and in December, 1948, assumed the position of Research Director of the Laboratory, his present title. Dr. Weinberg's special fields of interest include mathematical biophysics, nuclear energy, and the mathematical theory of nerve function.

❖

William A. Whitcraft, Jr. (S'47–A'48) was born on April 2, 1917, in Cambridge, Ohio. He received the A.B. degree in music from Harvard College in 1939, and the M.S. degree in communication engineering from Harvard University in 1947. From 1941 to 1946 he served in the Armed Forces, spending two years in the south and southwest Pacific, first as a ground radar officer and later as the IFF officer and assistant air radar officer of Headquarters, 13th Air Force.

W. WHITCRAFT, JR.

Since June, 1947, Mr. Whitcraft has been with the Raytheon Manufacturing Company of Waltham, Mass., engaged in the engineering research and development activities of that company on various Government contracts. The work has included pulse-handling circuit techniques, antennas, and problems of wave propagation in the high-frequency band.

❖

For a biography and photograph of EVERARD M. WILLIAMS, see page 1220 of the October, 1950, PROCEEDINGS OF THE I.R.E.

❖

Nicholas Yaru (S'47) was born in Canton, Ohio, on November 8, 1923. He received the B.S. degree in electrical engineering from Carnegie Institute of Technology in 1944. He was employed by E. I. DuPont and Company during the period 1944 to 1946, in the industrial engineering division.

In 1946, Mr. Yaru received an appointment to the electrical engineering research staff at the University of Illinois, where he has since been engaged in study, along with research work. He received the M.S. degree in electrical engineering in 1948, and is at present continuing his work and study at the University of Illinois. He is a member of Eta Kappa Nu and Sigma Xi.

NICHOLAS YARU

Institute News and Radio Notes

Professional Group Notes

The Professional Group Manual has been revised, and the new edition will be available within a short time. The revised version is currently being reviewed by the Professional Groups Committee.

The **IRE Professional Group on Vehicular Communications** will hold its annual conference at the Sheraton Hotel, Chicago, Ill., on October 25 and 26; Eugene S. Goebel is serving as Chairman of the Committee on Arrangements. This Group meeting will dovetail with the National Electronics Conference scheduled for October 22–24, and with the Radio and Television Manufacturers' Association meeting on October 27, which will complete a full week of electronic activities.

On July 10 the Constitutions of the **IRE Professional Groups on Airborne Electronics** and **Broadcast Transmission Systems** were approved by the Executive Committee.

There will be a joint meeting of the U. S. National Committee of the URSI and the **IRE Professional Group on Antennas and Propagation** on October 8, 9, and 10, at Cornell University, Ithaca, N. Y.

An Administrative Committee meeting of the **Professional Group on Information Theory** was held at IRE Headquarters on September 13. Membership rolls are now open, and interested persons should contact L. G. Cumming, Technical Secretary, for information.

The Professional Group on Instrumentation has reelected Ernst Weber of the Polytechnic Institute of Brooklyn as its Chairman. Also serving from July 1, 1951, to June 30, 1952, are I. G. Easton of the General Radio Co., Cambridge, Mass., Vice-Chairman, and H. J. Carlin of the Polytechnic Institute of Brooklyn, Secretary-Treasurer. Samuel N. Alexander has been elected to membership in the Group's Administrative Committee for a three-year-term, as substitute for H. S. Knowles. The Administrative Committee also voted to participate actively in the organization of a second symposium on "Improved Quality Electronic Components," to be held during the spring of 1952 in Washington, D. C. This Group will participate in the Houston, Texas, Conference of the Instrument Society of America, scheduled for September 10–14.

The Planning Committee of the **Professional Group on Nuclear Science** has made tentative plans to hold a meeting in co-operation with the Atomic Energy Commission at the Brookhaven National Laboratory on December 3, and 4, 1951. D. H. Loughridge, Chairman of the Program Committee, has outlined the activities of the December 3rd meeting which will include papers by seven members of the Laboratory. A panel discussion will be held on "The Role of Electronics Engineering in AEC Developments." On December 4, representatives of North Carolina State College, MIT, Stanford University, the Dow Chemical Co., and the Stanford Research Institute will present papers on the "Industrial Applications of Fission Products." Notices for this meeting are scheduled to be released to all members of this Group by September 15.

Calendar of COMING EVENTS

56th Annual International Municipal Signal Association Meeting, Mark Hopkins Hotel, San Francisco, Calif., September 17–20

4th Conference on Gaseous Electronics, General Electric Research Laboratory, Schenectady, N. Y., October 4–6

1951 National Electronics Conference, Edgewater Beach Hotel, Chicago, Ill., October 22–24

AIEE Fall General Meeting, Cleveland, Ohio, October 22–26

Optical Society of America 36th Annual Meeting, Hotel Sherman, Chicago, Ill., October 23–24

Professional Group on Vehicular Communications Annual Conference, Sheraton Hotel, Chicago, Ill., October 25, 26

Radio Fall Meeting, King Edward Hotel, Toronto, Ont., Canada, October 29–31

American Physical Society Meeting on Electron Emission from Surfaces, National Bureau of Standards, Washington, D. C., November 1–3

First JETEC General Conference, Absecon, N. J., November 29–December 1

Joint IRE/AIEE Computer Conference, Benjamin Franklin Hotel, Philadelphia, Pa., December 10–12

IAS-ION-IRE-RTCA Conference on Air Traffic Control, Astor Hotel, New York, N. Y., January 30

1952 IRE National Convention, Waldorf-Astoria Hotel and Grand Central Palace, New York, N. Y., March 3–6

Technical Committee Notes

The Administrative Committee of the **Standards Committee** held a meeting on June 14, with M. W. Baldwin, Jr., presiding in the absence of Axel G. Jensen. At the subsequent meeting of the Standards Committee itself, Mr. Baldwin also presided. It was agreed that the Designation Task Force will be used for working subdivisions of the Standards Committee.

The Institute has appointed John G. Brainerd to serve as IRE Representative on **ASA Sectional Committee C42—Definitions of Electrical Terms.**

The **Committee on Radio Transmitters** convened on June 12, M. R. Briggs, Chairman. This Committee has revised its scope to include the entire field of radio transmitters. The Chairman requested an outline of its scope and activity from each Subcommittee to enable the Radio Transmitters Committee to supervise more closely the work currently under way, and to avoid overlapping by the Subcommittees. A Task Group has been organized to provide information for the Annual Review progress report in the field of radio transmitters during 1951.

A meeting of the **Sound Recording and Reproducing Committee** was held on June 5, under the Chairmanship of H. E. Roys. This Committee is reviewing all available material on methods of calibrating frequency records. It is also planning to prepare standard methods of calibrating frequency records.

The **Committee on Electron Tubes and Solid-State Devices** held a meeting on June 1, A. L. Samuel presiding. L. S. Nergaard, former Chairman, gave a status report on standardizing work accomplished during the past year. Plans for the 1952 Conference on Electron Devices were discussed. W. J. Dodds was appointed Chairman of the Conference Committee. P. A. Redhead, the new Vice-Chairman, was also appointed Chairman of the Local Arrangements Committee. Reports on the activities in progress in the various Subcommittees were given by their Chairmen. The Committee on Electron Tubes and Solid-State Devices has proceeded with the initial steps in organizing a Professional Group on Electron Devices.

The **Joint AIEE-IRE Computer Conference Committee,** under the Chairmanship of J. C. McPherson, met at IRE Headquarters on June 21. Plans were discussed for the next Joint Computer Conference to be held on December 10, 11, and 12, 1951, in Philadelphia, Pa.

A meeting of the **Navigation Aids Committee** was held on June 18, P. C. Sandretto, Chairman. A Subcommittee has been formed for the purpose of developing standards for methods for determining the performance of direction-giving systems. Harry Davis was appointed Chairman. The Committee is also considering definitions of terms.

SECOND CALL!

AUTHORS FOR IRE NATIONAL CONVENTION!

W. H. Doherty, Chairman of the Technical Program Committee for the 1952 IRE National Convention, to be held March 3–6, requests that prospective authors submit the following information:

1. Name and address of author.
2. Title of paper.
3. A 100-word abstract and additional information up to 500 words (both in triplicate) to permit an accurate evaluation of the paper for inclusion in the Technical Program.

Please address all material to W. H. Doherty, Bell Telephone Laboratories, Inc., Murray Hill, N. J. The deadline for acceptance is November 5, 1951. Your prompt submissions will be appreciated.

Haraden Pratt, IRE Secretary, Named Telecommunications Adviser to Truman

HARADEN PRATT

Haraden Pratt, Secretary of the IRE and vice-president of the American Cable and Radio Corporation, was appointed by President Truman on July 31 to the newly-created post of Telecommunications Adviser to the President, the highest appointive position in the communications field. He will advise the President on broad national and international policies in the communications field, and will assist the President in discharging the powers vested in him over national communications.

Creation of this post was suggested last February by the President's Communication Policy Board. Mr. Pratt's responsibilities, as outlined by the Board, would include the following:

(1) The assignment of frequencies to Federal Government users, and the economical use of the frequency spectrum by them.

(2) The exercise of the President's emergency and war powers over the radio and wire communications of the country.

(3) By joint action with the FCC, the resolution of conflicts concerning frequency allocation arising between Government and non-Government users.

(4) The formulation of policies and positions for international telecommunications negotiations.

The Interdepartment Radio Advisory Committee (IRAC), consisting of representatives of the frequency-using Government agencies, will continue the detailed work of assigning frequencies to Government users, but under policies established by, and with the approval of, the office of the Telecommunications Adviser. The Federal Communications Commission will continue as the agency for regulation and control of private users, as before.

Mr. Pratt will operate directly as a member of the President's staff. Offices and personnel will be furnished by the National Security Resources Board. His appointment does not require Senate confirmation.

Long associated with the communications industry, Mr. Pratt has been a member of the IRE Board of Directors continuously since 1935. He served as President of the Institute in 1938, Treasurer in 1941 and 1942, and Secretary from 1943 through 1951.

In 1944 he was awarded the Medal of Honor, the Institute's highest award, in "recognition of his engineering contributions to the development of radio, of his work in the extension of communication facilities to distant lands, and of his constructive leadership in Institute affairs."

A biographical sketch of Mr. Pratt appeared on page 1362 of the December, 1949, issue of the PROCEEDINGS.

Interference Measurements Groups Hold Joint Meeting

A joint meeting of the JAN-I-225 Working Group of the Interference Reduction Panel, Research and Development Board, and the Measurements Techniques Task Group of Subcommittee No. 1, American Standards Association Sectional Committee C-63, was held at the Moore School of Electrical Engineering, University of Pennsylvania, on April 24 to 27. The first group is under the chairmanship of L. W. Thomas of the Bureau of Ships, and the second is headed by W. E. Pakala of the Westinghouse Electric Corporation. Organized to rewrite JAN-I-225 specifications on methods of radio-interference measurements, the Working Group has held several meetings during the past year with the result that two new drafts of JAN-I-225 have been written. The formulations of the new specification requires a considerable amount of time, since it is the aim of the group to include noise-measurement specifications in the new JAN-I-225 for all the Armed Services.

Subcommittee 1 of ASA C-63 has recently finished two tentative specifications on radio-noise meters (Specification C-63.2 and C-63.3) and issued them on a one-year trial basis. The Measurements Task Group was subsequently organized to develop methods of measurement of radio noise. The members of the group found that their interests paralleled those of the JAN-I-225 group in many respects, and it was felt that the two measurement specifications should not disagree in principle. Thus the joint meeting mentioned above was planned.

At the meeting it was decided to adopt the microvolt-per-meter-per-kilocycle bandwidth as the standard unit of measurement of radiated broad-band interference. Agreement was reached on the general characteristics of a power-line stabilization unit for measurement of conducted interference.

The term "interference" used by the Army-Navy Group will probably be replaced by "noise" in the ASA specification. Various members of the combined groups were assigned the writing of detailed measurement specifications for particular equipments such as engine generators, vehicles, communication equipment, aircraft equipment, and so forth. A third draft of the specification is expected to be issued shortly.

ASEE Sees Shortage of Technologists

At the 59th Annual Meeting of the American Society for Engineering Education held at Michigan State College June 25–29, 1,800 leading teachers of engineering and science pointed out that the gap between the nation's need for technologists and the sources of supply is widening each year.

The shortage, after the placement of this year's graduating class, was estimated at 60,000. In 1952 only 26,000 engineers will graduate, and by 1954 the supply will be down to 12,000. The annual peacetime need for engineers is approximately 30,000.

Most of the papers presented at the meeting stressed the urgency of using engineering manpower more efficiently and of extending research jobs and facilities.

IRE Convention Selected for First Show-Attendance Audit

The Radio Engineering Show of the 1951 IRE National Convention, held in New York City last March, became the first exhibition ever to have its attendance figures audited. The audit was performed by the newly-formed Exhibits Attendance Audit Bureau (EAAB) which will publish standardized statements of exhibit attendance and related information after they have been certified by an auditor's examination.

Information for the EAAB report on the IRE Convention was obtained from the registration cards of members, nonmembers, and exhibitors. The report verified the attendance as 22,919 and the number of exhibitors as 277, and gave data on business affiliations, job classifications, and geographic locations of the attendees.

IRE/RTMA Radio Fall Meeting

KING EDWARD HOTEL, TORONTO, ONT., CANADA—OCTOBER 29–31, 1951

Monday, 9:30 A.M., October 29

GENERAL SESSION

Chairman, W. R. G. Baker
General Electric Co.

"Welcome," R. A. Hackbush, President, RTMA of Canada.

"Greetings of the IRE," I. S. Coggeshall, IRE President.

"Noise in Television Receivers," S. J. H. Carew, Stromberg Carlson Co., Ltd.

"Suppression of Local Oscillator Radiation in Television Receivers," John Van Duyne, Allen B. DuMont Laboratories, Inc.

"Report of the RTMA Material Bureau," L. M. Clement, Crosley Division, Avco Mfg. Corp.

Monday, 2:00 P.M., October 29

Symposium on Reliability of Tubes and Circuits

(Sponsored by the IRE Professional Group on Broadcast and Television Receivers)
Chairman, J. R. Steen, Sylvania Electric Products Inc.

Tuesday, 9:00 A.M., October 30

Symposium on Color Television

(Sponsored by the IRE Professional Group on Broadcast and Television Receivers)
Chairman, D. B. Smith, Philco Corp.

Tuesday, 2:00 P.M., October 30

TELEVISION SESSION

(Sponsored by the IRE Professional Group on Broadcast and Television Receivers)
Chairman, D. D. Israel, Emerson Radio and Phonograph Corp.

"A New Miniature Triode for UHF TV Tuners," K. E. Loofbourrow and C. M. Morris, Radio Corporation of America

"Measurement of Television Gamma or Amplitude Linearity," W. K. Squires, Sylvania Electric Products Inc.

"A UHF Television Converter," H. R. Hesse, Allen B. DuMont Laboratories, Inc.

Tuesday, 6:45 P.M., Annual Fall Meeting Dinner

Toastmaster, F. S. Barton, former IRE Vice-President

"Report on the CCIR Meeting—Geneva, 1951," D. G. Fink, *Electronics*

Wednesday, 9:00 A.M., October 31

Symposium—The Receiver as a Link in the Audio Chain

(Sponsored by the IRE Professional Group on Audio)

Chairman, F. H. Slaymaker,
Stromberg-Carlson Co.

Wednesday, 2:00 P.M., October 31

TELEVISION SESSION

(Sponsored by the IRE Professional Group on Broadcast and Television Receivers)

Chairman, F. H. R. Pounsett,
Stromberg-Carlson Co., Ltd.

"Phase Linearity in TV Receivers," Herbert Kiehne and Stanley Mazur, Emerson Radio and Phonograph Co.

"The Chromatron—An Electronically Registered Tri-Color Cathode-Ray Tube," Robert Dressler, Chromatic Television Laboratories, Inc.

"Pencil Triode for Pulsed-Oscillator and Power-Amplifier Service," John W. Busby, Radio Corporation of America

Industrial Engineering Notes[1]

TELEVISION NEWS

A partial lifting of the nearly three-year-old "freeze" on television station construction is not possible at this time, the FCC announced recently in a "Third Report of Commission" on the involved television situation. Previously, on March 22 of this year, the FCC issued its "Third Notice of Further Proposed Rule Making" which indicated the possibility of a partial lifting of the "freeze" with respect to TV stations in Alaska, the Hawaiian Islands, Puerto Rico, and the Virgin Islands, the lifting of the "freeze" with respect to uhf-channel applications, and the granting of additional power to existing vhf stations. . . . The **National Television System Committee,** which recently released an ad hoc committee report on a new color television system, **has now reorganized and established nine new panels,** W. R. G. Baker, chairman, announced. The reorganization is the first step of the NTSC in carrying out the program announced by Dr. Baker in releasing the ad hoc committee report for the development of recommended standards for an NTSC color system. Appointment of Elmer Engstrom, RCA Laboratories Division, as vice-chairman of the NTSC also was announced by Dr. Baker. Other NTSC vice-chairmen are: D. G. Fink, McGraw-Hill Book Co., and David B. Smith, Philco Corp. The nine new panels and their chairmen and vice-chairmen are as follows: Subjective Aspects of Color—A. N. Goldsmith, chairman, D. E. Hyndman, Eastman Kodak Co., vice-chairman; Color System Analysis—D. G. Fink, chairman, A. G. Jensen, Bell Telephone Laboratories, vice-chairman; Color Video Standards—A. V. Loughren, Hazeltine Electronics Corp., chairman, W. T. Wintringham, Bell Telephone Laboratories, vice-chairman; Color Synchronizing Standards—D. E. Harnett, General Electric Co., chairman, M. R. Briggs, Westinghouse Electric Corp., vice-chairman; Compatibility—D. E. Noble, Motorola, Inc., chairman, Rinaldo DeCola, Admiral Corp., vice-chairman; Field Testing—T. T. Goldsmith, Allen B. DuMont Laboratories, chairman, G. E. Gustafson, Zenith Radio Corp., vice-chairman; Network—Frank Marx, American Broadcasting Co., chairman, R. E. Shelby, National Broadcasting Co., vice-chairman; Co-ordination—D. B. Smith, Philco Corp., chairman, I. J. Kaar, General Electric Co., vice-chairman; Definitions—R. M. Bowie, Sylvania Electric Products Inc., chairman, M. W. Baldin, Jr., Bell Telephone Laboratories, vice-chairman. . . . **Commercial television broadcasting will mark its tenth anniversary on July 1 with 107 stations on the air** and more than 400 applications on file pending the lifting of the present "freeze." On April 30, 1941, the FCC authorized commercial TV operation to start on July 1 of that year. Two New York stations, which had previously operated experimentally, were able to start commercial operation on July 1. They were WNBT and WCBS. By May of 1942 ten commercial TV stations were on the air. Six of these continued to provide service during World War II. . . . **The FCC has allocated the frequency band of 470 to 500 mc to the television-broadcasting service.** The new allocation, providing five new TV channels, was contained in the FCC's Fourth Report and Order in the television proceedings. In providing the new frequencies for TV, the Commission turned down a request of the Bell Telephone Laboratories for the allocation of these frequencies for broad-band mobile operation. Most of the 470–500-mc band, the FCC said, is already being used for experimental TV operation, though 470–475 mc had been allocated to facsimile broadcasting. The Commission points out that facsimile operation can be accomplished on existing broadcast stations, such as FM. The Commission concluded that there is need for further expansion of common-carrier mobile radio service, but pointed out that this can be accomplished by smaller separations between frequency assignments in bands below 160 mc, development and use of more efficient techniques, and utilization of geographic frequency sharing. . . . .**Television in Switzerland may become a reality next spring,** on an experimental basis, under terms of a proposal submitted to the Swiss Federal Assembly (parliament) by the Swiss Federal Council If the experiment is satisfactory, regular service will be initiated in 1955. Under the plan technical aspects of the experiment would be handled by the Federal Posts,

[1] The data on which these *NOTES* are based were selected, by permission, from *Industry Reports*, issues of June 22, June 29, July 6, and July 13, published by the Radio-Television Manufacturers' Association, whose helpfulness is greatly appreciated.

Telegraphs and Telephones, while the Swiss Broadcasting Association would be responsible for programs and operations. Commercial telecasting is opposed during the experimental period, but the way is left open for its possible adoption later. Technical standards contemplated are 625 lines per picture and 25 pictures per second, according to a report to the U. S. Government.

FCC Actions

The FCC has recently appointed Edward W. Allen, Jr., Chief Engineer, to succeed Curtis Plummer who has been moved up to head the newly-formed Broadcast Bureau. Mr. Allen, presently Chief of the Technical Research Division, will head the Office of the Chief Engineer of which that division is a component. He assumed his new duties upon his return from Geneva where he was a member of the U. S. delegation to the International Radio Consultative Committee (CCIR). A native of Portsmouth, Va., Mr. Allen received his electrical engineering degree from the University of Virginia in 1925 and obtained the LL.B. degree from George Washington University in 1933. . . . **The FCC has proposed to amend its Rules Governing the Low Power Industrial Radio Service** to provide for the assignment of certain microwave frequencies in this service. The proposed rulemaking would also relax the present limitation on maximum permissible separation between a transmitter in this service and the radiation portion of its associated antenna. Recent developments, the FCC stated, indicate that there are certain uses or microwave operation in the Low Power Industrial Radio Service. Chief among these are industrial direction and range devices. The new FCC proposals would extend to this service microwave uses now available for mobile operations in other industrial services.

Coy Denies FM Spectrum Space Cuts

FCC Chairman Wayne Coy has scotched rumors that the Commission is planning to take any spectrum space from FM. In a letter to Josh L. Horner of WFMA (FM), Rocky Mount, N. C., made public recently, Mr. Coy said "the FCC is not considering the deletion of the FM band or any part of it. The FCC is not considering allocating the FM band or any part of it to any other service."

Chairman Coy praised the strength of the service, "particularly when one considers that many manufacturers do not make sets and none of them have carried on continuously aggressive sales campaigns. In almost every area of the country there is an unfilled demand for FM receivers."

May TV Production Drops as Radio Output Rises

Television set production was cut back drastically in May—28 per cent below April and 54 per cent under the monthly average of the first quarter, according to RTMA estimates of the industry's output. The output of radio receivers, on the other hand, increased three per cent over the preceding month and declined by the same percentage under the quarter's average.

RTMA's estimates, which include production by members of the Association and nonmembers, showed a total of 339,132 TV sets and 1,372,609 radios manufactured in May. These compare with 469,157 television sets produced in April and a monthly average for the first 1951 quarter of 733,223 TV receivers. April's radio production aggregated 1,337,042 and the quarter's average was 1,411,866 sets.

RTMA Activities

A recent RTMA-sponsored **demonstration of uhf converters and other reception equipment at Bridgeport, Conn.,** indicated that conversion of vhf television receivers for uhf reception in areas where uhf stations eventually will be built will be relatively simple and inexpensive. . . . Chairman Wayne Coy of the FCC has suggested that **the FCC and RTMA jointly sponsor a uhf "road show"** for would-be broadcasters in order to demonstrate the technical effectiveness of uhf telecasting.

NPA to Aid Laboratories

The National Production Authority has issued an order (M-71) giving priority assistance to technical and scientific laboratories in the procurement of materials needed to carry on important research projects.

NPA provides a self-certification system in the new order to enable laboratories to obtain controlled materials and other products. Provisions also are made for giving assistance on a quarterly basis if requirements are for amounts greater than those permitted by the order. Affected by the action are all scientific laboratories (research, production control, testing, analytical, clinical, and instructional).

IRE People

James W. McRae (A'37–F'47) has been appointed vice-president of Bell Telephone Laboratories, Inc., in charge of the systems development organization. This organization was recently divided into the following departments: systems engineering, transmission development, and switching development, headed by **G. W. Gilman** (A'29–SM'47–F'50), **G. N. Thayer** (SM'47–F'51), **M. B. McDavitt** (M'46), respectively.

James W. McRae

Born in Vancouver, B. C., Canada, in 1910, Dr. McRae attended the California Institute of Technology where he received the Ph.D. degree in 1937. Upon completion of his studies he joined the staff of Bell Telephone Laboratories. His early work was concerned largely with transoceanic radio transmitters and microwave research, a branch of radio engineering which led him to participate in important military projects, including some early radar developments.

In 1942 he was commissioned a major in the Signal Corps, and was assigned to the Office of the Chief Signal Officer in Washington, D.C. In 1944 he was made chief of the engineering staff of the Signal Corps Engineering Laboratories at Bradley Beach, N. J., and subsequently became deputy director of the engineering division. Before his return to civilian life in 1945, he had attained the rank of colonel and was awarded the Legion of Honor.

In 1946 he was appointed director of radio projects and television research at the Bell Laboratories, in which capacity he was responsible for work on the New York–Boston radio relay system. He was made director of electronics and television research in 1947. Two years later he became assistant director of apparatus development, and then director of that department. Since 1949 he has been director of transmission development.

A member of the IRE Board of Editors since 1946, Dr. McRae has served on the Awards Committee, the Policy Development Committee, and the Tellers Committee. In 1948 and 1949 he was Chairman of the New York Section, and is at present active on the Executive Committee and the Board of Directors. He received honorary mention in the Eta Kappa Nu awards for outstanding young electrical engineers in 1943, and belongs to the American Institute of Electrical Engineers and to Sigma Xi.

❖

David C. Prince (A'45–SM'45), a vice-president of the General Electric Company on the president's staff, and formerly head of the company's General Engineering and Consulting Laboratory, has retired after 32 years of service, it has been announced. His plans are to enter the consulting engineering field and to maintain headquarters in Schenectady, N.Y.

David C. Prince

Responsible for many developments in the electrical-engineering field, Mr. Prince holds a total of 98 United States patents and was the recipient in 1940 of the Modern Pioneer Award for outstanding contributions to engineering science. In 1943

he received the honorary degree of Doctor of Science from Union College.

Mr. Prince is active in the American Institute of Electrical Engineers and served as its president for the term of 1941–1942. He received the AIEE Lamme Medal in 1946. He is a member, also, of the American Society of Mechanical Engineers, the Institute of Aeronautical Sciences, the Society of Automotive Engineers, the American Rocket Society, and the British Institution of Electrical Engineers.

❖

Allen B. DuMont (M'30–F'31), television pioneer, scientist, and industrialist, was among the nation's 12 foremost business leaders chosen in the *Forbes* Magazine poll. As a summary of his qualities the magazine published the following citation:

A. B. DuMont

"Dr. Allen B. DuMont, through sheer individual intellectual force, scientific perception and inventiveness, unremitting research, combined with acute business acumen, is hailed as the world's most fruitful pioneer in television. Recipient of some two-score 'awards' from scientific and other societies—and a similar number of exclusive patents. Essentially the type that has won America world-wide know-how leadership."

A Fellow of the American Institute of Electrical Engineers and of the Television Society, Dr. DuMont belongs also to Sigma Xi and has served as president of the Television Broadcasters Association. His Institute activities have included work on the Standardization, Standards, and Television Committees.

❖

Joseph T. Thwaites (SM'46) has been appointed manager of electronic research at Canadian Westinghouse Company, Ltd., Hamilton, in charge of what will soon be the largest laboratory of its kind in Canada.

Mr. Thwaites was the first person in Canada to take a formal course in electronics, and has the distinction of receiving three Certificates of Appreciation from the United States Government for wartime service—the first civilian to be so honored.

British-born, Mr. Thwaites was on loan to the U. S. War Department from Canadian Westinghouse, and serving in the United Kingdom at the time. Technically he was regarded as a United States citizen. Success of his efforts and those of his co-workers was responsible for some remarkable Allied technical victories.

Mr. Thwaites was born in Lancashire, England, and came to Canada in 1905. He attended public school in Hamilton until the age of 14. His first job was at Westinghouse in the transformer department. Working days at the plant, he attended night school for four years to obtain his junior and senior matriculation. With money he had saved while working, he enrolled at Queen's University in engineering physics. He graduated in 1925, and went to a two-year postgraduate course in electronics.

In 1929, upon his return to Westinghouse, he entered the radio-engineering department as radio-test engineer. The following year he joined the switchgear division and served as a special-products engineer until his appointment as division engineer in charge of electronics in 1939.

Between 1940 and 1943, Mr. Thwaites was instrumental in increasing the Canadian production of aluminum, greatly by means of large-scale applications of ignitrons. He also carried out pioneer work on X-ray penetration of steel, part of the program which led to X-ray inspection of welds and castings.

He was loaned to the U. S. Government in 1943 and sent to Great Britain the following year. His Certificates of Appreciation were from the U. S. Office of Scientific Research and Development, 1945; the U. S. War Department, 1946; and the U. S. War Department and Navy Department, 1948.

❖

R. Morris Pierce (A'30–M'42–SM'43) has been appointed executive engineer for the Voice of America, it was announced recently by the Department of State. In this capacity he will be especially concerned with problems of construction of new facilities for the expanded radio operation of the Voice.

Born in Chicago, Ill., in 1906, Mr. Pierce is a graduate of Cornell College, Mt. Vernon Iowa. He began his engineering career with the Zenith Radio Corporation, and then worked as chief engineer of Station WJAY, the Cleveland Police Radio System, and Station WGAR, becoming vice-president in charge of engineering of the latter, as well as of WJR, Detroit, and of KMPC, Los Angeles.

During the war, Mr. Pierce served in North Africa and Europe as chief radio engineer with the Psychological Warfare Branch of the Allied Forces Headquarters. More recently he was president of Station WDPK, Cleveland, Ohio.

A member of the American Institute of Electrical Engineers and the Cleveland Engineering Society, Mr. Pierce has served on several radio industry engineering committees, including the Executive Committee of the IRE Professional Group on Broadcast Transmission Systems, a joint body of the National Association of Broadcasters and the IRE Committee on Recording Standards, the FCC/Industry Committee on North American Regional Broadcasting Agreement, and the Engineering Committee of the National Association of Broadcasters.

❖

Donald H. Loughridge (M'42–SM'43), who has served for the past three years as senior scientific advisor to the Secretary of the Army, has been transferred to the post of assistant director of the reactor division of the Atomic Energy Commission.

Born in Lincoln, Neb., in 1899, Mr. Loughridge received the B.S. degree in 1923, and the Ph.D. in 1927, both from the California Institute of Technology.

His career has included work in magnetic analysis with the United States Steel Corporation, teaching positions at the University of Southern California, Los Angeles, Calif., and at the University of Washington, Seattle, Wash., and the post of principal physicist at the Department of Terrestrial Magnetism and at the National Bureau of Standards, where he was engaged in national defense research of a highly important nature during World War II.

Mr. Loughridge has served on the IRE Committee on Nuclear Studies during 1948 and 1949, and is a Fellow of the American Physical Society.

❖

Louis Kahn (A'31) has been appointed expert consultant for the Panel of Components, and also Chairman of the Capacitor Sub-Panel, Research and Development Board for the Armed Forces, it was announced recently. Mr. Kahn is director of research for the Aerovox Corporation of New Bedford, Mass., and director of Aerovox, Canada, Ltd.

Louis Kahn

Before joining the staff of Aerovox in 1937, Mr. Kahn was an instructor in electrical engineering at Rutgers University, New Brunswick, N. J. In 1947 the American Standards Association awarded him a certificate of appreciation for his contributions to the joint engineering studies and recommendations dealing with wartime capacitor problems. A leader in his field, Mr. Kahn has contributed extensively to the evolution of new impregnants climaxed by Aerolene, to new plastic-case materials, and to the commercialization of metallized paper capacitors.

❖

Wallace R. MacGregor (A'46), formerly common-carrier engineer on the staff of the Federal Communications Commission, has joined the Lenkurt Electric Sales Company as manager of government sales for carrier telephone and telegraph systems. He will head two new branch offices, one in Monmouth County, N. J., which serves the Signal Corps at Fort Monmouth, and the other in Washington, D. C.

W. R. MacGregor

Mr. MacGregor is a graduate of Clarkson College of Technology, Potsdam, N. Y., where he received the B.S. in electrical engineering in 1926. During the war he served with the Navy on the engineering of landline communications installations for both continental and advance-base naval shore establishments. Previously he had held various plant-supervisory posts with the New York Telephone Company. He is a Registered Engineer in the State of Maryland, and belongs to the Armed Forces Communications Association.

Books

Theory and Application of Industrial Electronics by John M. Cage

Published (1951) by McGraw-Hill Book Co., 330 W. 42 St., New York 18, N. Y. 281 pages+4-page index+2-page appendix+xi pages. 244 figures. 6×9¼. $4.85.

This is a new book written primarily for students, and particularly those who have learned the fundamentals of physics, electrical engineering, algebra, and elementary calculus. It aims to do for the industrial electronic field what numerous other books do for the student of radio engineering.

Its 14 chapters may be divided into a number of groups, such as timing circuits, high-frequency heating, and control circuits. Each may be studied without the need of the others as a background.

The chapter on the extensive and ever-growing science of electronic measurements and instrumentation is appropriately entitled merely a "survey" chapter on the subject.

The field of servomechanisms is covered in more detail than the other subjects in the book, and would appear to require more background than that of the average undergraduate, particularly in mathematics. However, as the author has pointed out, the reader may pass it by without losing anything necessary for the understanding of subsequent chapters.

The text includes a few errors, probably traceable to scanty proofreading and the lack of a thorough check. Also, it would have been helpful if the index had been made more complete, and if some of the terms had been defined when first introduced.

The pages are well supplied with diagrams and figures. Problems and a selected list of references are included at the end of each chapter.

W. C. White
General Electric Co.
Schenectady, N. Y

Electronics, Principles and Applications by Ralph R. Wright

Published (1950) by The Ronald Press, 15 E. 26 St., New York 10, N. Y. 376 pages+11-page index+ix pages. 314 figures. 6×9¼. $5.50.

In this new and complete work the author uses material that he has employed successfully in instructing electrical engineering students and physics majors. Chapters 1 through 3 present basic electronic principles; Chapter 4 is a review of dc and ac circuits; and Chapters 5 through 12 deal lucidly with applications of electron tubes. As each of the chapters is a more or less complete unit in itself, the actual order of use in teaching is flexible, and up to the instructor of the course.

A complete coverage of its subject, the book also has distinct value as a refresher reading course. The complication of derived equations is avoided by the use of basic equations only. The first 100 pages, easily readable, deal with electron-tube principles, and the ensuing chapters are instructive discussions of amplification, oscillation, modulation and detection, rectification cathode-ray tubes and applications, light-sensitive devices, X rays, high-frequency heating, and basic-control circuits.

The inclusion of 30 pages on the subject of cathode-ray tubes is praiseworthy. It is but 20 years since the cathode-ray oscillograph was made available commercially in this country for viewing electrical phenomena, and the subject has not often been treated as informatively as in Professor Wright's book. Twenty-two pages on X-ray principles and practice are warranted as there is hardly a town or hamlet in the country that does not have one or more X-ray installations.

The book will be found to have direct use in college instruction, and engineers already at work in the associated industries will find it a useful reference work.

Donald McNicol
25 Beaver St.
New York, N. Y.

Introduction to Industrial Electronics by R. Ralph Benedict

Published (1951) by Prentice-Hall, Inc., 70 Fifth Ave., New York 11, N. Y. 413 pages+8-page index+14-page appendixes+x Pages. 301 figures. 5½×8½. $6.35.

This well-written text, another volume in the series edited by W. L. Everitt, is intended primarily for the instruction of undergraduate engineering students, including those not in the electrical field. As such, it takes an elementary approach, confining demonstrations to high-school algebra and trigonometry. The treatment is primarily descriptive, but the quantitative aspects are well brought out in a number of numerical exercises at the end of each chapter. These represent, for the most part, practical problems in the measurement and computation of circuit values, selection of tubes, and so forth. The student who is required to work out the correct answers to a generous sample of these exercises will find himself well prepared to deal intelligently with the increasing number of electronic applications now requiring the attention of engineers in all fields. The book is not particularly well adapted to self-study, since only a few problems are worked out in the body of the text. With the services of an instructor available, however, the transition from the formulas to specific problem solutions should be readily made.

The subjects covered are as follows: high-vacuum diodes and triodes, space charge, emission, practical cathodes, diode- and triode-circuit analysis, multigrid-tubes, amplifiers, oscillator modulators, detectors, phototubes and photocells, cathode-ray tubes and equipment, gaseous conduction and gas-filled tubes, and specialized tubes. Among the specific applications are rectifier and controlled-rectifier circuits, industrial power conversion, induction and dielectric heating, electronic relay circuits, control of resistance welding, industrial instrumentation, motor control, process control and regulation.

The contents of this book have, of course, been treated by other authors, with about the same organization of the material; there are, perhaps, too many books on industrial electronics. But this is one of the better ones, particularly well suited to the would-be engineer who wants a working familiarity with electronic methods without having to devote his whole life to this all-pervasive subject.

Donald G. Fink
Electronics
330 W. 42 St.
New York, N. Y.

Time Bases, Second Edition by O. S. Puckle

Published (1951) by John Wiley & Sons, Inc., 440 Fourth Ave., New York 16, N. Y. 258 pages+9-page index+118-page appendixes+2-page bibliography +xxi pages. 257 figures. 5½×8½. $5.00.

The second edition of this very valuable little book dealing with time bases will be welcomed by engineers everywhere, and particularly by those who are specifically engaged in work dealing with pulse techniques, scanning generators, deflection circuits, and related apparatus utilizing the cathode-ray tube. It is an essential reference work which should be included in the libraries of practicing television engineers throughout the world.

Much new material has been added in this second edition, and the reviewer wishes to recommend especially the new material in Chapter IX dealing with the subject of Miller-capacitance time bases. The rather detailed information on trigger circuits which make use of negative feedback to improve trace linearity, positive feedback being employed to operate the trigger portion of the circuit, is particularly valuable.

The book is well written, and the information given under each topic heading is geared to the essentials. It is at once evident to the reader that Mr. Puckle is dealing with a subject of which he has a very eminent knowledge, and that he has accomplished his task in a highly professional manner.

In his vivid treatment of the subject's historical background he traces the measurement of time back to the sundial introduced into Greece from Babylon by Animaxander (611 to 547 B.C.), a pupil of Thales of Miletus, discoverer of "electrum." From these early times the author brings us up to the present day, with its cathode-ray oscillographs capable of measuring the passage of time in terms of fractions of microseconds. Such writing does much to make a strictly scientific subject intensely interesting for the student.

An appendix on the operation of gas-discharge triodes is of interest, the author successfully dispelling current misapprehensions with respect to their frequency limitations. Finally, a rather complete bibliography provides a selection of source material for the reader who would like to do further research on the subjects covered.

Scott Helt
Allen B. DuMont Laboratories, Inc.
2 Main Ave.
Passaic, N. J.

Sections*

Chairman		Secretary
R. L. Burtner Goodyear Aircraft Corp. 1210 Massillon Rd. Akron, Ohio	AKRON (4)	E. M. McCormick 2512 State Rd. Cuyahoga Falls, Ohio
E. S. Lammers, Jr. Westinghouse Electric Corp. Box 4808 Atlanta 2, Ga.	ATLANTA (6)	D. B. Buchanan 5130 Powers Ferry Rd., N.W. Atlanta, Ga.
D. G. Little 408 Old Orchard Rd. Baltimore 29, Md.	BALTIMORE (3)	G. R. White Bendix Radio Div. Towson 4, Md.
E. D. Coburn Box 793 Nederland, Texas	BEAUMONT-PORT ARTHUR (6)	C. B. Trevey 2555 Pierce St. Beaumont, Texas
L. E. Packard Technology Instrument Corp. 1058 Main St. Waltham 54, Mass.	BOSTON (1)	Beverly Dudley The Technology Review Mass. Inst. of Tech. Cambridge 39, Mass.
G. J. Andrews Fernandez Spiro 286 Acassuso, F.C.N.G.B.M. Buenos Aires, Argentina, S.A.	BUENOS AIRES	I. C. Grant Paseo Colon 995 Buenos Aires, Argentina, S.A.
R. E. Frazier R.D. 1. Center St. East Aurora, N. Y.	BUFFALO-NIAGARA (4)	W. K. Squires 115 St. John's Ave. Kenmore 23, N. Y.
V. R. Hudek 137 29 St. Drive S.E. Cedar Rapids, Iowa	CEDAR RAPIDS (5)	R. M. Mitchell 357 Garden St., S.E. Cedar Rapids, Iowa
Leroy Clardy Research Labs. Swift & Co. U.S. Yards Chicago 9, Ill.	CHICAGO (5)	A. A. Gerlach 4020 Overhill Ave. Chicago 34, Ill.
A. B. Bereskin University of Cincinnati Cincinnati, Ohio	CINCINNATI (5)	W. B. Shirk 6342 Hamilton Ave. Cincinnati 24, Ohio
T. B. Friedman 1900 E. 30 St. Cleveland 14, Ohio	CLEVELAND (4)	A. L. Hammerschmidt 111 Westbridge Dr. Berea, Ohio
D. C. Cleckner 1376 Aberdeen Ave. Columbus 3, Ohio	COLUMBUS (4)	J. H. Jaeger Ohio Bell Telephone Co. 42 E. Gay St. Columbus 15, Ohio
L. E. Williams Dept. of Elec. Eng. University of Connecticut Storrs, Conn.	CONNECTICUT VALLEY (1)	H. E. Rohloff The Southern New England Tel. Co. 227 Church St. New Haven, Conn.
E. A. Hegar 802 Telephone Bldg. Dallas 2, Texas	DALLAS-FORT WORTH (6)	J. K. Godbey 3990 Davilla Dr. Dallas 9, Texas
Joseph General 1116 Lexington Ave. Dayton 7, Ohio	DAYTON (5)	A. H. Petit 159 Aberdeen Ave. Dayton 9, Ohio
P. M. La Hue 3215 E. 34 Ave. Denver 5, Colo.	DENVER (5)	D. I. Peterson 933 Pontiac St. Denver, Colo.
G. A. Richardson Dept. of Elec. Eng. Iowa State College Ames, Iowa	DES MOINES-AMES (5)	A. D. Parrott 1515—45 Des Moines 11, Iowa
K. R. Schmeisser 13117 La Salle Blvd. Detroit 6, Mich.	DETROIT (4)	F. W. Chapman 1756 Graefield Rd. Birmingham, Mich.
W. R. Rolf 364 E. 5th St. Emporium, Pa.	EMPORIUM (4)	L. R. Maguire 4 E. 6 St. Emporium, Pa.
J. F. Sears 1736 Washington Ave. Evansville 14, Ind.	EVANSVILLE-OWENSBORO (5)	F. A. Gehres 2232 E. Powell Evansville 14, Ind.
J. F. Conway, Jr. 4610 Plaza Dr. Fort Wayne, Ind.	FORT WAYNE (5)	L. F. Mayle Capehart-Farnsworth Corp. Fort Wayne 1, Ind.
J. S. Turner 3422 Alani Dr. Honolulu, T.H.	TERRITORY OF HAWAII (7)	S. H. Lewbel Civil Aeronautics Admins. Box 4009 Honolulu, T.H.
S. A. Martin, Jr. Box 2180, Rm. 209 Houston 1, Texas	HOUSTON (6)	H. T. Wheeler 802 N. Avenue 'A' Bellaire, Texas
	INDIANAPOLIS (5)	R. T. Van Nimam 4441 Indianola Ave. Indianapolis 5, Ind.
J. H. Gregory 2002-A Ellis China Lake, Calif.	INYOKERN (7)	W. E. Vore 420-A Nimitz Ave. China Lake, Calif.
C. L. Foster 1901 W. 73 Terrace Kansas City 5, Mo.	KANSAS CITY (5)	Mrs. G. L. Curtis 6005 El Monte Mission, Kan.
F. P. Kehoe 1338 Brydges St. London, Ont., Canada	LONDON, ONTARIO (8)	R. B. Lumsden VE3ADB 332 Hale St. London, Ont., Canada
J. J. Fiske 128 W. Las Flores Ave. Arcadia, Calif.	LOS ANGELES (7)	Ellis King 3171 Federal Ave. Los Angeles 34, Calif.
R. B. McGregor 2100 Confederate Ct. Louisville, Ky.	LOUISVILLE (5)	M. I. Schwalbe Nichols Veterans Hospital Louisville 2, Ky.
P. H. Craig 1012 Catalonia Ave. Coral Gables, Fla.	MIAMI (6)	F. B. Lucas 5340 Davis Rd., S.W. South Miami 43, Fla.
W. H. Elliot 4747 N. Larkin St. Milwaukee 11, Wis.	MILWAUKEE (5)	D. A. Weller c/o WISN 540 N. Plankinton Ave Milwaukee 1, Wis.
N. R. Olding Canadian Broadcasting Corp. Box 6000 Montreal, P.Q., Canada	MONTREAL, QUEBEC (8)	R. W. Cooke 1417 Graham Blvd. Town of Mt. Royal Montreal, P. Q., Canada
B. J. Bittner 3110—42 Pl., Sandia Base Albuquerque, N. M.	NEW MEXICO (7)	G. A. Arnot, Jr. 401 N. 6 St. Albuquerque, N. M.
J. H. Mulligan, Jr. 14 Mitchell Pl. East Orange, N. J.	NEW YORK (2)	H. S. Moncton Sylvania Elec. Prods. Inc. Bayside, L. I., N. Y.
C. E. Hastings 117 Hampton Rd. Hampton, Va.	NORTH CAROLINA-VIRGINIA (3)	P. F. Hedrick 2472 Maplewood Ave. Winston-Salem 7, N. C.
O. A. Nash, Acting Chairman c/o CAA, AC-636 P. O. Box 1082 Oklahoma City, Okla.	OKLAHOMA CITY (6)	R. R. McClung, Acting Secretary-Treasurer 1615 Joane Street Oklahoma City, Okla.
F. W. Norris 3303 Woods Ave. Lincoln, Neb.	OMAHA-LINCOLN (5)	C. W. Rook Dept. of Elec. Eng. University of Nebraska Lincoln 8, Neb.
W. R. Wilson c/o Royal Canadian Mounted Police Ottawa, Ont., Canada	OTTAWA, ONTARIO (8)	D. V. Carroll Box 527 Ottawa, Ont., Canada
L. M. Rodgers 400 Wellesley Rd. Philadelphia 19, Pa.	PHILADELPHIA (3)	J. G. Brainerd Moore School of Elec. Eng. Univ. of Pennsylvania Philadelphia 4, Pa.
G. C. Rich Box 737 Scottsdale, Ariz.	PHOENIX (7)	A. M. Creighton, Jr. 2221 E. Osborn Rd. Phoenix, Ariz.
W. P. Caywood, Jr. 23 Sandy Creek Rd. Pittsburgh 21, Pa.	PITTSBURGH (4)	V. G. Shaw 17 Frankwood Rd. Pittsburgh 35, Pa.
L. C. White 3236 N. E. 63 Ave. Portland 13, Ore.	PORTLAND (7)	G. C. Ellison 11310 S. E. Market St. Portland 16, Ore.
W. H. Bliss 300 Western Way Princeton, N. J.	PRINCETON (3)	J. S. Donal, Jr. RCA Labs. Princeton, N. J.
J. A. Rodgers Huntington Hills Rochester 9, N. Y.	ROCHESTER (4)	J. C. O'Brien 283 Malden St. Rochester 13, N. Y.
W. F. Koch 1340 33 St. Sacramento 16, Calif.	SACRAMENTO (7)	H. C. Slater 1945 Bidwell Way Sacramento 18, Calif.
H. G. Wise 1705 N. 48 St. East St. Louis, Ill.	ST. LOUIS (5)	E. F. O'Hare 8120 Whitburn Drive Clayton 24, Mo.
L. S. Cole 696 E. 4 North St. Logan, Utah	SALT LAKE CITY (7)	E. C. Madsen 739 Scott Ave. Salt Lake City 6, Utah

* Numerals in parentheses following Section designate Region number.

Sections

Chairman		Secretary
W. J. Hamm St. Mary's University San Antonio 7, Texas	SAN ANTONIO (6)	Paul Tarrodaychik 215 Christine Dr. San Antonio 10, Texas
J. P. Day 3565 Ingraham St. San Diego 9, Calif.	SAN DIEGO (7)	I. L. McNally 2714 Azalea Dr. San Diego 6, Calif.
A. R. Ogilvie 51 Michael Lane Millbrae, Calif.	SAN FRANCISCO (7)	W. R. Abbott 274 Grizzly Peak Blvd. Berkeley 8, Calif.
Ernest S. Sampson 1402 Union St. Schenectady 8, N. Y.	SCHENECTADY (2)	J. D. Cobine 1498 Regent St. Schenectady, N. Y.
J. Emerson Hogg General Electric Co. 710 2 Ave. Seattle 11, Wash.	SEATTLE (7)	H. M. Swarm 6856 19 Ave., N.E. Seattle 5, Wash.
D. C. Pinkerton 312 Cherry Rd. Syracuse 9, N. Y.	SYRACUSE (4)	Samuel Seely College Applied Science Syracuse University Syrcause 10, N. Y.
H. N. Rowe Rowe Industries 1702 Wayne St. Toledo 9, Ohio	TOLEDO (4)	R. G. Larson 2647 Scottwood Ave. Toledo 10, Ohio
George Sinclair 304 Heath St., E. Toronto 12, Ont., Canada	TORONTO, ONTARIO (8)	J. R. Bain Dominion Sound Equip., Ltd. 386 Victoria St. Toronto, Ont., Canada
A. A. Cohen Eng. Research Assoc. 1902 W. Minnehaha Ave. St. Paul 4, Minn.	TWIN CITIES (5)	O. W. Muckenhirn Dept. of Elec. Eng. University of Minnesota Minneapolis 14, Minn.
G. C. Chandler 846 Howe St. Vancouver, B. C., Canada	VANCOUVER (8)	D. D. Carpenter 1689 W. 29 Ave. Vancouver, B. C., Canada.
P. De Forrest McKeel 9203 Sligo Creek Pkwy. Silver Spring, Md.	WASHINGTON (3)	H. P. Meisinger Hull Rd. & Old Courthouse Rd. Route 3 Vienna, Va.
F. H. Scheer College Park Lewisburg, Pa.	WILLIAMSPORT (4)	B. H. Bueffel, Jr. Dept. of Elec. Eng. Bucknell University Lewisburg, Pa.
D. G. Harmon Dept. of Elec. Eng. Texas Tech. College Lubbock, Texas	AMARILLO-LUBBOCK (6) (Dallas-Ft. Worth Subsection)	R. B. Spear 510 E. Hill St. Brownfield, Texas

Chairman		Secretary
L. H. Stantz 168 Moeller St. Binghamton, N. Y.	BINGHAMTON (4) (Syracuse Subsection)	E. L. Pittsley Reynolds Rd. R. D. 1 Johnson City, N. Y.
W. R. Smith Dept. of Elec. Eng. Pennsylvania State College State College, Pa.	CENTRE COUNTY (4) (Emporium Subsection)	H. F. Wischnia Dept. of Elec. Eng. Pennsylvania State College State College, Pa.
J. H. Pickett Aerovox Canada Ltd. 1551 Barton St., E. Hamilton, Ont., Canada	HAMILTON (8) (Toronto Subsection)	G. F. Beaumont 55½ Sherman Ave., S. Hamilton, Ont., Canada
E. E. Spitzer c/o RCA Victor Div. Radio Corp. of America Lancaster, Pa.	LANCASTER (3) (Philadelphia Subsection)	Werner Rueggeberg Research Lab. Armstrong Cork Co. Lancaster, Pa.
H. E. Webber Sperry Gyroscope Co. Lake Success, L. I., N. Y.	LONG ISLAND (2) (New York Subsection)	J. F. Craib R. D. 1 Hicksville, L. I., N. Y.
A. L. Samuel Electronics Labs. I.B.M. Corp. Plant 2, Dept. 532 Poughkeepsie, N. Y.	MID-HUDSON (2) (New York Subsection)	A. V. Platter R. D. 1 Salt Point Rd. Poughkeepsie, N. Y.
B. V. Blom 38 Lafayette St. Rumson, N. J.	MONMOUTH (2) (New York Subsection)	H. S. Bennett 31 Cedar Ave., Apt. 23 Long Branch, N. J.
J. F. Morrison Bell Telephone Labs. Whippany, N. J.	NORTHERN N. J. (2) (New York Subsection)	P. S. Christaldi Box 145 Clifton, N. J.
W. N. Eldred 60 Michaels Way Atherton, Calif.	PALO ALTO (7) (San Francisco Subsection)	O. G. Villard, Jr. Dept. of Elec. Eng. Stanford University Stanford, Calif.
George Weiler 1429 E. Monroe South Bend, Ind.	SOUTH BEND (5) (Chicago) Subsection)	A. R. O'Neil Apt. 302 6712 Lake St. Falls Church, Va.
R. M. Wainwright Dept. of Elec. Eng. University of Illinois Urbana, Ill.	URBANA (5) (Chicago Subsection)	M. H. Crothers Dept. of Elec. Eng. University of Illinois Urbana, Ill.
	WINNIPEG (8) (Toronto Subsection)	W. F. Souch Canadian Marconi Co. 149 Portage Ave., E. Winnipeg, Canada

Professional Groups

	Chairman
AIRBORNE ELECTRONICS	John E. Keto Wright Field Dayton, Ohio
ANTENNAS AND PROPAGATION	George Sinclair Dept. of Elec. Eng. University of Toronto Toronto, Ont. Canada
AUDIO	B. B. Bauer Shure Brothers, Inc. 225 W. Huron St. Chicago 10, Ill.
BROADCAST AND TELEVISION RECEIVERS	D. D. Israel Emerson Radio & Phonograph Co. 111 8 Ave. New York 11, N. Y.
BROADCAST TRANSMISSION SYSTEMS	Lewis Winner Bryan Davis Publishing Co., Inc. 52 Vanderbilt Ave. New York 17, N. Y.
CIRCUIT THEORY	J. G. Brainerd University of Pennsylvania Philadelphia, Pa.
ENGINEERING MANAGEMENT	Ralph I. Cole Griffiths Air Force Base Rome, N. Y.

	Chairman
INDUSTRIAL ELECTRONICS	Eugene Mittelmann 549 West Washington Blvd. Chicago 6, Ill.
INFORMATION THEORY	Nathan Marchand Sylvania Electric Products Inc. Bayside, L. I., N. Y.
INSTRUMENTATION	Ernst Weber Polytechnic Institute of Brooklyn Brooklyn, N. Y.
NUCLEAR SCIENCE	M. M. Hubbard Massachusetts Institute of Technology Cambridge, Mass.
QUALITY CONTROL	R. F. Rollman Allen B. DuMont Laboratories 1000 Main Ave. Clifton, N. J.
RADIO TELEMETRY AND REMOTE CONTROL	W. J. Mayo-Wells The Johns Hopkins University Silver Spring, Md.
VEHICULAR COMMUNICATIONS	Austin Bailey American Telephone and Telegraph Co. 195 Broadway New York, N. Y.

Abstracts and References

Compiled by the Radio Research Organization of the Department of Scientific and Industrial Research, London, England, and Published by Arrangement with that Department and the *Wireless Engineer*, London, England

NOTE: The Institute of Radio Engineers does not have available copies of the publications mentioned in these pages, nor does it have reprints of the articles abstracted. Correspondence regarding these articles and requests for their procurement should be addressed to the individual publications, not to the IRE.

The number in heavy type at the upper left of each Abstract is its Universal Decimal Classification number and is not to be confused with the Decimal Classification used by the United States National Bureau of Standards. The number in heavy type at the top right is the serial number of the Abstract. DC numbers marked with a dagger (†) must be regarded as provisional.

The Annual Index to these Abstracts and References, covering those published in the PROC. I.R.E. from February, 1950, through January, 1951, may be obtained for 2s.8d. postage included from the *Wireless Engineer*, Dorset House, Stamford St., London S.E., England. This index includes a list of the journals abstracted together with the addresses of their publishers.

ACOUSTICS AND AUDIO FREQUENCIES

534 1811

Program of the Fortieth Meeting of the Acoustical Society of America [Boston, Mass. 9th-11th November, 1950]—(*Jour. Acous. Soc. Amer.*, vol. 23, pp. 142–150; January, 1951.) Summaries are given of the papers presented, which included the following:—

A5—Attenuation of Sound in Water containing Air Bubbles—D. T. Laird and P. M. Kendig.

B5—On the Relation between the Sound Fields Radiated and Diffracted by Plane Obstacles—F. M. Wiener.

B6—Synthesis of Line Source Directivity Patterns—R. Hills, Jr.

B7—Viscosity Effects in Acoustic Inductances—A. W. Nolle.

B8—The Non-Linear Interaction of a Plane Progressive Wave with a Small Sphere—P. Westervelt.

B9—First- and Second-Order Acoustic Fields with Viscosity and Relaxation—J. J. Markham.

C3—Comparison of Absorption Coefficients Measured in a Reverberation Chamber with Statistical Coefficients from Impedance Values—H. C. Hardy, F. G. Tyzzer, L. G. Ramer, and J. E. Ancell.

C4—Damping Effects of Porous Absorbing Units in Rooms—R. W. Roop.

C5—The Record-Rerecord Test for Rooms—W. Rudmose.

D2—The Transmission of Sound through Single and Double Walls at Oblique Incidence—R. E. Beatty, Jr., R. H. Bolt, and J. Young.

D3—On the Design of Sound Absorbing Ducts—U. Ingard, J. J. Baruch, L. L. Beranek, and S. Labate.

D4—A Wide-Range Acoustic Termination—O. K. Mawardi.

D5—On the Non-Specular Reflection of Sound from Absorbent Surfaces—V. Twersky.

D6—A Comparison of Sound Pressures Developed in Earphone Couplers and in the Ear—E. L. R. Corliss, R. F. Brown, and K. T. Lemmon.

F1—New Assembly for the Measurement and Analysis of Sound—L. W. Sepmeyer.

F2—Non-Linear Distortion in Hearing Aids—A. Peterson.

F3—An Automatic Non-Linear Distortion Analyzer—H. F. Olson and D. F. Pennie.

F4—A Photographic Method for Displaying Sound Wave Space Patterns—W. E. Kock and F. K. Harvey.

F5—A Feedback-Controlled Calibrator for Phonograph Pick-Ups—J. G. Woodward.

F6—Equipment for the Field Measurement of Reverberation Times—W. Rudmose and H. Mims.

F7—Higher Order Gradient Microphones using a Single Diaphragm—M. E. Hawley and A. H. Kettler.

534:016 1812

References to Contemporary Papers on Acoustics—A. Taber Jones. (*Jour. Acous. Soc. Amer.*, vol. 23, pp. 240–247; March, 1951.) Continuation of 1541 of August.

534:577 1813

A Bibliography on Sonic and Ultrasonic Vibration: Biological, Biochemical, and Biophysical Applications—G. M. Naimark, J. Klair, and W. A. Mosher. (*Jour. Frank. Inst.*, vol. 251, pp. 279–299 and 402–408; February and March, 1951.) A list of 580 references for the period 1900 to 1950, grouped according to the year of publication and with both author and subject index.

534.22-14 1814

The Velocity of Sound in Sea Water—A. Weissler and V. A. Del Grosso. (*Jour. Acous. Soc. Amer.*, vol. 23, pp. 219–223; March, 1951.) Full paper. Summary abstracted in 514 of April.

534.231 1815

A New Expansion for the Velocity Potential of a Piston Source—A. H. Carter and A. O. Williams, Jr. (*Jour. Acous. Soc. Amer.*, vol. 23, pp. 179–184; March, 1951.) Full paper. Summary noted in 521 of April.

534.231 1816

On the Acoustical Radiation of an Emitter Vibrating in an Infinite Wall—J. Pachner. (*Jour. Acous. Soc. Amer.*, vol. 23, pp. 185–198; March, 1951.) The velocity-potential distribution for a circular emitter in an infinite wall is calculated by the King method for points immediately in front of the wall.

534.231 1817

On the Acoustical Radiation of an Emitter Vibrating Freely or in a Wall of Finite Dimensions—J. Pachner. (*Jour. Acous. Soc. Amer.*, vol. 23, pp. 198–208; March, 1951.) The radiation field of a source vibrating freely or in a finite wall is considered as made up of the field of the same source in an infinite wall, together with a field that can be computed from an integro-differential equation that follows from Rayleigh's formula. An abstract solution of the problem is given which can be applied for any shape of wall or wavelength of sound. Computation will be easier if the wall is circular, and if the wavelength is large in comparison with the wall dimensions.

534.232:621.315.612.4 1818

A Barium Titanate Transducer Capable of Large Motion at an Ultrasonic Frequency—W. P. Mason and R. F. Wick. (*Jour. Acous. Soc. Amer.*, vol. 23, pp. 209–214; March, 1951.) Full paper. Summary abstracted in 560 of April, for which the above UDC number is preferable.

534.241 1819

Analysis of Multiple-Echo Effect Arising from the Release of a Stored Wave Train—L. Gold. (*Jour. Acous. Soc. Amer.*, vol. 23, pp. 214–218; March, 1951.) Calculation of the dependence of the number of observable echoes on the threshold sensitivity of the detector, and on the absorption and reflection coefficients of the storage medium.

534.321.7 1820

Standard Musical Pitch—F. W. Alexander. (*BBC Quart.*, vol. 6, pp. 62–64; Spring, 1951.) The history of standard pitch is sketched briefly, and the method now used by the BBC, for deriving from a crystal-controlled 1-mc oscillator, the 440-cps international-standard-pitch tone broadcast before the start of the Third Program is described.

534.321.9:534.231-14 1821

Measurements of the Underwater Sound Field Generated by Quartz Transducers—W. Keck, G. S. Heller, and A. O. Williams, Jr. (*Jour. Acous. Soc. Amer.*, vol. 23, pp. 168–172; March, 1951.) The pressure distributions in the ultrasonic fields produced in water by quartz transducers of various shapes were displayed on a cro and photographed. The ultrasonic beams, pulsed at af, were swept backward and forward across a small microphone placed at various distances from the source. The microphone output was rectified and amplified before being applied to the cro. All the transducers were of X-cut quartz, about 2 cm in diameter, excited near resonance at about 1 mc. The results obtained show that simple piston theory is applicable, provided the baffles and

electrodes used satisfy certain geometrical conditions.

534.321.9:534.232 1822
High-Power Ultrasonic Siren—L. Pimonow. (*Ann. Télécommun.*, vol. 6, pp. 23–26; January, 1951.) The siren described was developed at the C.N.E.T., and is of the type in which a toothed rotor interrupts a powerful air current emerging from holes in a stator [see also 917 of 1948 (Allen and Rudnick)]. The frequency range is 5 to 25 kc, and a radiated acoustic power >2 kw can be obtained by introducing compressed nitrogen into the casing. Applications are discussed.

534.321.9:534.614-13 1823
Ultrasonic Velocities in Gases at Low Pressures—R. A. Boyer. (*Jour. Acous. Soc. Amer.*, vol. 23, pp. 176–178; March, 1951.) Measurements of velocity as a function of pressures down to about 2 mm Hg were made at a frequency of 970 kc. At the lowest pressure, the following increases in velocity over the values under standard conditions were observed: A, 27 per cent; N_2, 16 per cent; O_2, 20 per cent; dry CO_2-free air, 7 per cent.

534.321.9:621.395.61 1824
Effects of Reflected Signals and Electric Pick-Up at an Ultrasonic Microphone—A. O. Williams, Jr., and W. Keck. (*Jour. Acous. Soc. Amer.*, vol. 23, pp. 173–175; March, 1951.) The mixing process is analyzed for a particular arrangement of equipment, and experimental evidence is adduced in support of the conclusions that, (a) the main response pattern of the microphone shows space variations of the order of both λ and $\lambda/2$, (b) the $\lambda/2$ variation dies out, at sufficiently great distances from the source, at a rate showing that a single echo path together with a constant electric signal is responsible, (c) the direct, reflected, and electric-pickup signals can be resolved analytically.

534.374 1825
⅓-Octave Variable Filter—G. Fontanellaz. (*Tech. Mitt. schweiz. Telegr.-Teleph. Verw.*, vol. 29, pp. 48–51; February 1, 1951. In French and German.) This band-pass filter, designed for use in reverberation measurements, comprises a Zobel-type variable LC network. The range covered is 50 cps to 10 kc, using a 9-position and a 3-position switch, respectively, for octave and ⅓-octave selection. The circuit arrangement is described and attenuation characteristics are shown.

534.6:621.395.625 1826
Modulation Measurement at Points of Frequency-Dependent Maximum-Amplitude—K. H. R. Weber. (*Frequenz*, vol. 4, pp. 295–298; November, 1950.) The use of frequency compensation in the meter circuit, in order to obtain a true indication of amplitude, is described, with reference to the response curves of optical and disk recorders.

534.78 1827
Representations of Speech Sounds and Some of their Statistical Properties—Sze-Hou Chang, G. E. Pihl, and M. W. Essigmann. (Proc. I.R.E., vol. 39, pp. 147–153; February. 1951.) A 1950 IRE National Convention paper noted in 1319 of 1950. Properties of speech sounds and methods of transformation and analysis such as infinite clipping, autocorrelation, and spectrographic analysis are discussed with a view to the identification of essential elements of speech intelligibility.

534.846.3/.4 1828
Sound Reinforcing—D. W. Pipe. (*Wireless World*, vol. 57, pp. 117–119; March, 1951.) The sound distribution system installed in the Assembly Hall and three adjacent halls at Church House, Westminster, is described. In the Assembly Hall, low-level reinforcement from small loudspeakers secured to the seat backs is provided. The facilities installed include four-channel simultaneous interpretation; any member of the audience can select the interpretation he requires by operating a switch fitted in the loudspeaker panel, which controls the input to his headphones. Any speaker on the floor of the hall is within the zone of one of the eleven suspended microphones, the appropriate one being selected by the system operator in the balcony, who has an unobstructed view of the assembly.

534.846.3/.4:621.395.623.7 1829
From Decentralized to Central Sound Transmission—F. Spandöck. (*Elektrotech. Z.*, vol. 72, pp. 101–104; February 15, 1951.) The advantages of loudspeaker arrays as compared with distributed arrangements of loudspeakers are: lower installation costs; less amplifier power required; absence of zones of confusion; coincidence of directions of sight and sound. Microphone arrays have corresponding advantages, and when used in theaters, need not be restrictively close to the actors. In sound-reinforcement systems, the sharp directivity of the arrays lessens the danger of acoustic feedback. A formula is given for the amplification at which feedback commences; the calculated values are compared with measurements. Stereophonic applications of arrays are briefly considered.

534.844.1 1830
Automatic Apparatus for Measurement of Reverberation Time—F. J. v. Leeuwen. (*Tijdschr. ned. Radiogenoot.*, vol. 16, pp. 13–36; January, 1951. Discussion, p. 37.) The theory of reverberation time and its measurement is outlined, and apparatus for providing a moving strip record of the reverberation-time-frequency curve of a room is described. By means of a relay arrangement, a sound source within the room is periodically actuated and is interrupted when a steady state is reached. A microphone has its output circuit arranged so as to actuate a "reverberation-time relay" when the sound level drops to 40 db below the level prevailing on interruption of the source. Actuation of this relay causes reversal of the motion of the recording pen of a decibel meter, the distance between turning point and zero axis giving the reverberation time. A frequency scale is provided on the record by means of a Wien-bridge circuit connected to the tone generator.

534.85 1831
Thorn Needles—C. E. Watts, S. Kelly. (*Wireless World*, vol. 57, pp. 121–122; March, 1951.) Comments on 806 of May (Pollock).

534.85/.86:[621.396.645.029.3+621.395.623.7 1832
The FAS Audio System: Parts 3 and 4—M. B. Sleeper. (*FM-TV*, vol. 10, pp. 24–26; December, 1950. vol. 11, pp. 32–35, 38; February, 1951.) Description of (a) methods of adapting the FAS loudspeaker system to any good amplifier, (b) the construction of an 8-foot-air coupler, (c) experiments with 15-inch loudspeakers for high volume output. Parts 1 and 2: 805 and 804 of May.

534.86:621.396.712 1833
Developments in Studio Design—L. L. Beranek. (*Proc. IRE* (Australia), vol. 12, pp. 21–25; January, 1951.) Reprint. *See* 1847 of 1950.

621.3.018.78†:621.395.613.3 1834
Graphical Representation of Nonlinear Distortion—(*Radio Tech. Dig.* (France), vol. 4, no. 5, pp. 279–290; 1950.) French version of paper abstracted in 2964 of 1950 (Bressi and Sacerdote).

621.395.623.7 1835
Improving Loudspeaker Response with Motional Feedback—R. L. Tanner. (*Electronics*, vol. 24, pp. 142..240; March, 1951.) A negative feedback voltage is obtained from a feedback coil wound over the existing voice coil in a conventional loudspeaker. This voltage, induced by the movement of the voice coil, is fed back to the driving amplifier. Mechanical and magnetic data for the design of an amplifier-loudspeaker combination are listed for five typical loudspeakers.

621.395.623.7:621.3.018.78†:621.317.79 1836
An Automatic Nonlinear Distortion Analyzer [for loudspeakers]—H. F. Olson and D. F. Pennie. (*RCA Rev.*, vol. 12, pp. 35–44; March, 1951.) The system consists of the standard automatic recorder for obtaining the frequency-response curve, combined with a set of switched high-pass filters, which suppress the fundamental and pass the harmonics. The overall-amplitude-frequency characteristic and the distortion-amplitude-frequency characteristic are recorded on the same sheet, and the percentage distortion at any frequency is obtained by comparing the two curves.

621.395.625.3 1837
Magnetic Recording with A.C. Bias—R. E. Zenner. (Proc. I.R.E., vol. 39, pp. 141–146; February, 1951.) The function of ac bias in magnetic recording is analyzed in a manner similar to that used to explain AM. Certain simplifying assumptions are made to facilitate manipulation of mathematical expressions. The analytical results are compared with experimental observations of harmonic distortion amplitude of fundamental, spurious recorded frequencies, frequency response, difficulty of erasure, and others.

621.395.625.6 1838
Electron-Optical Sound-Recording Device—P. G. Tager. (*Compt. Rend. Acad. Sci.* (URSS), vol. 73, pp. 1181–1183; August 21, 1950. In Russian.) An arrangement of two cathode-ray tubes with x deflections synchronized at a frequency much higher than the highest af. One tube has also a y-deflection system controlled by microphone currents, and has a modulation-controlling mask of some desired pattern interposed in front of a signal plate. Film is traversed in the y direction past the fluorescent screen of the second tube, whose beam is switched on or off according as current is or is not flowing in the signal-plate circuit, as controlled by the mask.

621.395.92 1839
A Master Hearing Aid—E. Aspinall. (*Jour. Brit. IRE*, vol. 11, pp. 45–50; February, 1951.) Description of a speech transmission system with widely variable characteristics, suitable for speech tests on deaf patients. Automatic-level-control, peak-limitation, and attenuation-distortion circuits can be selected as desired, the merits of any transmission path being assessed by analysis of sound articulation scores.

621.395.92 1840
The Design of Commercial Hearing Aids—J. P. Ashton. (*Jour. Brit. IRE*, vol. 11, pp. 51–59; February, 1951.) A description of the engineering technique adopted in the design and construction of hearing aids with a view to providing instruments of the smallest possible size. Details of components and circuit elements are given.

ANTENNAS AND TRANSMISSION LINES

621.392.26† 1841
Cut-off Frequency in Two-Dielectric Layered Rectangular Waveguides—J. van Bladel and T. J. Higgins. (*Jour. Appl. Phys.*, vol. 22, pp. 329–334; March, 1951.) Equations for the modes and eigenvalues are derived for a guide containing a single dielectric layer, a dielectric

sandwich, or an air sandwich. Cut-off frequencies are shown graphically for a range of geometric and dielectric parameters.

621.392.26†:621.396.52 1842
U.H.F. Filters and Lenses—P. Marié. (*Radio Tech. Dig.* (France), vol. 4, nos. 5 and 6, pp. 291–312 and 359–364; 1950. vol. 5, no. 2, pp. 97–109; 1951.) The analogy between optical and radio waves and the general theory of transparency are discussed, with particular reference to a system consisting of a series of metal diaphragms in a waveguide. Expressions derived for attenuation, etc., are applied to the problems of design of a band filter, losses being assumed negligible; a numerical example is given. Effects of losses due to resistance, and of multiple reflections in the transient regime, are analyzed. The theory of em lenses is considered and the required phase rotation is determined. The elements of calculation are indicated for the design of lenses of the pseudo-dielectric, the accelerating, and the retarding types.

621.392.26†:621.396.67 1843
Radiation Characteristics of Open Rectangular Waveguides (Horns) for Fundamental and Harmonic Oscillations in the H-Mode—W. Reichardt. (*Frequenz*, vol. 5, pp. 23–27; January, 1951.) Theoretical determination of the radiation field for the H_{mn} mode for different values of m and n.

621.396.67 1844
The Field Radiated by Circular and Square Helical Beam Antennas—H. L. Knudsen. (*Trans. Dan. Acad. Tech. Sci.*, no. 8, 55 pp.; 1950.) Theoretical investigations, as well as measurements, have shown that the current distribution on a helical antenna radiating in the axial mode may be described, for the greater part of the helix, as a progressive current wave with constant amplitude and phase velocity, moving along the wire away from the feed point. Formulas for the em field, radiated from an arbitrary current distribution, are reviewed and applied to the calculation of the field radiated by a circular helical antenna. The field is expressed in the form of rapidly converging series. The general formulas are used to derive the field of a helix with an integral number of turns, and a numerical example is worked out. Corresponding calculations are made for a square helical antenna, the field components being obtained as closed expressions from which approximate formulas for the circular-helical antenna are derived. The series obtained for the circular helix are, however, so rapidly convergent and the closed expressions for the square helix are so simple that approximate formulas are hardly necessary.

621.396.67:621.397.6 1845
TV Receiving Antenna Research, Design and Production—R. G. Peters. (*TV Eng.*, vol. 2, pp. 8–10; February, 1951.) A report of methods used by some United States' manufacturers.

621.396.671.4 1846
Complex Radiation Impedance of an Aerial System Electromagnetically Coupled to Another Aerial System—R. G. Mirimanov. (*Compt. Rend. Acad. Sci.* (URSS), vol. 73, pp. 1177–1179; August 21, 1950. In Russian.) Formulas are derived for the case of two systems, each comprising a linear oscillator and a reflector having the form of a surface of revolution.

621.396.677 1847
Gain of Electromagnetic Horns—W. C. Jakes, Jr. (Proc. I.R.E., vol. 39, pp. 160–162; February, 1951.) An experimental investigation is described. For the horns tested it was found (a) that edge effects are <0.2 db, so that the gain may be computed to within that accuracy from their physical dimensions, using Schelkunoff's curves (2295 of 1943); (b) that for the transmission of power between two horns the ordinary transmission formula is valid, provided that the distance between the horns is measured between suitable reference points on the horns and not between their mouths.

621.396.677:538.56:535.312 1848
Experimental Determination of the Reflection Coefficient of Metal-Plate Media—Ruze and Young. (*See* 1880.)

621.396.677:538.56:535.312 1849
Reflection and Transmission at the Surface of Metal-Plate Media—Lengyel. (*See* 1879.)

621.396.677:621.396.9 1850
Microwave Radar Antenna—H. N. Chait. (*Electronics*, vol. 24, pp. 103–105; March, 1951.) The polarization characteristics are determined in the transmission-line system, where a magic-T junction is used with a variable-phase shifter. Any arbitrarily chosen elliptical polarization can be transmitted and received by proper adjustment of the phase shift and rotation of the antenna feed. A circularly polarized search radar system can be used with a single antenna, as the transmitter for a circular component and the receiver for the reflected circular component are located at different terminals of the junction.

CIRCUITS AND CIRCUIT ELEMENTS

517.92:621.396.611.1 1851
Topological Methods for Investigating Problems Relating to Nonlinear Oscillations—T. Vogel. (*Ann. Télécommun.*, vol. 6, pp. 2–10; January, 1951.) The methods considered are useful for giving a physical insight into the phenomena corresponding to nonlinear differential equations, and for demonstrating the influence of various parameters. Work done by Poincaré, Bendixson, and Dulac is surveyed, and the concepts of singular points, limit cycles etc. are discussed. The method is used to investigate the solutions of nonlinear second-order differential equations having applications in physics, and is particularly suitable for dealing with discontinuous phenomena, such as sawtooth oscillations. Topographical systems can be displayed on cro screens.

517.93:621.319.55 1852
On Amplitude Bounds for Certain Relaxation Oscillations—N. Wax. (*Jour. Appl. Phys.*, vol. 22, pp. 278–281; March, 1951.) Amplitude limits are derived for the unique periodic solution of the generalized Lienard equation

$$\ddot{x}+f(x)\dot{x}+g(x)=0,$$

when the functions $f(x)$ and $g(x)$ are suitably restricted. The restrictions are less severe for the lower than for the upper limits. A class of equations is noted, which includes the van der Pol equation and satisfies all the restrictions. Numerical results are given for the van der Pol equation.

621.314.2+621.318.42].003.1 1853
Minimum-Cost Transformers and Chokes—H. C. Hamaker and T. Hehenkamp. (*Philips Res. Rep.*, vol. 5, pp. 357–394; October, 1950.) The theoretical design of a transformer is governed by the dependence of the price on the dimensions, and the way the apparent power and losses depend on the dimensions, magnetic-flux density, and electric-current density. The problem of minimum cost, when power and losses are prescribed, is considered for various types of transformer. The solution is given in tabular form for practical application, and examples are calculated. This solution is, however, unsatisfactory in that it gives a design and price dependent only on the ratio of power to losses and not on their absolute magnitudes. Modifications of the theory to take account of limitations imposed by maximum temperature or flux density are discussed.

621.318.4:621-05 1854
Universal Coil Winding—E. Watkinson. (*Jour. Brit. IRE*, vol. 11, pp. 61–69; February, 1951.) Reprint. *See* 2993 of 1950.

621.392.012.8 1855
Study of a Meshed Hydraulic Network, by the Method of Equalization of Loads: Reduction to an Equivalent Electrical Network—C. Dubin and M. Magnien. (*Rev. gén. élect.*, vol. 60, pp. 70–74; February, 1951.)

621.392.5:621.3.015.3:518.3 1856
Spectrum Analysis of Transient-Response Curves—H. A. Samulon. (Proc. I.R.E., vol. 39, pp. 175–186; February, 1951.) A method of computing the amplitude and phase response of a network from its measured transient response is described. Tables and abacs are included to facilitate numerical evaluation.

621.392.52 1857
Resistance and Capacitance Twin-T Filter Analysis—L. G. Gitzendanner. (*Tele-Tech*, vol. 10, pp. 46–48, 71; February, 1951.) The twin-T circuit is redrawn in a way that makes its operation easier to understand. Formulas are developed for conditions of equal and unequal source and load impedance. Various applications in feedback circuits are discussed.

621.396.52:621.392.26† 1858
U.H.F. Filters and Lenses—Marié. (*See* 1842.)

621.392.54†:621.396.662 1859
A High Power Attenuating Tuner for a High-Q Ten-Cm Cavity—R. R. Perron. (*Rev. Sci. Instr.*, vol. 22, pp. 116–117; February, 1951.) A water-cooled attenuator constructed of polystyrene is described, which serves simultaneously to absorb about half the 900-kw peak output of a magnetron and to tune the cavity to the magnetron frequency.

621.396.611.1 1860
Alternative Ways in the Analysis of a Feedback Oscillator and its Application—E. J. Post and H. F. Pit. (Proc. I.R.E., vol. 39, pp. 169–174; February, 1951.) An oscillator is regarded as a closed loop comprising (a) an amplifier and (b) a passive frequency-determining network. Attenuation, introduced to limit oscillation amplitude, is often regarded as improving the phase discrimination of (b), but may equally well be regarded as improving the phase stability of (a) by negative feedback. Well-known oscillator circuits are examined from this viewpoint, and a 2-tube stabilized crystal oscillator incorporating a thermistor is analyzed.

621.396.611.21:534.133 1861
Thickness-Shear and Flexural Vibrations of Crystal Plates—R. D. Mindlin. (*Jour. Appl. Phys.*, vol. 22, pp. 316–323; March, 1951.) The theory of flexural motions of elastic plates, including the effects of rotatory inertia and shear, is extended to crystal plates. The equations are solved approximately for the case of rectangular plates, excited by thickness-shear deformation parallel to one edge. Results of computations of resonance frequencies of rectangular AT-cut quartz plates are shown and compared with experimental data. Simple algebraic formulas are obtained relating frequency, dimensions, and crystal properties for resonances of special interest.

621.396.611.4 1862
The Variation of Resonance Wavelength and Damping of Cavity Resonators on Introduction of Dielectric Rings—E. M. Philipp. (*Acta Phys. austriaca*, vol. 1, pp. 246–258; February, 1948.) The problem considered is that of the circuit in which a cavity resonator is sealed directly to a tube and is arranged for continuous tuning. The influence of the location of the dielectric member forming the boundary of the evacuated region is examined. Variation

of resonance wavelength and damping with position of the dielectric ring is shown in graphs. For minimum additional damping, the ring should be as near as possible to the cavity boundary, for example, in a region of low electrical field strength. The theory is confirmed by experiments.

621.396.611.4 1863

Phenomena in Electromagnetic Resonators near the Natural Frequency—V. B. Shteinshleiger. (*Compt. Rend. Acad. Sci.* (URSS), vol. 65, pp. 669–672; April 11, 1949. In Russian.)

621.396.615:621.384.612.1† 1864.

The Design of Cyclotron Oscillators—J. Backus. (*Rev. Sci. Instr.*, vol. 22, pp. 84–92; February, 1951.) The procedure used to design the oscillator for the 60-inch cyclotron at Berkeley is described.

621.396.645+621.396.727].012 1865

Comparative Graphical Study of Problems relating to the Cathode Follower and the Feedback Phase Inverter—(*Radio Tech. Dig.*, (France), vol. 4, pp. 259–269; 1950.) French version of papers abstracted in 1386 of 1950 and 298 of March (Malatesta).

621.396.645.015.7 1866

The Problem of the "Best" Pulse Receiver Comparison of Various Pulse Amplifiers—L. Huber and K. Rawer. (*Arch. elekt. Übertragung*, vol. 4, pp. 475–484 and 523–526; November and December, 1950.) Three types of circuit are analyzed, having response curves respectively peaked, multi-humped, and flat-topped. The optimum compromise between faithful reproduction and low-time lag on the one hand, and high amplification and sensitivity on the other is considered in relation to the different purposes for which the receiver may be required. Four-stage amplifiers of the three types are compared, and their advantages and disadvantages summarized.

621.396.645.35 1867

The Automatic Compensation of Zero-Drift Errors in Direct-Coupled Feedback Systems—F. A. Summerlin. (*Proc. IEE* (London), Part II, vol. 98, pp. 59–66; February, 1951.) Degenerative feedback cannot correct zero-drift errors of direct-coupled amplifiers; a method is described whereby an auxiliary amplifier is used for this purpose. With suitable switching, a single auxiliary amplifier can be used to correct continuously the balance of a number of main feedback systems. The effects of the balancing circuits on stability are discussed with particular reference to a position-control servo system.

621.396.645.35 1868

Direct-Coupled Amplifier Starvation Circuits—W. K. Volkers. (*Electronics*, vol. 24, pp. 126–129; March, 1951.) Stage gains of up to 2,500 have been obtained by using pentodes with very low screen-grid voltages and greatly increased anode loads. A "starved" direct-coupled two-stage amplifier requires fewer components than the normal *RC*-coupled amplifier. The frequency response is severely limited, but can be much improved by use of negative or regenerative feedback.

621.396.645.37:621.396.662 1869

Tuning Systems employing Feedback Amplifiers—P. G. Sulzer. (*Electronics*, vol. 24, pp. 252, 258; March, 1951.) The effective value of an inductance or capacitance can be altered by means of a feedback amplifier of high-input and low-output impedance. A cathode-follower circuit can be tuned over a wide-frequency range by potentiometer control. Wide-deviation-frequency modulation can thus be obtained at radio frequencies; two-stage circuits have been used for resistance-tuned audio oscillators.

621.396.662.22:538.533:621.398 1870

The Magnetic Variometer—A. Weis. (*Funk u. Ton*, vol. 4, pp. 508–518 and 559–568; October and November, 1950.) From a detailed theoretical treatment of the principle of varying the inductance of a hf coil by magnetic means, practical design requirements for a magnetic variometer are derived, particularly in respect of the magnetic characteristics of coil and core. Ferrite cores are specially suitable. For remote tuning of receivers the dust core of the hf coil may be arranged in the air gap of an electromagnet. This application and the use of the device for remote control of coupling are described.

621.397.645.37 1871

Linearization of the Frequency Response of Wide-Band Amplifiers by Negative Feedback—W. Dillenburger. (*Frequenz*, vol. 5, pp. 1–5; January, 1951.) The basic design of a video-frequency amplifier stage, with (a) compensated anode circuit, (b) selective feedback, is considered. The latter has better response at low frequencies and low-modulation depths but experiment shows that serious distortion of pulses with short rise time may occur.

GENERAL PHYSICS

534.1+538.56]:621.319.55 1872

A New Method of Studying Relaxation Processes—N. A. Tolstoi and P. P. Feofilov. (*Zh. Eksp. Teor. Fiz.*, vol. 19, pp. 421–430; May, 1949. In Russian.)

534.232:538.652 1873

Magnetostrictive Vibration of Prolate Spheroids. Preliminary Measurements—J. S. Kouvelites and L. W. McKeehan. (*Rev. Sci. Instr.*, vol. 22, pp. 108–111; February, 1951.)

535.42:538.56 1874

On Bethe's Theory of Diffraction by Small Holes—C. J. Bouwkamp. (*Philips Res. Rep.*, vol. 5, pp. 321–332; October, 1950.) The problem is considered of the diffraction of a plane-polarized-em wave incident, normally on a small circular hole in an infinite-plane-conducting screen. Bethe's theory of this problem [706 of 1945; see also 1378 of 1945 (Pekeris: Bethe)] is examined and his expression for the fictitious magnetic-current density in the aperture is found to be incorrect. This results in Bethe's formulas for the field near the hole being seriously in error although his results for the distant field are correct.

537.226 1875

Processes in Dielectrics containing Free Charges—B. Breyer and F. Gutmann. (*Jour. Roy. Soc. NSW*, vol. 83, Part 1, pp. 66–74; 1949.) The free electrostatic energy, capable of doing reversible work, stored in a space-charge filled capacitor is calculated, yielding an expression for the effective dielectric constant of a medium containing free charges. Analogies with thermal quantities are established and electrical entropy is defined. It is shown that a space-charge-filled capacitor may be loss free if the sum of the free charges is constant or proportional to the potential difference across the plates.

537.311.33 1876

The Fermi Limiting Energy of Electronic Semiconductors—H. Muser. (*Z. Naturf.*, vol. 5a, pp. 18–25; January, 1950.) The concepts of the Wilson semiconductor model are examined quantitatively, and the dependence of the Fermi-limiting energy on temperature and on the nature and concentration of the impurity centers is calculated. The limiting energy is shown to be the determining factor for the electrical behavior of the semiconductor.

537.581 1877

Convenient Methods for Thermionic Emission Calculations—H. F. Ivey and C. L. Shackelford. (*Tele-Tech*, vol. 10, pp. 42–43, 68; February, 1951.) *See* 1902 of 1950.

538.56:535.312 1878

A Note on Reflection and Transmission—B. A. Lengyel. (*Jour. Appl. Phys.*, vol. 22, pp. 263–264; March, 1951.) Propagation through the interface of two media is dependent on their reflection coefficients and transmission coefficients. Relations between these four quantities are applied to the calculation of reflection from dielectric sheets and from metal-plate structures.

538.56:535.312:621.396.677 1879

Reflection and Transmission at the Surface of Metal-Plate Media—B. A. Lengyel. (*Jour. Appl. Phys.*, vol. 22, pp. 265–276; March, 1951.) The theory of Carlson and Heins (2756 and 3504 of 1947) has been extended; an expression is found for the reflection coefficient applicable in the presence of a diffracted beam. Tables and graphs are included for the coefficients associated with electromagnetic phenomena at the surface of metal-plate media. The magnitude of the reflection coefficient was measured at normal incidence and the phase of the transmission coefficient for angles of incidence from 0 to 25°. A satisfactory agreement with theory is obtained.

538.56:535.312:621.396.677 1880

Experimental Determination of the Reflection Coefficient of Metal-Plate Media—J. Ruze and M. Young. (*Jour. Appl. Phys.*, vol. 22, pp. 277–278; March, 1951.) A method of measurement at 3-cm wavelength is described. Back reflections are eliminated by means of an absorbing wedge. The results obtained for structures of very thin plates are in good agreement with the theory of Carlson and Heins (2756 and 3504 of 1947). For plates of moderate thickness the measured reflection near normal incidence is higher than that predicted for an infinitely thin set of plates with identical index of refraction.

538.566 1881

Wave Packets, the Poynting Vector, and Energy Flow: Part I—Non-Dissipative (Anisotropic) Homogeneous Media—C. O. Hines. (*Jour. Geophys. Res.*, vol. 56, pp. 63–72; March, 1951.) The object of the present analysis is to correlate the results obtained from the two commonly used methods for finding the velocity of propagation of energy in em waves, the one method involving wave packets and the other the Poynting vector. For nondissipative media the two methods are found to give the same direction of propagation of energy.

538.566.2 1882

The Propagation of Electromagnetic Waves in Slightly Heterogeneous Layers—G. Eckart. (*Compt. Rend. Acad. Sci.* (Paris), vol. 232, pp. 1294–1296; March 28, 1951.) A method developed by Schelkunoff is used to derive formulas representing the propagation of a plane wave in a system consisting of a layer whose dielectric constant varies linearly with one co-ordinate, and which is bounded along that co-ordinate by two layers with uniform dielectric constant. The formulas indicate that small departures from uniformity of the dielectric constant cannot be determined from the reflections and deformations of pulses, though large departures can be so determined.

537.122/.123 1883

Negative Ions [Book Review]—H. S. W. Massey. Publishers: Cambridge University Press, New York, N. Y. 2nd ed., 1950, 133 pp., $2.50. (*Jour. Frank. Inst.*, vol. 251, pp. 301–302; February, 1951.) "A unique and satisfying combination of theory and experimental data and description is contained in this book on negative ions in the gas phase at pressures lower than a few mm of Hg."

GEOPHYSICAL AND EXTRATERRESTRIAL PHENOMENA

523.4:621.396.11 1884

Shortwave Radio Propagation Correlation with Planetary Positions—Nelson. (*See* 1997.)

523.5:621.396.9 1885
The Interpretation of Radar Echoes from Meteor Trails—J. Feinstein. (*Jour. Geophys. Res.*, vol. 56, pp. 37–51; March, 1951.) Maxwell's equations are applied to investigate the scattering of em waves by a column of electrons, for various cylindrically symmetrical distributions of electron density within the column, in particular for a linear radial variation and for a uniform density distribution. Results are presented graphically in terms of the average effective dielectric constant, the ratio of cylinder circumference to wavelength, and the polarization of the incident wave. A new picture of the trail-decay process is developed from a comparison of these results with published observational data.

523.746 1886
Mean Areas and Heliographic Latitudes of Sunspots in the Year 1945—(*Mon. Not. R. Astr. Soc.*, vol. 110, no. 5, pp. 501–504; 1950.)

523.746"1950.10/.12" 1887
Provisional Sunspot—Numbers for October to December, 1950—M. Waldmeier. (*Jour. Geophys. Res.*, vol. 56, p. 130; March, 1951.)

523.75:550.385 1888
On the Expulsion of Corpuscular Streams by Solar Flares—F. D. Kahn. (*Mon. Not. R. Astr. Soc.*, vol. 110, no. 5, pp. 477–482; 1950.) The corpuscular stream, which is the probable cause of terrestrial magnetic disturbances associated with solar flares, is thought to arise from the action of the flares themselves. The minimum momentum density of the stream required to produce a magnetic storm is calculated. Analysis of the effects of atomic reasonance absorption and ionization, produced by radiation pressure, shows that this pressure alone is insufficient to expel such a stream from the sun.

523.75:550.385 1889
An Investigation into the Possibility of Observing Streams of Corpuscles Emitted by Solar Flares—F. D. Kahn. (*Mon. Not. R. Astr. Soc.*, vol. 110, pp. 483–490; 1950.)

523.752:537.591 1890
An Increase of the Primary Cosmic-Ray Intensity following a Solar Flare—M. A. Pomerantz. (*Phys. Rev.*, vol. 81, pp. 731–733; March 1, 1951.) An increase of about 15 per cent in the cosmic-ray intensity at altitudes of about 100,000 feet occurred about 19 hours after the commencement of the solar flare of May 10, 1949.

523.8:538.12 1891
The Strength of Interstellar Magnetic Fields—L. Davis, Jr. (*Phys. Rev.*, vol. 81, pp. 890–891; March 1, 1951.) Discussion of the possibility of the existence of magnetic fields as strong as 10^{-4} gauss in interstellar space.

538.12:523.7 1892
Magneto-hydrostatic Fields—S. Lundquist. (*Ark. Fys.*, vol. 2, pp. 361–365; December 28, 1950.) Theoretical investigation of the properties of magnetic fields existing in electrically conducting fluids at rest. Such fields may have an important bearing on solar and terrestrial magnetism and may be responsible for trapping cosmic rays.

538.712 1893
The 1950 World Isogonic Chart—A. M. Weber and E. B. Roberts. (*Jour. Geophys. Res.*, vol. 56, pp. 81–84; March, 1951.) An account of the process used by The United States Coast and Geodetic Survey for compiling the new edition. Punched-card machines were used. The results have been published by The United States Navy Hydrographic Office in one mercator and two polar charts.

550.38"1950.07/.09" 1894
International Data on Magnetic Disturbances, Third Quarter, 1950 J. Bartels and J. Veldkamp. (*Jour. Geophys. Res.*, vol. 56, pp. 127–129; March, 1951.)

550.38"1950.10/.12" 1895
Cheltenham [Maryland] Three-Hour-Range Indices *K* for October to December, 1950—R. R. Bodle. (*Jour. Geophys. Res.*, vol. 56, p. 130; March, 1951.)

550.385"1950.07/.12" 1896
Principal Magnetic Storms [July-Dec. 1950]—(*Jour. Geophys. Res.*, vol. 56, pp. 141–133; March, 1951.)

551.5:621.396.11 1897
Meteorological Aspects of Very-Short-Wave Propagation in the Atmosphere—Hauer. (*See* 1998.)

551.510.535 1898
Fine Structure of the Lower Ionosphere—R. A. Helliwell, A. J. Mallinckrodt, and F. W. Kruse, Jr. (*Jour. Geophys. Res.*, vol. 56, pp. 53–62; March, 1951.) Night-time vertical-incidence *h't* records taken in California, at frequencies of 100 and 325 kc, show a series of reflections at heights between 90 and 130 km. The characteristics and polarization of the echoes are described, and several tentative explanations discussed. It is concluded that the region is divided into a series of partially reflecting strata, by a mechanism yet to be explained.

551.510.535 1899
Characteristics of the E_s Region at Brisbane—R. W. E. McNicol and G. de V. Gipps. (*Jour. Geophys. Res.*, vol. 56, pp. 17–31; March, 1951.) The region was studied over the period 1943 to 1949, and the seasonal and diurnal changes are described and discussed. Two types of E_s region are distinguished, the one being formed at greater heights and descending to its final position (E_{ss}), while the other is formed in situ (E_{sc}). E_{ss} is predominant in summer, blankets strongly, and probably has a uniform ionization density; E_{sc} is a winter type, blankets little, and probably has lateral irregularities. No correlation is found between either type and sunspot number, ionospheric storms, or meteoric activity.

551.510.535 1900
An Investigation of Certain Properties of the Ionosphere by means of a Rapid-Frequency-Change Experiment—B. H. Briggs. (*Proc. Phys. Soc.* (London), vol. 64, pp. 255–274; March 1, 1951.) Apparatus is described in which the receiver is kept in tune with the transmitter by afc circuits, operated by the direct pulse from the transmitter. The tuning is corrected by each pulse and remains fixed during the intervals between pulses. A frequency range of 1 mc, selected anywhere in the range 2 to 20 mc, can be covered in 1 second. Applications of the equipment are described and typical records are reproduced.

"The irregularities of ionization present in the normal regions are investigated by observing the irregular variations of the amplitude of the reflected wave, which are produced when the frequency is altered. Irregularities of ionization are sometimes found to be localized in height. Observations of the reflection coefficient of the abnormal region *E* suggest that there are two distinct types of region, one an irregular region consisting of scattering clouds, the other a coherent layer with a thickness of the order of 5 km. The apparatus is also used to study the behavior of the subsidiary critical frequencies, often present below the main critical frequency of region *E*. It is found that these are always decreasing whenever they are observed. Records of amplitude and group path near the critical frequency of a region can be used to determine the collision frequencies of electrons. The treatment is mainly descriptive, and a full discussion of those records which require a detailed quantitative analysis is reserved for a later paper."

551.510.535 1901
Vertical-Incidence Ionosphere Absorption at 150 kc—A. H. Benner. (PROC. I.R.E., vol. 39, pp. 186–190; February, 1951.) Recordings over a period of one year, using 150 μs pulses with a folded-dipole antenna 3,000 feet long and 96 feet high, have shown that, (a) vertical-incidence absorption at night is of the order of 1 neper, (b) maximum absorption in the daytime varies from 2 nepers in midwinter to about 7 nepers (too high to measure) in midsummer, (c) the exponent of cos χ (χ = sun's zenith angle) that relates it to the total absorption is about 0.7 for the morning and 0.6 for the afternoon, (d) the exponent necessary to explain the seasonal change is considerably larger than that given by the diurnal curves, and (e) absorption lags behind the value of χ.

551.510.535:534.21 1902
On the Propagation of Sound over Great Distances—Veldkamp. (*See* 1542 of August.)

551.510.535:621.396.11 1903
Ionosphere Review: 1950—T. W. Bennington. (*Wireless World*, vol. 57, pp. 109–111; March, 1951.) The variations of the monthly mean values of the F_2 layer-critical frequency, for Slough at noon and midnight, are considered and related to corresponding variations for earlier years. The variation in relative sunspot number is similarly considered. A general indication is given of the probable trend of ionospheric conditions during 1951. The incidence during 1950 of recurrent ionospheric storms, as observed at the BBC receiving station at Tatsfield, is discussed with reference to the forecasting of ionospheric conditions.

551.510.535:621.396.11 1904
The Work of the [Australian] Radio Research Board—Munro. (*See* 1999.)

551.510.535:621.396.11 1905
The Gyro-Frequency in the Arctic E-Layer—Scott. (*See* 2001.)

551.594.11 1906
The Semidiurnal Fluctuations of Atmospheric Potential Gradient—H. Israel. (*Arch. Met. Geophys. Bioklimatol. A*, vol. 1, pp. 247–251; December 4, 1948.) The double-hump curve representing the variation of atmospheric potential gradient with time of day is interpreted as consisting of two superposed curves, (a) a simple fluctuation with a minimum in the early morning and a maximum in the afternoon, and (b) a depression during the daytime, caused by turbulent exchange. The second of these components depends on the season and on the location of the observation station, in respect of distance from large towns, where the content of nuclei and large ions in the atmosphere is high.

551.594.221 1907
The Approximate Mean Height of the Thundercloud Charges taking part in a Flash to Ground—V. Barnard. (*Jour. Geophys. Res.*, vol. 56, pp. 33–35; March, 1951.) Measurements are described. The results obtained from 10 flashes give an over-all mean of 5.2 km, in agreement with those obtained previously by another method.

551.594.5 1908
Southern Extent of Aurora Borealis in North America—C. W. Gartlein and R. K. Moore. (*Jour. Geophys. Res.*, vol. 56, pp. 85–96; March, 1951.) "Results are presented for the first 11 years of a study of the frequency of overhead auroras in North America, as a function of latitude in a region south of the auroral zone. The data have been averaged in various ways so that monthly and annual variations are demonstrated. It appears that there is a relatively constant level of auroral

activity throughout the year in the region 58° to 60° geomagnetic latitude, while auroras appearing overhead south of these latitudes are more frequent during equinoctial periods. Auroras have been seen as far south as 52°, during this period every month of the year. Correlation of auroral frequency with sunspot number is not high on a month-by-month or three-month running-mean basis."

551.594.5:621.396.11 1909
A V.H.F. Propagation Phenomenon Associated with Aurora—Moore. (*See* 2002.)

551.594.6 1910
On the Measurement and Nature of Atmospherics Produced by Electric Discharges in Snow Squalls and from Other Sources—H. Norinder. (*Tellus*, vol. 1, pp. 1–13; May, 1949.) The differences between atmospherics originating within snow squalls and those produced by lightning discharges are pointed out. Methods of measuring atmospherics using an open-wire antenna and cro indicator are described. Examples are given of typical meteorological situations associated with the occurrence of these atmospherics, and of typical discharge waveforms observed.

LOCATION AND AIDS TO NAVIGATION

621.396.9 1911
The Design and Application of a Marine Radar System—F. W. Garrett. (*Marconi Rev.*, vol. 14, pp. 23–38; 1st Quarter, 1951.) The trend of present practice as applicable to merchant-shipping requirements is reviewed and a detailed description is given of prototype "Radiolocator" equipment, including particulars of the transmitter, the display console, the antenna scanning unit, motor generator, and control apparatus. Typical installations in ships are illustrated; performance is well within the Ministry of Transport specification.

621.396.9 1912
Harbour-Control Radar—(*Wireless World*, vol. 57, pp. 105–107; March, 1951.) A brief description of Decca radar, type I. A simple corner-fed "half-cheese" antenna is used, having an aperture of 9 feet; this type of antenna shows lower side-lobe amplitudes than the conventional cheese antenna. The pulse duration used in the equipment is 0.06 μs. Examples of the high-range discrimination of the system are quoted. Arrangements are incorporated for using three display consoles up to 1,000 yards from the scanner. The possibility is mentioned of using centimeter-wave links to relay information to a central office, in circumstances where it is necessary to use a number of scanners to cover a harbor adequately.

621.396.9:523.5 1913
The Interpretation of Radar Echoes from Meteor Trails—Feinstein. (*See* 1885.)

621.396.9:621.396.677 1914
Microwave Radar Antenna—Chait. (*See* 1850.)

621.396.9.082:523.5 1915
A Circuit for Simultaneously Recording the Range, Amplitude, and Duration of Radar-Type Reflections—V. C. Pineo and R. C. Peck. (*Rev. Sci. Instr.*, vol. 22, pp. 112; February, 1951.) The circuit briefly described was developed at the National Bureau of Standards for observing meteor-trail reflections of durations ranging from less than one up to several hundred seconds. A specially adapted cro display was used in conjunction with an automatic camera recorder.

621.396.932 1916
New Crystal-Controlled Radar Beacon—J. W. Busby. (*Tele-Tech*, vol. 10, pp. 24–26, 70; January, 1951.) The model TB-140 "ramark" beacon, used in conjunction with marine radar receivers having a bandwidth of about 6 mc, radiates on a frequency of 9.31 kmc, with square-wave modulation at 100, 200, or 300 kc. The radio frequency is derived by multiplication from a crystal-controlled master oscillator. Final multiplication is performed by a newly developed klystron tube, the SMX 32, which acts as a frequency doubler and power amplifier with an output of 2.5 w. The modulator is crystal controlled and is applied to one of the intermediate multiplying stages. Three of these units have been installed on the Ambrose Lightship outside New York harbor, the Detour Reef Lighthouse on Lake Huron, and Lightship 116 in Chesapeake Bay.

621.396.933:621.396.11.029.51 1917
Low-Frequency Radio-Wave Propagation by the Ionosphere, with particular reference to Long-Distance Navigation—Williams. (*See* 1761 of August.)

621.396.933.2 1918
Distance-Measuring Equipment for Civil Aircraft: Part 2—D.M.E. Responder Beacons—J. P. Blom and J. D. Gilchrist. (*Proc. IRE* (Australia), vol. 12, pp. 9–20; January, 1951.) Part 1: 1392 of July (Lindsay, Blom, and Gilchrist). See also 1659 of August.

621.396.933.4:621.396.5 1919
Multi-Carrier Air Communications—(*See* 2016.)

MATERIALS AND SUBSIDIARY TECHNIQUES

531.788.7 1920
The Measurement of High Vacuum by Electrical Methods—F. Wade. (*Electronic Eng.* (London), vol. 23, pp. 30–34 and 44–48; January and February, 1951.) A review of methods depending on (a) the thermal conductivity of gases, (b) ionization phenomena, and comparison of various types of gauge, with a table showing their optimum pressure ranges.

535.376:549.621.22 1921
Cathodoluminescence of Zinc Orthosilicate with Manganese Activator—S. Larach and R. E. Shrader. (*Jour. Appl. Phys.*, vol. 22, p. 362; March, 1951.) The results of measurements of the light output, at constant current, as a function of accelerating voltage are shown for three different thicknesses of screen material. In the range investigated, 10 to 50 kv, equations of the form $L = KV^n$ do not fit the results, except possibly for the thickest screen (9 mg/cm²), where n is approximately 0.8.

535.376:621.385.832 1922
The Luminescence of Cathode-Ray-Tube Screens—R. Roulaud. (*Rev. gén. élect.*, vol. 60, pp. 61–70; February, 1951.) The theoretical bases of luminescence in gases, liquids, and solids are discussed. The luminous intensity of cathode-ray-tube screens is calculated. Factors influencing the luminous efficiency are considered, and methods of improving efficiency and life are indicated.

535.376:621.397.621.2 1923
Saturation of Fluorescence in Television Tubes—A. Bril and F. A. Kröger. (*Philips Tech. Rev.*, vol. 12, pp. 120–128; October, 1950.) Fluorescence efficiency decreases with high beam density, due to the limited number of activator centers. For continuous bombardment, saturation depends on the activator concentration and average life-time. For discontinuous irradiation, as in television, there is no dependence on the life time if this lies between the time for two successive passages and the time required to scan a certain spot. Sulphide phosphors are preferable for the smaller current densities, while silicates are better for conditions of heavy loading. The matching of screen-material components, to avoid color change in white-fluorescing mixtures at high current densities, is discussed. Color change may still occur with defocused beams, even for mixtures with uniform characteristics.

537.228.1:546.472.21 1924
The Piezoelectric Constant of Zinc-Sulphide—B. D. Saksena. (*Phys. Rev.*, vol. 81, pp. 1012–1015; March 15, 1951.) The piezoelectric constant is calculated by a method previously used for α quartz (2538 of 1948), for which good agreement was obtained with measurements.

537.311.32:539.234:546.23 1925
The Electrical Properties of Selenium Coatings—P. H. Keck. (*Jour. Opt. Soc. Amer.*, vol. 41, pp. 53–55; January, 1951.) Conductivity measurements were made on thin evaporated Se layers, unilluminated and illuminated. The results indicate that for coating temperatures below 50°C only vitreous Se is formed, whereas, for higher coating, temperatures crystalline Se is formed. From the rectifier properties of the layers, it is deduced that p-type conduction occurs in vitreous Se and n-type in the crystalline material.

537.311.33 1926
On the Aggregation of Trapping Centers in Semiconductors or Insulators—T. Hibi and T. Matsumura. (*Phys. Rev.*, vol. 81, pp. 884–885; March 1, 1951.)

537.311.33 1927
Measurement of Semiconductor Impurity Content—C. N. Klahr and L. P. Hunter. (*Phys. Rev.*, vol. 81, pp. 1059–1060; March 15, 1951.) Formulas and curves are given for calculating impurity concentration from measurements of conductivity σ and Hall constant R at a low temperature (e.g. 10° to 20°K for Ge) and of R at a temperature in the exhaustion range. The analysis is based on the assumption of scattering by lattice defects, by ionized impurities, and by nonionized impurities.

537.311.33:546.289 1928
The Mobility and Life of Injected Holes and Electrons in Germanium—J. R. Haynes and W. Shockley. (*Phys. Rev.*, vol. 81, pp. 835–843; March 1, 1951.) "The mobilities of holes injected into n-type germanium and of electrons injected into p-type germanium have been determined by measuring transit times between emitter and collector in single-crystal rods. Strong electric fields, in addition to those due to injected current, were employed so that spreading effects due to diffusion were reduced. The mobilities at 300°K are 1,700 cm per vcm for holes and 3,600 cm per vcm for electrons, with an error of probably less than 5 per cent. The value for electrons is about 20 per cent higher than the best estimates obtained from the conventional interpretation of the Hall effect, and the difference may be due to curved energy-band surfaces in the Brillouin zone. Studies of rates of decay indicate that recombination of holes and electrons takes place largely on the surface of small samples with constants varying from 10^2 to $>10^4$ cm for special treatments.

537.311.33:546.482.21 1929
Dependence of Electrical Properties of Cadmium Sulphide Crystals on Electrode Arrangement—I. Broser and R. Warminsky. (*Z. Naturf.*, vol. 5a, pp. 62–63; January, 1950.) Experiments are reported which indicate the practicability of using CdS crystals for rectifiers or triodes or as photosensitive elements.

537.311.33:549.351.11 1930
On the Semiconductor Bornite—C. W. Horton. (*Jour. Appl. Phys.*, vol. 22, pp. 364; March, 1951.) The dc voltage characteristics published by El Sherbini and Yousef (2959 of 1939 and 1647 of 1941) are used to derive the energy levels for bornite between 120° and 170°C.

537.533:546.883 1931
Periodic Deviations in the Schottky Effect for Polished Tantalum—G. B. Finn, W. B. LaBerge, and E. A. Coomes. (*Phys. Rev.*,

vol. 81, p. 889; March 1, 1951.) Schottky data for polished Ta wire show no significant difference from data for unpolished wire, for fields below 5×10^4 per cm.

538.221 1932

Measurement of the Gyromagnetic Constant of the Ferromagnetic Elements and of some Isoelectronic Alloys of the Iron Group—A. J. P. Meyer. (*Ann. Phys.* (Paris), vol. 6, pp. 171–210; January and February, 1951.)

538.221 1933

The Use of Eddy Currents for Investigating Ferromagnetic Substances—I. Épelboin. (*Rev. gén. élect.*, vol. 60, pp. 74–84; February, 1951.) The technique of electrolytic polishing, coupled with the study of eddy currents, has materially assisted investigations into the behavior of inhomogeneous-ferromagnetic substances, subjected to weak alternating magnetic fields. The anomalous behavior of high-permeability specimens in these fields is due partly to a nonuniform distribution of permeability with depth,—the macroscopic magnetic structure of the material,—and partly to a magnetic-viscosity effect, associated with the diffusion of impurities. The application of successive electrolytic polishings permits the separation of these effects, but involves the destruction of the specimen. The comparative study of eddy currents provides, in a limited range of cases, a nondestructive technique for determining the structure. Technical applications are indicated and figures are quoted showing that electrolytic polishing produces a marked increase of permeability and a diminution of eddy-current losses in various standard ferromagnetic alloys. A bibliography of 41 references is appended.

538.221 1934

A Survey of the Possible Applications of Ferrites—K. E. Latimer and H. B. MacDonald. (*Commun. News*, vol. 11, pp. 76–90; September, 1950.) The general mechanical and magnetic properties of ferrites, particularly those of the Mn-Zn ferrite now produced commercially as "ferroxcube III," are described. Ferrites are homogeneous ceramics and may be molded to shape and conveniently machined by grinding. The initial permeability of ferroxcube III is 700 to 1,500 and its resistivity 20 to 100 Ω./cm.[3] Engineering applications for which ferrites have been tried, and others for which it is suggested they may be suitable, are discussed. Graphs, references, and dimensioned sketches are given in illustration of the examples. The applications include filter coils of small size and high Q factor, hf transformers for frequencies from 10 kc to 50 mc, power transformers for carrier frequencies, harmonic generators, and delay lines.

538.652 1935

Magnetostriction of Fe/Pd and Ni/Pd Alloys—Z. I. Alizade. (*Compt. Rend. Acad. Sci.* (URSS), vol. 73, pp. 79–81; July 1, 1950. In Russian.)

538.652 1936

The Magnetostriction Hysteresis of High-Coercivity Alloys—D. I. Volkov. (*Compt. Rend. Acad. Sci.* (URSS), vol. 73, pp. 87–89; July 1, 1950. In Russian.)

541.183.26:546.78 1937

The Formation of Mobile and Immobile Films of Oxygen on Tungsten—R. C. L. Bosworth. (*Jour. Roy. Soc. NSW*, vol. 83, part 1, pp. 31–38; 1949.) At low temperatures, the condensation of O_2 on W follows Roberts' theory. At higher temperatures, the process proceeds the more slowly, the higher the temperature or the lower the pressure.

549.514.51 1938

The Use of Quartz in Radio Equipment—C. Warenghem. (*Rev. gén. élect.*, vol. 60, pp. 49–56; February, 1951.) An account of the properties of natural quartz and of current practice in cutting, calibrating, and mounting the finished crystals. Large scale production methods are described, and the precautions necessary to secure a high quality product are indicated.

549.514.51:621.396.611.21 1939

Interferometric Studies on the Vibration of Piezoelectric Plates—S. Tolansky and W. Bardsley. (*Proc. Phys. Soc.* (London), vol. 64, pp. 224–230; March 1, 1951.) Description of multiple beam interference investigations. A stroboscopic method, in which the intensity of the light source is modulated at the crystal frequency, reveals the phase relations between the vibrations of different parts of the crystal surface. Typical interference patterns are illustrated.

549.514.51:621.396.611.21.002.2 1940

The Manufacture of Quartz Oscillator-Plates: Part 3—Lapping and Final Frequency Adjustment of the Blanks—W. Parrish. (*Philips Tech. Rev.*, vol. 12, pp. 166–177; December, 1950.) Description of the principles and operation of the planetary lap machine, which can deal with 30 to 55 plates simultaneously. The resonance frequency of the crystals can be measured during lapping by using the piezoelectric emf set up by mechanical vibration. Final frequency adjustment is made by etching in ammonium bifluoride. Part 2: 664 of April.

621.3.011.5:547.38 1941

Dielectric Properties of Ketones—V. Daniel and K. H. Stark. (*Trans. Faraday Soc.*, vol. 47, pp. 149–155; February, 1951.) Experiments are described which prove that Muller's results published in 1937 and 1938 do not support Fröhlich's theory (3304 of 1946).

621.314.632:546.289 1942

Significance of Composition of Contact Point in Rectifying Junctions on Germanium—W. G. Pfann. (*Phys. Rev.*, vol. 81, p. 882, March 1, 1951.) During forming, certain metal electrodes pass donors or acceptors to the semiconductor, modifying the properties of the junction. Donors can pass from phosphor-bronze to p-type Ge, thereby lowering the effective work function for electrons leaving the metal, and therefore, improving the rectification ratio. Furthermore, the current multiplying factor of an n-type Ge transistor increases with increasing donor (Sb) concentration in the collector electrode.

621.314.634 1943

A Study of Electrical Forming Phenomena at Selenium Contacts—H. K. Henisch and J. Ewels. (*Proc. Phys. Soc.* (London), vol. 64, pp. 277–278; March 1, 1951.) Discussion on 926 of May.

621.315.33:679.57 1944

Wire and Cable Insulating Materials with Polyvinyl Chloride as Base—E. A. J. Mol. (*Phillips Tech. Rev.*, vol. 12, pp. 97–110; October, 1950.) A comprehensive review of the mechanical, electrical, and chemical properties of polyvinyl chloride insulation, with descriptions of the extrusion method of coating wire and of the principal types of "Podur" wire.

621.315.612.4:546.431.82 1945

The Dielectric Properties of $BaTiO_3$ at Low Temperatures—W. J. Merz. (*Phys. Rev.*, vol. 81, pp. 1064–1065; March 15, 1951.) Measurements on single-domain crystals from room temperature to 4.2°K are described. Dielectric loss and spontaneous polarization remain constant, while permittivity decreases and the coercive field strength increases with decreasing temperature.

621.315.613.1 1946

Progress in Synthetic Mica—R. D. Jackel. (*Elec. Mfg.*, vol. 45, pp. 99–103, 192; March, 1950.) A report on investigations being made by several USA government agencies into the problem of growing, on a commercial scale, large crystals having properties comparable with those of natural mica.

621.318.3/.4.013.5 1947

Magnetic Field Leakage at the Edges of Airgaps—E. Bergtold. (*Elektrotech Z.*, vol. 72, pp. 111–113; February 15, 1951.) The leakage field is investigated and shown graphically for a number of common cases, and an empirical formula is given for determining the extent of the associated increase of effective cross section of the field.

621.318.323.2.042.15 1948

Some Properties and Tests of Magnetic Powders and Powder Cores—C. E. Richards, P. R. Bardell, S. E. Buckley, and A. C. Lynch (*Proc. IEE* (London), Part II, vol. 97, pp. 236–245; April, 1950. *Elec. Commun.* (London), vol. 28, pp. 55–69; March, 1951.) Conversion factors are given relating various recognized systems of expressing the electrical losses in powder cores. Test apparatus and methods used in the laboratory and in production control are described. Relevant properties of many materials are tabulated.

669.198.865:621.385.032.2 1949

Aluminum-Clad Iron for Electron Tubes—W. Espe and E. B. Steinberg. (*Tele-Tech*, vol. 10, pp. 28–30, 72; February, 1951.) Materials developed in Germany and in The United States as substitutes for nickel are described; properties and manufacturing procedures are tabulated.

669.75:621:357.7 1950

Antimony Plate—A. Bregman. (*Metal Progress*, vol. 59 pp. 245–247; February, 1951.) Plating techniques are described which render Sb suitable as a substitute for Ni and Cr in a variety of applications, including radio and radar equipment requiring protection against corrosion.

MATHEMATICS

517.54 1951

An Epitomization of the Basic Theory of the Generalized Schwarz-Christoffel Transformations as used in Applied Physics—T. J. Higgins. (*Jour. Appl. Phys.*, vol. 22, pp. 365–366; March, 1951.) Basic theory is outlined and 26 references are given to books and papers on these transformations, which are being increasingly used in hf circuit theory.

681.142 1952

Universal High-Speed Digital Computers: Small-Scale Experimental Machine—F. C. Williams, T. Kilburn, and G. C. Tootill. (*Proc. IEE* (London), Part II, vol. 98, pp. 13–28; February, 1951.) The electronic machine described uses the serial binary-digital system of number representation. Its principle of operation is explained in detail. The storage is by cathode-ray tube. When extended, as allowed for in the design, the machine will be intrinsically capable of performing any computation automatically.

681.142 1953

The General Purpose Analog Computer—A. A. Currie. (*Bell Lab. Rec.*, vol. 29, pp. 101–109; March, 1951.) Description of computer based on a three-stage negative-feedback amplifier, for performing addition, subtraction, multiplication, division, integration, and differentiation.

681.142 1954

Problem Solving with the Analog Computer—E. Lakatos. (*Bell Lab. Rec.*, vol. 29, pp. 109–114; March, 1951.)

512,831 1955

Matrizen [Book Review]—R. Zurmühl. Publishers: Springer-Verlag, Berlin, Germany, 1950, 427 pp., DM25.20. (*Frequenz*, vol. 4, pp. 301–302; November, 1950.) An introduction

to matrix methods in analysis, starting from fundamental principles and including many examples of their application. " . . . can be recommended to anyone concerned with matrix calculus."

517.93 1956

Ordinary Nonlinear Differential Equations in Engineering and Physical Sciences [Book Review]—N. W. McLachlan. Publishers: Clarendon Press, Oxford, 1950, 201 pp., $4.25. (*Jour. Frank. Inst.*, vol. 251, p. 303; February, 1951.) "The book is *not* an analytical treatise with technical applications. It aims to show how certain types of nonlinear problems may be solved, and how experimental results may be interpreted by aid of nonlinear analysis. The contents of the book include: General Introduction, Equations Readily Integrable, Equations Integrable by Elliptic Integrals and Functions, Equations Having Periodic Solutions, Method of Slowly Varying Amplitude and Phase, The Equivalent Linear Equation, Equations having Periodic Coefficients, and Graphical and Numerical Solutions."

518.12+517.392 1957

Numerical Mathematical Analysis [Book Review]—J. B. Scarborough. Publishers: Johns Hopkins Press, Baltimore, Md., 2nd edn., 1950, 511 pp., $6.00 (*Jour. Frank. Inst.*, vol. 251, pp. 303–304; February, 1951.) "Chapters have been included on the numerical solution of partial differential equations and on integral equations. The chapters on the numerical solution of ordinary differential equations and on numerical integration have been thoroughly revised and enlarged."

MEASUREMENTS AND TEST GEAR

621.317.029.6:061.3 1958

Conference on High-Frequency Measurements, Washington, D. C., 10th–12th January 1951—(Proc. I.R.E., vol. 39, pp. 208–211; February, 1951.) Summaries are given of the following technical papers presented:

1—Program for Atomic Frequency and Time Standards—A Survey—H. Lyons.
2—Improved NBS Ammonia Clock—B. F. Husten.
3—The Stabilization of a Microwave Oscillator with an Ammonia Absorption Line Reference—E. W. Fletcher and S. P. Cooke.
4—Performance of Oscillators Frequency-Controlled by Gas Absorption Lines—L. E. Norton.
5—Millimeter-Wave Measurements—W. Gordy.
6—Quartz-Crystal Frequency Standards—W. D. George.
7—High-Frequency Crystal Units for Primary Frequency Standards—A. W. Warner.
8—Inflection-Point Method of Measuring *Q* at Very-High Frequencies—N. E. Beverly.
9—A Precise Sweep-Frequency Method of Vector Impedance Measurement—D. A. Alsberg.
10—Precision Coaxial Resonance Line for Impedance Measurements—H. E. Sorrows, R. E. Hamilton, W. E. Ryan, and Ming S. Wong.
11—A 2,600- to 4,000-MC VSWR-Measuring Set—S. F. Kaisel and J. W. Kearney.
12—Measurement of Waveguide and Coaxial-Line Impedances with a Circular Waveguide—A. E. Laemmel.
13—Survey of Microwave Dielectric Techniques for Small Liquid and Solid Samples—G. Birnbaum.
14—Microwave Spectroscopy with Application to Chemistry, Nuclear Physics, and Frequency Standards—L. J. Rueger, R. G. Nuckolls, and H. Lyons.
15—Recording Atmospheric Index of Refraction at Microwaves—G. Birnbaum, S. J. Kryder, and R. R. Larson.
16—Measurement of Microwave Field Patterns using Photographic Techniques—W. E. Kock.
17—Absolute Microwave Power Measurements—A. C. Macpherson and D. M. Kerns.
18—Broad-Band Bolometer Development—W. E. Waller.
19—Calibrating Ammeters above 100 MC—H. R. Meahl and C. C. Allen.
20—A Microwave Oscillograph—W. B. Sell and J. V. Lebacqz.
21—Precision Millidecibel Waveguide-Attenuation Measurements—J. H. Vogelman.
22—Dissipative and Piston Attenuator Corrections—C. M. Allred.
23—A Field-Strength Meter for 600 MC—J. A. Saxton.
24—Measuring Techniques for Broad-Band Long-Distance Radio Relays—W. J. Albersheim.
25—Wide-Band Swept-Frequency Measurements Applicable to Traveling-Wave Tubes—F. E. Radcliffe.
26—Microwave Techniques in the 28,000- to 300,000-MC Region—L. Swern.
27—Measurement of Characteristics of Crystal Units—L. F. Koerner.
28—Reflecting Surface to Simulate an Infinite Conducting Plane at Microwave Frequencies—S. J. Raff.

621.317.3.001.4.621.396.615.142.2 1959

3-cm Low-Voltage Reflex Klystron, Type RHK 6332—Chantereau, Musson-Genon, and Metivier. (*See* 2069.)

621.317.335 1960

The Double-Superheterodyne Principle applied to Dielectric Measurements—E. B. Baker. (*Rev. Sci. Instr.*, vol. 22, pp. 34–36; January, 1951.) Description, with circuit diagrams, of generator-detector equipment for the range 0 to 16 kc, which includes two mixers and a common variable-frequency local oscillator. Advantages are (a) single-dial tuning, (b) freedom from relative frequency drift and (c) improved signal-noise ratio. The equipment is particularly suitable for use with automatic-balancing bridges. Extension of the range to 600 kc is practicable.

621.317.335.2.088 1961

The Influence of Mutual and Self Inductances on the Accurate Determination of Capacities—A. Michels and C. A. ten Seldam. (*Appl. Sci. Res.*, vol. B2, pp. 73–76; 1951.) Formulas indicating the effect of lead inductances are presented. To avoid measurement errors, common leads should be avoided.

621.317.336/.34.029.6 1962

Applications of Directional Couplers to Amplitude-Ratio and Phase Measurement at Very High Frequencies—B. M. Sosin. (*Marconi Rev.*, vol. 14, pp. 39–57; 1st Quarter, 1951.) A critical survey is made of methods of accurate measurement of impedance or admittance at vhf, and a new technique is described in which two waves are sampled independently by directional couplers and compared in amplitude and phase. Essential parts of the apparatus are discussed and procedures are outlined for input impedance measurement, matching of input impedance, matching of discontinuities, and for measurements of insertion-loss, crosstalk, power division at a junction, and attenuation constant of a transmission line. The method of setting up the equipment is described and an estimate made of the probable errors.

621.317.336.088 1963

Evaluation of Coaxial-Slotted-Line Impedance Measurements—H. E. Sorrows, W. E. Ryan, and R. C. Ellenwood. (Proc. I.R.E., vol. 39, pp. 162–168; February, 1951.) The errors introduced by probe coupling, attenuation, and by the slot can be estimated and those due to structural defects can be measured. The errors in measuring the voltage SWR and the position of the nodes are analyzed, and the accuracy of the resultant impedance calculation is determined.

621.317.351 1964

The Radiospectroscope SFM 101—W. C. van B. Jutting. (*Commun. News*, vol. 11, pp. 120–125; December, 1950.) The apparatus comprises fm oscillator, sawtooth oscillator, mixer, amplifiers, detector, and cro, and is adapted to work in conjunction with any receiver having an IF between 400 and 500 kc. The observation frequency band is ±50 kc with respect to a center frequency of 140 kc +receiver IF. Application is particularly for measurement of frequency deviation, carrier shift and modulation distortion in fm transmitters, and of modulation depth and parasitic fm and asymmetrical modulation in AM transmitters.

621.317.361 1965

A Modern Frequency Measuring Installation—H. A. Taylor and E. C. Rundquist. (*Electronics*, vol. 24, pp. 98–102; March, 1951.) An account of RCA equipment and methods providing, through receiving stations at Riverhead, Long Island, Point Reyes, California, and Manila, a commercial service with worldwide coverage except at vhf and uhf, where the effective range is limited to 200 to 500 miles, depending on propagation conditions. The primary frequency standards are 100-kc quartz crystal oscillators, which are frequently compared with observatory time signals and with standard-frequency radio transmissions. The main equipment measures frequencies over the range from 100 kc to 26 mc, with extensions to provide measurements from 15 kc to 100 kc and from 26 mc to 500 mc. The average deviation of the primary standard-frequency source is approximately 1 cycle in 5×10^8, while the possible error in the interpolation system is less than 2 cps at any frequency from 15 kc to 26 mc. The antenna arrays permit a wide choice of directive pattern, so that interference can be largely eliminated.

621.317.7:621.392.26† 1966

Some Aspects of Waveguide Technique—A. E. Pannenborg. (*Commun. News*, vol. 11, pp. 65–75; September, 1950.) See 946 of May.

621.317.723 1967

Circuits and Tubes for Ultra-Sensitive Electrometers—F. E. O'Meara. (*Rev. Sci. Instr.*, vol. 22, pp. 106–108; February, 1951.)

621.317.725:621.396.622.7 1968

The Audion Valve Voltmeter—H. Boucke. (*Frequenz*, vol. 4, pp. 281–289; November, 1950.) Discussion of the design details of the instrument, particularly component values in the detector circuit, methods of calibration and adjustment, and stabilization. The circuit comprises basically a grid-leak detector and a compensating tube in two arms of a bridge circuit. Methods are described for extending the range.

621.317.727.027.213 1969

High-Sensitivity Automatic Recording Potentiometer—S. Ekelöf and B. Nilsson. (*IVA, Stockholm*, vol. 21, no. 4, pp. 153–162; 1950.) The arrangement includes a standard potentiometer circuit and an automatically balancing feedback circuit consisting of null galvanometer, photocell, and two-stage dc amplifier. Voltage variations <0.001 per cent can easily be recorded. Accuracy is to within 5 to 10 per cent of full-scale deflection. Possible applications include investigation of the stability of dc voltage sources such as primary batteries.

621.317.79:621.3.018.78†:621.395.623.7 1970

An Automatic Nonlinear Distortion Analyzer [for loudspeakers]—Olson and Pennie. (*See* 1836.)

621.317.79:621.396.619 1971
The N.R.U. [Nederlandse Radio Unie] Modulation Monitor Type ON301—R. Y. Drost. (*Tijdschr. ned. Radiogenoot.*, vol. 16, pp. 1–11. Discussion p. 12; January, 1951.) The unit described forms part of the equipment standardized for use in stations of the Netherlands Union of Broadcasting Corporations. The scale of the instrument is logarithmic for modulation depths up to 50 per cent and linear above that value. Pulses of amplitude within the linear scale range and of duration below a given time interval (e.g. 500 ms) are automatically lengthened to enable their value to be correctly indicated. Light-spot indicators are used.

621.396.619.13:[621.317.761+621.317.7:621.396.619 1972
Communication-System Monitor—J. E. Stiles. (*FM-TV*, vol. 11, pp. 16–18; February, 1951.) General description, with block diagram and simplified circuit diagrams of the discriminator and reference oscillator, of the Hewlett-Packard fm monitor, Model 337, which enables measurements to be made of both carrier frequency and peak modulation swing of transmissions in the range 30 to 175 mc.

621.317 1973
Basic Electrical Measurements [Book Review]—M. B. Stout. Publishers: Prentice-Hall, New York, N. Y., 1950, 504 pp., $5.75. (*Jour. Frank. Inst.*, vol. 251, p. 304; February, 1951.) "The book would make a fine text for an electrical engineering course."

621.317.323 1974
High-Frequency Voltage Measurements. National Bureau of Standards Circular 481 [Book Review]—M. C. Selby. Publishers: U. S. Department of Commerce, 14 pp., $0.20. (*Tijdschr. ned. Radiogenoot.*, vol. 16, p. 54; January, 1951.) Principles and methods are given for both high-accuracy (to within 1 per cent and medium-accuracy (to within 5 per cent) measurements. The frequency range covered is from about 10 kc to about 100 mc. A useful list of references is included.

OTHER APPLICATIONS OF RADIO AND ELECTRONICS

534:577 1975
A Bibliography on Sonic and Ultrasonic Vibration: Biological, Biochemical and Biophysical Applications—Naimark, Klair, and Mosher. (*See* 1813.)

534.321.9.001.8 1976
Latest Developments in Ultrasonics—A. R. Laufer. (*Electronics*, vol. 24, pp. 82–86; March, 1951.) Discussion of the generation and use of ultrasonic energy, with particular reference to the high-power generator in use at the University of Missouri. Some methods of mounting quartz crystals in ultrasonic oscillators are illustrated. A short-range optical communication system, in which the modulator is a xylene-filled ultrasonic-diffraction cell, can be used for distances up to 5,000 yards at night with an infrared filter.

537.533 1977
On the Spherical Aberration of Electron Emission Systems—O. Klemperer and Y. Klinger. (*Proc. Phys. Soc.* (London), vol. 64, pp. 231–233; March 1, 1951.) Both the spherical aberration and the apparent source diameter for a "hairpin" emission system are found to be less than the corresponding values for various other emission systems.

621.317.083.4 1978
Radio Telemetry—M. H. Nichols and L. L. Rauch. (*Rev. Sci. Instr.*, vol. 22, pp. 1–29; January, 1951.) An extensive theoretical survey of possible methods and discussions of characteristics. Frequency and time-division types are considered in detail, and comparisons of crosstalk and fluctuation noise, complexity, and reliability are made. Recording and instrumentation are considered, and crosstalk due to overload and restricted bandwidth are calculated. Information theory is applied and the efficiency of various systems estimated.

621.38.001.8 1979
Detecting Tramp Metal in Logs and Iron Ore—C. W. Clapp. (*Electronics*, vol. 24, pp. 88–93; March, 1951.) Based on a 1950 National Electronics Conference paper. Analysis of the problem of detecting a small metal sphere in an ac field, and a description of practical application to the detection of (a) bullets and shell fragments in logs floating down a flume, (b) broken drills in highly magnetic taconite iron ore carried on a conveyor belt.

621.38.001.8 1980
Microwaves offer New Control Functions—W. C. White. (*Elec. Mfg.*, vol. 45, pp. 86–89, 170; March, 1950.) A general account is given of methods suitable for radiating and detecting microwaves, and the particular conditions under which microwave relays can usefully supplant photocell relays are discussed.

621.384.612.1†:621.396.615 1981
The Design of Cyclotron Oscillators—J. Backus. (*Rev. Sci. Instr.*, vol. 22, pp. 84–92; February, 1951.) The procedure used to design the oscillator for the 60-inch cyclotron at Berkeley is described.

621.384.612.2† 1982
An Air-Cored Synchro-Cyclotron for 400-MeV Protons—L. Riddiford. (*Proc. Phys. Soc.* (London), vol. 64, pp. 218–224; March 1, 1951.

621.385.38:621.316.7.076.7 1983
Thyratron Grid-Circuit Design—J. H. Burnett. (*Electronics*, vol. 24, pp. 106–111; March, 1951.) Seven basic methods for phase control of firing in thyratrons, and four primary sources of noise voltages in thyratron circuits are analyzed, with circuit diagrams and waveforms. Criteria for reliable operation are based on consideration of maximum critical grid current, transients, and frequency.

621.385.833 1984
Investigation of Electron Optical Properties of an Electrostatic Focusing System—W. E. Spear. (*Proc. Phys. Soc.* (London), vol. 64, pp. 233–243; March 1, 1951.) Paraxial ray tracing, together with a dynamical determination of electron trajectories in the cathode region, leads to a complete analysis of electron-optical immersion systems. The method is applied to an electrode arrangement for use in a fine-focus X-ray tube [1450 of July (Ehrenberg and Spear)].

621.385.833 1985
Electron-Optical Systems with Helical Axis—D. Gabor. (*Proc. Phys. Soc.* (London), vol. 64, pp. 244–255; March 1, 1951.) Systems with curved axes can be designed which are equivalent to centered systems in the Gaussian approximation, but have chromatic error of opposite sign and thus can be used as correcting elements. Theory is given of such systems with a helical axis, with a helical electrostatic field shaped so as to eliminate first-order astigmatism. The properties of such systems, and their applications, are discussed.

621.385.833 1986
Electron Microscopes—M. Locquin. (*Electronique* (Paris), pp. 5–21, 44–49; October, 1950.) A comprehensive illustrated survey of models available on the world market, compiled from information supplied by the makers.

621.385.833 1987
International Congress on Electron Microscopy—(*Électronique* (Paris), pp. 22–38; October, 1950.) Summaries are given in French and English of papers presented at the congress held in Paris, September 14–22, 1950.

621.385.833:621.396.615.141.2 1988
Electron Optical Exploration of Space Charge in a Cut-Off Magnetron—D. L. Reverdin. (*Jour. Appl. Phys.*, vol. 22, pp. 257–262; March, 1951.) Detailed account of the work noted in 2315 of 1950.

621.387.4† 1989
The Elimination of the End Effects in Counters—A. L. Cockroft and S. C. Curran. (*Rev. Sci. Instr.*, vol. 22, pp. 37–42; January, 1951.

621.387.4† 1990
A Note on the Successive Peaks of Spurious Counts in G-M Tubes—J. E. Kupperian, Jr., P. C. Murray, and H. Feeny. (*Rev. Sci. Instr.*, vol. 22, pp. 60–61; January, 1951.)

621.396.662.22:538.533:621.398 1991
The Magnetic Variometer—Weis. (*See* 1870.)

621.385.833 1992
The Electron Microscope, Its Development, Present Performance and Future Possibilities [Book Review]—D. Gabor. Publishers: Chemical Publishing Co., New York, N. Y., 2nd ed., 1948, 164 pp., $4.95. (*Jour. Opt. Soc. Amer.*, vol. 40, pp. 879–880; December, 1950.) Written from the point of view of the physicist; mathematical details are kept to a minimum.

PROPAGATION OF WAVES

538.566 1993
Wave Packets, the Poynting Vector, and Energy Flow: Part 1—Non-Dissipative (Anisotropic) Homogeneous Media—Hines. (*See* 1881.)

538.566.2 1994
The Propagation of Electromagnetic Waves in Slightly Heterogeneous Layers—Eckart. (*See* 1882.)

621.396.11 1995
Fluctuations of the Angle of Departure of Ionospheric Waves—W. Budde. (*Arch. elekt. Übertragung*, vol. 4, pp. 509–516; December, 1950.) A method is described which enables the vertical and azimuthal components of the angle of departure to be determined in one step. The equipment comprises in principle two pairs of transmitting antennas whose base lines, 2λ long, are set at a given angle. The total phase difference D between the radiations from the antennas, of a single pair, is the sum of the difference due to the geometrical separation, δ, and the electrical phase difference, Δ. δ is kept constant while Δ is varied until the field strength recorded at the receiver is zero, i.e., $D=\pi$; δ is thus determined. The direction of departure is found from the phase differences for the two pairs of antennas. For a transmission distance of 1,500 km fluctuations of elevation angle of 5° to 10° were measured. The deviations from great circle ranged from 3° to 5°. Operating frequency was 9.8 mc.

621.396.11 1996
World Charts in Short-Wave Engineering—T. W. Bennington. (*BBC Quart.*, vol. 6, pp. 43–54; Spring, 1951.) The importance of the ionosphere in making possible long-distance communication is discussed. Advance information on ionospheric conditions several months ahead is desirable to enable frequency allocations to be used efficiently. A qualitative description is given of the methods used in deriving the maximum usable frequency for propagation via the ionosphere. The effects of ionospheric absorption and noise at the receiver site on the lowest usable frequency are described.

621.396.11:523.4 1997
Shortwave Radio Propagation Correlation with Planetary Positions—J. H. Nelson. (*RCA Rev.*, vol. 12, pp. 26–34; March, 1951.) Consideration is given to "planetary configurations" in which the radius vectors of two planets include an angle equal to zero or a multiple of 90°. The distribution in time of such configurations was compared with observations of disturbances in SW propagation conditions over the North Atlantic; good correlation is claimed.

621.396.11:551.5 1998
Meteorological Aspects of Very-Short-Wave Propagation in the Atmosphere—A. Hauer. (*Tijdschr. ned. Radiogenoot.*, vol. 16, pp. 39–52; January, 1951.) An outline is given of the theory of refraction and scattering of radio waves in the troposphere, and of the influence of humidity and temperature gradients on propagation. The criterion for a ray to be refracted back to earth is discussed. Meter waves can be received beyond the horizon, even when the vertical gradient of modified refractive index is not negative; when this gradient is negative, ducts are formed and superrefraction occurs. Measurements made over the Caribbean Sea, on a wavelength of 9 cm, are compared with calculated values of signal strength as a function of distance from the transmitter, and of the scattering due to 4-, 6-, and 8-cm atmospheric "blobs." Agreement is good. A comparison also indicates some correlation between radiosonde measurements and the observed quality of certain 3-m communication links in Holland.

621.396.11:551.510.535 1999
The Work of the [Australian] Radio Research Board—G. H. Munro. (PROC. IRE (Australia), vol. 12, pp. 41–43; February, 1951.) The history of the Board is reviewed and the development of the ionospheric prediction service during the war period 1939 to 1946, is described. Post-war investigations of movements in the ionosphere *F* layer are surveyed, and other investigations are discussed briefly.

621.396.11:551.510.535 2000
Ionosphere Review: 1950—Bennington. (*See* 1903.)

621.396.11:551.510.535 2001
The Gyro-Frequency in the Arctic *E*-Layer—J. C. W. Scott. (*Jour. Geophys. Res.*, vol. 56, pp. 1–16; March, 1951.) Calculation of the gyrofrequency in the *E* layer in Northern Canada, from measurements of critical-frequency differences, gives a lower value of terrestrial magnetic field than extrapolation from ground-level values. At one station, a large semidiurnal variation with maxima at 0600 and 1800 LMT was found. The explanation given for similar effects in the *F* layer (1471 of July) is not applicable. In the *E* layer, the effects may be caused by a variable concentration of heavy ions, rising to over 4,000 times the density of free electrons.

621.396.11:551.594.5 2002
A V.H.F. Propagation Phenomenon Associated with Aurora—R. K. Moore. (*Jour. Geophys. Res.*, vol. 56, pp. 97–106; March, 1951.) Abnormal propagation has been observed at frequencies between 28 and 148 mc, during auroral activity. The effects observed include a very high rate of fading, such as to render radio-transmitted speech unintelligible, the absence of any skip effect, and the necessity for the transmitting and receiving antennas to be pointed northwards. The correlation of these effects with the southerly limit of auroral displays is examined.

RECEPTION

621.316.726:621.396.62 2003
Automatic Frequency Control for Single-Sideband Receivers—J. L. Arends. (*Commun. News*, vol. 11, pp. 101–119; December, 1950.) A brief explanation is given of ssb operation, and the elements of an afc circuit are discussed. Two forms of afc are distinguished, viz., electronic and electromechanical; a combination of the two is required for ssb reception during fading. A description is given of an electromechanical system using the "flotor," a small variable capacitor comprising a tube of insulating material containing oil, within which a metal core is able to move freely. Special problems arising when afc is used in conjunction with frequency-shift telegraphy are mentioned.

621.396.621 2004
Communication Receiver Design—D. Heightman. (*Radiotronics*, pp. 99–105, 121; October, 1950.) Reprint. *See* 1235 of 1950.

621.396.645.015.7 2005
The Problem of the "Best" Pulse Receiver. Comparison of Various Pulse Amplifiers—Huber and Rawer. (*See* 1866.)

621.396.397.82 2006
Open-Field Test Facilities for Measurement of Incidental Receiver Radiation—C. G. Seright. (*RCA Rev.*, vol. 12, pp. 45–52; March, 1951.) Description of a test setup for measuring interference radiation from television and fm receivers.

621.397.8 2007
Investigation of Ultra-High-Frequency Television Transmission and Reception in the Bridgeport, Connecticut, Area—Guy. (*See* 2037.)

621.396.62.004.67:621.397.62 2008
Wireless Servicing Manual [Book Review]—W. T. Cocking. Publishers: Iliffe and Sons, London, Eng., 8th ed., 1950, 296 pp., 12s. 6d. (*Jour. Brit. IRE*, vol. 11, p. vi; February, 1951.) Revised and brought up to date; the chapter on television has been completely rewritten. Problems of hum and distortion are treated very thoroughly.

STATIONS AND COMMUNICATION SYSTEMS

621.39.001.11 2009
Maxwell's Demon cannot operate: Information and Entropy: Part 1—L. Brillouin. (*Jour. Appl. Phys.*, vol. 22, pp. 334–337; March, 1951.) "In an enclosure at constant temperature, the radiation is that of a "black body," and the demon cannot see the molecules. Hence, he cannot operate the trap door and is unable to violate the second principle. If we introduce a source of light, the demon can see the molecules, but the over-all balance of entropy is positive. This leads to the consideration of a cycle.

Negentropy→Information→Negentropy

for Maxwell's demon as well as for the scientist in his laboratory. Boltzmann's constant k is shown to represent the smallest possible amount of negative entropy [negentropy] required in an observation."

621.39.001.11 2010
Physical Entropy and Information: Part 2—L. Brillouin. (*Jour. Appl. Phys.*, vol. 22, pp. 338–343; March, 1951.) "The laws of statistical thermodynamics are used for the definition of entropy, and it is shown that the definition of information can be reduced to a problem of Fermi-Dirac statistics or to a generalized Fermi statistics. With these definitions, the entropy of a certain message can be defined, and the information contained in the message can be directly connected with the decrease of entropy in the system.

This definition leads directly to the formulas proposed by C. E. Shannon [455 of March (Shannon and Weaver)] for the measure of information, and shows that Shannon's "entropy of information" corresponds to an equal amount of negative entropy in the physical system. The physical background of the whole method is discussed and found in agreement with previous discussions."

621.39.001.11:061.3 2011
Survey of the Work of the Conference on Information Theory—M. D. Indjoudjian. (*Ann. Télécommun.*, vol. 6, pp. 27–31; January, 1951.) An account of the proceedings at the symposium held in London in September, 1950. An account in English was noted in 984 of May (Jackson).

621.39.001.11:621.397.5 2012
Television and the Transmission of Information—Delbord. (*See* 2028.)

621.395.44:621.396.619.2 2013
A 48-Channel Carrier Telephone System: Part 2—Apparatus Design—G. H. Bast, D. Goedhart, and J. F. Schouten. (*Commun. News*, vol. 11, pp. 91–100; September, 1950.) Reprint. See 3251 of 1949. Reprint of part 1 noted in 739 of April.

621.396.216:621.396.619.24 2014
The Single-Sideband System of High Frequency Radio Transmission—E. T. Wrathall and C. P. Beanland. (*Marconi Rev.*, vol. 14, pp. 2–22; 1st Quarter, 1951.) A simple and general treatment of the subject is given. The theoretical advantages of a ssb system over dsb systems, considered from the signal-noise bandwidth, and carrier-suppression viewpoints, are shown to be borne out in practice. A comparison of radiated-power requirements and dc anode input powers shows a marked economy in favor of the ssb transmission. Five ways of using the sideband spectrum for music, speech, and telegraph channels are outlined, and the power distribution per channel is considered for each case.

Diagrams of typical ssb generating equipment and monitoring circuits for carrier level, distortion, and interchannel crosstalk are given. Details of the power amplifier circuits of the transmitter are discussed. The process of multiple heterodyning in a typical ssb receiver, to produce sidebands related to a nominal carrier and their demodulation and separation, are described. The benefits of using spaced-antenna reception, especially when receiving telegraph signals on a ssb system, are explained.

621.396.5:621.395.632 2015
The Auto-Call—R. V. Anderson. (*CQ*, vol. 7, pp. 33–35; February, 1951.) Description of a device which can be fitted to a standard receiver to enable a station not "on the air" to be called from any mobile station. The caller whistles a sequence of pulses into his microphone. At the receiver, these pulses operate an anode-circuit relay controlling a stepping switch which connects the loudspeaker to the output tube, at the same time cutting out a high-pass audio filter inserted to prevent false operation by speech modulation. Conversation can then be carried on as usual.

621.396.5:621.396.933.4 2016
Multi-Carrier Air Communications—(*Wireless World*, vol. 57, pp. 92–94; March, 1951.) A brief description of a vhf system of radiotelephony for the control of civil aircraft, with particular reference to arrangements in the southern part of England. To ensure adequate coverage, five combined transmitting and receiving stations are dispersed over the area, all being operated from a common control point. Outline particulars of the transmitting and receiving equipment are given and the arrangements by which more than one receiver or more than one transmitter can be used, with a single antenna, are described. The scheme for frequency allocation is indicated. See also

Electronic Eng. (London), vol. 23, pp. 86–91; March, 1951.

621.396.619:621.391.1 2017

The Assessment of Modulation Systems using the Communication-Theory Concept of Channel Capacity—R. Piloty. (*Arch. elekt. Übertragung*,. vol. 4, pp. 493–508; December, 1950.) Channel capacity is defined in terms of the highest possible rate of transmission of single-valued signals of a given duration. Formulas are developed giving the capacity for both continuous and discrete channels, by a method less rigorous than that of Shannon (1361 and 1649 of 1949). The theory is used to compare the frequency-band and signal-noise-ratio requirements for various modulation systems for the same channel capacity; results are shown in graphs. Pulse code modulation is shown to be advantageous from this point of view.

621.396.65 2018

Emergency Wire-Line to Radio Circuits—D. Talley. (*Electronics*, vol. 24, pp. 195, 215; March, 1951.) Description of the construction and operation of equipment for temporary connection of a radio circuit, which is essentially a 4-wire system, to a 2-wire telephony network.

621.396.712 2019

B.B.C. Stations—(*Wireless World*, vol. 57, p. 104; March, 1951.) An up-to-date list of BBC medium- and long-wave stations, stating the program transmitted and the wavelength and power used.

SUBSIDIARY APPARATUS

621–526 2020

The Position Synchronization of a Rotating Drum—F. C. Williams and J. C. West. (*Proc. IEE* (London), Part II, vol. 98, pp. 29–34; February, 1951.) Description of a servo system, using a crystal reference oscillator, for controlling, within fine limits, the angular speed and angular position of a drum.

621:526 2021

Ascertaining the Critical Servo Gain—A. Schlang. (Proc. I.R.E., vol. 39, p. 290; March, 1951.) A simplified method is described for determining, from the system-determinantal equation, the critical gain resulting in instability.

621–526:659.25.001.11 2022

A General Scheme relating to a Problem in Cybernetics—S. Colombo (*Compt. Rend. Acad. Sci.* (Paris), vol. 232, pp. 1287–1288; March 28, 1951.) General formulas are given representing the operation of the system comprising apparatus to be regulated, comparator-discriminator, and servo-control mechanism.

621–526:659.25.001.11 2023

Reduction of a Problem in Cybernetics to a Problem of "Pursuit" in a Hilbert Space—R. Vallée. (*Compt. Rend. Sci.* (Paris), vol. 232, pp. 1288–1290; March 28, 1951.) Development of a particular method of considering the problem dealt with in 2021 above.

TELEVISION AND PHOTOTELEGRAPHY

621.397.5 2024

Perspective Distortion in TV Pictures—E. C. Lloyd. (*TV Eng.*, vol. 2, pp. 12–15 and 18–22; January and February, 1951.) "Proper viewing distance" is defined; the perspective distortion introduced at other viewing distances is evaluated quantitatively, and methods are developed for minimizing this distortion and for assessing the adequacy of standards of picture definition.

621.397.5 2025

The Sharpness of the Television Picture when the Picture Element has a Bell-Shaped Illumination-Intensity-Distribution Curve—E. Schwartz. (*Arch. elekt. Übertragung*, vol. 4, pp. 517–522; December, 1950.) Theoretical investigation of the form of the photocell-current curve obtained when a circular spot, across which the electron density decreases from center to periphery, is scanned across a line where the picture brightness changes suddenly. A formula is developed in the form of a power series, of which the independent variable is proportional to the distance between the center of the scanning spot and the brightness discontinuity. The resulting curve is S shaped, and its slope on crossing the discontinuity is greater than that of the straight line, corresponding to a uniform-intensity-square scanning spot. Thus, for the same sharpness the circular spot may be larger.

621.397.5:535.623/.624 2026

Colour Television—M. Alixant. (*Radio Tech. Dig.* (France), vol. 4, nos. 4 and 5, pp. 221–243 and 271–274. Bibliography, pp. 275–278; 1950.) Review with illustrated descriptions of the features of different transmission and reception systems, particularly American, classified according to principle of operation.

621.397.5:535.623 2027

Analysis of Synchronizing Systems for Dot-Interlaced Color Television—T. S. George. (Proc. I.R.E., vol. 39, pp. 124–131; February, 1951.) A mathematical analysis of random-phase error due to noise, and of static-phase error caused by variations in frequency from crystal to crystal in two systems, which might be used to synchronize the receiver dot or sampling frequency, viz: (a) a simple high-Q resonant filter and (b) an oscillator with afc calculations made for IF-carrier-noise ratios of 1, 3, and 5 (the critical range) show that for a phase-error tolerance of 10°, receivers operating without manual control of the dot frequency could probably be designed for carrier-noise ratios down to about 2.

621.397.5:621.39.001.11 2028

Television and the Transmission of Information—Y. Delbord. (*Ann. Télécommun.*, vol. 6, pp. 11–22; January, 1951.) A paper given at the symposium on Signal and Information Theory, Paris, April to May, 1950. Television is compared with various other ways of transmitting information, such as telegraphy, telephony, teleprinting, and so forth. The comparison is relatively easy for still material, and indicates that all the systems make approximately equally good use of the frequency channel. For a moving picture, the assessment is more difficult; the frequency band required in this case is 1,000 to 2,000 times that for transmitting a still picture. Methods both old and new for reducing this factor are considered, for example, line interlacing, division of the vision frequency spectrum into sub-bands transmitted sequentially, use of receiver-cathode-ray tube with long-persistence screen. Reduction of the frequency spectrum would make possible the use of lower-carrier frequencies and hence, a great extension of television.

621.397.5:778.1 2029

Some Factors in Pictorial Reproduction Processes with Special Reference to Television—R. G. Hopkinson, R. B. Mackenzie and R. D. Nixon. (*Photogr. Jour.*, vol. 91B, pp. 2–10; January to February, 1951.) The factors which determine the quality of pictorial reproduction in general are discussed, and their application in television practice is indicated.

621.397.5(73) 2030

Television Broadcasting in the United States, 1927–1950—D. G. Fink. (Proc. I.R.E., vol. 39, pp. 116–123; February, 1951.) A review of the development of transmission methods and equipment, receivers, and theater and color television.

621.397.6:621.396.67 2031

TV Receiving Antenna Research, Design and Production—R. G. Peters. (*TV Eng.*, vol. 2, pp. 8–10; February, 1951.) A report of methods used by some United States, manufacturers.

621.397.62 2032

P-M [permanent-magnet] Focus Devices for Picture Tubes—K. James and R. T. Capodanno. (*Electronics*, vol. 24, pp. 94–97; March, 1951.) A discussion of the requirements of a good permanent-magnet-focusing system, and of the various imperfections often occurring in practice. The stray field must be reduced to a minimum, and a uniform-focus field is essential. This entails the use of pole pieces of good mechanical design operated at flux densities below saturation.

621.397.62:[621.396.662+621.396.645 2033

Use of New Low-Noise Twin Triode in Television Tuners—R. M. Cohen. (*RCA Rev.*, vol. 12, pp. 3–25; March, 1951.) A full description of the use of the 6BQ7 in "driven grounded-grid" circuits, whose merits are discussed. Data are given on noise figure, image rejection, gain, and standing-wave ratio, for frequencies in the vhf television bands. The use of the 6BQ7 in an IF preamplifier for uhf television receivers is also discussed.

621.397.62:621.397.84 2034

Locked-in Oscillator for TV Sound—M. S. Corrington. (*Electronics*, vol. 24, pp. 120–125; March, 1951.) The characteristics of fm receivers can be improved by decreasing the frequency deviation before discrimination. The instantaneous frequency of the incoming signal is divided by a factor of five, by means of a locked-in oscillator. The input to this oscillator must be sufficient to ensure that locking takes place. The method is not suitable for the reception of weak stations with low-sensitivity receivers. A receiver incorporating this circuit is found to give better performance than a conventional receiver, when an interfering signal in the same channel is present.

621.397.621.2:535.376 2035

Saturation of Fluorescence in Television Tubes—Bril and Kröger. (*See* 1923.)

621.397.645.37 2936

Linearization of the Frequency Response of Wide-Band Amplifiers by Negative Feedback—Dillenburger. (*See* 1871.)

621.397.8 2037

Investigation of Ultra-High-Frequency Television Transmission and Reception in the Bridgeport, Connecticut, Area—R. F. Guy. (*RCA Rev.*, vol. 12, pp. 98–142; March, 1951.) During the year 1950, systematic comparisons were made between the experimental uhf (530 mc) and commercial vhf (67 mc) transmissions. The receiving stations included numerous homes in which either uhf receivers or converters were installed. The effects of various types of transmission line, antenna, and locations are described. The quality ratings of the uhf and vhf pictures were compared and related to field-strength tests made with a mobile equipment. The uhf field strength was more than 20 db below the theoretical level assuming a smooth earth.

621.397.6 2038

Television, Vol. 5 (1947–1948) and Vol. 6 (1949–1950). [Book Review]—A. N. Goldsmith, A. F. Van Dyck, R. S. Burnap, E. T. Dickey, and G. M. K. Baker (Eds.). Publishers: *RCA Review*, Princeton, N. J., 1950, 458 and 402 pp., $2.50 per volume. (*Jour. Soc. Mot. Pic. & Telev. Eng.*, vol. 56, p. 132; January, 1951.) Reprints of articles by RCA authors.

621.397.62:621.396.62.004.67 2039

Wireless Servicing Manual [Book Review]—Cocking. (*See* 2008.)

TUBES AND THERMIONICS

621.383.012 2040

Modification of Current/Voltage Characteristics of a Gas-Filled Photocell with Plane Cathode under the action of a Magnetic Field Perpendicular to the Cathode—R. Birebent. (*Compt. Rend. Acad. Sci.* (Paris), vol. 232, pp. 1296–1298; March 28, 1951.) Measurements of the variation of current with voltage were made on an argon-filled photocell, for different values of illumination, with and without a magnetic field of 250 oersted. The current/voltage characteristic can be represented by an exponential function involving the ionization-potential of the filling gas. Application of the magnetic field leads to an increase of current, by preventing diffusion of electrons and ions towards the walls.

621.383.27† 2041

Secondary-Electron Multipliers and their Technical Significance—K. Nentwig. (*Frequenz*, vol. 4, pp. 328–332; December, 1950.) Review of German development, showing details of construction and sensitivity characteristics of new photomultiplier tubes. These include an 11-stage tube mounted on a 13-pin base, with sensitivity of the order of 10 a/lumen, though for continuous operation, a much smaller current of about 0.5 ma should not be exceeded; for pulsed operation the current may be increased to about 10 ma.

621.383.4 2042

Infra-Red Photoconductivity of Certain Valence Intermetallic Compounds—G. N. Braithwaite. (*Proc. Phys. Soc.* (London), vol. 64, pp. 274–275; March 1, 1951.) Short account of investigations of the properties of evaporated layers of Cu_2Te, Ag_2Te, ZnTe, HgTe, Tl_2Te, Sb_2Te_3, Mo_2Te, W_2Te, U_2Te, Zn_3As_2, SnS, and Sb_2Se_3, with a table showing, (a) the peak wavelength, (b) the long-wave threshold, (c) the greatest wavelength at which signals were detected.

621.383.49:546.683.1.221 2043

On the Photoconductivity of Thallous Sulfide Cells—A. W. Ewald. (*Phys. Rev.*, vol. 81, pp. 607–611; February 15, 1951.) "An investigation of the rise and decay of the photocurrent in Tl_2S cells shows that the simple bimolecular recombination theory, on which previous quantitative discussions of the photoeffect in Tl_2S were based, is inadequate for the complete explanation of these curves. The dependence of the initial slopes of the response curves on light intensity is that to be expected for a homogeneous photoconductor, but the temperature dependence of these slopes suggests the presence of barriers, which influence the conductivity through the mobility. The variations of both the initial slopes and the steady-state photoconductivity with temperature indicate an exponential dependence of the mobility upon temperature, with an activation energy of 0.19 ev."

621.385:621.318.572 2044

Wide-Band A.T.R. and T.R. Gas-Discharge Switches—R. Musson-Genon, R. Métivier, and R. Palièr. (*Rev. tech. Comp. franç. Thomson-Houston*, pp. 23–34; November, 1950.) The functions and operation of transmit-receive and anti-transmit-receive switches in radar apparatus are described and analyzed. Design and performance testing of ATR switches, Types RH. 0331 and 0332, and TR switch Type RH. 0531 for use in the X band (8.5 to 9.6 kmc) are considered, and their characteristics are given.

621.385.001.4:519.283 2045

Statistical Evaluation of Life Expectancy of Vacuum Tubes Designed for Long-Life Operation—E. M. McElwee. (Proc. I.R.E., vol. 39, pp. 137–141; February, 1951.) A 1950 IRE National Convention paper noted in 2104 of 1950.

621.385.029.64/.65 2046

Transmission-Line Equivalent of Electronic Traveling-Wave Systems—W. E. Mathews. (*Jour. Appl. Phys.*, vol. 22, pp. 310–316; March, 1951.) The small-signal properties of long electron beams may be analyzed in terms of traveling-space-charge waves; this suggests an equivalence between such beams and transmission lines moving longitudinally. The analysis of certain electronic devices in terms of coupled-distributed-parameter lines in motion is equivalent to a rigorous field-theory analysis. The results for the idealized helix and thin cylindrical-electron beam are presented.

621.385.029.64/.65 2047

Periodic-Waveguide Traveling-Wave Amplifier for Medium Powers—G. C. Dewey, P. Parzen, and T. J. Marchese. (Proc. I.R.E., vol. 39, pp. 153–159; February, 1951.) A theoretical and experimental investigation of singly corrugated-coaxial-transmission lines is described. The properties of such structures are calculated, and the effect of an axial-electron beam is taken into account by a field method. Values of gain and bandwidth are derived. The theoretical results agree fairly well with experimental values. An amplifier giving an output of 50 w, with a gain of 20 db and bandwidth of 100 mc at a wavelength of 6.5 cm has been produced. The maximum output obtained was 125 w and the highest efficiency 7 per cent.

621.385.029.64/.65:621.317.755 2048

The Traveling-Wave Cathode-Ray Tube—H. E. Hollmann. (Proc. I.R.E., vol. 39, pp. 194–195; February, 1951.) Comment on 503 of March (Owaki et al.). The prototype of the traveling-wave deflection system is the multiphase system (see 1128 of 1939). The ultradynamic Lissajous figures in the Japanese paper are the same as those obtained by Hollmann many years ago (see 544 of 1940). See also 3536 of 1940 and back references.

621.385.032.2:669.198.865 2049

Aluminum-Clad Iron for Electron Tubes—Espe and Steinberg. (*See* 1949.)

621.385.032.213 2050

Boride Cathodes—J. M. Lafferty. (*Jour. Appl. Phys.*, vol. 22, pp. 299–309; March, 1951.) See 3207 of 1950.

621.385.032.216 2051

On Poisoning of Oxide Cathodes by Atmospheric Sulfur.—H. A. Stahl. (Proc. I.R.E., vol. 39, p. 193; February, 1951.) Measurements on oxide cathodes exposed in the open air showed a large decrease of emissivity, with increasing sulphur content. Only by sealing the cathodes in a vacuum immediately after the manufacture could the formation of BaS (detected by electron diffraction) be prevented.

621.385.032.216 2052

The Leaky-Condenser Oxide-Cathode Interface—A. Eisenstein. (*Jour. Appl. Phys.*, vol. 22, pp. 138–148; February, 1951.) "The time dependence of current passed by commercial pentodes has been studied under pulsed conditions of operation. A decay of current is observed in the microsecond time range for those tubes operated for long periods under cutoff conditions. This decay has been interpreted in terms of the resistance and capacitance of the interface layer, known to exist from X-ray diffraction studies. Techniques are developed and applied to the measurement of this interface resistance and capacitance as a function of temperature. Following the initial-current decay, a partial recovery is observed when long pulses are used. This effect results from Joule heating of the interface layer."

621.385.032.216 2053

The Barium-Oxide-on-Tungsten Cathode Interface—H. P. Rooksby and E. G. Steward. (*Jour. Appl. Phys.*, vol. 22, pp. 358–359; March, 1951.) The results of investigations on oxide cathodes lead to conclusions different from those put forward by Hensley and Affleck (263 of February). Compounds similar in structure to the interface compounds have been synthesized by heat treatment of alkaline-earth carbonates and tungstic oxide in the molecular proportions of 3:1; they have the formula R_3WO_6, R representing the alkaline-earth metal. Such compounds give X-ray patterns consistent with face-centered-cubic symmetry and thus differing from the perovskite structure.

621.385.032.216 2054

The Barium-Oxode-on-Tungsten Cathode Interface—E. B. Hensley and J. H. Affleck. (*Jour. Appl. Phys.*, vol. 22, p. 359; March, 1951.) Further investigations confirm the conclusions of Rooksby and Steward (2053 above) that the interface compound is Ba_3WO_6 and not $BaWO_3$ as suggested previously (263 of February).

621.385.032.216:546.41+546.42+546.431]-31 2055

Pulsed Emission from the BaO-SrO-CaO System—L. E. Grey. (*Nature* (London), vol. 167, p. 522; March 31, 1951.) Dependence of pulsed emission on molecular composition is shown by means of contours on a triangular diagram. A maximum of about 8 a/cm² occurs for the composition BaO:SrO:CaO::47:43:10.

621.385.15:621.385.032.216 2056

Secondary-Emitting Surfaces in the Presence of Oxide-Coated Cathodes—S. Nevin and H. Salinger. (Proc. I.R.E., vol. 39, pp. 191–193; February, 1951.) Describes experiments to show that the deleterious effect of oxide cathodes, on Ag-Mg-secondary-emission surfaces, can be overcome by using Ta instead of Ni as the base metal for the oxide coating.

621.385.2 2057

The Transit Time, Electron Paths, Cathode Field-Strength and Potential of the Space-Charge Diode for All Values of Initial Velocity, Initial Direction and Current—A. O. Barut. (*Z. angew. Math. Phys.*, vol. 2, pp. 35–42; January 15, 1951.) The basic equations for the space-charge field in a planar diode lead to a nonlinear equation of the third degree and third order, for the x component of the electron-velocity potential. This differential equation and its solution can be used to calculate, without integration of the Poisson equation, the electron-transit time, the cathode field, the potential and the electron paths, as functions of only two reduced parameters for all values of initial velocity and current, under conditions of partial or complete space charge. The generality of the solution is discussed and other possible applications of the method are mentioned.

621.385.2:537.525.92 2058

The Space-Charge Smoothing Factor—C. S. Bull. (*Proc. I.E.E.* (London), Part III, vol. 98, pp. 149–152; March, 1951.) A relation between the anode-current fluctuations and the fluctuation in the total emission of a planar diode is derived; the total-emission fluctuations are, in general, much greater than the full shot noise. The space-charge smoothing factor can be expressed simply and its value can be determined experimentally from measurements of (a) the characteristic at two slightly different cathode temperatures and (b) the distance from cathode to anode; no measurement of temperature or total emission is necessary.

621.385.2:546.289 2059

Germanium Diodes—R. T. Lovelock and

J. H. Jupe. (*Wireless World*, vol. 57, pp. 57–60; February, 1951.) Description of method of manufacture and short discussion of characteristics and uses.

621.385.2.012:[546.28+546.289 2060
Semiconductor Diodes—(*Electronics*, vol. 24, pp. 112–113; March, 1951.) Summary of the characteristics of Si and Ge crystal diodes, with dimensions and terminal data of available United States' types.

621.385.28/.38:537.525.92 2061
Measuring the Deionisation Time of Gas-Filled Diodes and Triodes—K. W. Hess. (*Phillips Tech. Rev.*, vol. 12, pp. 178–184; December, 1950.) A method is described for determining quickly the order of magnitude of deionization time in a triode; an alternating voltage is applied to the anode, while the grid is connected via a resistance to a negative voltage source, the grid voltage giving a direct indication of the number of positive ions present. The cases of a triode in a polyphase-rectifying installation and of a diode in a relay circuit are also investigated.

621.385.4:621.396.61 2062
Two Transmitting Valves for Use in Mobile Installations—E. G. Dorgelo and P. Zijlstra (*Philips Tech. Rev.*, vol. 12, pp. 157–165; December, 1950.) Two double tetrodes, types QQE 06/40 (indirectly heated) and QQC 04/15 (directly heated) are described, in which the screen grids for the two halves form a single structure When used in an output stage, the two halves are preferably connected in push pull; for frequency multiplication, they can be connected in cascade. At frequencies up to 200 mc, the QQE 06/40 can generate 90 w with an efficiency of about 75 per cent, and at 300 mc, 70 w with 65 per cent efficiency. The corresponding figures for the QQC 04/15 are 22.5 w with over 70 per cent efficiency and 9 w with 34 per cent efficiency. See also *Commun. News*, vol. 11, pp. 126–132; December, 1950.

621.385.5 2063
Low-Noise Miniature Pentode for Audio Amplifier Service—D. P. Heacock and R. A. Wissolik. (*Tele-Tech*, vol. 10, pp. 31–33, 69; February, 1951.) Design features of the RCA Type 5879 tube are described, which result in low values of interelement leakage and of coupling between heater and other parts.

621.385.832:681.142 2064
The Selective Electrostatic Storage Tube—J. Rajchman. (*RCA Rev.*, vol. 12, pp. 53–97; March, 1951.) The tube is intended for high-speed handling of digital information in the form of on-off signals, and has a storage capacity of 256 signals. Electrons from an extended cathode system are directed to the whole target area, but are prevented from reaching all but one selected window area, by means of a complex control-grid system consisting of two orthogonal sets of spaced-parallel bars. The characteristics of the tube, the design of the associated circuits, and the arrangement of the bar connections are described.

621.396.615.14 2065
The Design of Low-Power Valves for V.H.F. and U.H.F.—R. Stuart. (*Radio franç.*, pp. 1–5; January, 1951.) Discussion of the principles governing the design of triodes and tetrodes for the frequency range 500 to 1,500 mc. Factors considered include type of structure, electrode connections and disposition, anode voltage, and cathode emission. Operating characteristics of seven typical French tubes are tabulated. See also 2096 of 1950.

621.396.615.141.2 2066
3-cm Magnetrons—J. Lazzeri. (*Rev. tech. Comp. franç. Thomson-Houston*, pp. 35–46; November, 1950.) An account is given of the operating principles, design, and manufacture of magnetrons, with particular reference to 12-cavity magnetrons suitable for use in radar on a wavelength of about 3 cm. Characteristics are given of three types, each capable of an output of 40 kw, with an efficiency of about 30 per cent, one with frequency adjustment of 200 mc centered on 9.37 kmc.

621.396.615.141.2:621.385.833 2067
Electron Optical Exploration of Space Charge in a Cut-Off Magnetron—Reverdin. (*See* 1988.)

621.396.615.142 2068
Amplification by Acceleration and Deceleration of a Single-Velocity Stream—L. M. Field, Ping King Tien and D. A. Watkins. (PROC. I.R.E., vol. 39, p. 194; February, 1951.) The waves described by Hahn (3521 of 1939) and Ramo (4352 of 1939) not only change in length as the beam velocity changes but also change in amplitude. By a suitable combination of gradual decelerations and sudden accelerations, the amplitude may be increased. An amplifier constructed on these lines provided a net gain of 22 db at 3 kmc.

621.396.615.142.2:621.317.3.001.4 2069
3-cm Low-Voltage Reflex Klystron, Type RHK 6332—J. Chantereau, R. Musson-Genon, and R. Métivier. (*Rev. tech. Comp. franç. Thomson-Houston*, pp. 47–57; November, 1950.) A detailed description of the construction and test methods used. With an anode potential of 300 v, and a maximum anode dissipation of 12 w, the tube gives an output of more than 20 mw over the frequency band 8.5 to 9.66 kmc. See also 683 of April.

621.396.622.63:546.28 2070
Silicon Crystal Detectors—J. Mercier. (*Rev. tech. Comp. franç. Thomson-Houston*, pp. 9–21; November, 1950.) The manufacture, adjustment, and performance testing of silicon crystals, for use as frequency changers in radar receivers, are described in detail. Characteristics are given of a range of crystals for use as frequency changers and as detectors in the 8 5 to 9.6 kmc band and below 4 kmc.

621.396.822 2071
Transit-time Phenomena in Electron Streams: Part 3—The Electron-Ion Plasma and Beam Fluctuations—D. K. C. MacDonald. (*Phil. Mag.*, vol. 42, pp. 515–522; May, 1951.) A continuation of earlier papers (2408 of 1949 and 1038 of May) on the fluctuations in an electron beam. In this case, the equilibrium fluctuations are considered, taking full account of the interaction of the electrons and the field as expressed by Poisson's law. A discussion is also given of "lattice" models of electron and electron-ion plasma. The noise per unit bandwidth is frequency dependent up to a certain limiting frequency, above which it is constant (pure shot effect). The results are considered in relation to some practical tube problems.

621.385:[621.396.621+621.397.62 2072
Receiving Tube Substitution Guide Book [Book Review]—H. A. Middleton. Publishers: J. F. Rider, New York, N. Y., 1950, 224 pp., $2.40. (*Electronics*, vol. 24, pp. 144, 148; February, 1951.) A list of permissible substitutes for about 750 types of receiving tube is given, with diagrams showing socket changes or adapter construction where necessary. A table of receiving-tube characteristics is included and also a section dealing with television-receiver models.

061.4(41) 2073
Festival of Britain—(*Wireless World*, vol. 57, pp. 173–174; May, 1951.) A list of most of the modern radio gear included in the South-Bank and Land-Travel Exhibitions, in the "Campania" Festival Ship and in the Kelvin Hall, Glasgow.

MISCELLANEOUS

519.283:53+621.3].001.5 2074
The Control Chart as a Tool for Analyzing Experimental Data—E. B. Ferrell. (PROC. I.R.E., vol. 39, pp. 132–137; February, 1951.) A 1950 IRE National Convention paper.

55+621.3].001.5 2075
Research in 1950—(*Metrop. Vick. Gaz.*, vol. 23, pp. 312–319; February, 1951.) A review of the work in various branches of physics and engineering carried out in the Metropolitan Vickers research laboratories, with a list of papers published by members of the staff.

621.3 2076
Electrical Transmission of Power and Signals [Book Review]—E. W. Kimbark. Publishers: J. Wiley and Sons, New York, N. Y., and Chapman and Hall, London, Eng., 461 pp., 48s. (*P.O. Elec. Eng. Jour.*, vol. 43, p. 218; January, 1951.) "A general textbook covering basic theory appropriate to the transmission of power, telephony, and ultra-high-frequency signals."

621.3.029.6 2077
Ultrahigh-Frequency Engineering [Book Review]—T. L. Martin, Jr. Publishers: Prentice-Hall, New York, N. Y., 1950, 356 pp., $6.00. (*Jour. Frank. Inst.*, vol. 251, p. 301; February, 1951.) "It is highly recommended to electronic engineers and physicists who encounter design and operating problems in ultra-high frequencies."

621.39 2078
Radio Technology [Book Review]—B. F. Weller. Publishers: Chapman and Hall, London, Eng., 3rd ed., 420 pp., 30s. (*Electrician*, vol. 146, p. 1131; April 6, 1951.) Primarily for students of radio engineering. "The chapter on antennas and radiation has been considerably lengthened and a new chapter on uhf technique added."

621.39 Heaviside 2079
The Heaviside Centenary Volume [Book Review]—Publishers: Institution of Electrical Engineers, London, Eng., 10s. (*Engineering* (London), vol. 171, p. 90; January 26, 1951.) "The volume contains the papers which were read at the centenary meeting on May 18, 1950."

621.396.029.6 2080
Short Wave Wireless Communication [Book Review]—A. W. Ladner and C. R. Stoner. Publishers: Chapman and Hall, London, Eng., 5th ed., 1950, 717 pp., 50s. (*Jour. Brit. IRE*, vol. 11, p. vi; February, 1951.) Material no longer topical has been replaced by chapters on sound and vision intelligence, waveguides, and wireless telegraph circuits.

621.396.6.001.4.004.67 2081
Electronic Equipment Construction [Book Review]—Publishers: Department of Commerce, Office of Technical Services, Washington, D. C., 300 pp., $7.00. (*Electronic Eng.* (London), vol. 23, p. 116; March, 1951.)

"This book is a compendium of recent advances in construction techniques and components designed to facilitate servicing and maintenance of electronic equipment. It has been compiled by a team of scientists from the Stanford Research Institute, who have visited companies and government establishments both in the United States and England, in order to get the widest coverage on their subject."

FIT

FOR A KING *after* THE "ROYAL TASTER"

Prudently, kings of old employed the "taste-it-first" method to test the presence of lethal power in bulk food and drink. Wary but wise, you'd say...

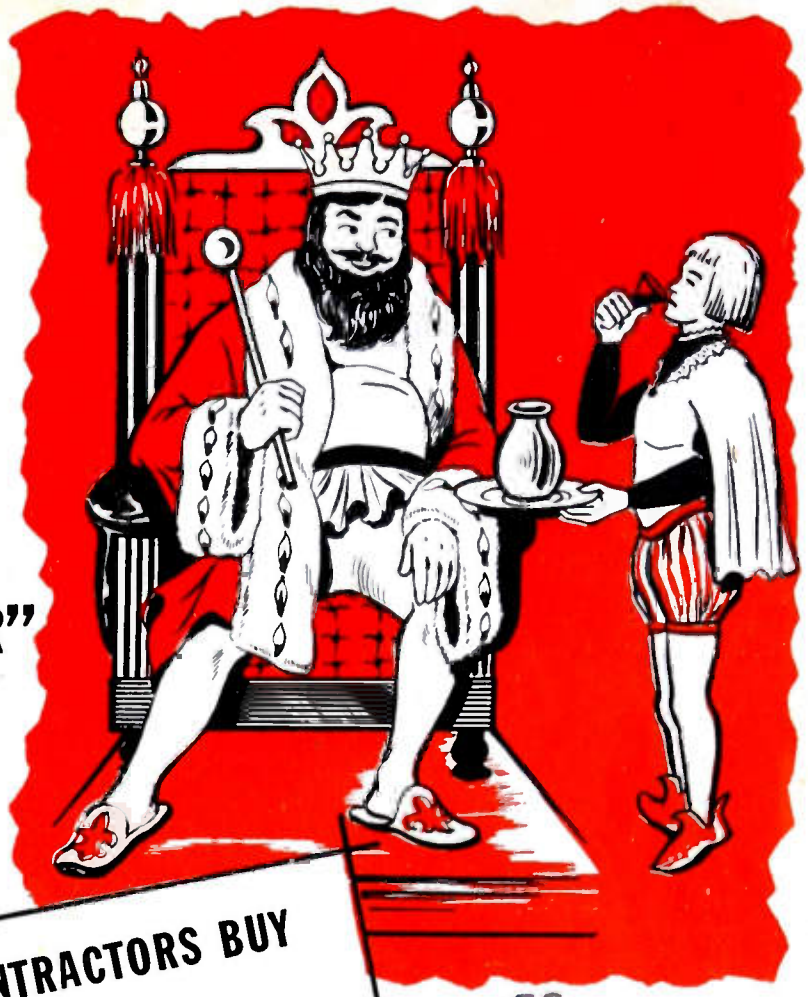

NOW GOVERNMENT CONTRACTORS BUY *Transformers* ON A "PROVE-IT-FIRST" BASIS!

We are prepared to submit a production sample GRACOIL TRANSFORMER (hermetically sealed to JAN-T-27 or MIL-T-27 Government specifications or one of open type construction), if your equipment is to be used for awarded prime or sub-contract work. Put your production sample to any test. Then order production quantities with absolute confidence of physical and electrical correctness, uniformity and substantial savings on profit-tight contracts.

James M. Blacklidge
PRESIDENT

VERTICAL BLOCKING OSCILLATING TRANSFORMER HERMETICALLY SEALED BUILT TO MIL-T-27

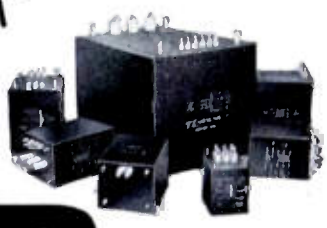

PLATE TRANSFORMER SHOWN (l to r) WITH POWER, FILAMENT, CHOKE, DRIVER, FILAMENT AND SMALLER PLATE TRANSFORMERS ALL BUILT TO MIL-T-27 SPECIFICATIONS. HERMETICALLY SEALED

One good Turn—or a Million

FILAMENT
AUDIO
TRANSFORMERS
•
FILTER REACTORS
•
ISOLATION-STEP-UP
STEP-DOWN
TRANSFORMERS
•
WINDINGS

GRAMER

TRANSFORMER CORPORATION

2736-K NO. PULASKI ROAD • CHICAGO 39, ILLINOIS

SEND YOUR B/P SPECIFICATIONS

SECTION MEETINGS

BEAUMONT-PORT ARTHUR

Inspection Tour of KPRC-TV by H. Wheeler Chief Engineer; July 17, 1951.

BUFFALO-NIAGARA

"High Quality Reproduction of Sound," by R. T. Bozak, R. T. Bozak Loudspeaker Co.; May 16, 1951.

DALLAS-FT. WORTH

Southwestern IRE Conference, Keynote Address by D. G. Fink, Banquet Address by Hon. G. E. Sterling, F.C.C., and twelve technical papers given; April 20–21, 1951.

Anniversary dinner celebrating 10th Anniversary of Section, presentations by Dr. W. H. Rust, Regional Director; May 24, 1951.

FORT WAYNE

"Color Television," by Arthur V. Loughren, Vice President, Hazeltine Corp.; June 11, 1951.

HOUSTON

Tour of Television Station KPRC-TV by Pau Huhndorff, Chief Engineer; June 19, 1951.

"Television, Past, Present and Future," by Jack Harris, General Manager, Radio KPRC and KPRC-TV; May 15, 1951.

"Fluid Mapping," by Prof. A. D. Moore, Faculty, University of Michigan; April 12, 1951.

INDIANAPOLIS

"Stroboscopes and Stroboscopic Techniques," by Kipling Adams, General Radio Company; March 30, 1951.

"Printed Circuits and Metalizing Insulators," by H. F. Fruth, Consulting Physicist; April 18, 1951.

"Electronic Tone Generators," by Serge Krauss, C. G. Conn Company; May 4, 1951.

"Response Characteristics of the Human Being," by Lt. Col. R. C. Gibson, Faculty, U.S.A.F. Institute of Technology; May 11, 1951.

"The Analog Computer," by Dr. J. D. Ryder, Faculty, University of Illinois; June 8, 1951.

LOS ANGELES

"Remote TV Pickups," by C. G. Pierce, panel discussion on Television by H. W. Pangborn, R. W. Clark, and F. G. Albin, and election of officers; June 5, 1951.

MILWAUKEE

"Third Surge of the Chemical Industry," by Frank C. Byrnes, Western Editor of "Chemical Engineering"; April 18, 1951.

"Home Beautification," by John E. Voight, Whitnall Park Botanical Gardens; April 19, 1951.

"Characteristics and Limitations of Resistors and Capacitors," by E. T. Sherwood, Globe-Union, Inc.; April 25, 1951.

"Your Chances in Life," by Roy Smith, Railway and Industrial Engineering Co.; May 2, 1951.

"Television Facilities of WTMJ-TV," by Phil Laesser, Chief Engineer of Television and FM facilities; May 25, 1951.

NEW MEXICO

Installation of new officers; June 23, 1951.

NORTH CAROLINA-VIRGINIA

"Dynamic Demonstration With Trouble Shooting in TV Sets," by J. V. Yakmas, General Electric Co.; June 22, 1951.

PITTSBURGH

"Electronic Aspects of Nuclear Power Plants," by Mortimer A. Schultz, Westinghouse Electric Corporation; June 11, 1951.

(Continued on page 36A)